The Structure and Evolution of the Newfoundland Basin, Offshore Eastern Canada

by

Kathryn D. Sullivan

Submitted in partial fulfilment
of the requirements for the degree of
Doctor of Philosophy,
Department of Geology, Dalhousie University.

April, 1978

Barrie, Many thanks for providing support, incentive and friendship - I've enjoyed it!
Kathy

Approved by

_____ _____

_____ _____

_____ _____

DALHOUSIE UNIVERSITY

Date 28 April , 1978

Author KATHRYN D. SULLIVAN

Title THE STRUCTURE AND EVOLUTION OF THE NEWFOUNDLAND BASIN, OFFSHORE EASTERN CANADA.

Department or School GEOLOGY

Degree Ph.D. Convocation SPRING Year 1978

Permission is herewith granted to Dalhousie University to circulate and to have copied for non-commercial purposes, at its discretion, the above title upon the request of individuals or institutions.

Signature of Author

TABLE OF CONTENTS

ABSTRACT

The ocean-continent boundary in the Newfoundland Basin is defined on the basis of seismic reflection and magnetic data as the seaward boundary of the continental margin magnetic smooth zone. The boundary is diachronous, being coincident with the J-anomaly (115 Ma) between the Southeast Newfoundland Ridge and the Newfoundland Seamounts and being of younger, but uncertain age north of the seamounts. These data are combined with recently-published data to define a pre-drift fit for Iberia-North America that is without gaps and continental overlaps.

Active seafloor spreading began in the southern Newfoundland Basin at J-anomaly time (115 Ma); rifting began much earlier, perhaps in Triassic time (concomitant with the opening of the main Atlantic basin to the south). Changes in magnetic anomaly trends document two pole shifts prior to anomaly 31/32: At about 102 Ma the spreading axis shifted from the 015° J-anomaly trend to 055°, and spreading occurred simultaneously in the Newfoundland Basin and the Bay of Biscay about a pole located northeast of Paris; at about 80 Ma (anomaly 34) the spreading shifted to the Cenozoic geometry evident in the pattern of magnetic anomalies 34 through 1.

The Southeast Newfoundland Ridge formed on oceanic crust along the southeastern extension of the Newfoundland Fracture Zone. Two processes were involved: migration of a leaky transform fault along the trend from 102-80 Ma and differential vertical movements in post-Middle Cretaceous time. The Newfoundland Seamounts represent volcanic activation of two structural trends, the seaward prolongation of a

major continental structure (evident gravimetrically) and the fracture zones formed during the Biscay-Newfoundland Basin spreading phase. Late-stage trachytic volcanics on Scruncheon Seamount ($^{40}Ar/^{39}Ar$ age = 97.7 ± 1.5 Ma) and the formation of a shallow-water limestone cap on Shredder Seamount (Early-Middle Cretaceous fauna) indicate that seamount volcanism had largely ceased by mid-Cretaceous time.

Three acoustic stratigraphic sedimentary units are defined on the basis of seismic reflection profiles and sonobuoy data. These correlate well with the units defined by Horizons β and A in the Northwest Atlantic and with the sedimentary sequence drilled on the Iberian and Biscay margins by the Deep Sea Drilling Project. The distribution and character of the Newfoundland Basin units document the uplift of the southern Grand Banks and Southeast Newfoundland Ridge in Early Cretaceous time and the onset of active bottom currents (turbidity and/or contour currents) in the Late Cretaceous or Early Tertiary.

Magnetic surveying and modelling in the southern Newfoundland Basin confirm the existance of magnetic lineations in oceanic crust of Late Cretaceous (Cretaceous Normal Polarity Interval) age that appear to be due to field reversals. It is shown here that chemical alteration or tectonic rotation of crustal blocks could account for the observed lineations without field reversals.

LIST OF SYMBOLS AND ABBREVIATIONS

Ma	Million years or million years before present, as required by context
nT	Nano-teslas; lnT = 1 gamma.
mgal	milligal
km	kilometer
m	meter
emu/cc	electromagnetic unit per cubic centimeter.
rms	root-mean square
DSDP	Deep Sea Drilling Project
SENR	Southeast Newfoundland Ridge

LIST OF FIGURES

LIST OF TABLES

ACKNOWLEDGEMENTS

I thank all the members of my supervisory committee, Drs. D. B. Clarke, C. E. Keen, M. J. Keen and D. J. W. Piper, for the guidance and support they offered during all phases of this project. I am particularly grateful to Charlotte Keen, the primary supervisor of this thesis, for her advice, encouragement and tremendous patience.

I am also grateful to Dr. S. Barr for initiating my involvement in the Newfoundland Basin study and to Blaine Hall for his continuing interest and support in this research. The advice and comments of the many people with whom I have discussed various aspects of this work are appreciated. Frequent and particularly valuable conversations were had with Drs. F. M. Gradstein, A. C. Grant, J. M. Hall, R. T. Haworth, L. F. Jansa, H. Schouten, S. P. Srivastava and J. A. Wade and Mr. R. L. Houghton.

Many friends at Bedford Institute and Dalhousie University helped with the collection and processing of the data in this thesis, and I am grateful to them all. I also thank the officers and crews of the Bedford Institute oceanographic vessels for their willing and capable assistance. The Geology Departments at St. Mary's University, Halifax, and Memorial University of Newfoundland very kindly provided X-ray fluorescence analyses of numerous samples.

I thank J. Aumento and A. Scott for drafting most of the figures in the text and M. Annand for patiently typing and re-typing the manuscript.

To Wint and Mary Sparling and the crew of Finally, who offered kind encouragement and much-needed diversion during the long final stages of this thesis, I give special thanks. Last, but far from least, I owe a special debt of gratitude to Ian and Dan for their unfailing understanding and patience.

CHAPTER 1: INTRODUCTION

An extensive body of literature dealing with the pre-drift positions of the circum-Atlantic continents and the relative motions of the plates in that region has accumulated in the past ten years. There is now widespread agreement on a basic model for the evolution of the North Atlantic which, between the Azores-Gibraltar line and the Charlie-Gibbs Fracture zone, is well-constrained from the present back to anomaly 31/32 (Bullard et al., 1965; Pitman and Talwani, 1972; LePichon and Fox, 1971). Interest is now shifting towards resolution of more specific paleogeographic and plate kinematic problems. Two such problems are the initial position of Iberia with respect to North America and the geometry and chronology of the pre-anomaly 31/32 (73 Ma) relative motions of these plates (Fig. 1.2).

Some progress has been made on these fronts since the early works of Wegener (1924) and Choubert (1935). Carey (1958) showed that a closer fit was obtained when the seaward limits of continental crust were matched instead of present-day coastlines, and Bullard et al. (1965) proved the geometrical validity of the morphological fits. However, the now-classical Bullard fit (Fig. 1.2b) and most subsequent reconstructions (Fig. 1.2c; Laughton, 1972, 1975; Dewey et al., 1973) fail to arrive at a pre-drift position for Iberia that does not involve either overlaps between continental areas or large, unexplained gaps. The pre-drift positions of the various sunken continental fragments in this part of the North Atlantic (Rockall Bank, Porcupine Bank, Orphan Knoll, Flemish

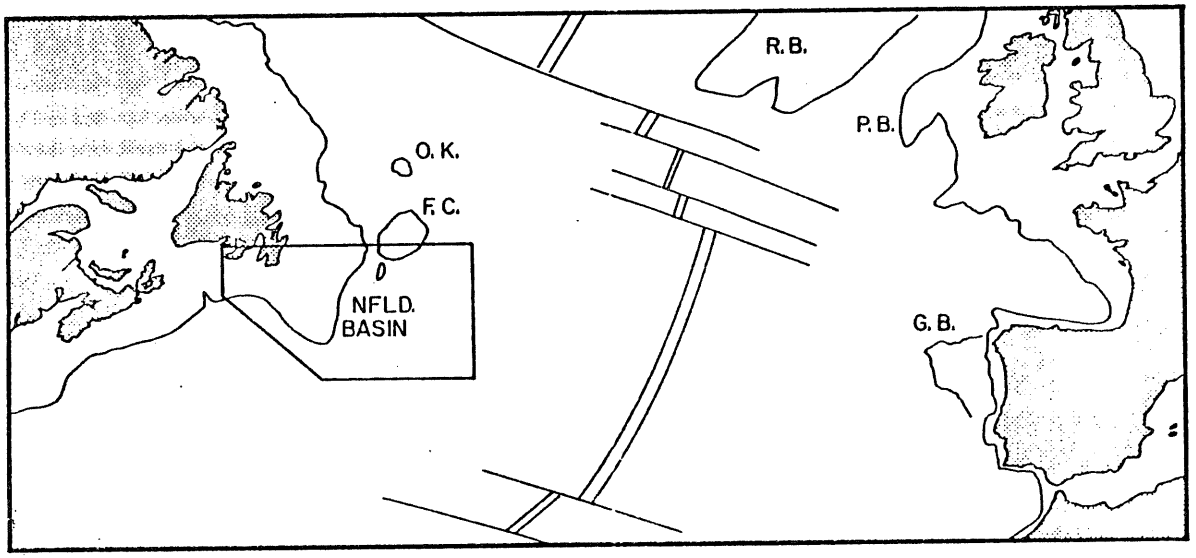

Figure 1.1
Location map. F.C.=Flemish Cap; O.K.=Orphan Knoll; R.B.=Rockall Bank; P.B.=Porcupine Bank; G.B.=Galicia Bank.

Cap; Galicia Bank; Figure 1.1) have proved especially difficult to determine.

More recently, Arthaud and Matte (1975, 1977) have shown that intensive crustal fragmentation was produced in the former Iberia-Grand Banks continental region during several Paleozoic tectonic episodes. The significant influence this fragmentation exerted upon the pattern of subsequent rifting is stressed by both Arthaud and Matte (1977) and LePichon et al. (1977). The latter authors express some doubt that a successful reconstruction of this part of the North Atlantic will ever be achieved, in view of the extreme complexity of the pre-drift structures. However, the apparent success of a reconstruction recently proposed by Haworth (in prep.) seems to indicate that detailed studies combining continental, continental margin and deep-sea data may provide a means for considerably improving upon the earlier, less satisfactory reconstructions.

Haworth (in prep.) approaches the task of reconstructing the pre-drift positions of the North Atlantic continents from both an oceanic and a continental viewpoint. Tectono-stratigraphic zones of Newfoundland are traced across the North American continental shelf and margin on the basis of detailed geophysical surveys (Haworth and MacIntyre, 1975) and correlated with similar features on the European and Iberian margins (Lefort, 1975; Roberts, 1975; Riddihough and Max, 1976; Lefort and Haworth, in press). These correlations are then used to refine the reconstruction of the Labrador Sea and North Atlantic proposed by Srivastava (1978) on the basis of detailed marine geophysical studies.

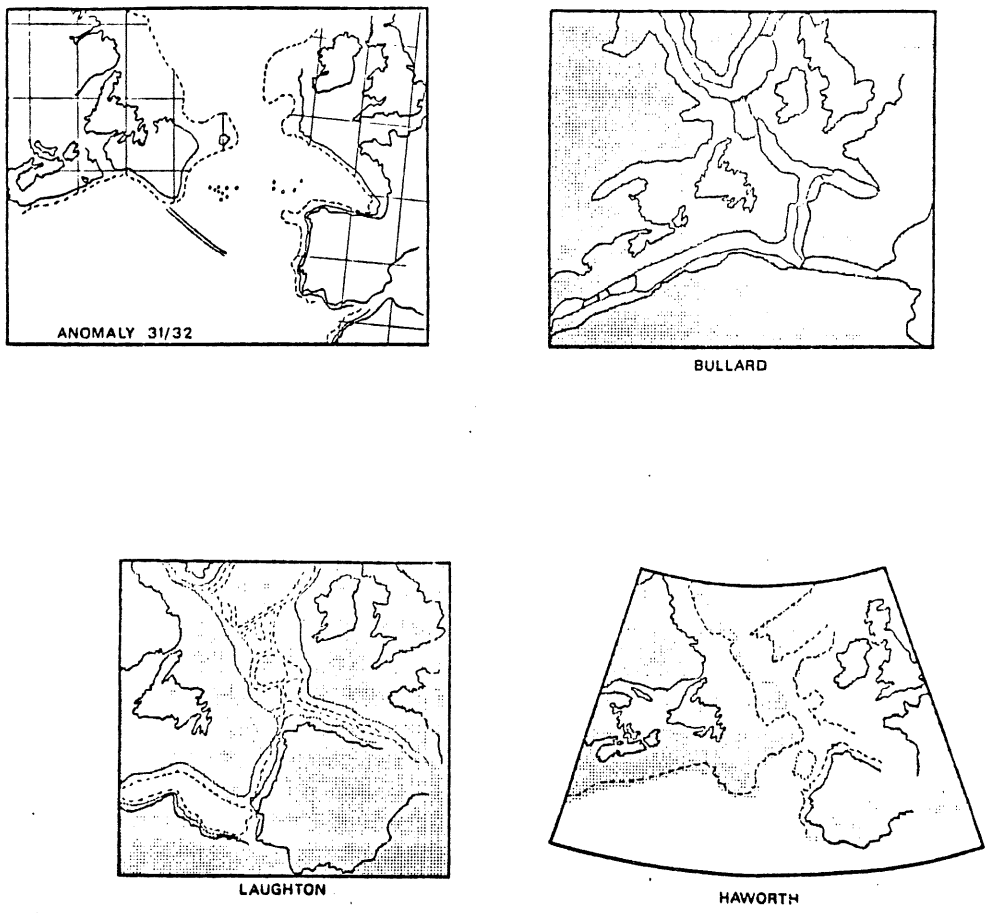

Figure 1.2
Paleogeographic reconstructions

Anomaly 31/32 from C.E. Keen et al (1977); pre-drift fits from Bullard et al. (1965), Laughton (1977) and Haworth (in prep).

Haworth's final model (Figure 1.2) succeeds in eliminating continental overlaps with minimal movement of the various continental fragments (only a small displacement of Galicia Bank is required) but still leaves a gap of several hundred kilometers between the southern Grand Banks and western Portugal.

Objectives

The position of Iberia with respect to North America in the Haworth reconstruction was not determined directly, but rather is a consequence of the Iberia-Europe and Europe-Greenland-North America fits. The need to use this indirect approach stemmed from the lack of comprehensive geophysical studies of the continental margins and oldest oceanic crust adjacent to Portugal and the Grand Banks. The recent publication of drilling results and site-survey data collected during Legs 47B and 48 of the Deep Sea Drilling Project (Groupe Galice, 1977; Montadert, Roberts et al., 1977; Ryan, Sibuet et al., 1976) partially removes this limitation by providing crucial data from the Iberian plate west of Portugal.

On the North American plate the Newfoundland Basin (Fig. 1.1), comprising the continental margins of the eastern Grand Banks and Flemish Cap and the adjacent seafloor west of anomaly 31/32 (Heirtzler et al., 1968; Pitman and Talwani, 1972; Srivastava, 1978) was very poorly known until recently. The first seismic reflection and refraction data in the southern Newfoundland Basin and across the eastern Grand Banks continental margin were obtained in 1973 (H. R. Jackson et al., 1975), and systematic multiparameter geophysical surveys and seamount studies were

undertaken between 1974 and 1976. The magnetic data collected during the latter surveys have been compiled and interpreted by B. R. Hall (1977) and C. E. Keen et al. (1977). Initial studies of the Newfoundland Seamounts were presented by Sullivan and Keen (1977).

One objective of the present study is to complete the task of assembling the geological and geophysical data base for the Newfoundland Basin and to integrate this with currently available data from the surrounding continental and oceanic areas. Specific scientific objectives of this effort are: delineation of present structure and stratigraphy; determination of the seaward extent of continental crust and continental structural elements; determination of the age and nature of the Newfoundland Seamounts.

The second broad objective of this study is to apply this new knowledge to the problem of the pre-drift Iberia-North America fit and to establish the early (pre-73 Ma) history of rifting and seafloor spreading between Iberia and the Grand Banks. This involves integration of the data from the North American plate compiled in this study with the currently-available data from the Iberian plate (Groupe Galice, 1977; Montadert, Roberts et al., 1977; Ryan, Sibuet et al., 1976; Williams, 1975; Montadert et al., 1974). Again, a number of specific points of interest are included within this general topic: the orientation and identification of magnetic anomalies older than anomaly 31/32 (73 Ma) in the Newfoundland Basin; the extent of the J-anomaly (identified by B. R. Hall, 1977) within the Newfoundland Basin; the age for the initiation of active seafloor spreading between North America and Iberia;

the relationship between spreading in the Newfoundland Basin and spreading in the Bay of Biscay; the origin of the Southeast Newfoundland Ridge and the Spur Ridge.

Organization of the thesis

A review of current knowledge of the continental shelves surrounding the Newfoundland Basin and the structures that form the southern boundary of this area, the Southeast Newfoundland Ridge and Spur Ridge (Fig. 2.1), is given in Chapter 2. The data assembled during this study are presented in Chapters 3-6, which also include short discussions of certain specific geological or geophysical topics. Data bearing on the nature and age of Newfoundland Seamounts are discussed in Chapter 7, and a model is presented which attempts to define the significance of the seamount volcanic activity in the evolution of the Newfoundland Basin as a whole. Chapter 8 synthesizes the data and interpretations presented in the thesis and combines these with recent data from the Bay of Biscay and western Portugal to define the initial positions of the continents and to develop a model for Iberia-Europe-North America relative motions prior to anomaly 31/32. A summary statement and suggestions for future research are given in Chapter 9.

CHAPTER 2: GEOLOGICAL SETTING

Many studies of continental break-up and passive margin formation have confirmed the idea, initially put forth by LePichon and Fox (1971) and LePichon and Hayes (1971), that the structural fabric of the splitting continental block exerts a significant influence upon the pattern of rifting and the early phases of the seafloor spreading history. Pre-rift structures are believed to have been particularly significant in the opening of the Atlantic north of the Southeast Newfoundland Ridge (LePichon et al., 1977; Arthaud and Matte, 1977; Haworth, in prep.). In the Newfoundland Basin, one would expect to find evidence that the early history was in part controlled by structures on the Grand Banks and Flemish Cap; effects of the complex interactions of the North American, Iberian and African plates should also be evident along the southern boundary of the area.

Some familiarity with the geology and geophysics of these continental areas and of the structures formed along the seaward extension of the Newfoundland Fracture Zone (Auzende et al., 1970; M. J. Keen and Keen, 1971) is essential background for the other chapters in this thesis.

2.1 Grand Banks

The Newfoundland Basin lies seaward of the northern Appalachian structural province of Canada (Figure 2.1; H. Williams et al., 1974). The Paleozoic Appalachian mountain system runs sub-parallel to the Atlantic coast of North America from the southeastern United States to

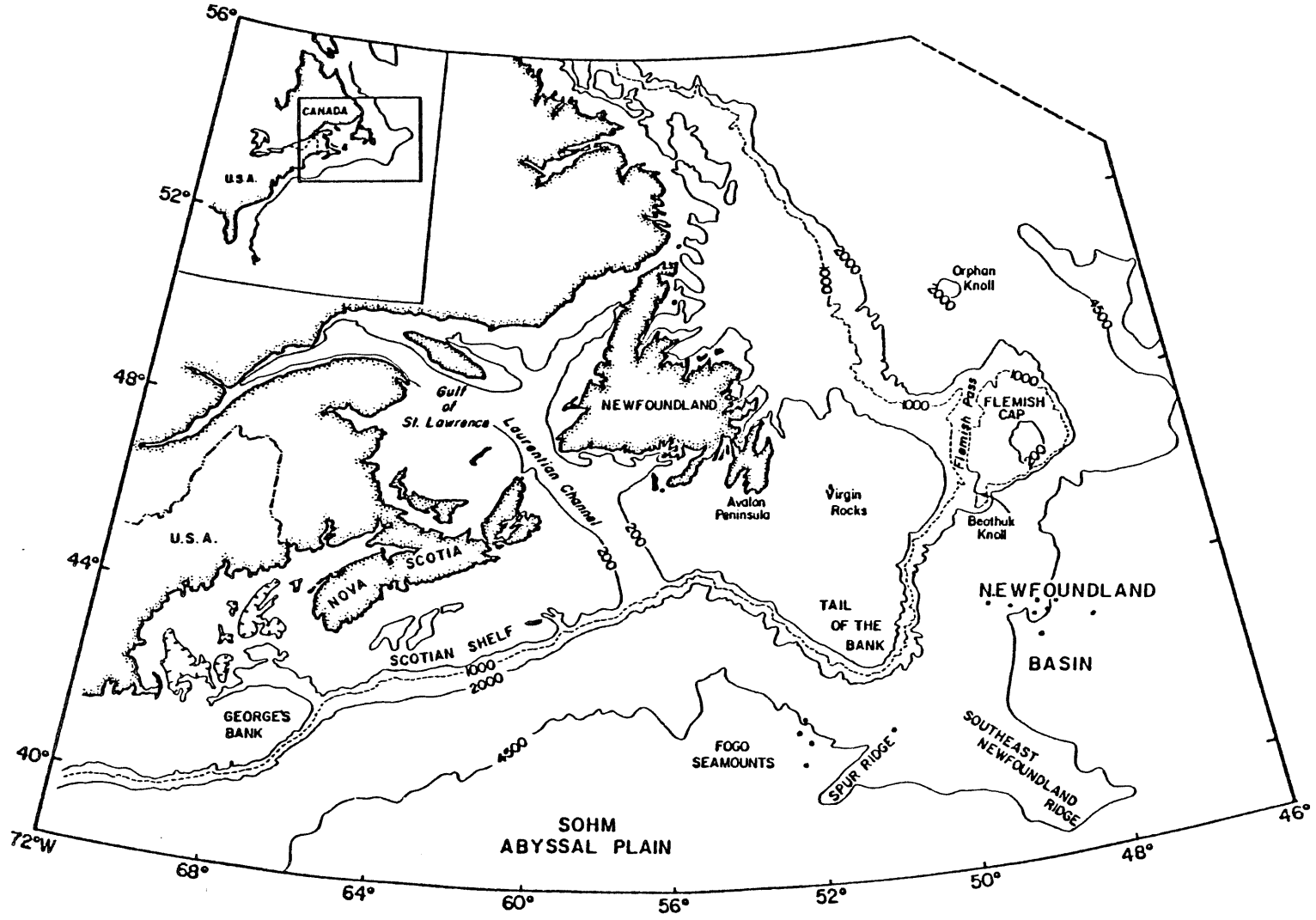

Figure 2.1
Location of the Newfoundland Basin in relation to Atlantic Canada

Newfoundland, a distance of over 3,500 km. On the island of Newfoundland the Appalachians consist of a central Paleozoic mobile belt bounded both to the Northwest and the southeast by zones of Precambrian and Lower Paleozoic sedimentary and volcanic rocks (H. Williams, 1964). The southeastern belt is known as the Avalon Platform or Avalon Zone (H. Williams et al., 1974), and it is the rocks of this zone which are believed to constitute continental basement on the Grand Banks and Flemish Cap (Haworth and Lefort, in prep.).

2.1.1 Geophysics

Numerous seismic refraction studies have been conducted on the continental shelf surrounding Newfoundland in order to determine crustal structure and to map the seaward extent of the various Appalachian zones (Press and Beckmann, 1954; G. N. Ewing et al., 1966; Dainty et al., 1966; C. E. Keen and Loncarevic, 1966; Sheridan and Drake, 1968; Fenwick et al., 1968; H. R. Jackson et al., 1975). Unfortunately, the coverage on the Grand Banks southeast of the Avalon Peninsula is insufficient to accurately reveal the crustal structure on this portion of the shelf. Basement velocities measured on the central and southeastern Banks are 6.0-6.6 km/sec. Sheridan and Drake (1968) correlate this velocity range with the igneous and metamorphic rocks of the Avalon Zone.

Seismic refraction coverage is also sparse on the eastern continental margin of the Grand Banks. H. R. Jackson et al. (1975) report on one airgun-sonobuoy line in this area. They find approximately 4 km of sediment overlying basement (5.8 km/s) on the continental slope here (sonobuoy 33, Table 4.1). More detailed seismic coverage, including two

crustal refraction profiles, is available on the southwestern Grand Banks margin. H. R. Jackson et al. (1975) identify oceanic layer 2 within 100 km of the shelf break on reflection profiles southwest of the Tail of the Bank and present refraction results which indicate that the transition from oceanic to continental crust occurs in a relatively narrow region (about 40 km) on this margin.

The extensive body of potential field data collected in the Grand Banks area during the past 15 years has recently been compiled and interpreted in terms of the plate tectonic evolution of this region (Haworth and MacIntyre, 1975; Haworth, 1975; Haworth and Lefort, in prep). The region between the Avalon Peninsula of Newfoundland and Flemish Cap is characterized by a group of sinuous potential field anomalies (Fig. 2.2, 2.3) which Haworth and Lefort (in prep.) show are quite similar in amplitude and character to the anomalies observed over the terrestrial Avalon Platform; the continuation of the latter zone to the east beneath the Grand Banks is thus inferred. The "Collector Anomaly", a band of positive gravity and magnetic anomalies extending from Nova Scotia to the southwestern Grand Banks, is believed to mark the southern boundary of the Avalon Zone on the Banks (Haworth and Lefort, in prep.).

The northern boundary of the Avalon Platform east of Newfoundland is geophysically less distinct. Basement structures, inferred from magnetic anomaly trends, cross the high-amplitude shelf-edge gravity anomaly northeast of Newfoundland, suggesting that the continental structures producing the magnetic anomalies continue to the northeast into the Orphan Knoll Basin (Haworth, in prep.; Haworth and Lefort,

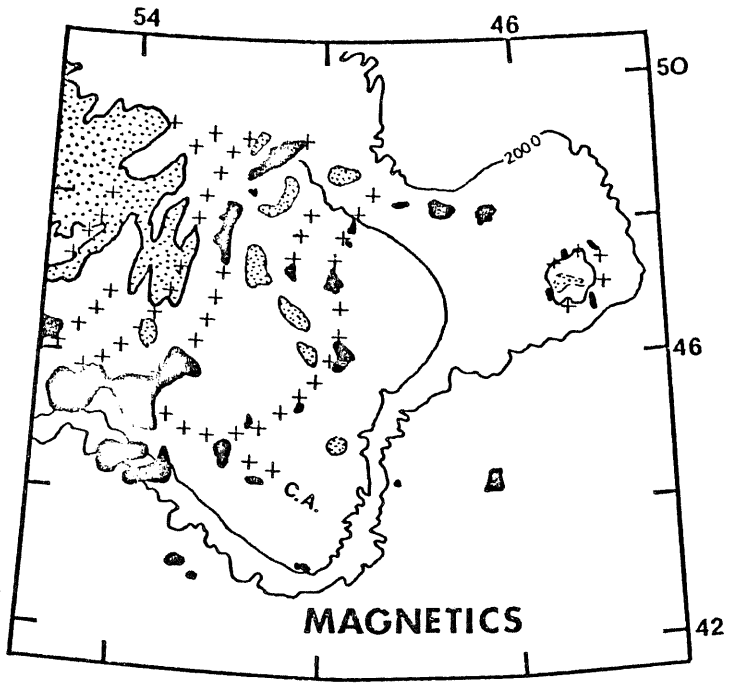

Figure 2.2

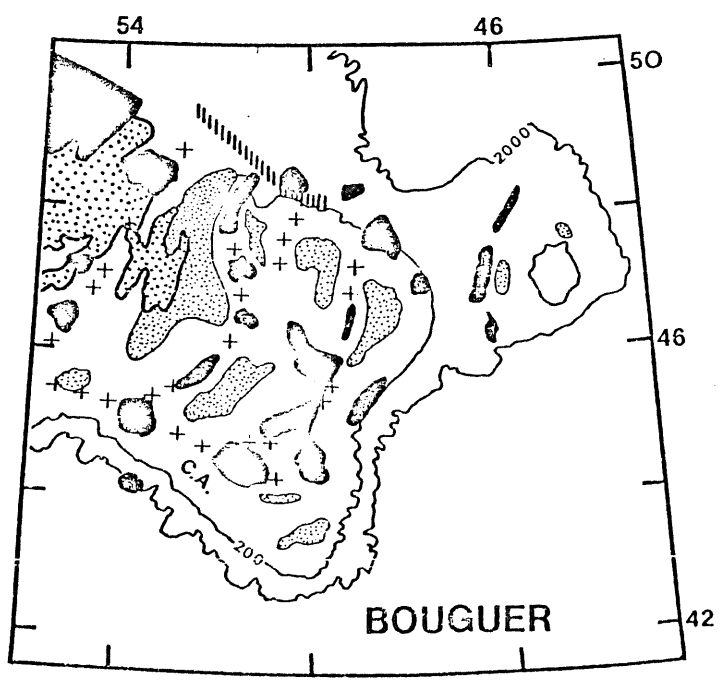

Figure 2.3

Magnetic and Bouguer anomaly trends on the Grand Banks (after Haworth, 1975)
Black=positive anomalies; fine stipple=negative anomalies; + = linear positive trends; hachured line = gravity gradient.

in prep.). The transition from continental to oceanic crust must therefore lie seaward of a line joining Orphan Knoll and Flemish Cap (A. C. Grant, 1975; Haworth and Lefort, in prep.).

2.1.2 Structural Framework

The development of structures related to the present phase of Atlantic seafloor spreading appears to have begun in Early or Middle Triassic time on both the Grand Banks and the Scotian margin. This development is discussed in detail in Jansa and Wade (1975), from which the following summary has been taken.

The Avalon Uplift trends southeast from the Avalon Peninsula of Newfoundland to the Tail of the Bank (Fig. 2.4), separating the Scotian margin and southwestern Grand Banks area from the Newfoundland Basin and northeastern Banks areas. The Uplift is subdivided into six tectonic elements: The South Whale, Whale, Horseshoe, Jeanne d'Arc and Carson Sub-basins and the South Bank High.

The sub-basins are structurally complex fault-bounded troughs (Fig. 2.5) which contain 4-12 km of sediment. Exploratory wells on the Grand Banks and Scotian shelf indicate that the South Whale Basin is more closely related structurally and stratigraphically to the Scotian Basin than to the other Grand Banks sub-basins (Jansa and Wade, 1975; Gradstein et al., 1975).

The South Bank High is underlain by a large basement block, which Jansa and Wade (1975) interpret as having been a positive element until late Early Cretaceous time. The Bittern exploratory well on the flank

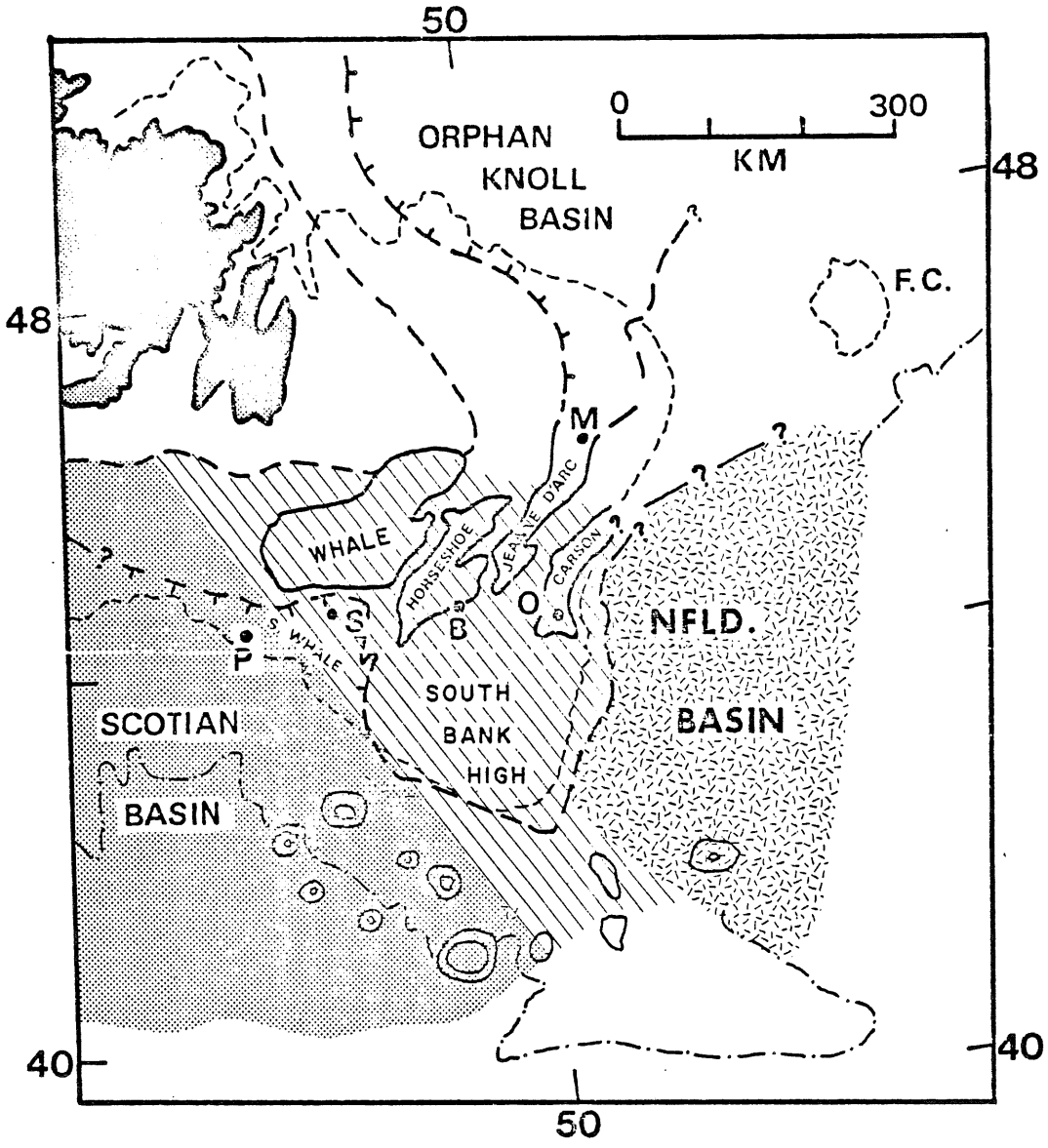

Figure 2.4

Structural elements on the Grand Banks (after Jansa and Wade, 1975) with locations of exploratory wells Puffin (P); Skelly Mallard (S); Bittern (B); Osprey (O); and Murre (M). 200 m and 4,000 m bathymetric contours shown.

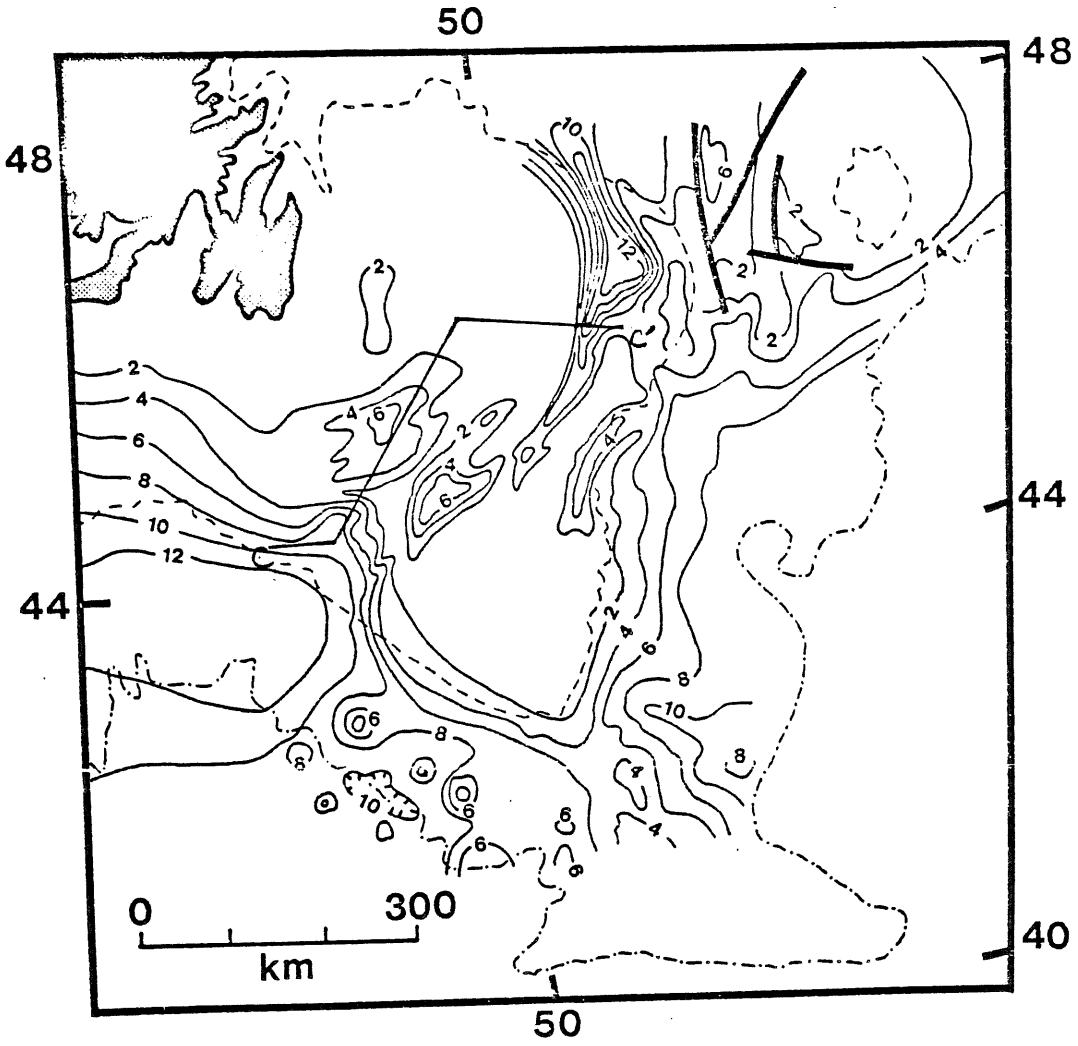

Figure 2.5a

Basement structure on the Grand Banks: contours on economic basement (kilometers below sealevel). After Jansa and Wade (1975).

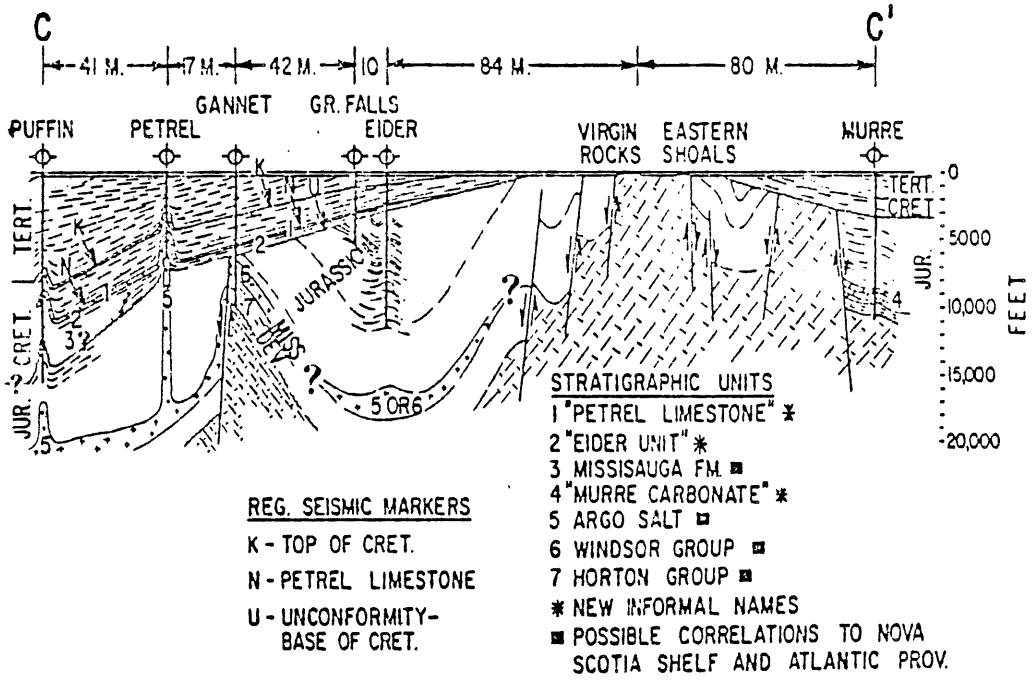

Figure 2.5b

Basement structures on the Grand Banks (after Jansa and Wade, 1975): Diagrammatic cross-section from Puffin to Murre well (see Fig. 2.4 for location).

of the High ("B", Fig. 2.4) bottomed in Early Devonian granite (Amoco, 1969). However, study of seafloor outcrops (Lilly, 1966) and of the potential fields over this region (Haworth, 1975; Haworth and Lefort, in prep) suggest that basement may consist of a variety of Precambrian to Devonian igneous and metamorphic rocks.

The Orphan Knoll Basin lies between the northeastern Newfoundland shelf edge and the Orphan Knoll and Flemish Cap bathymetric highs (Fig. 2.4). Sediment thicknesses here may locally exceed 12 km. On the basis of combined structural and geophysical studies it is believed that the floor of this basin consists of foundered continental crust (A. C. Grant, 1975; Haworth and MacIntyre, 1975). The Jeanne d'Arc Sub-basin forms a southerly branch of the Orphan Knoll Basin that extends to the South Bank High.

The area of the present study is the final major basin shown in Figure 2.4. Jansa and Wade (1975) give little information about this area, noting only that approximately 6 km of sediment lie beneath the lower slope on the eastern Grand Banks margin. They interpret the sediment fill as mainly of post-Early Cretaceous age.

2.1.3 Stratigraphy

Comprehensive reviews of the stratigraphic succession on the Scotian Shelf and the Grand Banks, as revealed by exploratory well-drilling operations, are given in Jansa and Wade (1975) and Gradstein et al. (1975). The following brief synopsis presents the points that are relevant to the present study:

1. The few wells that have bottomed in basement indicate that Devonian intrusive rocks and pre-Devonian metamorphic rocks comprise the basement complex.

2. Paleozoic (Ordovician-Silurian and Carboniferous) sediments have been drilled at several localities on the Grand Banks, but the oldest sediments in most areas are Triassic-Early Jurassic continental and marginal marine sediments deposited in linear, fault-bounded troughs; these strata sometimes attain thicknesses of 3,000 m.

3. Deposition of progressively shallower water facies continued without interruption from Triassic into earliest Jurassic time. Upward-coarsening sequences of Early-Middle Jurassic age signal the beginning of uplift in the terranes from which these deposits were derived.

4. A major change in the structural framework of the region during latest Jurassic and Early Cretaceous is indicated by the deposition of coarse clastic sediments across the Jurassic-Cretaceous boundary and the development of a major unconformity (see Point 5, below). This phase of tectonism broke the Jurassic Georges Bank-Orphan Knoll basin into four separate basins (Jansa and Wade, 1975). These are the Georges, Scotian, Orphan Knoll and Newfoundland Basins shown in Fig. 2.4.

5. Over much of the Grand Banks the Early Cretaceous is a period of erosion or non-deposition, marked by the Avalon Unconformity. This hiatus is most extensive on the South Bank High, where Devonian basement rocks are directly overlain by Cretaceous or Tertiary sediments. The maximum spatial extent of the unconformity occurred near the end of the Early Cretaceous, when erosion or non-deposition spread as far west as the Puffin well (Fig. 2.4). In contrast, the Early Cretaceous section

in the Scotian and Orphan Knoll Basins consists of thick continental margin deposits (alluvial plain and deltaic sequences; Gradstein et al., 1975).

6. The Early Cretaceous tectonism was accompanied by the eruption of basaltic rocks and trachytes at the Skelly Mallard well on the south-western Grand Banks ("S", Fig. 2.4; Gradstein et al., 1977).

7. Establishment of open marine conditions over much of the area in Late Cretaceous time resulted in reduced sedimentation rates and deposition of pelagic facies.

8. Several widespread carbonate and chalk horizons occur in the Cretaceous section. Two most noteworthy of these units are the Petrel Limestone Member of the Dawson Canyon Formation and the Wyandot Chalk Formation. The former is of Turonian age in the Scotian Basin and Turonian-Coniacian age in the Grand Banks sections; the latter is absent in wells on the Avalon Uplift, but may be present in the East Newfoundland Basin (possible correlatives have been recognized in seismic profiles) and on Orphan Knoll (DSDP Site 111; Laughton et al., 1972).

9. The Tertiary section on the Avalon Uplift and northeastern Grand Banks is thinner and of shallower-water facies than is that in the Scotian Basin and the South Whale Basin.

2.2 Flemish Cap

Flemish Cap (Fig. 2.1) is a submerged continental structure which became partially detached from North America during an early phase of seafloor spreading (A. C. Grant, 1971). The geology and geophysics of

this area are described by A. C. Grant (1971, 1972), Monahan and McNab (1975) and Haworth and Lefort (in prep), whose findings are summarized below.

Seismic and magnetic results indicate that Flemish Cap consists of a central area of basement material surrounded by outward-dipping sedimentary strata which attain thicknesses of 4-6 km. Core and dredge samples indicate that basement lithologies and ages are similar to those of bedrock in the Avalon Zone of Newfoundland; the potential field analysis of Haworth (1975) and Haworth and Lefort (in prep.) corroborate this. The overlying sedimentary cover includes Orbitulina limestones of Early-Middle Cretaceous age (Sen Gupta and Grant, 1972).

Flemish Cap is separated physiographically from the northeastern Grand Banks by Flemish Pass (Fig. 2.1). The Pass is 265 km in length and 20-45 km wide, the narrowest zone occurring near the southern end. Seismic and potential field studies show that both margins of the Pass are underlain by basement ridges. The eastern ridge, which may continue south beyond the end of the Pass to form Beothuk Knoll (Fig. 2.1) is coincident with a linear band of high-amplitude magnetic and gravity anomalies. The western ridge has a similar high gravity signature, but is not marked by any significant magnetic anomaly. The Pass itself contains substantial thicknesses of sediment and is characterized by relatively low-amplitude gravity and magnetic anomalies.

2.3 Southeast Newfoundland Ridge and Spur Ridge

The Southeast Newfoundland Ridge (SENR; Fig. 2.1) extends approximately 900 km to the southeast of the Tail of the Bank, roughly on

strike (130°) with the southwestern transform-fault margin on the Grand Banks (M.J. Keen and Keen, 1971). The Sohm Abyssal Plain (5300 m-5500 m) lies to the southwest of the SENR and the Newfoundland Basin (4,000-4,800 m) lies to the northeast. At 46°W the SENR is intersected by the smaller Spur Ridge (Renwick, 1973; "J-anomaly Ridge" of Tucholke, Vogt et al., 1975).

The entire Grand Banks-SENR lineament is commonly referred to as the 'Newfoundland Fracture Zone' (Auzende et al., 1970; LePichon and Hayes, 1971; LePichon et al., 1977). Although the seafloor topographic expression of the ridge terminates between 43°W and 45°W, Watson and Johnson (1970) and Laughton and Whitmarsh (1974) believe that the fracture zone continues to the east, being correlative with the Pico Fracture Zone on the present-day Mid-Atlantic Ridge. C. E. Keen et al. (1977) point out that significant vertical movements have also occurred across the SENR. The evidence for this is the 1 km difference in the present depths below sea level of coeval shallow-water limestones on the Spur Ridge (Tucholke, Vogt et al., 1975) and on the easternmost of the Newfoundland Seamounts (Chapter 7; Appendix II). Both limestones are of Early-Middle Cretaceous age, so the differential subsidence must be post-Middle Cretaceous.

Watson and Johnson (1970), Auzende et al. (1970) Renwick (1973) and H. R. Jackson et al. (1975) present seismic and magnetic data collected over the SENR and Spur Ridge and interpret these data as indicating that both ridges are underlain by faulted oceanic crust. This conclusion is supported by the work of B. R. Hall (1977), which shows that the oceanic

J-magnetic anomaly is observed on the northern flank of the SENR near the Tail of the Bank and by the observation that the J-anomaly, a prominent seafloor spreading isochron which is consistently associated with distinctive basement structures in the North Atlantic (Tucholke, Vogt et al., 1975; Ballard et al., 1976; B. R. Hall, 1977), is coincident with the Spur Ridge.

In contrast, A. C. Grant (1977) and Gradstein et al. (1977) propose that continental crust underlies much of all of the Spur Ridge and SENR. This alternative interpretation is based largely on examination of multi-channel seismic profiles across the Tail of the Bank and on the north-western limits of the ridges; Gradstein et al. (1977) also note similar subsidence histories for the Spur Ridge (based on DSDP Site 384, Vogt et al., 1975) and the southwestern Grand Banks (based on exploratory wells; Gradstein et al., 1975) as further support for their hypothesis. Seismic and magnetic data relevant to this question are presented in Chapters 4 and 5 of this study, and the problem of the boundary between oceanic and continental crust is discussed in greater detail in Chapter 8.

CHAPTER 3: PHYSIOGRAPHY

Strictly speaking, the entire Newfoundland Basin lies within the continental margin physiographic province (Johnson et al., 1971; Emery and Uchupi, 1972). However, subsequent chapters will show that significant structural and geophysical boundaries exist at the upper rise-lower rise transition. It is therefore more convenient for the purposes of this paper to consider the "continental margin" as extending from depths of 200 m or less to 4,000 m and to consider the lower continental rise (deeper than 4,000 m) separately.

This section is based on the bathymetric map prepared for the Wood's Hole Oceanographic Atlas (Uchupi, 1971) (Fig. 3.1). Data collected on Bedford Institute cruises to the Newfoundland Basin since 1971 permit refinement of this map in the southern Newfoundland Basin and SENR areas (section 3.2) and in the vicinity of the Newfoundland Seamounts (Section 3.3).

3.1 Continental Margins

The continental margin province (depths of less than 200 m to 4,000 m) varies in total width from about 60 km at the southeastern corner of Flemish Cap to 150 km at the southeastern Grand Banks. On the basis of the bathymetry shown in Figure 3.1 the margin can be divided along its length into four segments (Fig. 3.3), herein termed the Tail of the Bank segment, the Eastern Banks segment, the Flemish Pass segment and the Flemish Cap segment. Subsequent sections of this

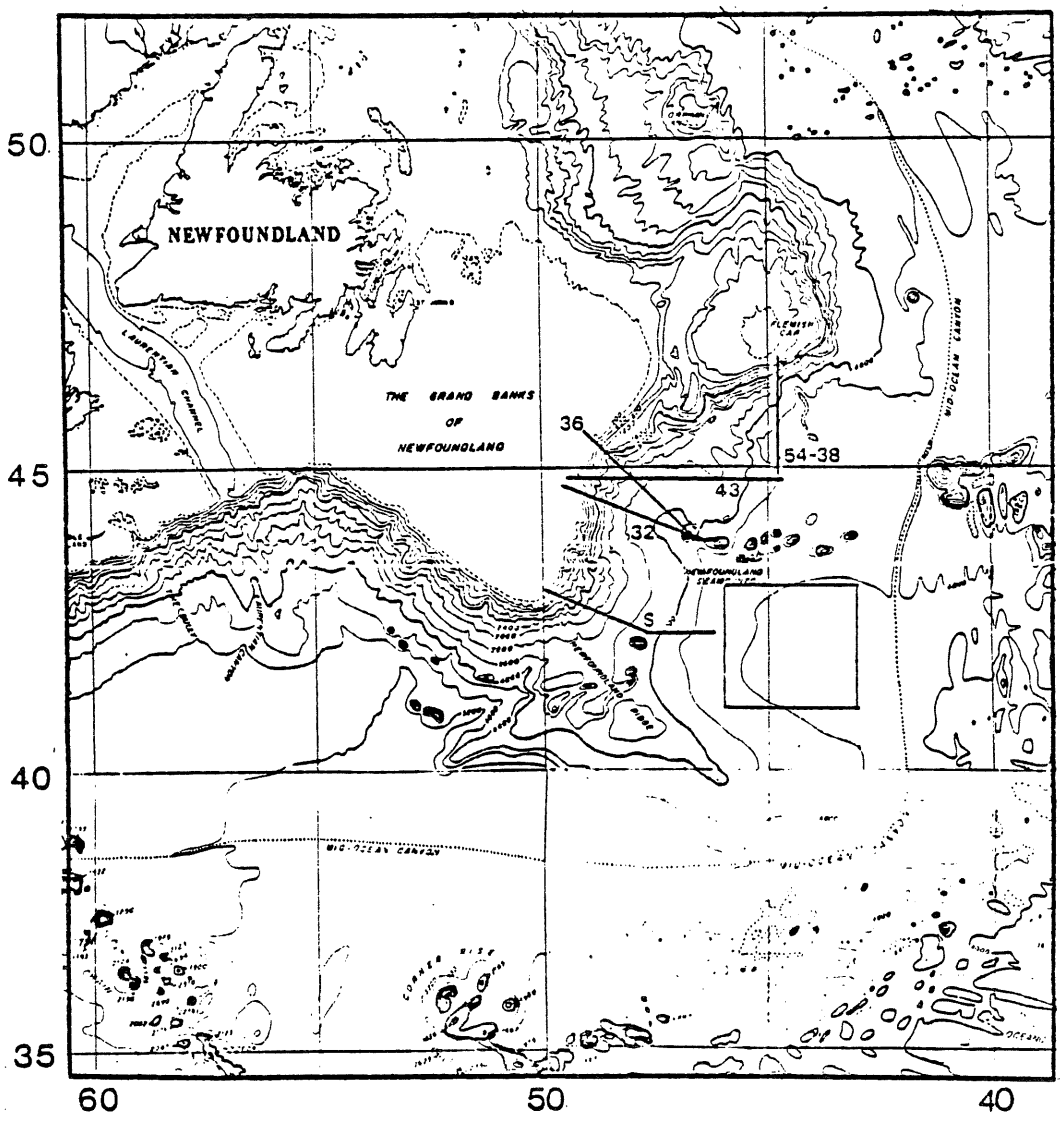

Figure 3.1

Bathymetry of the Newfoundland Basin and adjacent areas as given in Wood's Hole Oceanographic Atlas (Uchupi, 1971). Locations of profiles shown in Figure 3.4 and survey area in Figure 3.5 also shown.

Figure 3.2: Physiographic provinces of the Newfoundland Basin.

Figure 3.3: Segmentation of the continental margin.

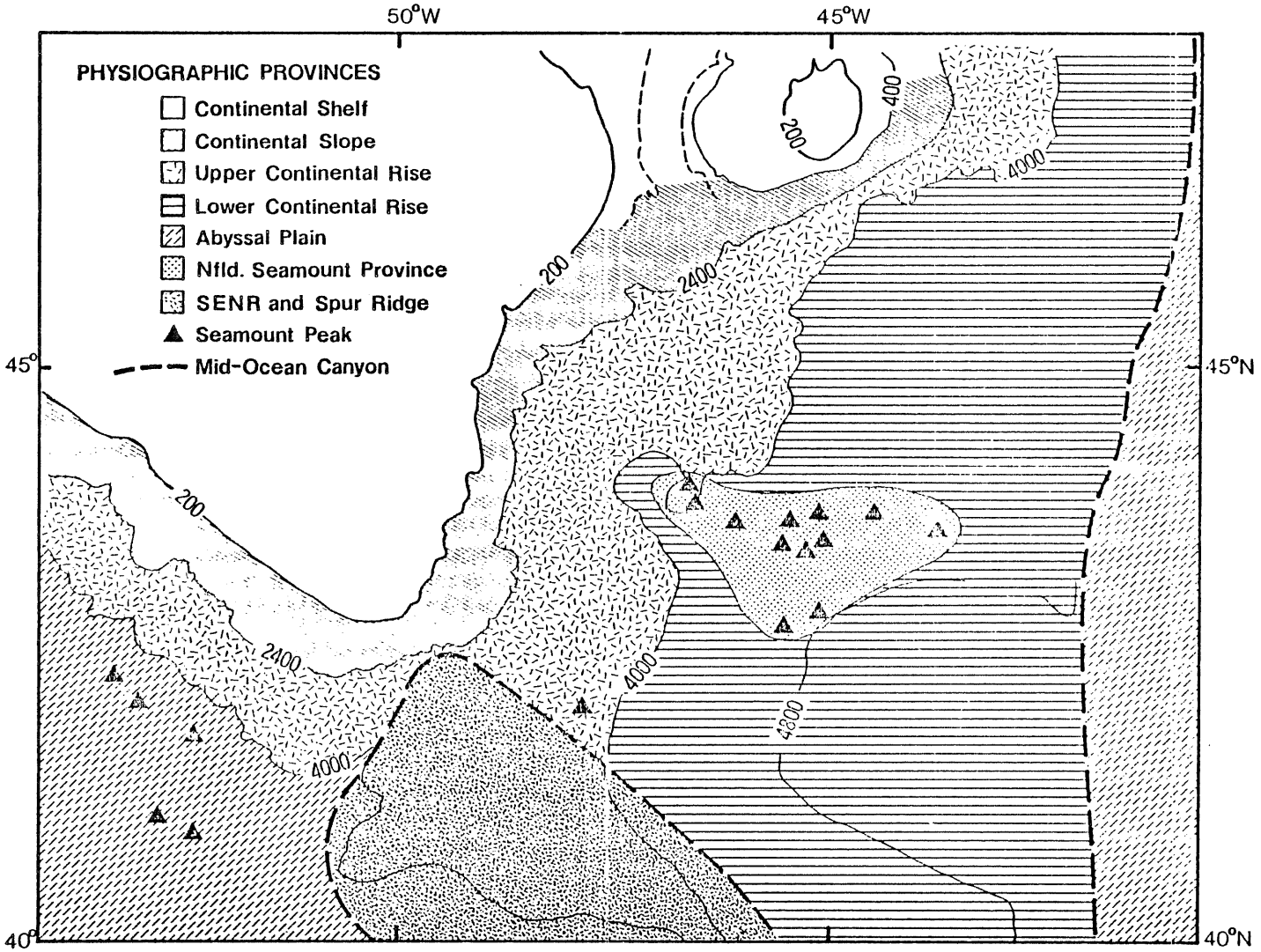
50°W
45°W
PHYSIOGRAPHIC PROVINCES
Continental Shelf
Continental Slope
Upper Continental Rise
Lower Continental Rise
Abyssal Plain
Nfld. Seamount Province
SENR and Spur Ridge
Seamount Peak
Mid-Ocean Canyon
45°
45°N
40°
40°N
200
400
4000
2400
4800

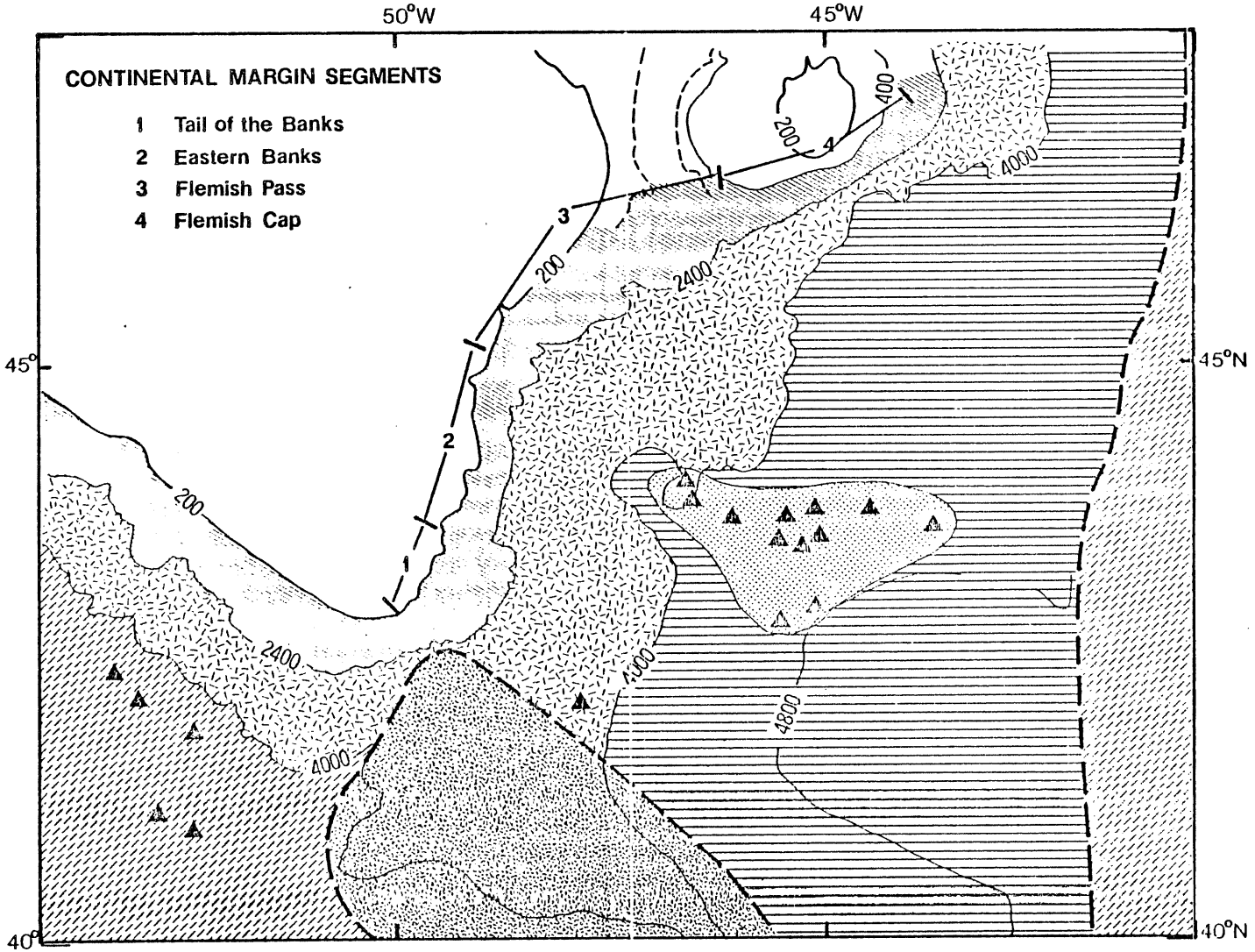
50°W
45°W
CONTINENTAL MARGIN SEGMENTS
1 Tail of the Banks
2 Eastern Banks
3 Flemish Pass
4 Flemish Cap
45°
45°N
40°
40°N
200
400
2400
4000
4800

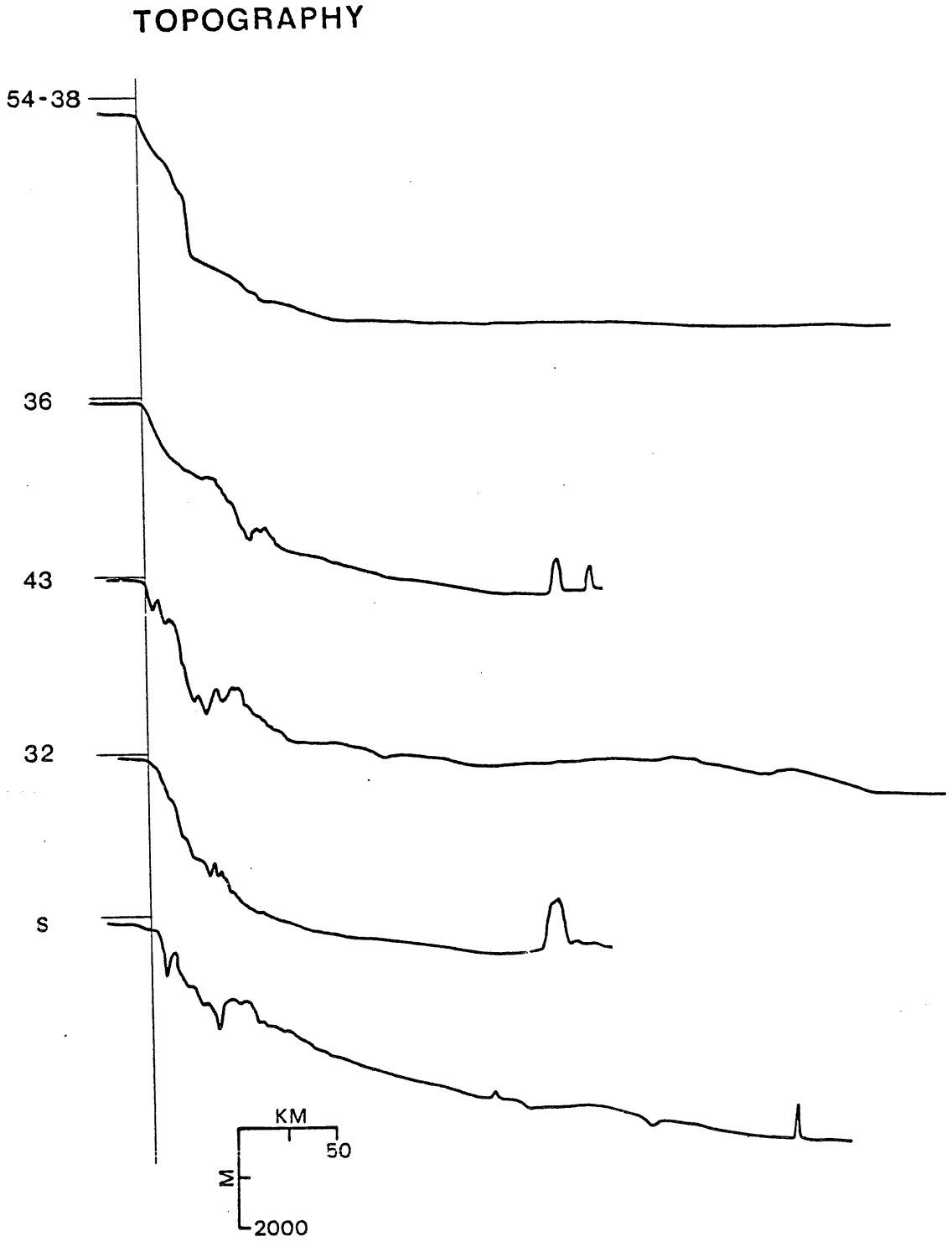

Figure 3.4

Continental margin bathymetric profiles.
See Fig. 3.1 for location.

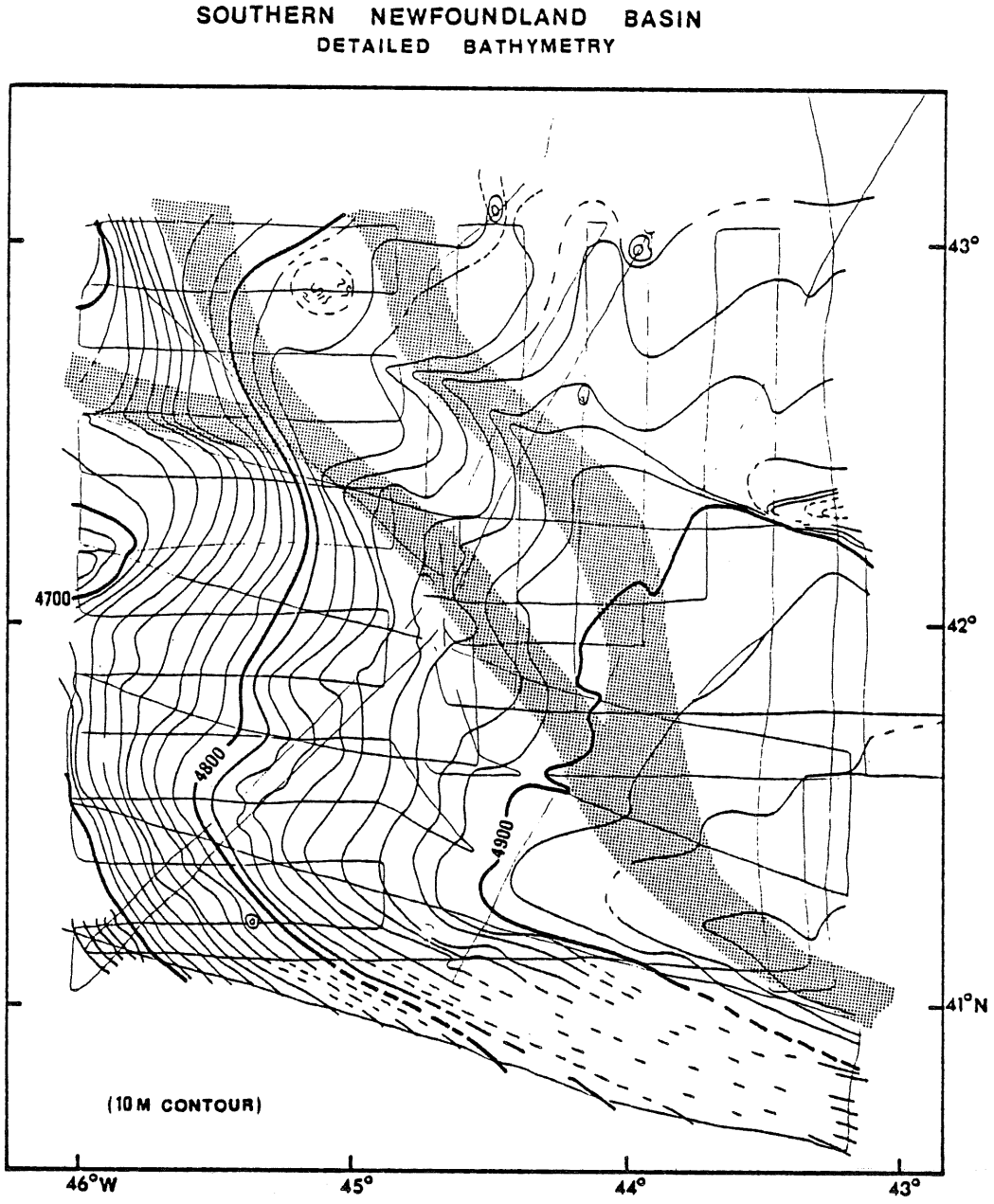

Figure 3.5

Detailed bathymetry, Southern Newfoundland Basin
See Fig. 3.1 for location of area.

report will show that this segmentation is also reflected in geophysical characteristics. Bathymetric profiles across the various margin segments are shown in Figure 3.4. No continuous profiles are available from the eastern portion of the Flemish Pass region.

The Eastern Banks and Flemish Cap margin segments are relatively straight, with much narrower and steeper continental slopes (35-40 km wide, 3.5-4.0° slopes) and fewer canyons than the other two sections. The continental rise widens westward along the Flemish Cap segment.

In contrast, the Tail of the Bank and Flemish Pass segments are characterized by wider slope and upper rise regions, with more numerous large canyons and rather less distinct shelf breaks. This may reflect the greater structural complexity of these two margin segments, which lie at the intersection of major structural features: The southwest and southeast Grand Banks continental slopes and the SENR intersect at the Tail of the Bank; Flemish Pass and the northeast Grand Banks and Flemish Cap slopes intersect in the Flemish Pass section.

3.2 Lower Continental Rise

The lower continental rise comprises those regions lying at depths greater than 4,000 m (Fig. 3.2). The Newfoundland Seamounts divide this physiographic province into a northern and southern section. Detailed bathymetry to supplement the Wood's Hole chart is available only for the southern section.

Depths in the northern section of the lower rise range from 4,000 m to 4,800 m, with slopes of 0.8° between 4,000 m and 4,400 m and 0.1°

between 4,400 m and 4,800 m. The strike of the 4,000 m isobath, which roughly defines the landward boundary of the lower rise, changes at 45°30'N from 010° (between the SENR and the Newfoundland Seamounts) to 030° (along Flemish Cap).

The southern section of the lower rise is a roughly square area lying between the seamounts and the SENR. Depths as great as 4,930 m are recorded in the southeastern portion of this area. Detailed bathymetry in the southern area collected during Hudson cruise HU75-009 reveals two linear trends on the seafloor (Fig. 3.5). The first of these, at the southern limit of the survey area, is the northern flank of the southeast Newfoundland Ridge. The second linear trend (approximately 42°15'N, 43°15'W) is the seafloor expression of a prominent basement scarp (Seismic line 39, Fig. 4.3c). Also indicated in the figure are locations of shallow seafloor channels mapped by Dr. D. J. W. Piper during the survey. The floors of the channels are stronger acoustic reflectors than are the adjacent levees, suggesting that coarser sediment is deposited in the channel axis and finer material in the levee. The orientation of the channels suggests that the currents producing these features move primarily downslope.

3.3 The Newfoundland Seamounts

Most published bathymetric maps of the Newfoundland Basin (for example, Figure 3.1) show the Newfoundland Seamounts to be a roughly linear group of about ten peaks striking east-west between 43° and 44°N. However, a comparison of maps from several sources reveals discrepancies

in the positions and morphology of many of the seamounts that stem from the limitations of the data previously available in this area.

A new bathymetric data base for the seamount region has been compiled during this study. This comprises data from five cruises undertaken between 1973 and 1976 by ships from Bedford Institute (Table 3.1). Navigation on all cruises was by Loran-C in the range-range mode and navigational satellite, giving a positioning accuracy of ± 300 m at the 95% confidence level (S. Grant, 1973). Five seamounts have been surveyed in some detail during these cruises (Fig. 3.7, 3.8) and the average spacing of ship's tracks in the seamount area has been reduced considerably (Figure 3.6). Some small seamounts may have been overlooked in these studies, but the positions and morphology of the seamounts shown in Figure 3.6 are accurate. Seamounts that do not at present have official names are given numerical designations in this report.

Examination of these new data reveals that the seamounts occupy a roughly triangular area within the Newfoundland Basin (Fig. 3.2) with most of the seamounts lying in an east-west zone extending from 43°15' to 44°15'N. Five seamounts (Scruncheon, Touten, Dipper, Number 4, Number 5) lie along a southeasterly trend which branches off this east-west band at Scruncheon Seamount; seismic reflection data described in the next chapter show that several large basement highs in the southern section of the lower continental rise also lie along this trend (open triangles, Fig. 3.6).

A number of significant physiographic and geophysical parameters for the eleven seamounts shown in Figure 3.6 are presented in Table 3.2. The data show that the seamount summits lie at depths of 2400 m

TABLE 3.1

SEAMOUNT	CRUISE(S)	DAY OR DAY/TIME
Screech	73-011	154
	75-009	157
# 2	73-011	154
	74-021	172
Scruncheon	73-011	152-154
	74-021	169
Touten	73-011	154
	74-021	171
Dipper	74-019	169-170
	74-021	171
# 1	73-011	151-152
	74-021	170
SHREDDER	75-009	159,165
# 3	73-011	154
	74-021	172
	75-009	157
# 4[1]	76-031	283/0800-1000
# 5[1]	75-009	163/1900-2100
# 6[1]	75-009	173/0300-0500

1 denotes single track across this seamount

TABLE 3.2

SEAMOUNT[+]	DIST. TO SHELF BREAK (km)	SEAFLOOR DEPTH(m)	SUMMIT DEPTH(m)	SEDIMENT THICKNESS(km)	TOTAL RELIEF	DIMENSIONS AT SEAFLOOR (km)	APPROX. VOL (km^3)	RATIO DIAMETERS MAJOR: MINOR AXIS	DIRECTION OF ELONGATION	NO. OF PEAKS	F.A. GRAV. mgal	MAG SIGN
SCREECH[D]	272	4080	3361	2.3 (N,W) 1.5 (S,E)	3.0 2.2	11x16	124	1.45	NNE	1	40	+
# 3	1299	4013	3525	2.0 (S,E)	2.5	10x14	212	1.40	NNE	1	65	+
# 2	342	4000	3112	1.8	2.7	20?	159	nd	nd	nd	30	+
SCRUNCHEON[D]	374	4500(S,E) 4100(N,W)	2400(E) 2860(W)	1.8	3.9 3.0	15x41	708	2.73	EW-ENE	2	40-60	+
TOUTEN	381	4550	3088	1.8	3.1	15x17	208	1.13	NONE	1	15	+
DIPPER[D]	409	4500	2900	1.5*	3.1 2.6	22x35	659	1.59	ENE	2	40	+
# 1	444	4630	2850	1.4	3.2	15x20?	242?	nd	ENE	nd	60	+
SHREDDER[D]	524	4685	2389	1.3	3.1	37x37	1111	1.00	NONE	1	120	+
# 4[1]	433	4800	4200	1.0	1.6	10x15	42?	1.5	NE	nd	15	+
# 5[1]	470	4820	4643	0.8	1.0	nd	nd	nd	nd	nd	12	+
# 6[1]	446	4820	3195	1.3*	2.9	16x12?	149	1.3?	nd	2	50	+

+ : D denotes seamount which has been dredged; 1 denotes seamount crossed by only one track.

* : thickness approximated from nearest seismic profile.

(Scruncheon) to 4643 m (Number 5), while the surrounding seafloor ranges in depth from 4000 m (Number 2, Number 3) to 4820 m (Number 5, Number 6). The relief above the seafloor thus varies from approximately 200 m to 2100 m. This variation is due in part to differences in the thickness of sediment surrounding the seamounts and in part to a real difference in seamount size (columns 5 and 6). The maximum true relief of six of the eleven seamounts tabulated is between 2.7 and 3.2 km.

The shape of the seamounts at the seafloor and their approximate volumes vary considerably throughout the area (columns 7-11, Table 3.2; Fig. 3.6), but it is not clear from the morphological data which, if any, of the apparent trends are significant.

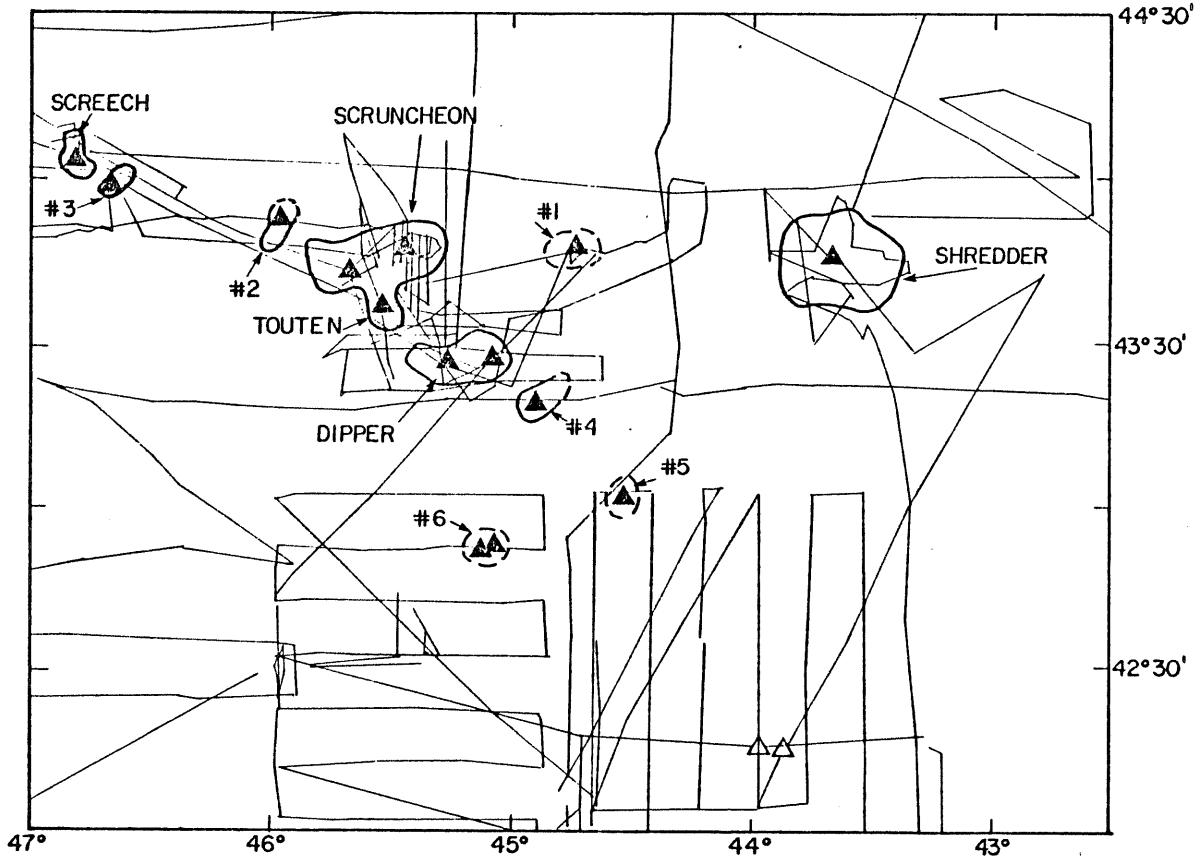

Figure 3.6

Ship's tracks in Newfoundland Seamounts region. Outline of seamounts at seafloor and location of peaks (solid triangles) also shown; open triangles are buried basement highs on seismic reflection line 39.

Figure 3.7: Contoured bathymetry, Newfoundland Seamounts

a. Scruncheon, Touten and Dipper Seamounts.
b. Shredder Seamount.
c. Number 1 Seamount
d. Screech Seamount

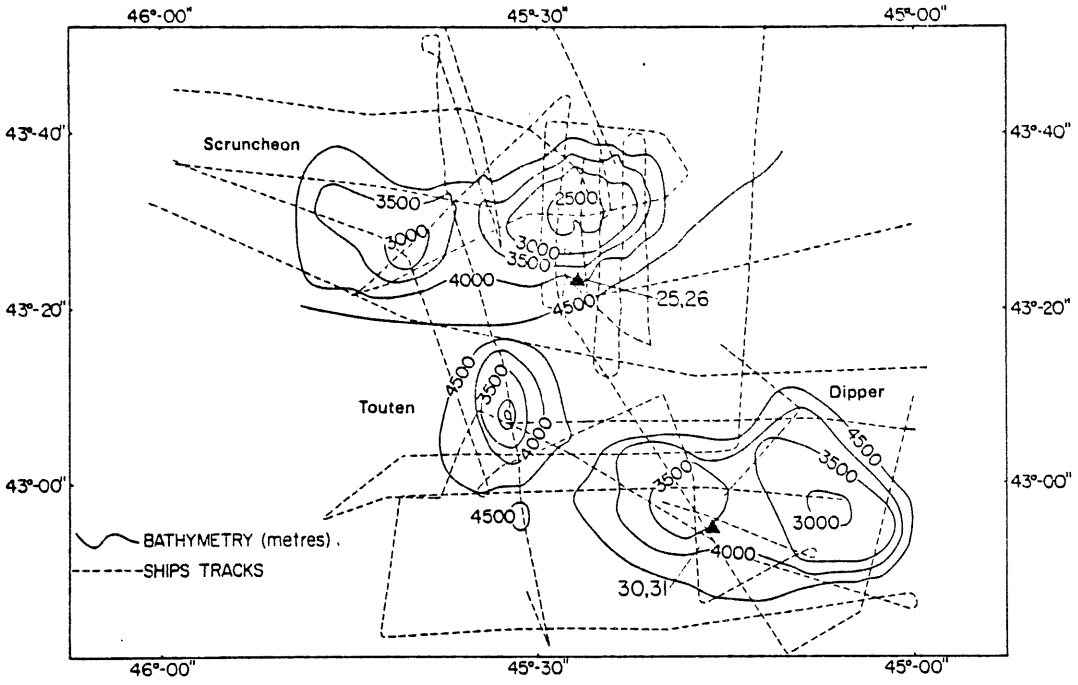

Figure 3.7a

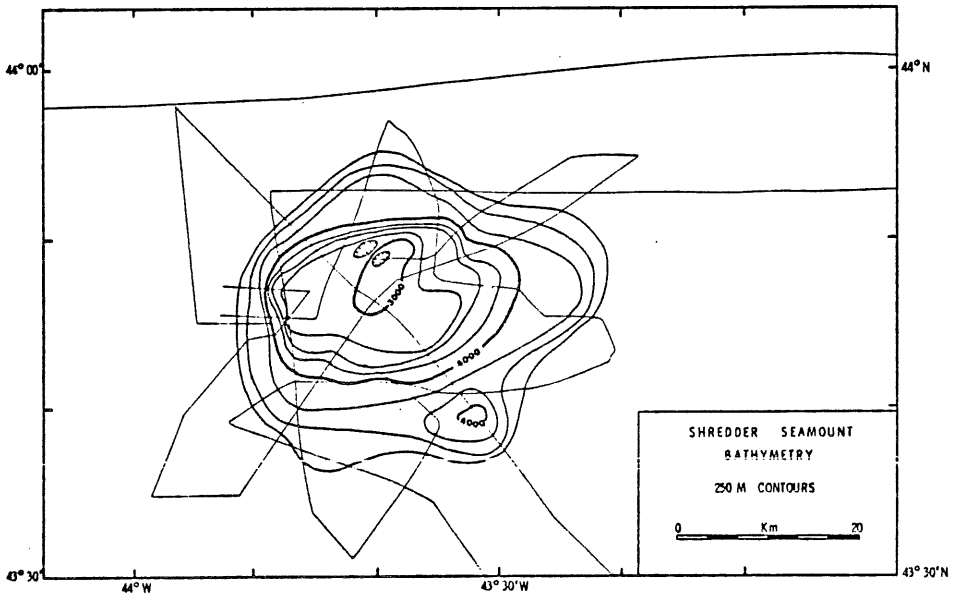

Figure 3.7b

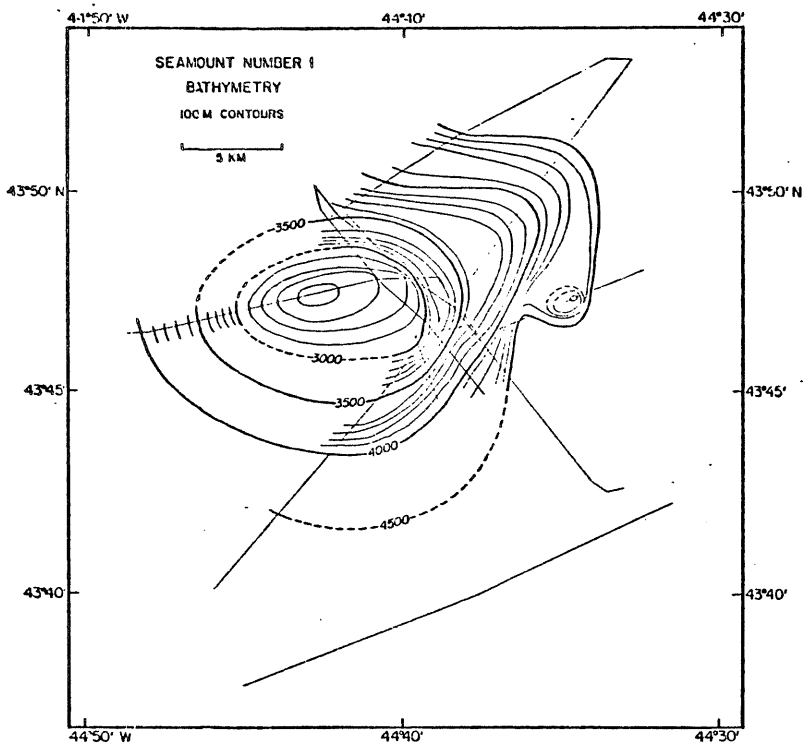

Figure 3.7c

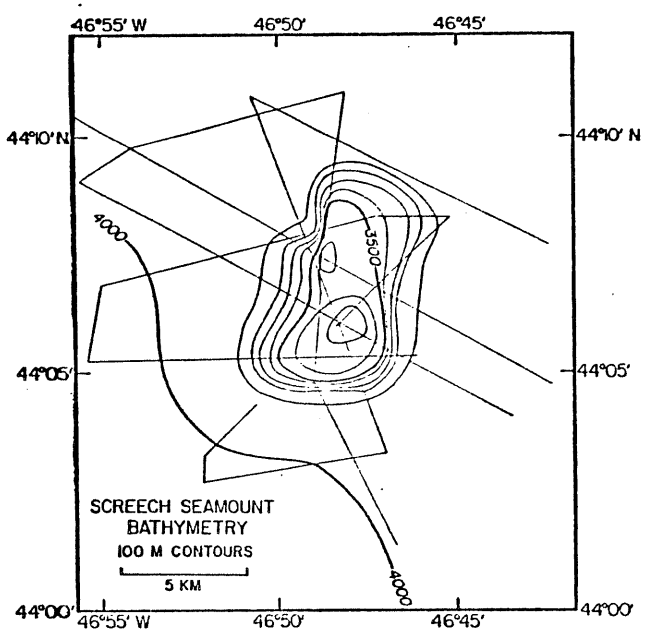

Figure 3.7d

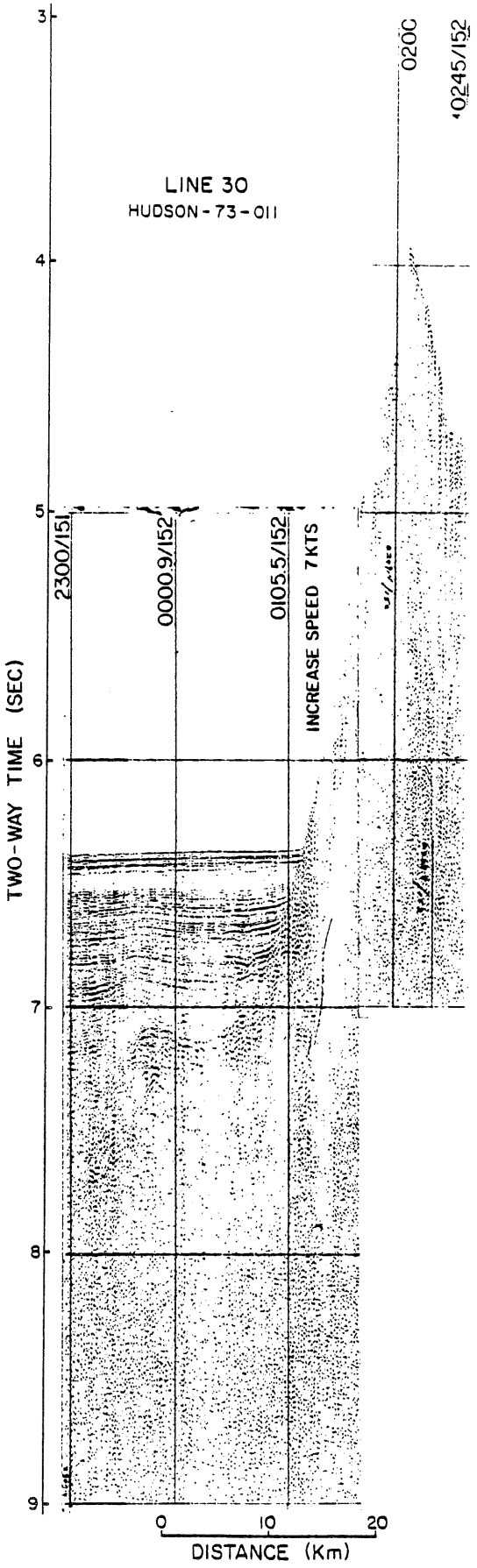

Figure 3.8a
Seamount Number 1

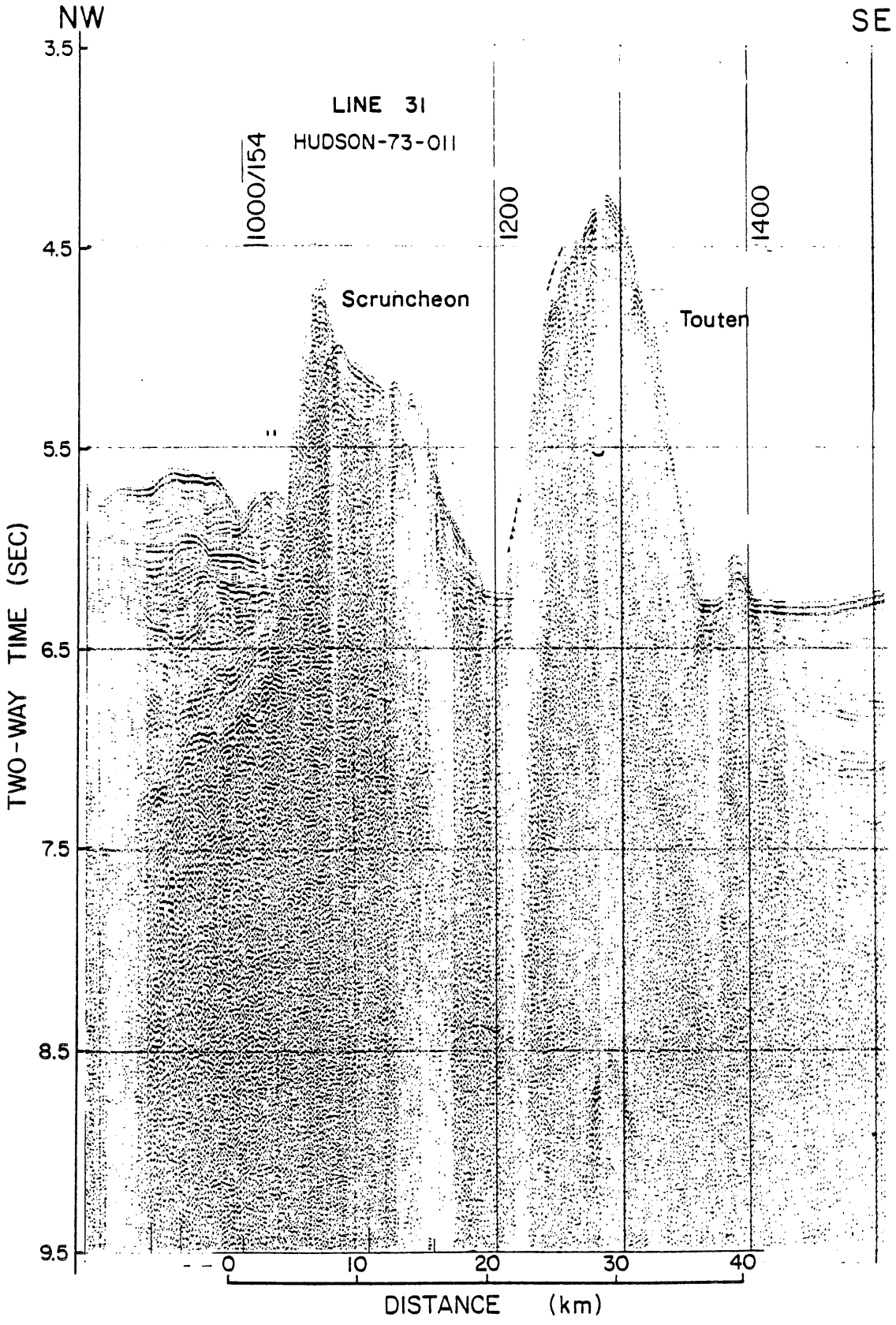
NW
SE
LINE 31
HUDSON-73-011
1000/154
1200
1400
Scruncheon
Touten
TWO-WAY TIME (SEC)
3.5
4.5
5.5
6.5
7.5
8.5
9.5
0
10
20
30
40
DISTANCE (km)

Figure 3.8c

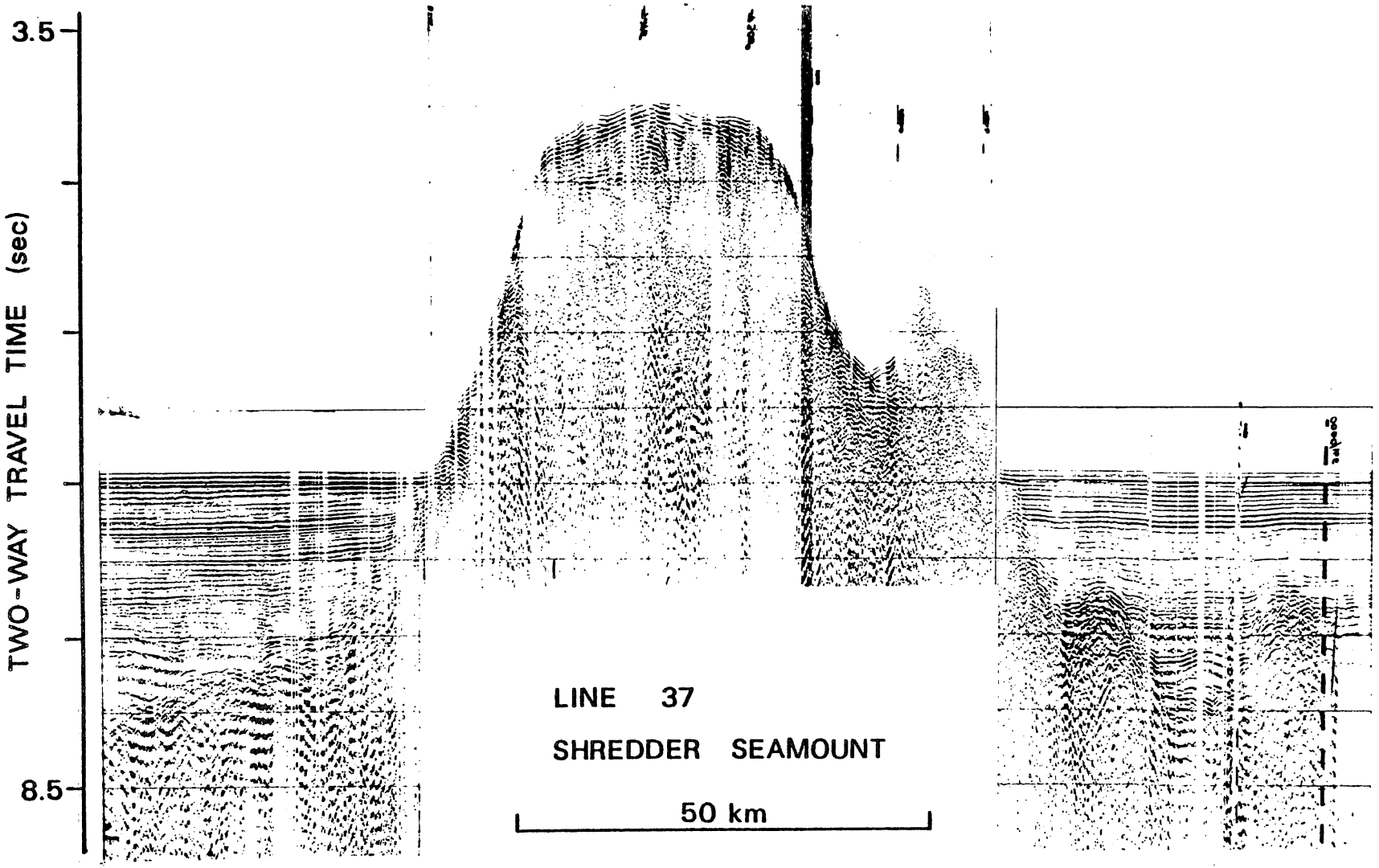

Figure 3.8c

CHAPTER 4: SEISMIC DATA

Bedford Institute of Oceanography has collected over 4,000 km of continuous single-channel seismic reflection profiles, 23 expendable sonobuoy profiles and one crustal refraction profile in the Newfoundland Basin (Fig. 4.1, Table 4.1). A considerable amount of published multi-channel and single-channel reflection data from this and surrounding areas (Fig. 4.2) have also been examined during the course of this study. The sources for the latter data are: Watson and Johnson (1970), Johnson et al. (1971), Auzende et al. (1970), Jansa and Wade (1975) and A. C. Grant (1977).

Selected Bedford Institute seismic profiles are presented in Figure 4.3 as interpretive line drawings with accompanying geophysical data. The significant basement and sedimentary features observed on seismic profiles in each of the physiographic provinces within the Basin are described in Section 4.1, followed by the expendable sonobuoy results (Section 4.2). Section 4.3 summarizes the important points brought out in the reflection profile and sonobuoy analysis. Possible correlations between the acoustic stratigraphy of the Newfoundland Basin and the well-known sections of the Grand Banks, the western Portugese continental margin and the North Atlantic south of the Southeast Newfoundland Ridge are discussed in Section 4.4.

A few points regarding the terminology used here and the interpretation of seismic profiles need clarification.

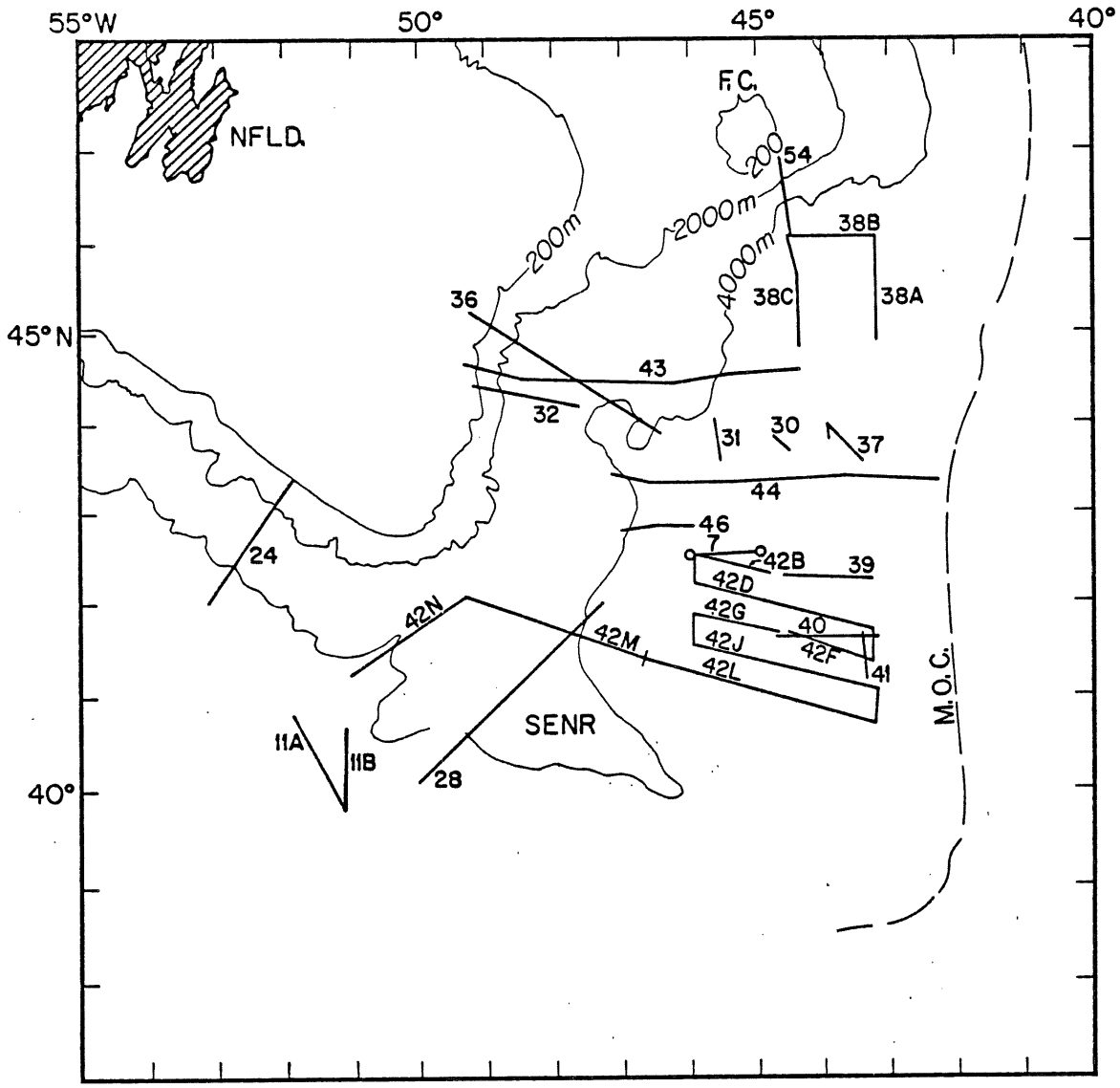

Figure 4.1a

Location map, Bedford Institute seismic data in the Newfoundland Basin. M.O.C. = Northwest Atlantic Mid-Ocean Canyon; solid line with open circles indicates crustal refraction line; solid lines are single-channel air-gun seismic profiles.

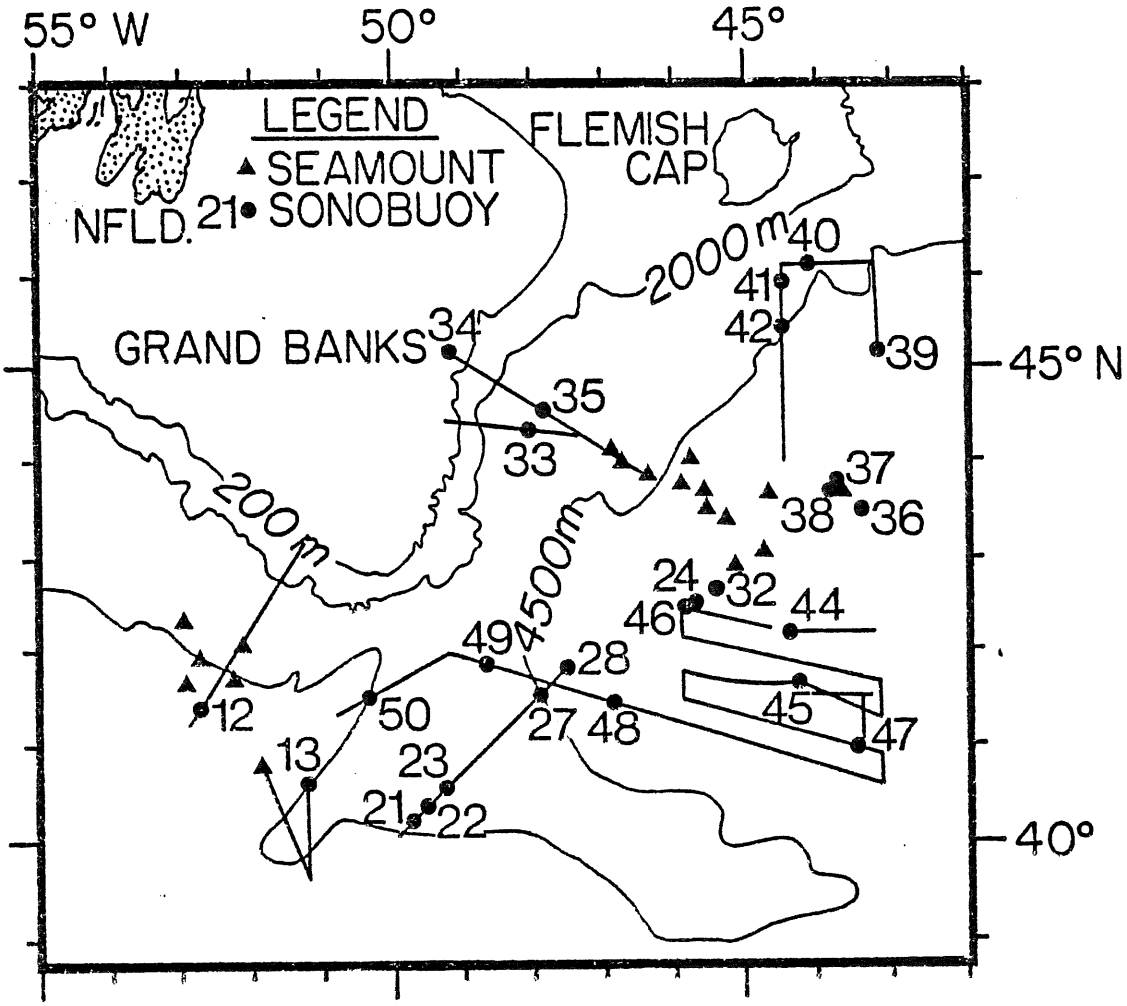

Figure 4.1b

Location map, Bedford Institute reflection profiles and expendable sonobuoy stations.

TABLE 4.1

B.I.O. Seismic Reflection Profiles

PROFILE NUMBER	CRUISE	START LAT (N) LONG (W)	START DAY/TIME	FINISH LAT (N) LONG (W)	FINISH DAY/TIME
11A	72-021	40.82 51.95	208/2200	39.71 51.18	209/1100
11B	72-021	39.71 51.18	209/1100	40.68 51.23	209/2300
28	73-011	40.04 50.06	148/1700	41.85 45.57	149/2300
29	73-011	42.50 46.00	150/0845	42.50 45.30	150/1200
30	73-011	43.66 44.50	151/2300	41.82 44.72	152/0245
31	73-011	43.91 45.65	154/0830	43.37 45.49	154/1500
32	73-011	44.23 47.74	155/0300	44.43 49.20	155/1500
36	75-009	45.22 49.31	156/0423	43.95 46.43	157/0312
37	75-009	43.48 49.31	164/2345	43.73 43.74	165/1032
38A	75-009	44.92 43.13	167/0458	45.95 43.14	167/1317
38B	75-009	45.95 43.13	167/1317	45.96 44.43	167/2151
38C	75-009	45.96 44.43	167/2151	44.90 44.30	168/0749
39	75-009	42.29 44.72	169/0350	42.29 43.32	169/1245
40	75-009	41.61 43.21	169/1930	41.61 44.74	170/0507
41	75-009	41.61 43.16	171/1450	41.11 43.39	171/2012
42A	75-009	42.28 44.68	175/2252	42.32 44.83	176/0000
42B	75-009	42.32 45.95	176/0000	42.54 45.95	176/1200
42C	75-009	42.54 45.95	176/1200	42.22 45.98	176/1530
42D	75-009	42.22 45.98	176/1530	41.68 43.25	177/0900

TABLE 4.1 (continued)

PROFILE NUMBER	CRUISE	START LAT (N) LONG (W)	START DAY/TIME	FINISH LAT (N) LONG (W)	FINISH DAY/TIME
42E	75-009	41.68 43.25	177/0900	41.31 43.25	177/1200
42F	75-009	41.31 43.25	177/1200	41.66 44.56	177/1900
42G	75-009	41.63 44.58	178/0130	41.87 45.98	178/0930
42H	75-009	41.87 45.98	178/0930	41.52 45.98	178/1300
42J	75-009	41.52 45.98	178/1300	40.96 43.21	179/0500
42K	75-009	40.96 43.21	179/0500	40.62 43.29	179/0800
42L	75-009	40.62 43.29	179/0800	42.10 49.35	180/2050
42M	75-009	42.10 49.35	180/2050	41.69 50.32	181/0200
43	76-031	44.65 49.31	277/1420	44.58 44.28	279/0030
44A	76-031	43.88 41.22	281/0900	43.37 41.98	281/0700
44B	76-031	43.46 41.91	282/0430	43.46 47.21	284/0300
45	76-031	43.46 47.21	284/0300	42.90 46.02	289/1217
46	76-031	42.81 45.89	284/1341	42.85 46.70	284/2030

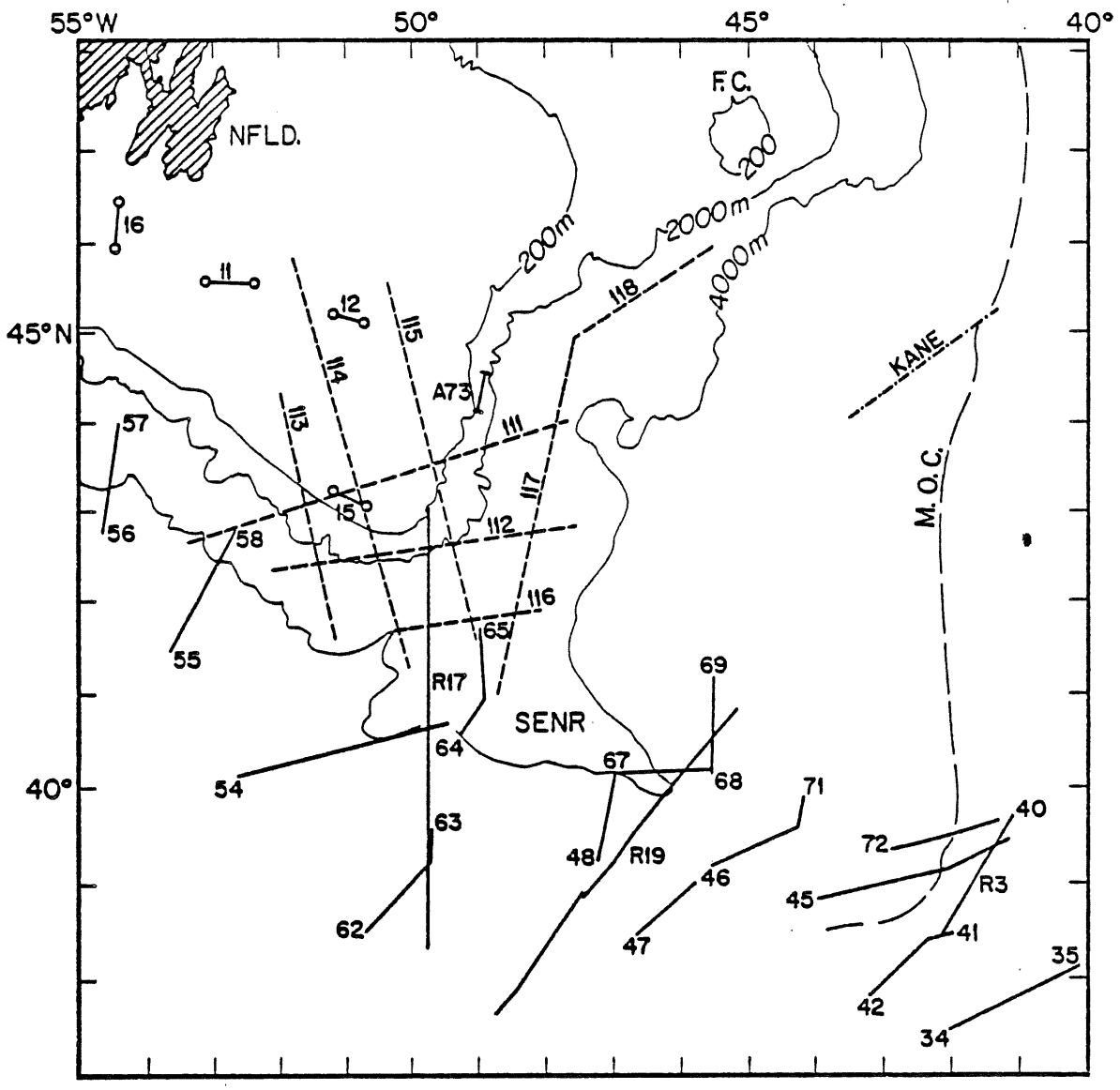

Figure 4.2

Location map, published seismic reflection and refraction data. Dashed lines: multi-channel profiles (Jansa and Wade, 1975); dot-dash line: USNS Kane profile (Johnson et al., 1971; solid lines: single-channel profiles (Watson and Johnson, 1970); refraction profiles (and) from Sheridan and Drake (1968).

Several descriptive terms are used in reference to the character of reflectors in various sedimentary units (e.g. "wavy-laminated", "disrupted"). This usage is convenient for description of records but may be misleading if genetic significance is carelessly attached to the descriptive terms. In the absence of direct sampling the geological or sedimentological significance of acoustic characteristics can only be inferred by comparison with areas where similar acoustic facies have been sampled. Correlative studies of this type have shown that uniformly well-laminated intervals of continuous, moderate to strong reflectors characterize distal turbidite deposits (Davies and Laughton, 1972). Wavy or inclined laminations and rippled or scoured seafloor surfaces are commonly attributed to contourites, i.e. sediments deposited by geostrophic bottom-currents flowing along the western margins of the Atlantic basin (Heezen et al., 1966; Johnson and Schneider, 1969; Johnson et al., 1971; Hollister and Heezen, 1972; Flood and Hollister, 1974). However, proximal turbidites might display many similar features (Stow, 1977). Since the nature of the currents depositing such units cannot be clearly determined on the basis of seismic profiles alone, the term "bottom-current" is used in this chapter as a general term that does not imply a specific mechanism.

Unless otherwise specified, the term "basement" is used throughout this chapter in reference to acoustic basement, which is the deepest primary reflector observed on the seismic record. Without direct sampling it is impossible to determine with certainty that the basement reflector actually represents the top of the crustal layer beneath the

sediments. In the present study this uncertainty gives rise to three particularly important problems:

a. An interval of relatively high-velocity sediments of variable thickness commonly occurs at the base of the sedimentary section (Section 4.2, 4.4), and reflections from this layer can mask true basement.

b. It is often difficult, especially in the SENR area and the southern part of the lower rise, to distinguish constructional volcanic from tectonic (fault-controlled) basement relief. Deep layers of strongly-reflective sediments may also obscure the original relief in places, complicating the matter.

c. It is often difficult to determine whether large basement highs are in fact acoustically continuous with the adjacent basement surface, because the airgun systems and vertical scales used in recording these profiles cannot resolve the junction between these two surfaces. This leaves the true nature of these features and the crust surrounding them open to some doubt, unless sampling or potential field data provide corroborating evidence.

The ambiguities arising from these elementary pitfalls in seismic reflection interpretation can be very troublesome, particularly when attempting to define the boundary between oceanic and continental crust.

All times quoted in the text are two-way travel times in seconds.

4.1 Reflection Profiles

The major upper crustal and sedimentary structures of the

Newfoundland Basin and its margins are illustrated by the seismic reflection profiles indicated in Figure 4.1. This section describes interpretive line drawings of selected profiles (Fig. 4.3) and highlights significant features of the accompanying geophysical data. Copies of the original records for all profiles shown in Fig. 4.1 are given in Appendix V.

4.1.1 Flemish Cap continental margin (Profiles 38A, 38B, 38C; 54; Fig. 4.3a)

Profiles 54 and 38C together provide the only currently-available crossing of the entire Flemish Cap margin. Basement and sedimentary reflectors on the Cap appear to be truncated at the shelf-break, and basement may be exposed on the very steep continental slope in this region. Between 40 km on Line 54 and 45 km on Line 38C, basement is frequently too deep to be observed. South of the peak at 80 km basement lies at 7.3-7.5 seconds sub-bottom.

The latter basement high separates two distinctly different sedimentary regimes: to the north one finds a substantial thickness of sediments deposited in fault-bounded troughs (Lines 54, 38C, 38B). These units are bounded above by a strong seaward-dipping reflector. Above the latter horizon there is a southward-thinning wedge of sediments characterized by wavy-laminated and disrupted reflectors (hereafter called the 'Flemish Cap wedge'). South of the basement high a turbidite unit lies directly on basement. The turbidites appear to unconformably overlie the Flemish Cap wedge between 35 and 75 km (Fig. 4.4).

Figure 4.3: Line drawings of seismic profiles.

a. Flemish Cap margin:
Lines 38A, 38B, 54-38C.

b. Eastern Banks margin:
Lines 36, 43.

c. Southern Newfoundland Basin:
Lines 39, 42D, 42L, 44, 46.

d. SENR and Spur Ridge:
Lines 42M, 42N, 28, 11A.

e. Newfoundland Seamounts:
Lines 30, 31, 37.

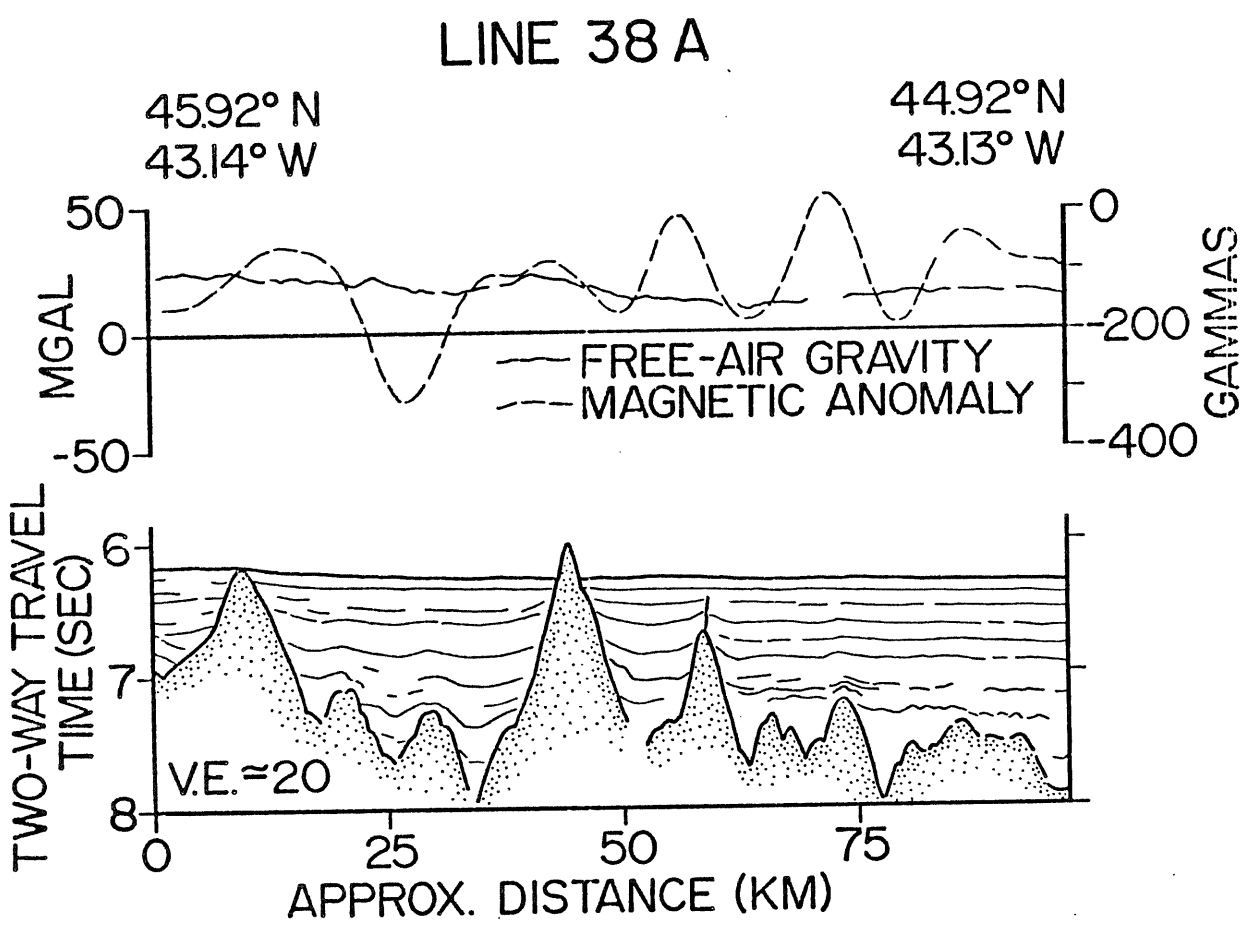
LINE 38 A
45.92° N
43.14° W
44.92° N
43.13° W
50
0
-50
MGAL
0
-200
-400
GAMMAS
FREE-AIR GRAVITY
MAGNETIC ANOMALY
TWO-WAY TRAVEL TIME (SEC)
6
7
8
V.E.≈20
0
25
50
75
APPROX. DISTANCE (KM)

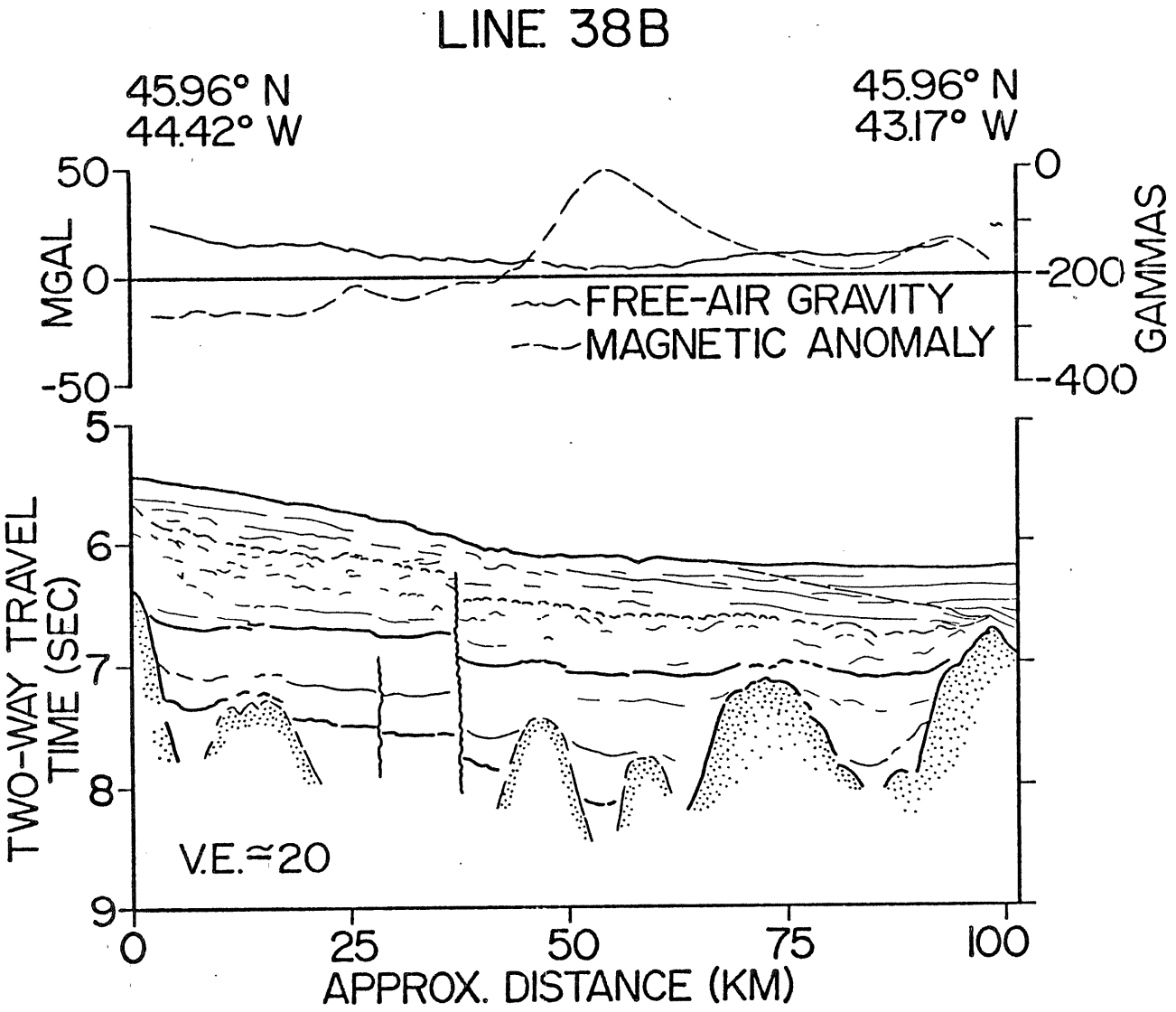
LINE 38B
45.96° N
44.42° W
45.96° N
43.17° W
50
0
-50
MGAL
0
-200
-400
GAMMAS
FREE-AIR GRAVITY
MAGNETIC ANOMALY
5
6
7
8
9
TWO-WAY TRAVEL TIME (SEC)
V.E.≈20
0
25
50
75
100
APPROX. DISTANCE (KM)

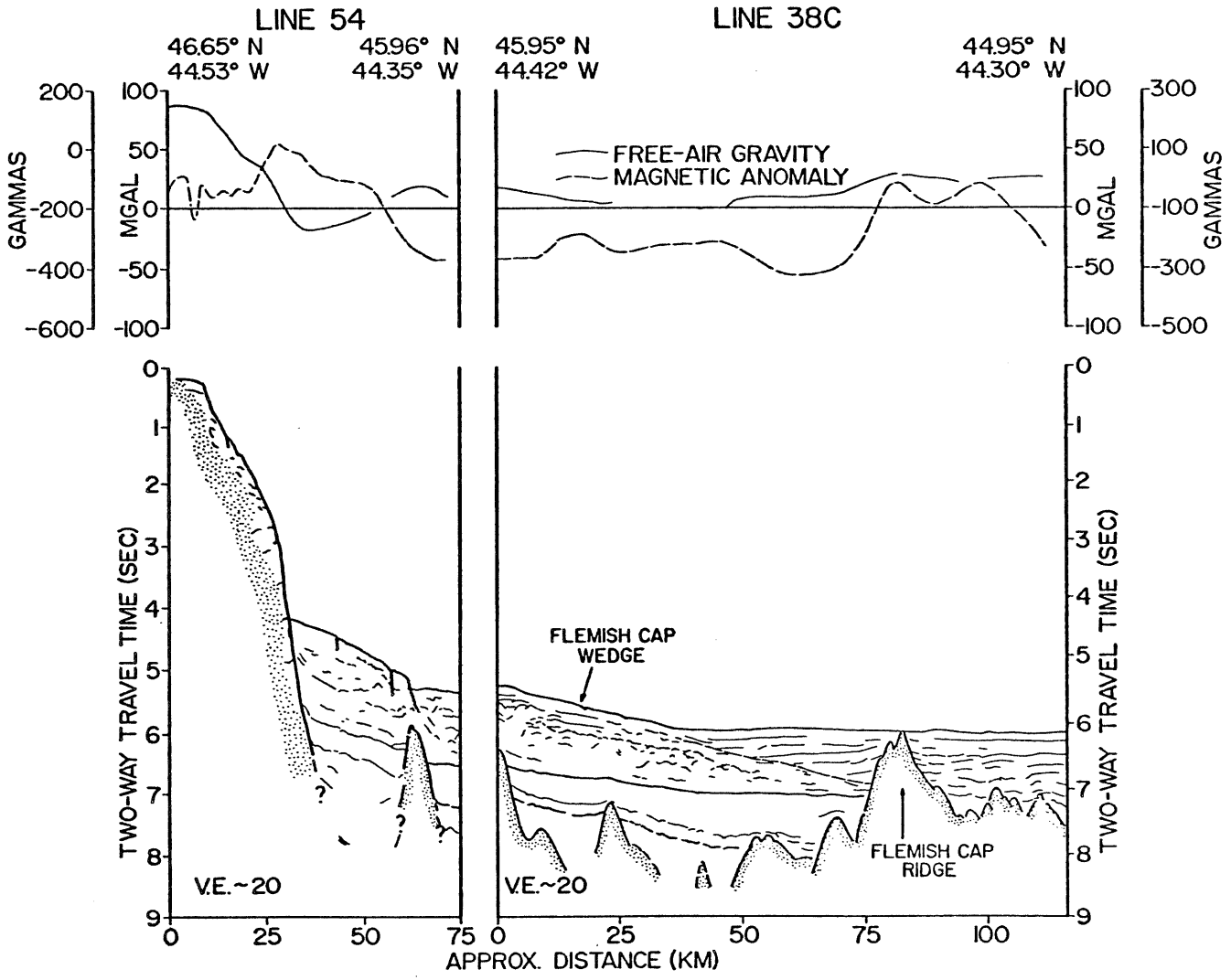
LINE 54
LINE 38C
46.65° N
44.53° W
45.96° N
44.35° W
45.95° N
44.42° W
44.95° N
44.30° W
FREE-AIR GRAVITY
MAGNETIC ANOMALY
GAMMAS
MGAL
MGAL
GAMMAS
200
0
-200
-400
-600
100
50
0
-50
-100
100
50
0
-50
-100
300
100
-100
-300
-500
TWO-WAY TRAVEL TIME (SEC)
TWO-WAY TRAVEL TIME (SEC)
0
1
2
3
4
5
6
7
8
9
FLEMISH CAP
WEDGE
FLEMISH CAP
RIDGE
V.E.~20
V.E.~20
0
25
50
75
0
25
50
75
100
APPROX. DISTANCE (KM)

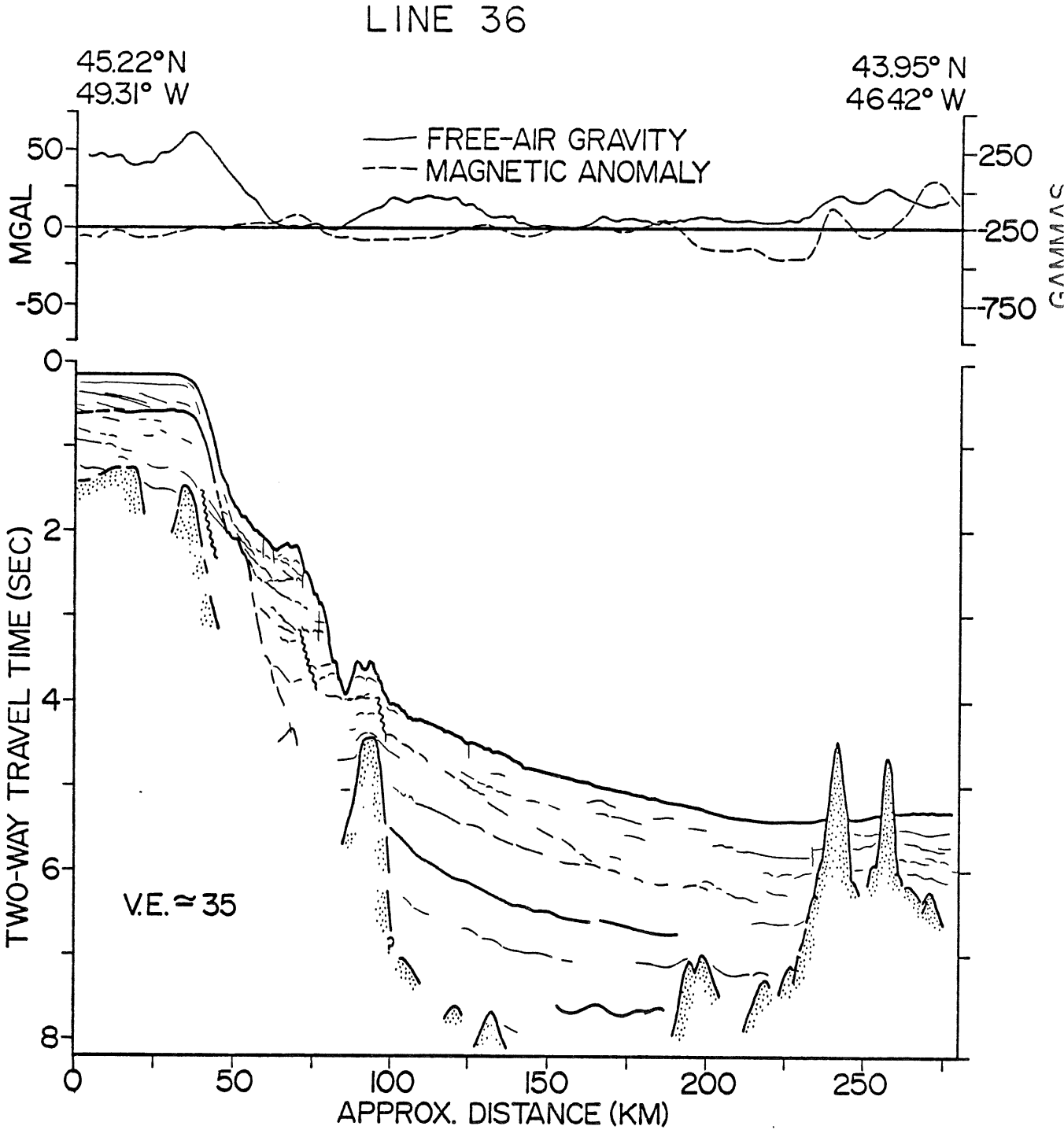
LINE 36
45.22°N
49.31° W
43.95° N
46.42° W
FREE-AIR GRAVITY
MAGNETIC ANOMALY
MGAL
50
0
-50
250
-250
-750
GAMMAS
TWO-WAY TRAVEL TIME (SEC)
0
2
4
6
8
V.E. ≃ 35
0
50
100
150
200
250
APPROX. DISTANCE (KM)

LINE 43

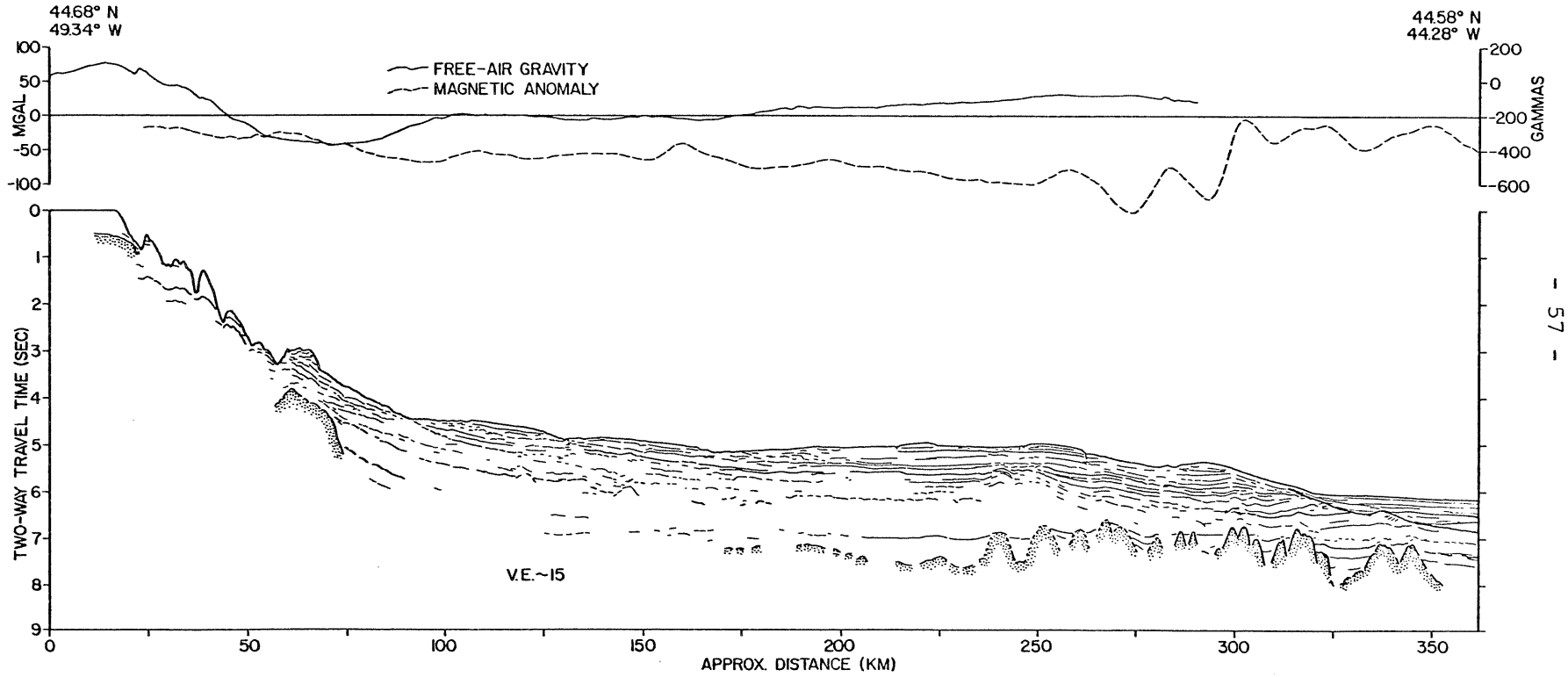
44.68° N
49.34° W
44.58° N
44.28° W
FREE-AIR GRAVITY
MAGNETIC ANOMALY
MGAL
GAMMAS
TWO-WAY TRAVEL TIME (SEC)
V.E.~15
APPROX. DISTANCE (KM)

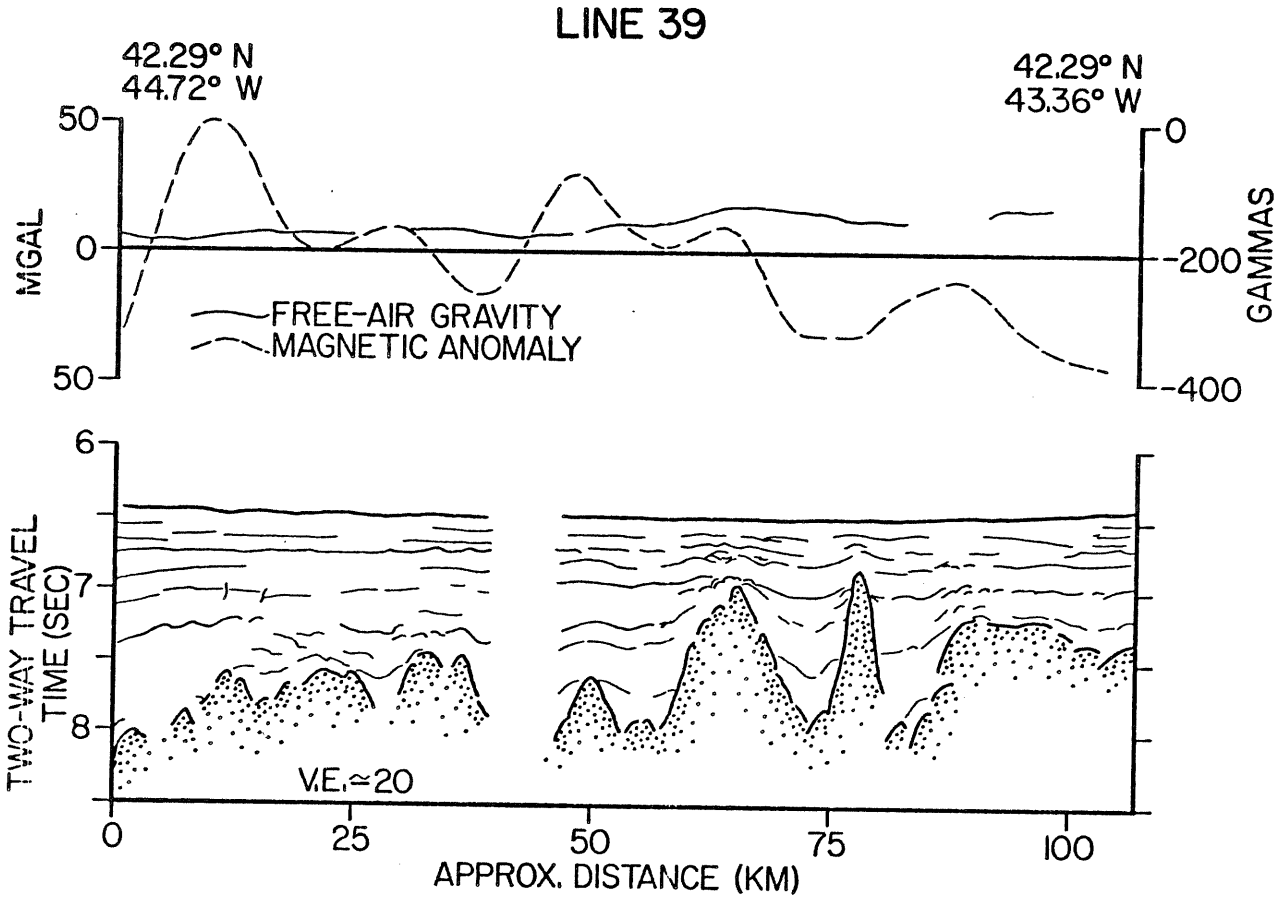
LINE 39
42.29° N
44.72° W
42.29° N
43.36° W
50
0
50
MGAL
0
-200
-400
GAMMAS
FREE-AIR GRAVITY
MAGNETIC ANOMALY
6
7
8
TWO-WAY TRAVEL TIME (SEC)
V.E.≈20
0
25
50
75
100
APPROX. DISTANCE (KM)

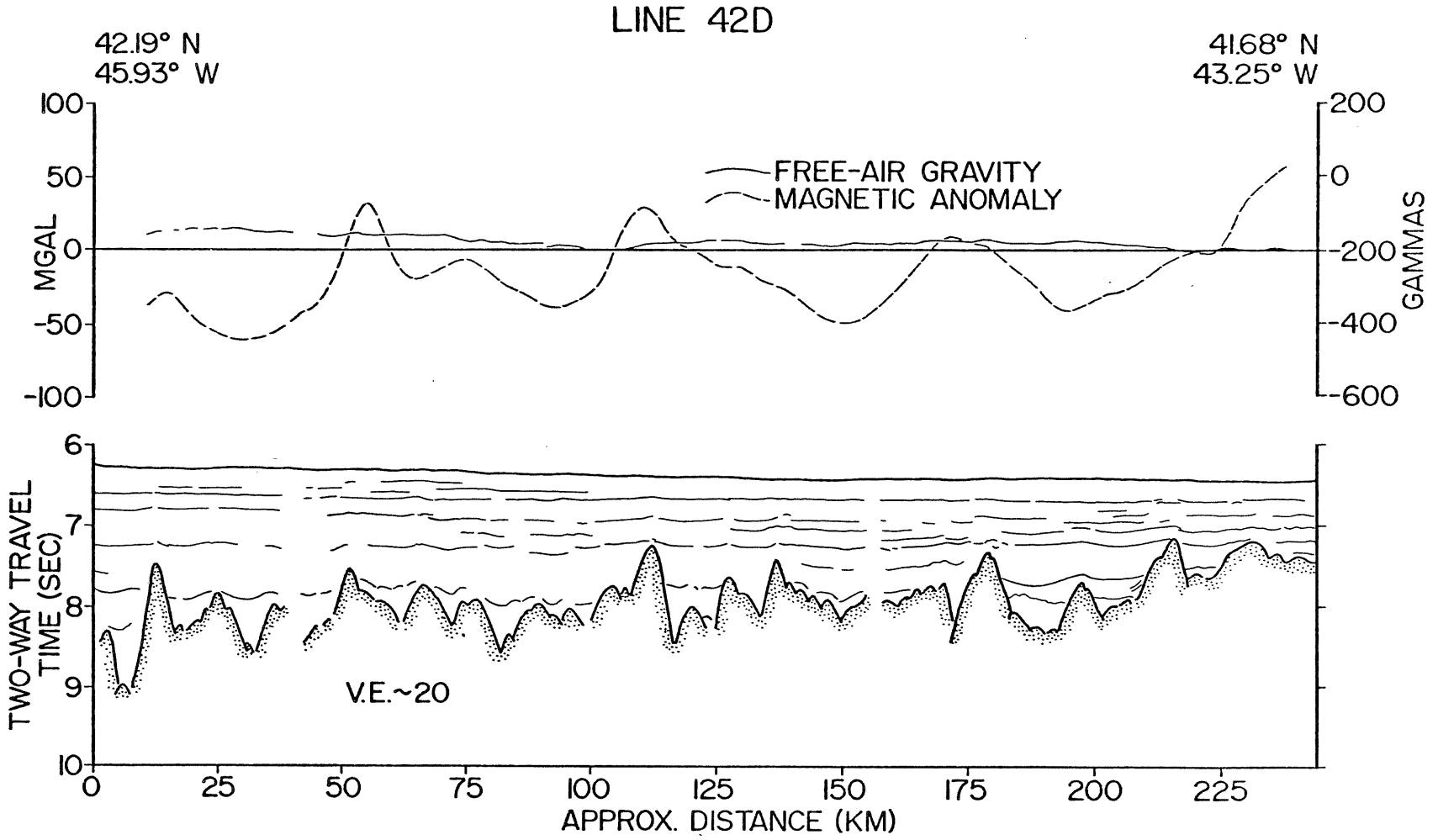
LINE 42D
42.19° N
45.93° W
41.68° N
43.25° W
100
50
0
-50
-100
MGAL
FREE-AIR GRAVITY
MAGNETIC ANOMALY
200
0
-200
-400
-600
GAMMAS
6
7
8
9
10
TWO-WAY TRAVEL TIME (SEC)
V.E.~20
0
25
50
75
100
125
150
175
200
225
APPROX. DISTANCE (KM)

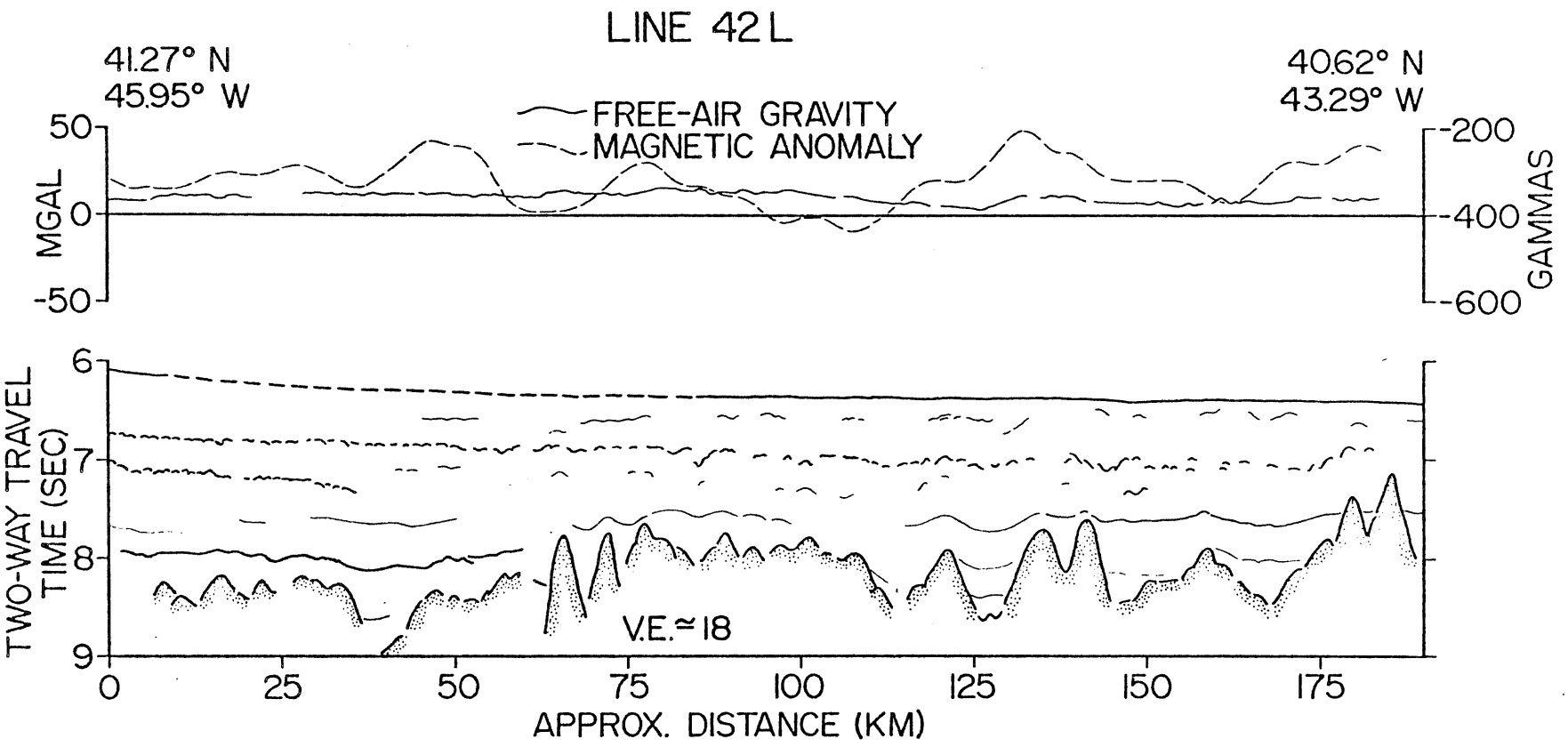
LINE 42 L
41.27° N
45.95° W
40.62° N
43.29° W
FREE-AIR GRAVITY
MAGNETIC ANOMALY
50
0
-50
MGAL
-200
-400
-600
GAMMAS
6
7
8
9
TWO-WAY TRAVEL TIME (SEC)
V.E.≃18
0
25
50
75
100
125
150
175
APPROX. DISTANCE (KM)

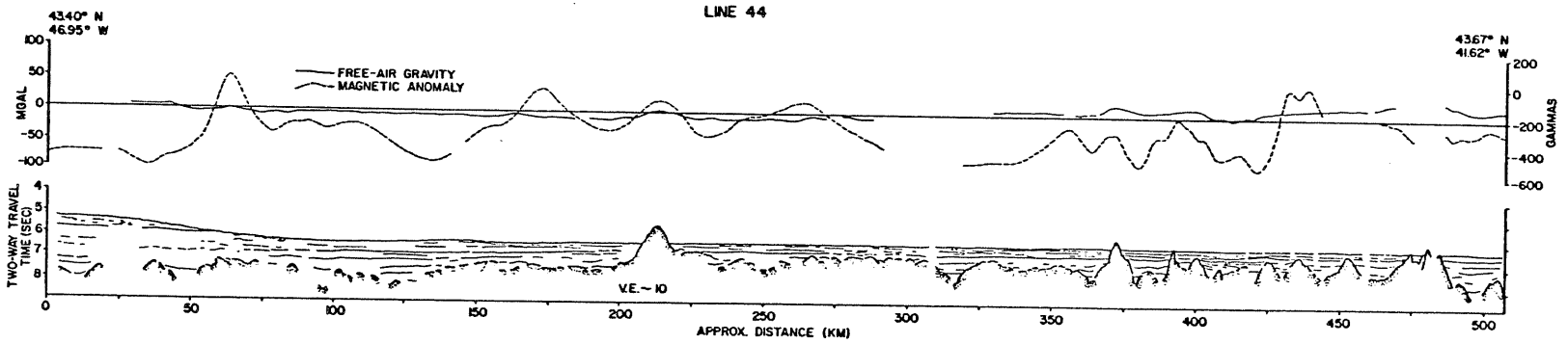
LINE 44
43.40° N
46.95° W
43.67° N
41.62° W
FREE-AIR GRAVITY
MAGNETIC ANOMALY
MGAL
GAMMAS
TWO-WAY TRAVEL TIME (SEC)
V.E.~ 10
APPROX. DISTANCE (KM)

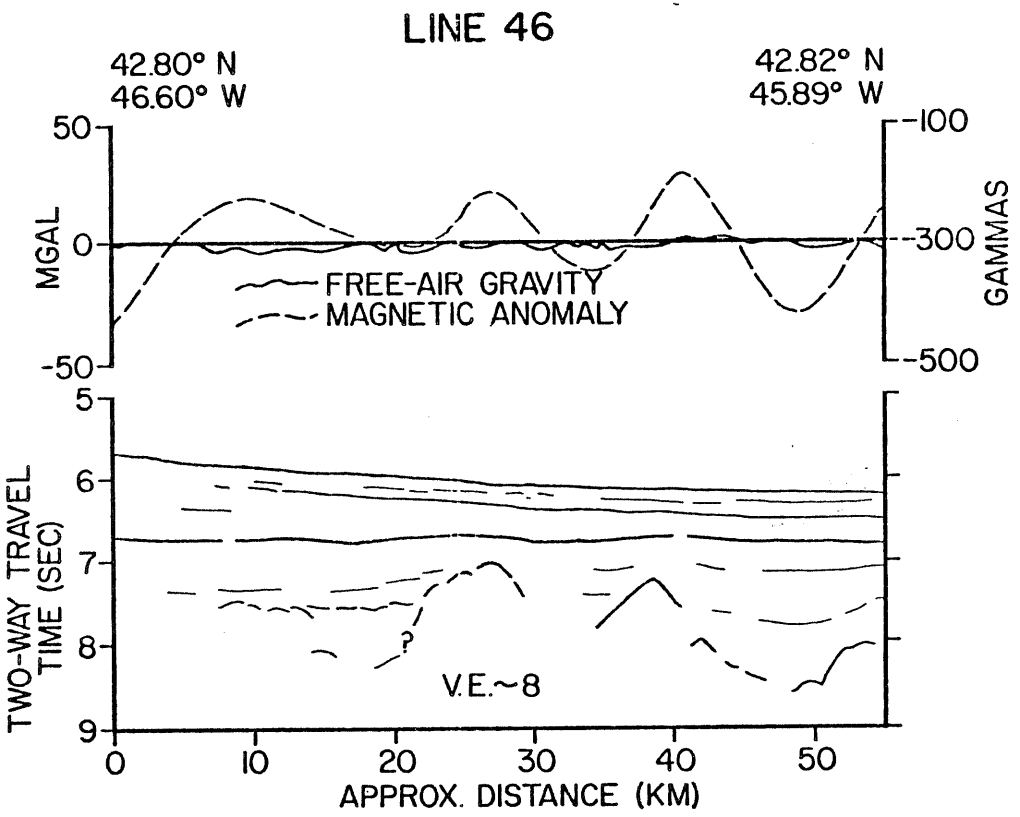
LINE 46
42.80° N
46.60° W
42.82° N
45.89° W
50
0
-50
MGAL
-100
-300
-500
GAMMAS
FREE-AIR GRAVITY
MAGNETIC ANOMALY
5
6
7
8
9
TWO-WAY TRAVEL TIME (SEC)
?
V.E.~8
0
10
20
30
40
50
APPROX. DISTANCE (KM)

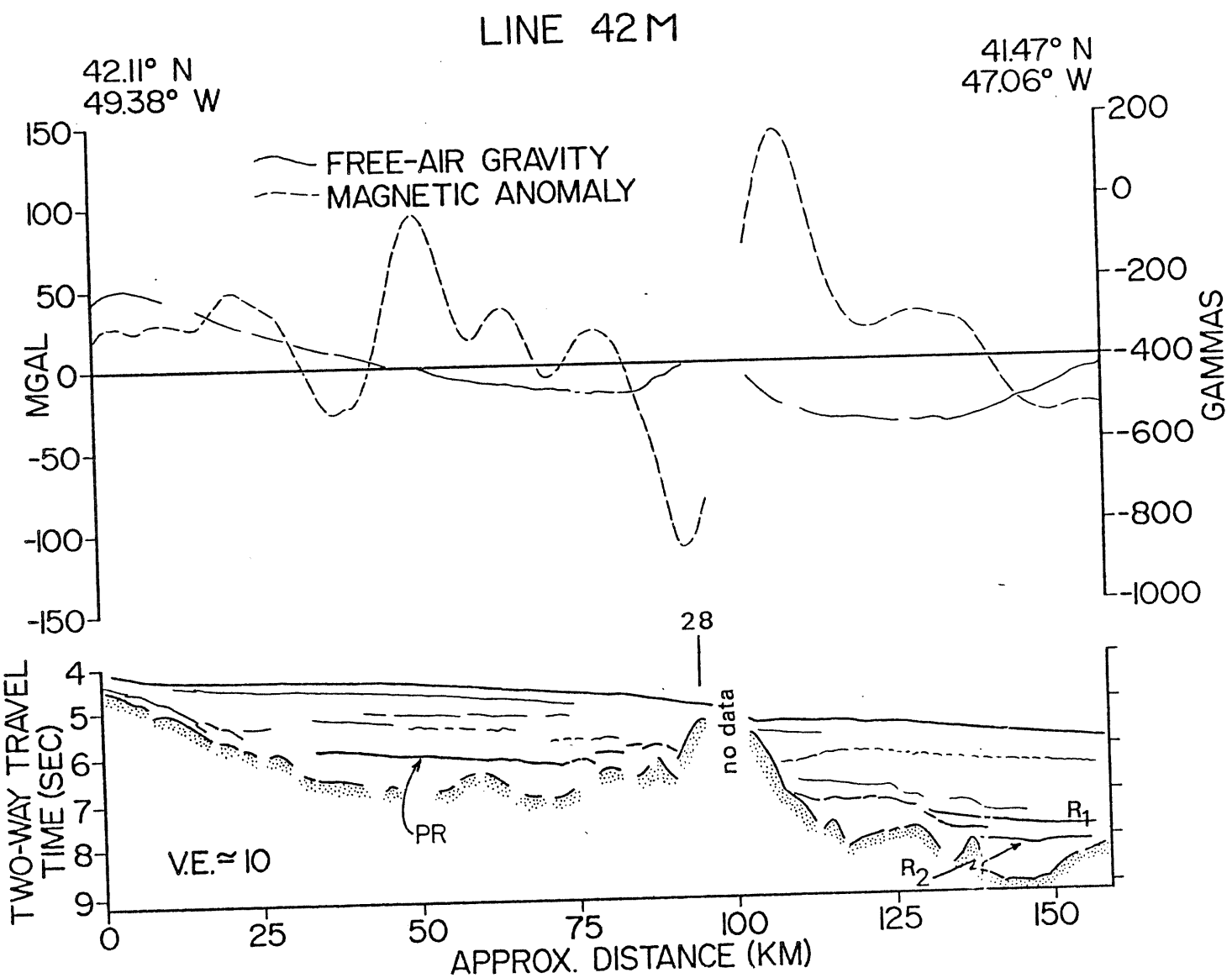
LINE 42 M
42.11° N
49.38° W
41.47° N
47.06° W
FREE-AIR GRAVITY
MAGNETIC ANOMALY
MGAL
GAMMAS
150
100
50
0
-50
-100
-150
200
0
-200
-400
-600
-800
-1000
28
no data
TWO-WAY TRAVEL TIME (SEC)
4
5
6
7
8
9
PR
R1
R2
V.E.≈ 10
0
25
50
75
100
125
150
APPROX. DISTANCE (KM)

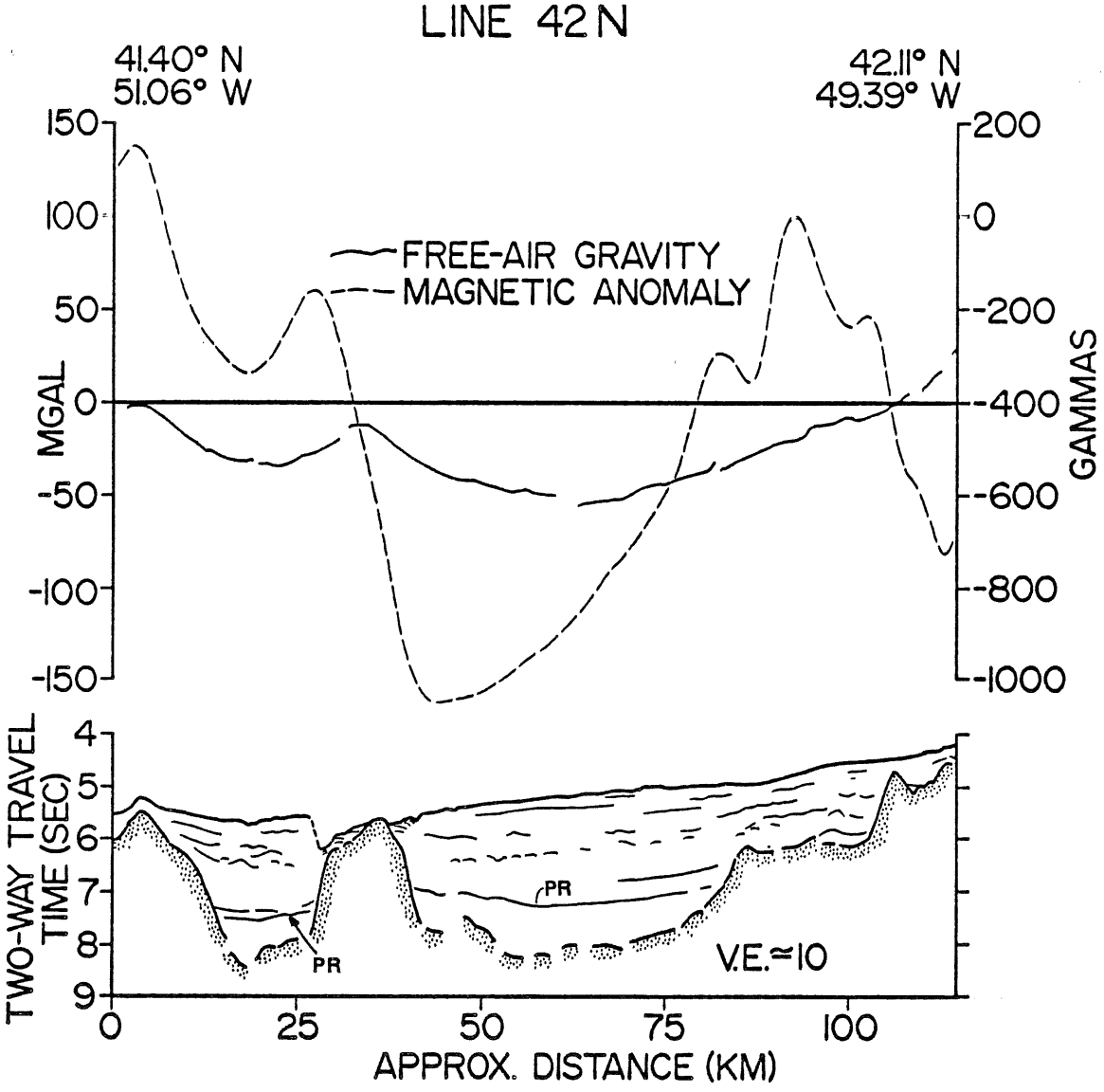
LINE 42 N
41.40° N
51.06° W
42.11° N
49.39° W
150
100
50
0
-50
-100
-150
MGAL
200
0
-200
-400
-600
-800
-1000
GAMMAS
FREE-AIR GRAVITY
MAGNETIC ANOMALY
TWO-WAY TRAVEL TIME (SEC)
4
5
6
7
8
9
PR
PR
V.E.≃10
0
25
50
75
100
APPROX. DISTANCE (KM)

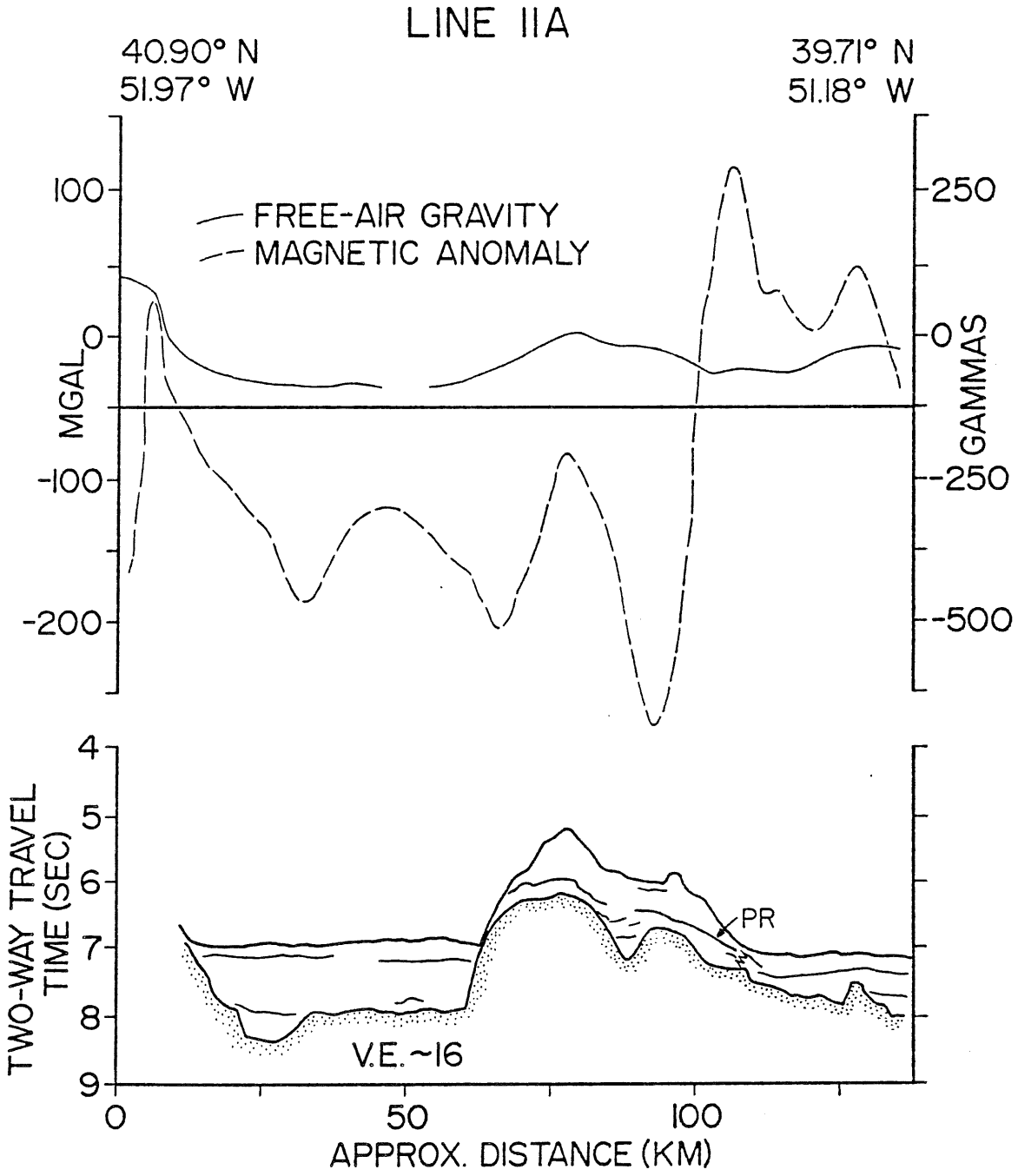
LINE IIA
40.90° N
51.97° W
39.71° N
51.18° W
FREE-AIR GRAVITY
MAGNETIC ANOMALY
100
0
-100
-200
MGAL
250
0
-250
-500
GAMMAS
4
5
6
7
8
9
TWO-WAY TRAVEL TIME (SEC)
PR
V.E.~16
0
50
100
APPROX. DISTANCE (KM)

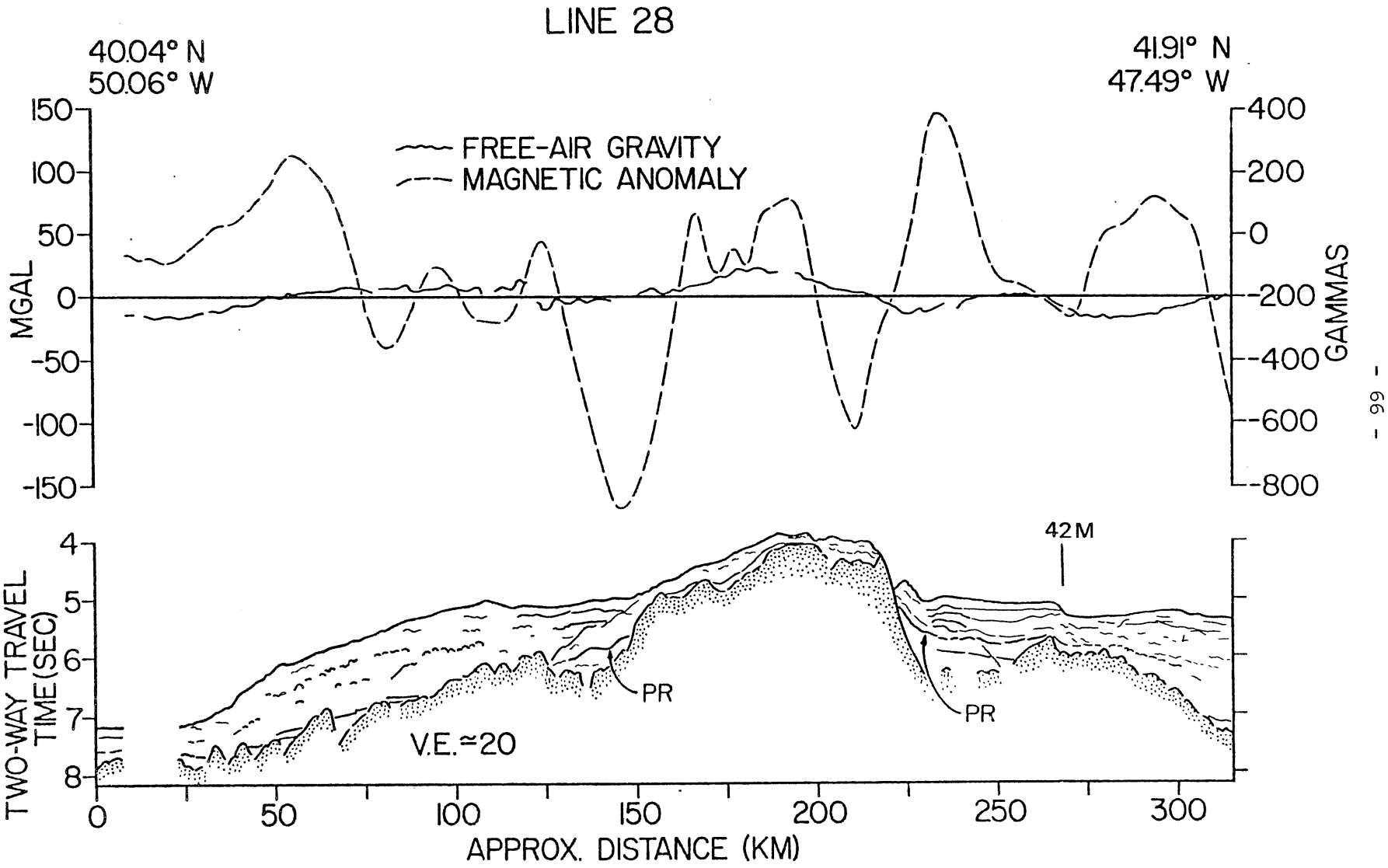
LINE 28
40.04° N
50.06° W
41.91° N
47.49° W
FREE-AIR GRAVITY
MAGNETIC ANOMALY
MGAL
GAMMAS
150
100
50
0
-50
-100
-150
400
200
0
-200
-400
-600
-800
42M
PR
PR
V.E.≈20
TWO-WAY TRAVEL TIME (SEC)
4
5
6
7
8
0
50
100
150
200
250
300
APPROX. DISTANCE (KM)

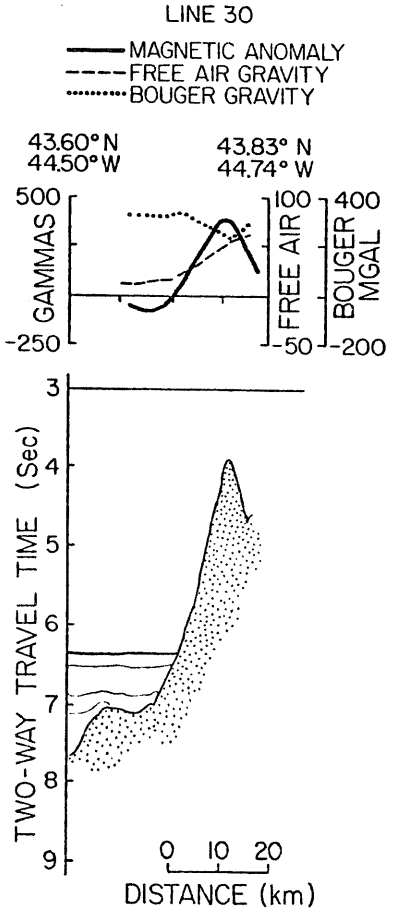
LINE 30
MAGNETIC ANOMALY
FREE AIR GRAVITY
BOUGER GRAVITY
43.60° N
44.50° W
43.83° N
44.74° W
500
GAMMAS
-250
100
FREE AIR
-50
400
BOUGER
MGAL
-200
3
4
5
6
7
8
9
TWO-WAY TRAVEL TIME (Sec)
0
10
20
DISTANCE (km)

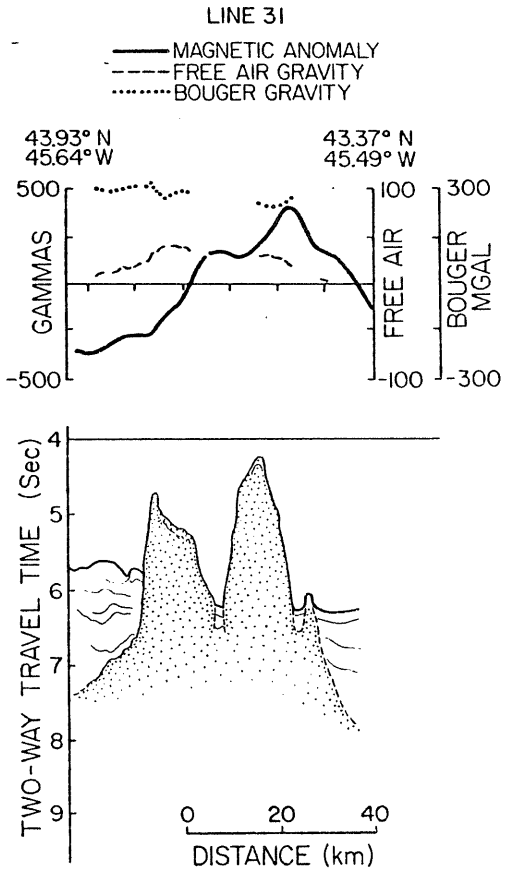
LINE 31
MAGNETIC ANOMALY
FREE AIR GRAVITY
BOUGER GRAVITY
43.93° N
45.64° W
43.37° N
45.49° W
500
GAMMAS
-500
100
FREE AIR
-100
300
BOUGER
MGAL
-300
4
5
6
7
8
9
TWO-WAY TRAVEL TIME (Sec)
0
20
40
DISTANCE (km)

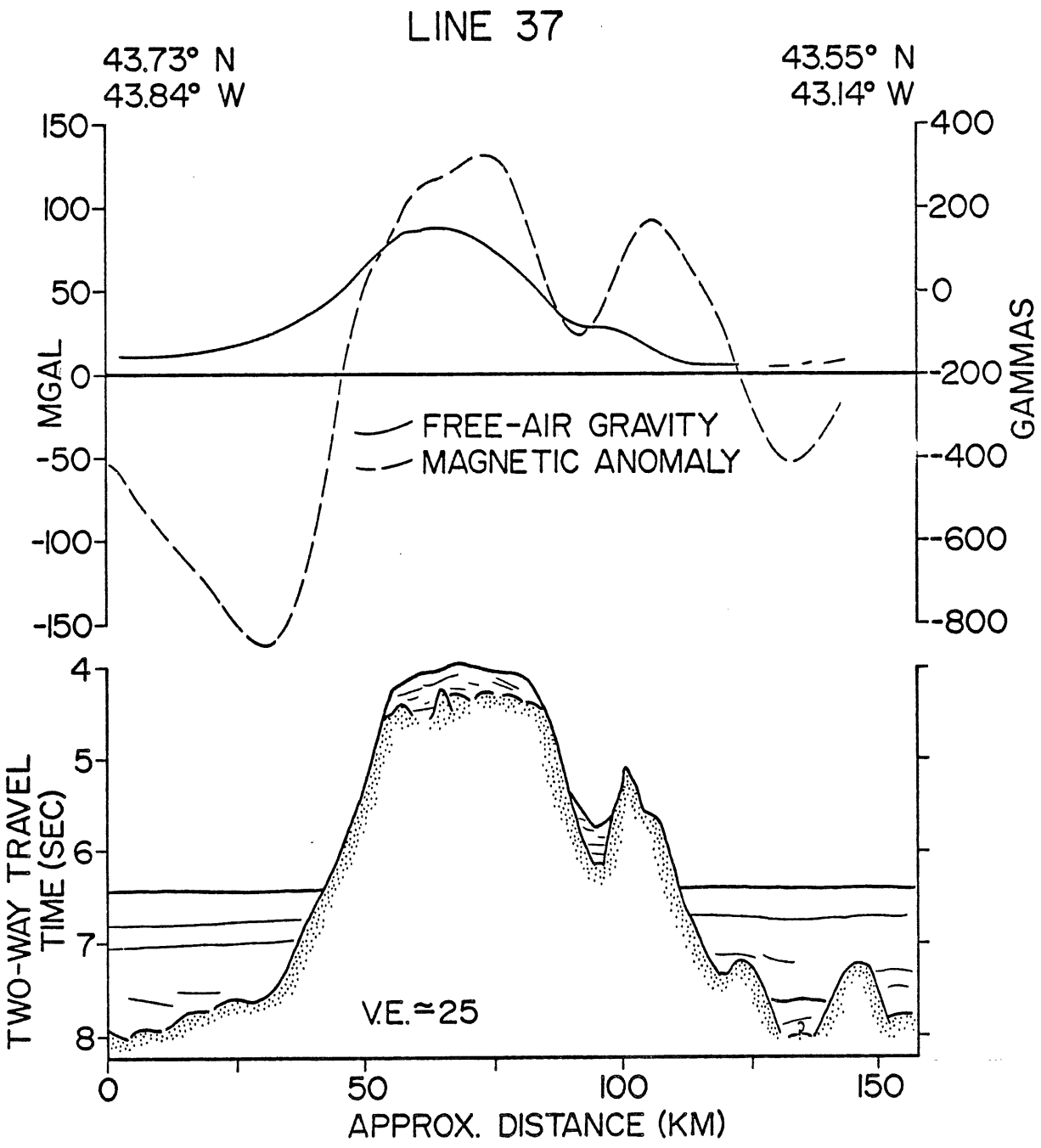
LINE 37
43.73° N
43.84° W
43.55° N
43.14° W
150
100
50
0
-50
-100
-150
MGAL
400
200
0
-200
-400
-600
-800
GAMMAS
FREE-AIR GRAVITY
MAGNETIC ANOMALY
4
5
6
7
8
TWO-WAY TRAVEL TIME (SEC)
V.E.≈25
0
50
100
150
APPROX. DISTANCE (KM)

Figure 4.4: Detail of seismic record, Line 38C.

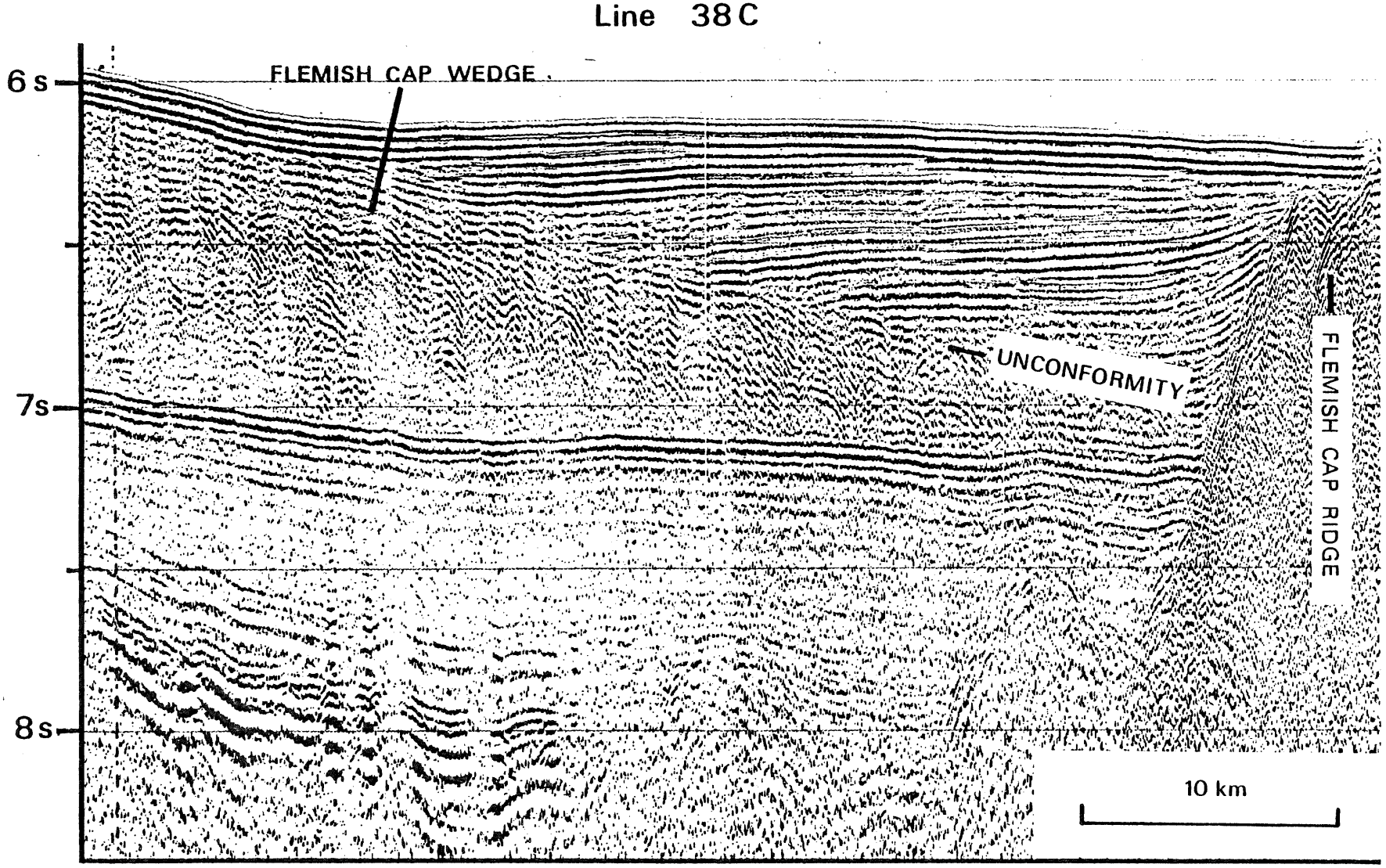
Line 38C
6 s
7s
8s
FLEMISH CAP WEDGE
UNCONFORMITY
FLEMISH CAP RIDGE
10 km

Profiles 38A and 38B provide some indication of the trends and spatial limits of the features described above. Very deep sediments are observed between 20 km and 60 km on 38B, with basement shallowing east of this. The Flemish Cap wedge extends, at the seafloor, to 70 km on line 38B. Profile 38A does not extend sufficiently far north to observe the deep sedimentary basins, but the toe of the Flemish Cap wedge can be seen abutting a basement high at the northern end of the line. This basement structure is thus inferred to be the continuation of the basement high seen at 80 km on line 38C. The strike of this feature, hereafter called the 'Flemish Cap Ridge' is 060°.

4.1.2 Eastern Banks continental margin (Profiles 36 and 43; Fig. 4.3b)

Profiles 36 and 43 present views of the Eastern Banks margin which, at first glance, appear to be quite different. This impression is due primarily to differences in profile orientation with respect to both structure and bathymetry and to differences in vertical exaggeration.

Both profiles show that basement beneath the shelf (approximately 1.0 seconds sub-bottom) is faulted at the shelf-edge and cannot be detected with certainty between the shelf break and the slope-rise transition. The slope-rise transition is underlain by a distinctive, block-shaped basement structure. It is important to note that, with the possible exception of some of the very youngest sedimentary horizons, no reflectors continue across this structure (this point is treated further in Section 4.3). Seaward of the base-of-slope structure on line 36 basement disappears beneath a 100 km wide graben. Clear

basement reflections appear again at 190 km, from which point basement can be traced eastward to the Newfoundland Seamounts. On line 43 basement reflections are quite weak between the base of the slope and 125 km, in part because of high hydrophone noise-levels prevailing during rough seas; clear reflections are first evident at about 160 km and shallowing, very rough basement occurs east of 190 km.

The most prominent feature in the sedimentary section on the shelf is the angular unconformity at 0.5 seconds sub-bottom. This correlates well with the Early Cretaceous Avalon Unconformity (Chapter 2; Jansa and Wade, 1975; C. E. Keen et al., 1977). The unconformity can be traced, with some difficulty, across the shelf break onto the slope, but it cannot be traced beyond the basement structure at the foot of the slope.

The sedimentary fill in the graben at the base of the continental slope on Line 36 is over 3 seconds thick. One unit that wedges out to the southeast can be seen near 5.0 seconds on the landward side of the graben; overlying sediments are unconformable with this unit. Both northwest and southeast of the seamounts, the uppermost sedimentary units have a wavy-laminated character, suggestive of bottom-current influence in the vicinity of the seamounts.

Line 43 shows that the sediments of the upper continental rise north of the seamounts have been deposited as a series of off-lapping units. It is not possible with only one section to determine whether slumping, erosional, or other processes dominate rise sedimentation. The abrupt variations in reflector strength and continuity within the

Figure 4.5: Details of seismic record, Line 43, upper continental rise sediments.

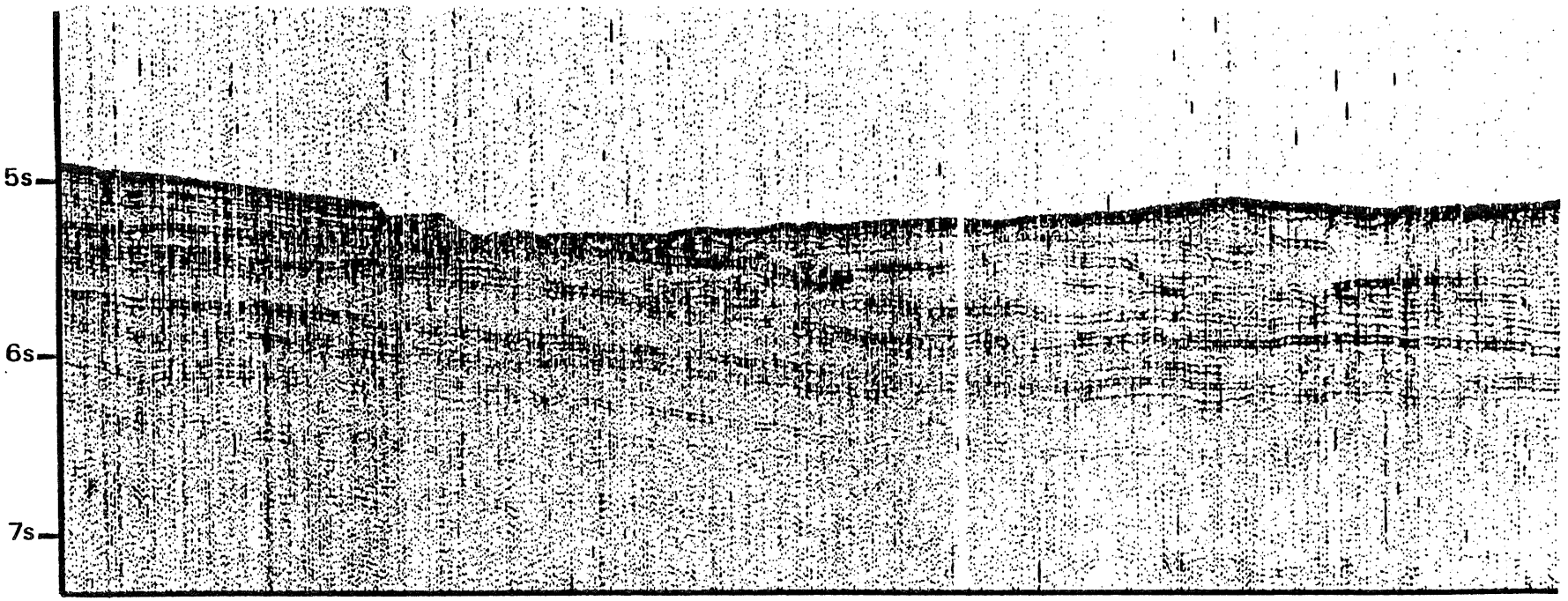
5s
6s
7s
25 km

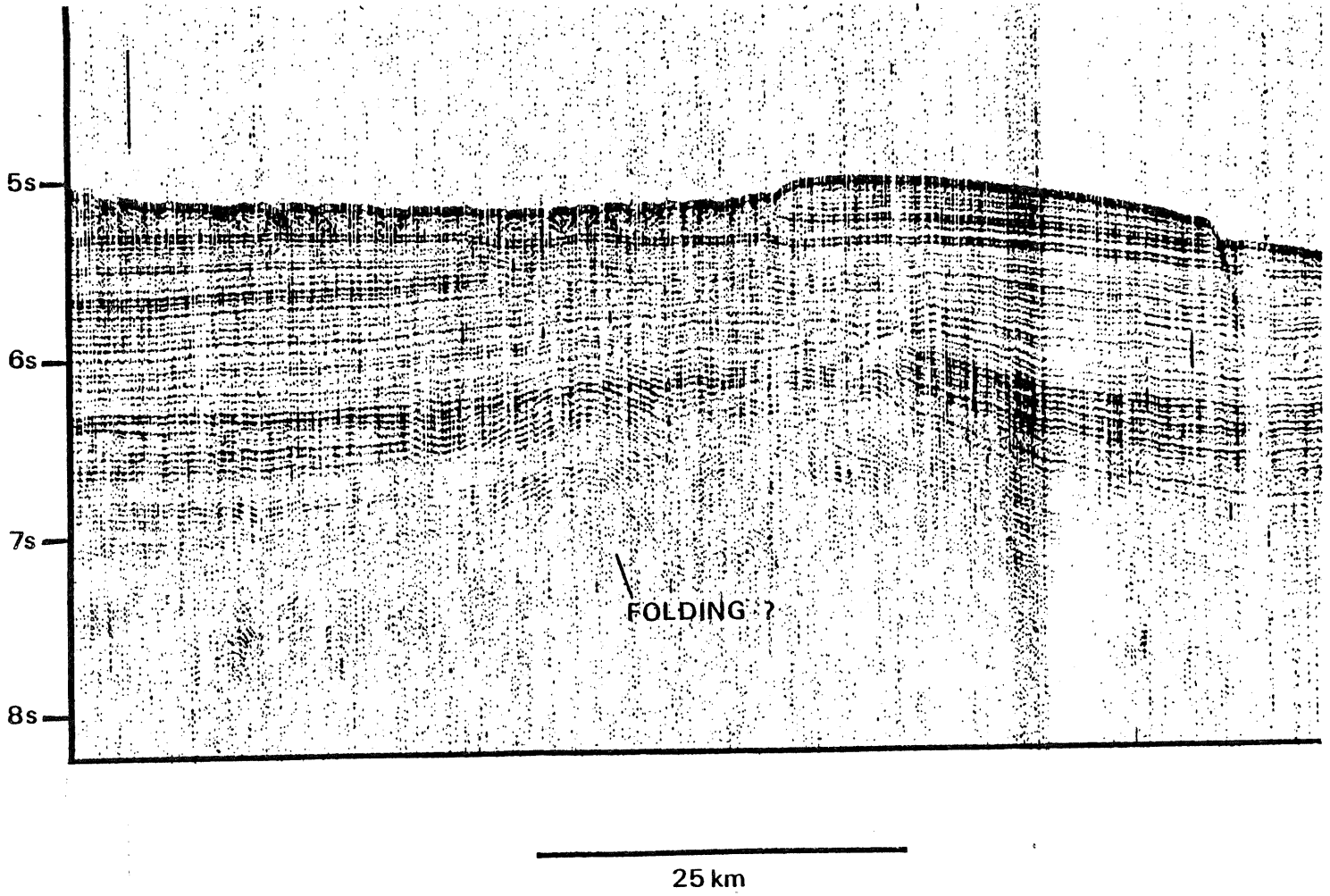
5s
6s
7s
8s
FOLDING ?
25 km

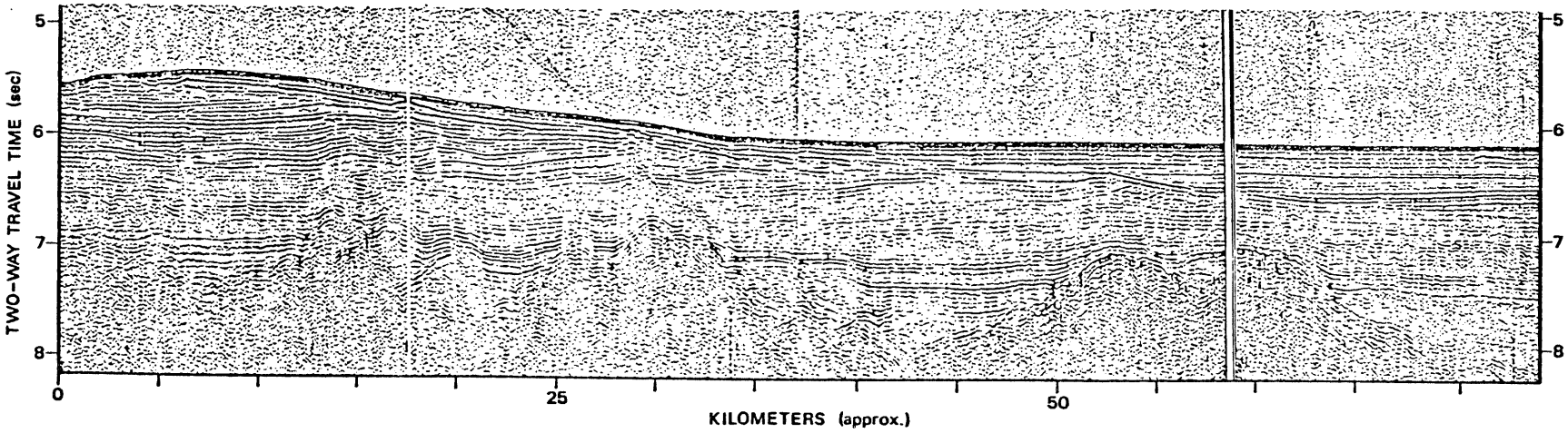

Figure 4.6

Expanded section, eastern end of Line 43.

upper 1 second of section (Fig. 4.5) suggests that both scouring and slumping have been and continue to be active agents in shaping the rise. Very similar sedimentary features seen in profiles across the continental rise off the eastern United States have been attributed to slumping and turbidity current activity (Emery and Uchupi, 1972) with penecontemporaneous and subsequent modification by contour-following bottom currents (Hollister and Heezen, 1972).

At 190 km on line 43 all reflectors above 5.5 seconds undergo a significant change in dip as they pass above a relatively transparent zone in the record (Figure 4.5). The cause of this very marked change is not known. One possible explanation is that the transparent zone represents a sedimentary ridge, like the Gardar or Eirik Ridge (Johnson and Schneider, 1969; Johnson et al., 1971), over which younger sediments are draped.

Figure 4.6 shows a less vertically-exaggerated view of the easternmost 170 km of line 43. This figure shows that the reflectors in the upper unit of the rise sequence take on a wavy form as they pass over a series of basement highs. The angular unconformity between the sediments of the rise prism and the younger turbidites may outcrop between 25 and 35 km. A prominent reflector at 7.5 seconds continues eastward beneath the turbidites.

4.1.3 Southern Newfoundland Basin (Profiles 39, 42D, 42L, 44, 46; Fig. 4.3c)

Profiles 39, 42D and 42L, from the southern survey area, illustrate the nature of acoustic basement and the typical sedimentary sequence of

the southern Newfoundland Basin.

This region is characterized by gently westward-dipping, rugged basement with average relief of about 0.5 seconds. Basement peaks up to 1.5 seconds high are observed on several profiles (one shown in Fig. 4.3c) in the eastern half of the survey area. The closer-than-average track-spacing here (10 km and less) permits correlation of these features between profiles; a NNE direction of elongation is indicated.

Lines 42D and 39 show basement shallowing abruptly to a smoother, bench-like feature at the eastern limit of the survey area. The eastern extent of this feature is not known. Three other seismic lines (Appendix V, Lines 40, 42F, 42J) also cross this scarp. Correlation between these profiles indicates that the scarp strikes 015° south of line 40; the strike north of this is unknown. Profile 39 also crosses the fracture zone which B. R. Hall (1977) identified on the basis of magnetic anomaly disruptions (40 km).

Line 42L, at the southern limit of the seismic coverage, shows rough basement extending west to about 50 km, where it abruptly becomes smoother and begins to deepen more rapidly. These changes may be related to volcanic activity on the SENR (smoothing basement relief) and sediment loading near the continental margin.

Profiles 44 and 46 provide coverage to the north and west, respectively, of the lines just described. From east to west on line 44 there are three zones of distinctly different basement topography: High-relief, relatively deep (500 to 360 km); smooth, shallow (360 km to 125 km); deep, blocky (125 to 0 km). The smooth shallow basement

in the central part of the record occurs in the region of the Newfoundland Seamounts, and is presumed to reflect modification of the original, high-relief surface formed at the ridge crest by subsequent seamount volcanism. The rugged topography on the eastern end of the line closely resembles basement topography on the USNS `Kane line north and east of the seamounts (Johnson et al., 1971; Fig. 4.2). Basement topographic zones on line 44 do not appear to correlate with those observed further south in the Basin.

Line 46 crosses basement structures very similar to those seen between 25 and 50 km on the western end of Line 44. Distinctive magnetic signatures are associated with these basement structures in both localities. On line 46 the basement highs observed between 25 and 40 km lie just east of a sharp 700-nT decrease in the magnetic anomaly. Basement is not visible west of this ridge.

Two prominent sedimentary reflectors observed throughout most of this region divide the sedimentary section into three units (Fig. 4.7).

Unit C, the oldest unit in the southern Newfoundland Basin acoustic stratigraphic sequence, occurs only where basement is deeper than 8 seconds (Fig. 4.11). The upper surface of this unit, reflector R_2, is generally quite flat, except for what appears to be draping over basement highs. However, significant dips are occasionally observed both on R_2 and on other reflectors within Unit C.

Unit B, the interval between R_1 and R_2, either directly overlies basement or unconformably overlies Unit C (Fig. 4.7). The reflectors within Unit B vary in strength from very weak to moderate and are essentially flat-lying. Disruption of upper Unit B reflectors near base-

Figure 4.7: Acoustic stratigraphic units.

4.7a: Definition of units, Line 42D.

4.7b: Illustrative sections, southern Newfoundland Basin.

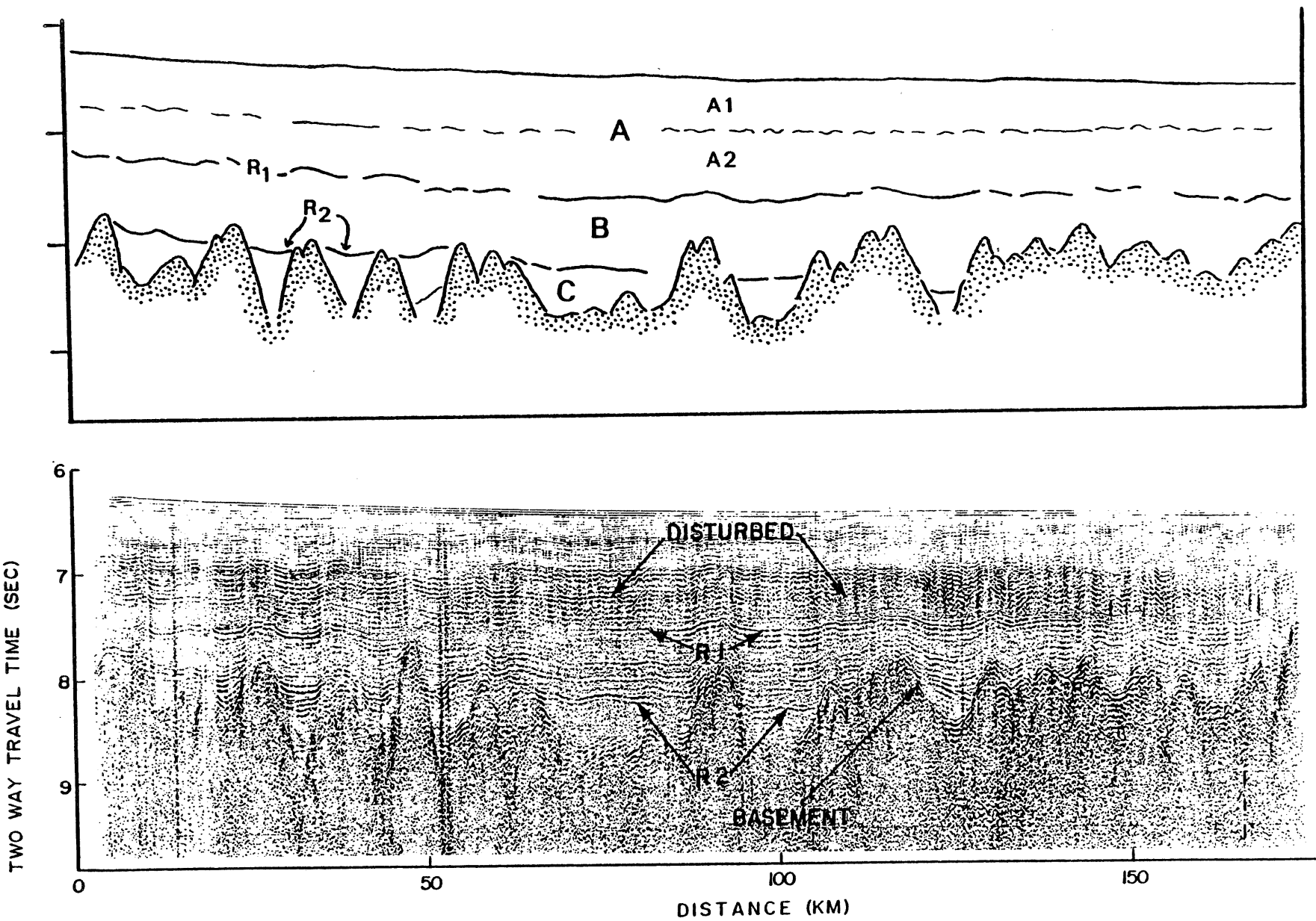
A1
A
A2
R1
R2
B
C
DISTURBED
R1
R2
BASEMENT
TWO WAY TRAVEL TIME (SEC)
6
7
8
9
0
50
100
150
DISTANCE (KM)

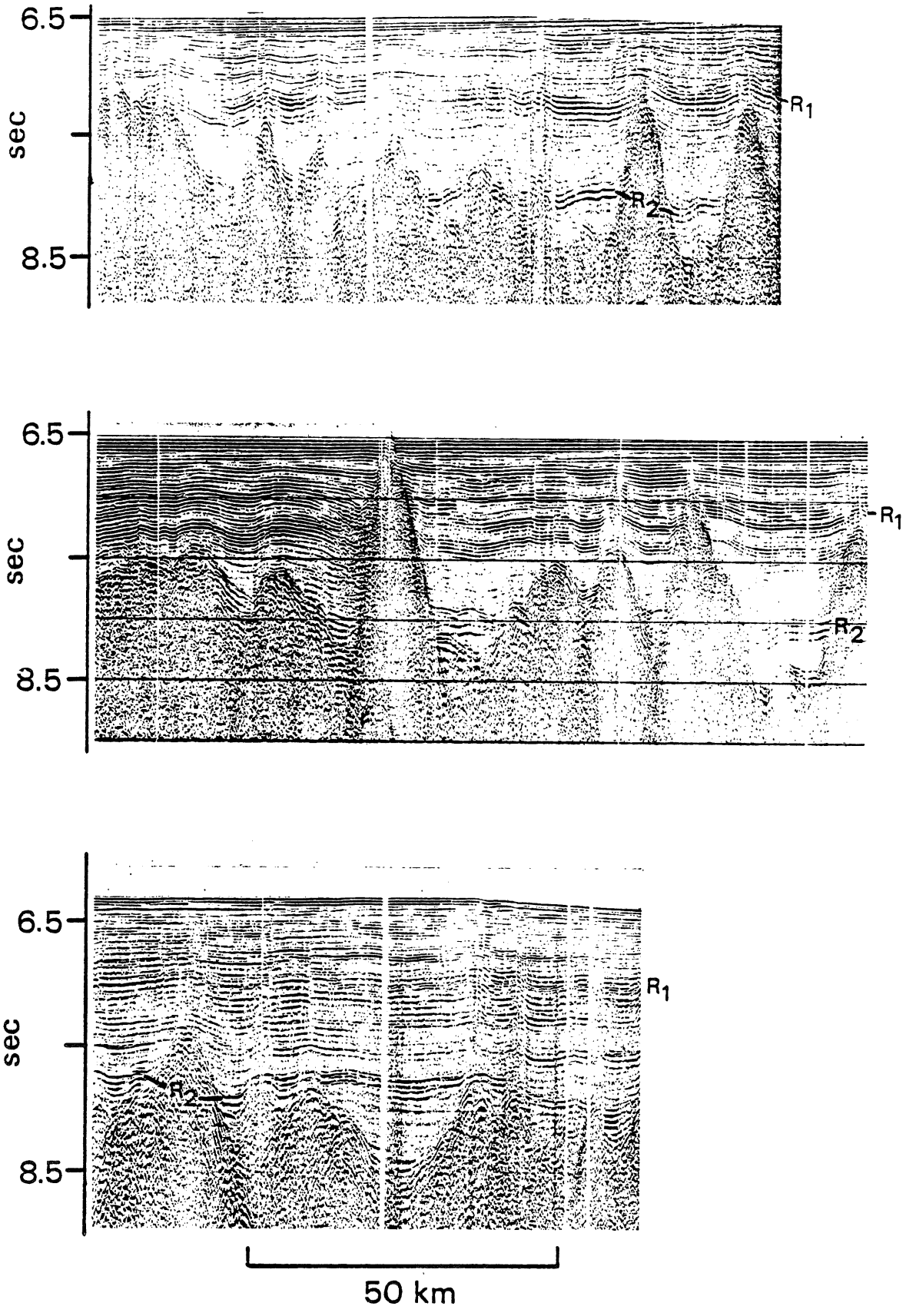
6.5
sec
8.5
R1
R2
6.5
sec
8.5
R1
R2
6.5
sec
8.5
R1
R2
50 km

ment highs might be due to: a) acoustic effects alone, b) depositional draping or post-depositional differential compaction, or c) bottom-current effects near topographic features.

Unit A is the final section in the sequence (Fig. 4.7). It appears to unconformably overlie Unit B in most places; occasionally it rests directly on basement. A relatively strong reflector occurs near or above the mid-point of Unit A, and several profiles show evidence of an angular discordance between the sections above and below this horizon; an upper (A1) and lower (A2) section of Unit A are thus distinguished. Most of Unit A is well-stratified, and the wavy or disrupted character of the reflectors suggests that bottom-currents exerted a significant influence upon deposition. These characteristics are accentuated in the vicinity of basement and seafloor topographic features such as the SENR and the basement scarp in the south-eastern part of the area. The recent activity of down-slope bottom currents (turbidity currents) in this area is indicated by the discovery of a network of shallow channels on the seafloor (Section 3.2). Horizontal or contour-following bottom currents related to those described off the eastern United States by Hollister and Heezen (1972), Emery and Uchupi (1972) and others may also be involved in controlling sedimentation here.

Tentative correlation of Units A, B and C with the sedimentary units observed on reflection profiles across the Newfoundland Basin continental margins (Fig. 4.3a, b) can be made on the basis of the depth to reflecting horizons and the distinctive characteristics of Unit A. Using Line 38C (Fig. 4.3b) as an example, Unit C can be correlated with the sediments beneath the 7.0-8.0 second reflector (0-50 km), Unit B with

the section between this horizon and the 6.5 second reflector (0-75 km) and Unit A with the overlying stratified and wavy-laminated units. This correlation is supported by the similarity in the velocity structures measured at expendable sonobuoy stations near the margin and in the southern Newfoundland Basin.

4.1.4 SENR and Spur Ridge (Profiles 42M, 42N, 11A, 28; Fig. 4.3d)

The nature of the Spur Ridge and the SENR is illustrated by profiles 11A (Renwick, 1973) and 28 (H. R. Jackson et al., 1975), respectively.

The Spur Ridge at the crossing of line 11A is 40 km wide, and is underlain by a basement ridge about 1.5 sec. high. Northwest of the ridge relatively flat basement lies beneath about 1 second of sediment; the flank of one of the Fogo Seamounts (J. M. Hall et al., 1977) can be seen at the very end of the profile. Shallower and rougher basement is observed to the southeast of the ridge. Up to one second of sediment caps the ridge. One strong reflector is observed immediately above basement, but the remainder of this unit shows little internal structure.

Line 28 shows that the SENR is also a structurally-controlled basement and sedimentary feature. The seafloor to the southwest is 700 m deeper than that to the northeast, although no offset in basement depth is apparent. Faults on the northeastern side exhibit the greatest throw (up to 2 seconds).

Three distinctive units comprise the sedimentary cover of the SENR on Line 28 (Fig. 4.8). The strongest reflector in the section ("PR")

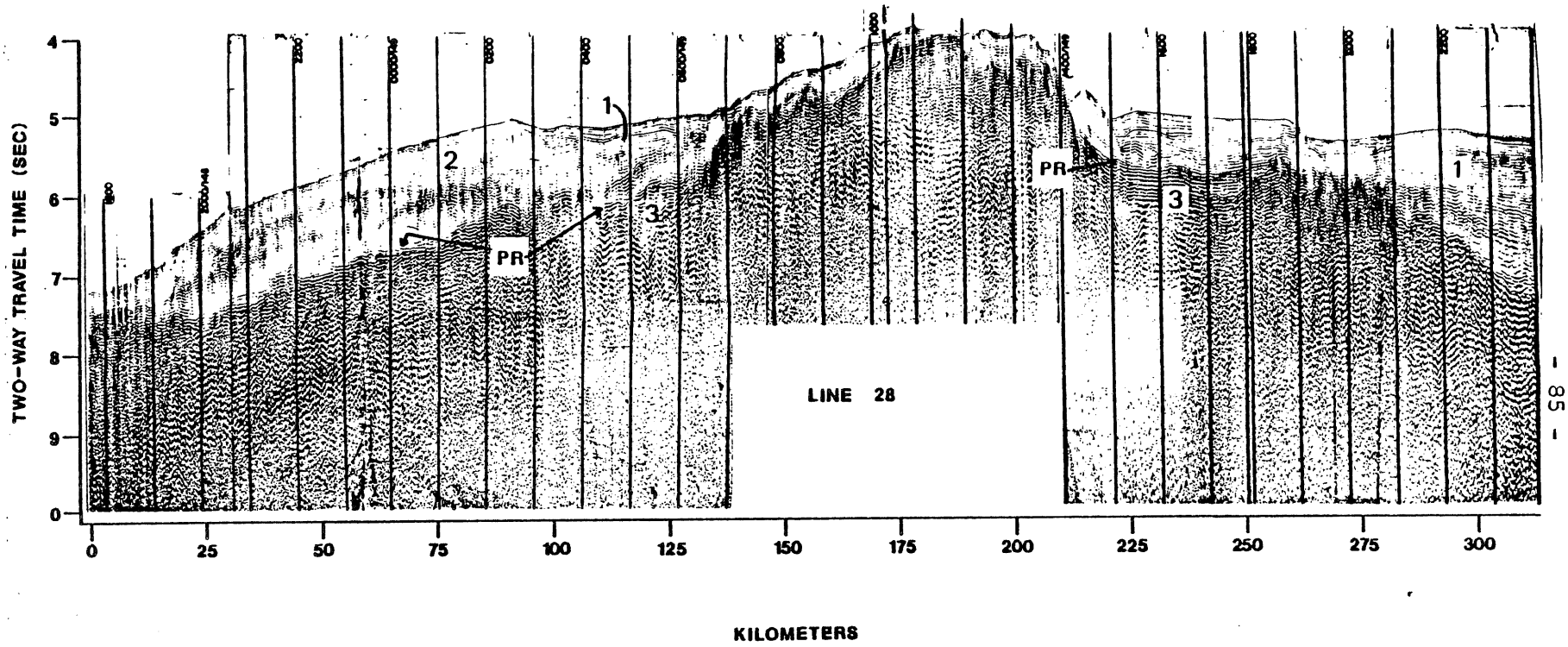

Figure 4.8
Sedimentary units on the SENR
PR=prominent reflector; 1, 2 and 3 are units
referred to in the text.

is observed just above basement and in small sediment ponds perched on the ridge flanks. The sediments which unconformably overlie this prominent deep reflector on the southwestern flank of the ridge (Unit 2) are characterized by wavy or disrupted reflectors. The contact between Unit 2 and the more coherently laminated sediments of the abyssal plain to the southwest is not shown by the seismic record; to the northwest Unit 2 wedges out against an irregular reflector near the crest of the ridge. No acoustically similar unit is seen on the northeastern ridge flank.

On the southwest flank of the ridge, the youngest unit in the section (Unit 1) occurs in a small depression within Unit 2 (at 130 km). Acoustically similar sediments unconformably overlie reflector PR or basement on the northeastern flank. The wavy form of the relatively continuous reflectors in Unit 1 and the evidence of scouring adjacent to the basement scarp at 225 km may indicate that significant bottom-current activity is occurring here.

Profile 42N shows an oblique section across the western flank of the Spur Ridge. Basement deepens rapidly coming down off the ridge (115-60 km) and two large basement highs (buried seamounts ?) are observed at the southwest end of the profile. A prominent, nearly flat-lying reflector (PR) is observed in both of the sediment ponds crossed by Line 42N. As on Line 28, the sediments overlying PR (Unit 2) are wavy laminated and there is evidence for recent current activity near the basement highs (i.e. the apparently erosional seafloor scarp at 30 km).

Profile 42M crosses the northeastern flank of the SENR at a low angle, providing a section approximately normal to that of Line 28 and a tie line with the southern Newfoundland Basin profiles (Fig. 4.1). The smooth character of basement along this line and the prominent basement high at 100 km are noteworthy. The particularly high-amplitude magnetic anomaly associated with the latter feature has been correlated with the J-anomaly (B. R. Hall, 1977; C. E. Keen et al., 1977; Chapter 5.)

Sedimentary reflectors R_1 and R_2 can be traced continuously from Line 42L onto Line 42M (these are actually sections of a continuous profile). The reflector identifications are shown at the eastern end of Line 42M. It appears that R_1 fades and then pinches out on basement or older strata between 110 km and 130 km, and R_2 terminates near 135 km. Reflector PR, observed in the sediment pond between 25 km and 90 km on Line 42M (the same pond is crossed by Line 28, 225-260 km) and elsewhere on the SENR and Spur Ridge (Profiles 11A, 11B, 42M), is believed to be correlative with reflector R_2; the expendable sonobuoy results presented below support this. The wavy-laminated character of the sedimentary units above PR suggests that these are correlative with Unit A. The absence of Unit B may indicate that the tectonism which produced the SENR and Spur Ridge was occurring during the time represented by Unit B in the Newfoundland Basin proper. It is quite probable that this represents the Early Cretaceous tectonism on the Grand Banks (Sections 2.1.2, 2.1.3).

4.1.5 Newfoundland Seamounts (Profiles 30, 31, 36, 37, Fig. 4.3b,e)

The general point demonstrated by the seismic profiles in Figure

4.3e is that the Newfoundland Seamounts are constructional volcanic features whose flanks are acoustically continuous (within the limits of resolution of the reflection techniques) with oceanic basement as identified by H. R. Jackson et al. (1975) and by sonobuoy results reported below.

Unfortunately, none of the profiles extends sufficiently far from the seamount summits to permit thorough study of basement and sedimentary structures associated with the seamounts. Nevertheless, several interesting points emerge from examination of these records.

Three of the four profiles show an offset in basement depth across the seamounts (the fourth profile only shows one flank of the seamount). In profiles 36 and 37 deeper basement lies to the northwest, whereas profile 31 shows deeper basement to the southeast.

Profiles 30 and 37 cross what appear to be steeply-dipping faults of considerable throw (1 km, assuming 3.0 km/sec sediment velocity in the deep sediments) in basement southeast and south of the seamounts profiled.

The central and western seamounts (Scruncheon and Touten, profile 31; Screech and Number 1, profile 36) have clearly exerted a strong influence on continental rise sedimentation. Profile 31, north of Scruncheon Seamount, gives particularly clear evidence of this. Note the thick accumulation of wavy-laminated sediments and the evidence of scouring at the intersection of the seamount flank and the seafloor.

4.2 Expendable Sonobuoy Results

Expendable sonobuoys provide valuable information on true sediment

TABLE 4.2
EXPENDABLE SONOBUOY RESULTS

ESB no.	lat N / long W	velocity + km/sec	thickness° km	remarks	ESB no.	lat / long	velocity	thickness	remarks
21*	40°10.0'	1.50	5.25	water	28*	41°47'	1.50		incomplete;
	40°49.0'	2.20	1.08	assumed		47°41'	2.14		lack of data
		3.75	0.53	reflector			5.36		
		5.43		refractor					
					49	41°56'	1.50	3.30	water
22*	40°20.0	1.50	4.57	water		48°46'	1.95	0.25	reflector
	49°34.0'	2.09	1.44	reflector			1.71	0.35	reflector
		3.95	0.84	reflector			2.51	1.14	refractor
		4.96		refractor			2.90		refractor
23*	40°30.0'	1.50	4.02	water	50	41°35'	1.50	4.20	water
	49°24.0'	1.94	1.24	reflector		50°30'	2.60	2.00	reflector
		3.70	1.49	assumed			incomplete section		
		5.67		refractor			4.64a		refractor
							6.58a		refractor
27*	41°30'	1.50	3.74	water	48	41°28'	1.50	4.40	water
	48°06'	2.14	0.99	reflector		47°04'	2.40	2.30	reflector
		3.80	0.88	assumed			incomplete section		
		4.95		refractor			5.69		refractor
							6.06a		refractor
							7.96a		refractor
				EASTERN GRAND BANKS MARGIN					
33*	44°17'	1.50	3.79	water	35	44°33'	1.50	3.61	water
	48°05'	1.64	0.66	reflector		47°43'	1.73	0.50	reflector
		2.60	1.28	reflector			2.38	2.13	reflector
		3.43	2.23	reflector			2.80	2.59	reflector
		5.82		refractor			6.25		refractor
34	45°12'	1.50	0.07	water					
	49°14'	2.03	0.91	refractor					
		4.78		refractor					
				NEWFOUNDLAND BASIN					
29*	42°30'	1.50	4.71	water	40	45°57'	1.50	4.20	water
	45°43'	2.12	1.48	reflector		44°03'	1.95	1.18	reflector
		3.60	1.53	assumed			2.10	0.89	reflector
		5.23		refractor			3.07	0.72	refractor
32*	42°27'	1.50	4.74	water			4.60		refractor
	45°20'	3.09		reflector			6.7a		refractor
		5.55		refractor					
					41	45°50'	1.50	4.19	water
36	43°32'	1.50	4.99	water		44°24'	1.88	0.39	reflector
	43°24'	1.83	0.27	reflector			2.18	0.77	reflector
		2.08	0.80	reflector			2.86	0.86	reflector
		2.98	0.42	reflector			3.00	1.08	assumed
		3.16	0.45	reflector			3.99		refractor
		5.50		refractor			5.01a		refractor
							6.60a		refractor
37	43°54'	1.50	4.80	water					
	43°44'	1.64	0.36	reflector	45	41°36'	1.50	4.88	water
		incomplete section				44°24'	1.80	0.70	reflector
		4.40a		refractor			2.50	1.50	reflector
							3.52	0.61	refractor
38	43°52'	1.50	4.80	water			6.26		refractor
	43°56'	1.76	0.28	reflector					
		2.50	1.29	reflector	46	42°11'	1.50	4.65	water
		6.3		refractor		45°54'	1.86	0.44	reflector
							2.42	0.61	reflector
39	45°03'	1.50	4.78	water			6.70a		refractor
	43°04'	1.80	0.52	reflector			7.50a		refractor
		2.70	0.79	reflector					
					47	41°00'	1.50	4.89	water
42	45°25'	1.5	4.61	water		43°27'	1.88	0.52	reflector
	44°18'	1.8	0.49	reflector			2.26	1.08	reflector
		2.4	0.69	reflector			3.37	0.71	refractor
							4.55		refractor

+ standard deviation less than 0.05
° standard deviation less than 0.02
* H. R. Jackson et al. (1975)

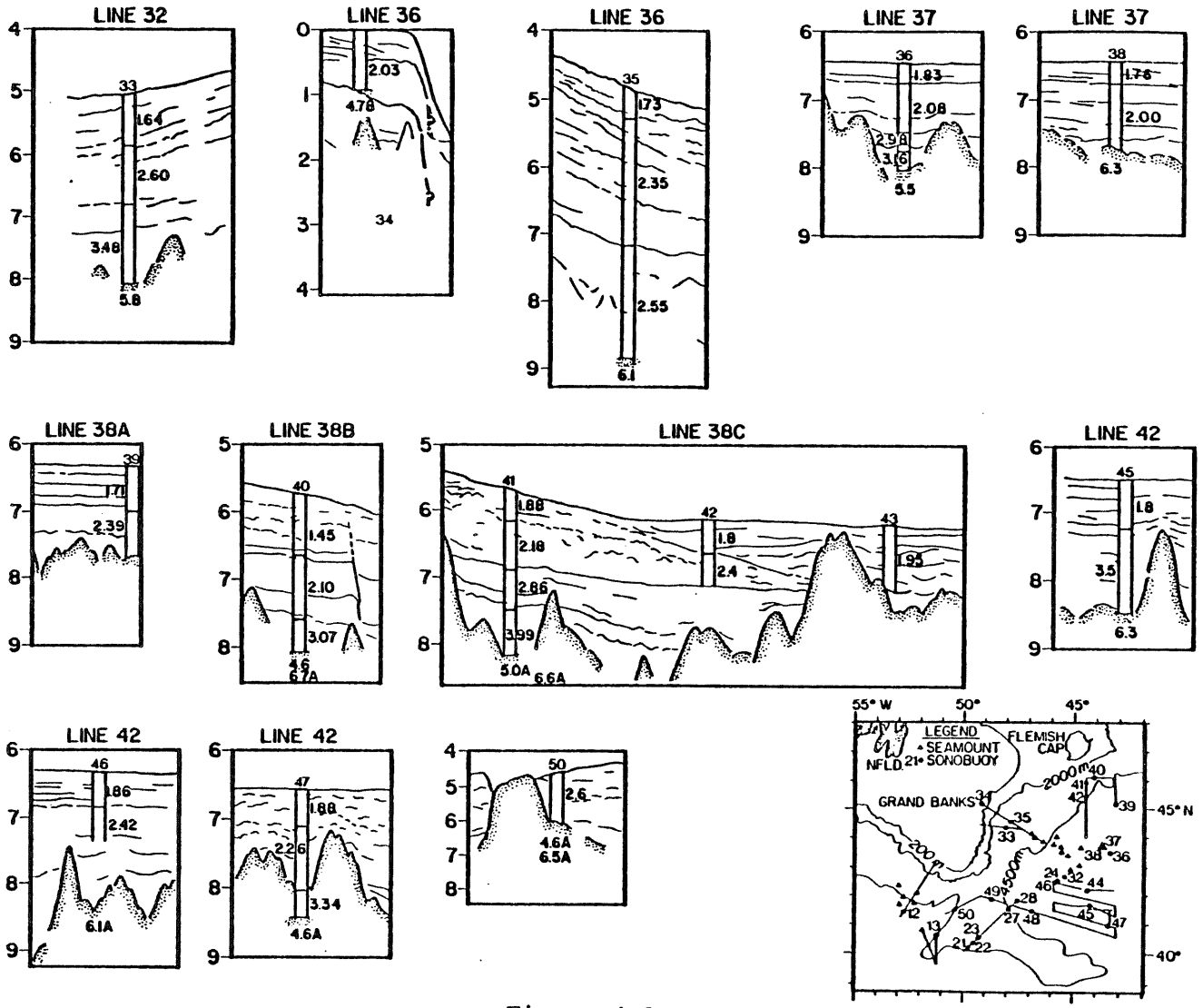

Figure 4.9

Expendable sonobuoy results

observed above the reflector PR on the vertical-incidence records (Units 1 and 2, Fig. 4.8). The lower interval measured on these sonobuoy records corresponds to Unit 3 (Fig. 4.8) and has velocities 2.9-3.0 km/sec. This compares quite well with the range of velocities measured for Unit C in the southern Newfoundland Basin and so supports the correlation of reflectors PR and R_2.

Sonobuoys 33, 35, 40 and 41 (Fig. 4.9) show that the Eastern Banks and Flemish Cap upper continental rise sections contain 4-5 km and 2-3 km of sediment, respectively. The interval velocities determined at these sonobuoy stations correlate moderately well with the three velocity ranges given in Table 4.3, suggesting that R_1 and R_2 may in fact correspond to the reflectors indicated on these sections in Fig. 4.9.

Only one sonobuoy was deployed on the Grand Banks (sonobuoy 34). A single sediment unit 0.91 km thick, with a velocity of 2.03 km/sec, was measured at this station.

4.2.2 Basement

Basement velocities were measured at 22 expendable sonobuoy stations in the Newfoundland Basin and on the SENR, and at one station on the Grand Banks (Fig. 4.10). Refractors with velocities of 4.4 km/sec to about 5.6 km/sec were generally associated with reflections from the upper surface of basement observed on the vertical-incidence reflection profiles. Velocities greater than 5.6 km/sec, in the range 6.1-8.0 km/sec, are associated with an unseen interface beneath base-

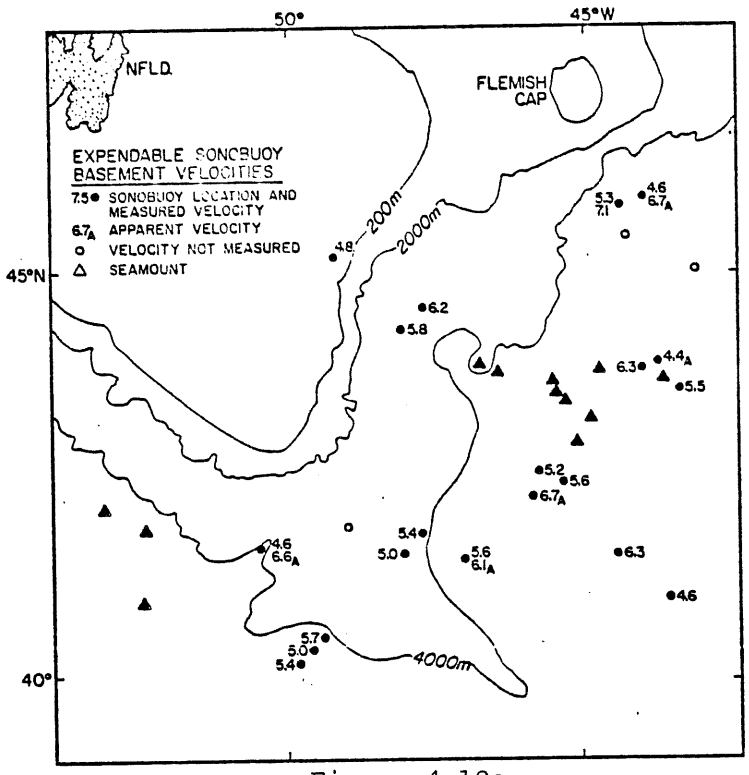

Figure 4.10a
Expendable sonobuoy basement velocities.

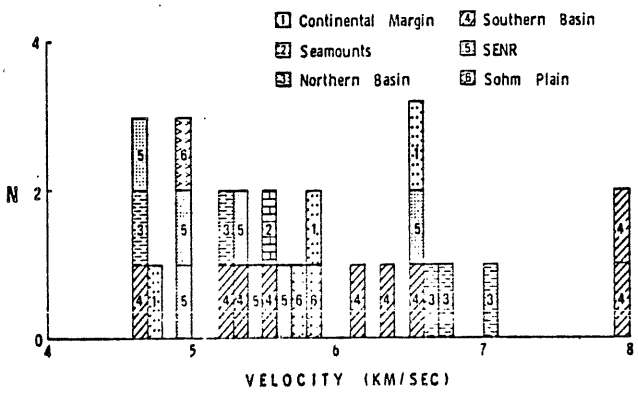

Figure 4.10b
Expendable sonobuoy refractor velocities.

ment. Figure 4.10 gives apparent velocities where the depth to the top of the refracting half-space is unknown or where complex topography on this surface prevented calculation of a true refractor velocity.

The basement velocities alone provide little indication of changes in crustal structure. The measured velocities are consistent with velocities reported for a wide variety of oceanic and continental lithologies (Press and Beckmann, 1954; Sheridan and Drake, 1968; Christensen and Salisbury, 1973) and no geographic variation in velocity is apparent (Fig. 4.10). Section 8.1 discusses the basement velocity data in further detail, using magnetic data in conjunction with these results and previously published seismic data to permit interpretation of the velocities in terms of oceanic and continental crustal regimes.

4.3 Summary

It is worthwhile to review briefly the most significant points brought out in the preceding sections and to clarify the geographic relations between the major features identified on the seismic profiles (Fig. 4.11).

Basement on the Eastern Banks margin is truncated by a fault beneath the shelf edge and, in general, cannot be seen beneath the thick sediment of the continental slope. A basement high (without prominent geophysical signature) observed near the slope-rise transition marks the seaward limit of shelf and slope sediment units.

The Flemish Cap continental slope at line 54 appears to be an exposed, faulted basement surface; recovery of Devonian rocks in a

dredge haul from the southern face of the Cap (Ruffman and van Hinte, unpubl.) supports this observation.

A basement high with about 3 km of relief (estimated using sonobuoy 44 results) underlies the continental rise approximately 120 km south of the Flemish Cap shelf break. This Flemish Cap Ridge strikes 060° between Lines 38C and 38A and is associated with two important boundaries: The transition from smooth (toward Flemish Cap) to disturbed (toward the Basin) magnetic field signature and the seaward limit of the base-of-slope grabens and the Flemish Cap wedge.

Lines 39-46 tie in directly with crustal refraction Line 7 (H. R. Jackson et al., 1975). Basement on these lines correlates with the top of oceanic layer 2 measured on Line 7.

Several distinct structural fabrics are observed in the southern part of the Newfoundland Basin (Fig. 4.11): Rough, deep basement in the southern and western areas of the Basin; rough, shallow basement northeast of the seamounts and along the eastern end of line 44; smooth, shallow basement at the eastern limit of the detailed survey area in the southern Basin and along line 44 in the seamount region; deep, block-faulted basement beneath the continental rise, associated with a smooth magnetic signature; block-faulted basement beneath the SENR; constructional volcanic basement features (buried and emergent seamounts) that pre-date most or all of the sediment cover.

Three sedimentary units are recognized in the Southern Basin on the basis of both sonobuoy and vertical-incidence reflection results. Units B and C, beneath reflectors R_1 and R_2, respectively, are essen-

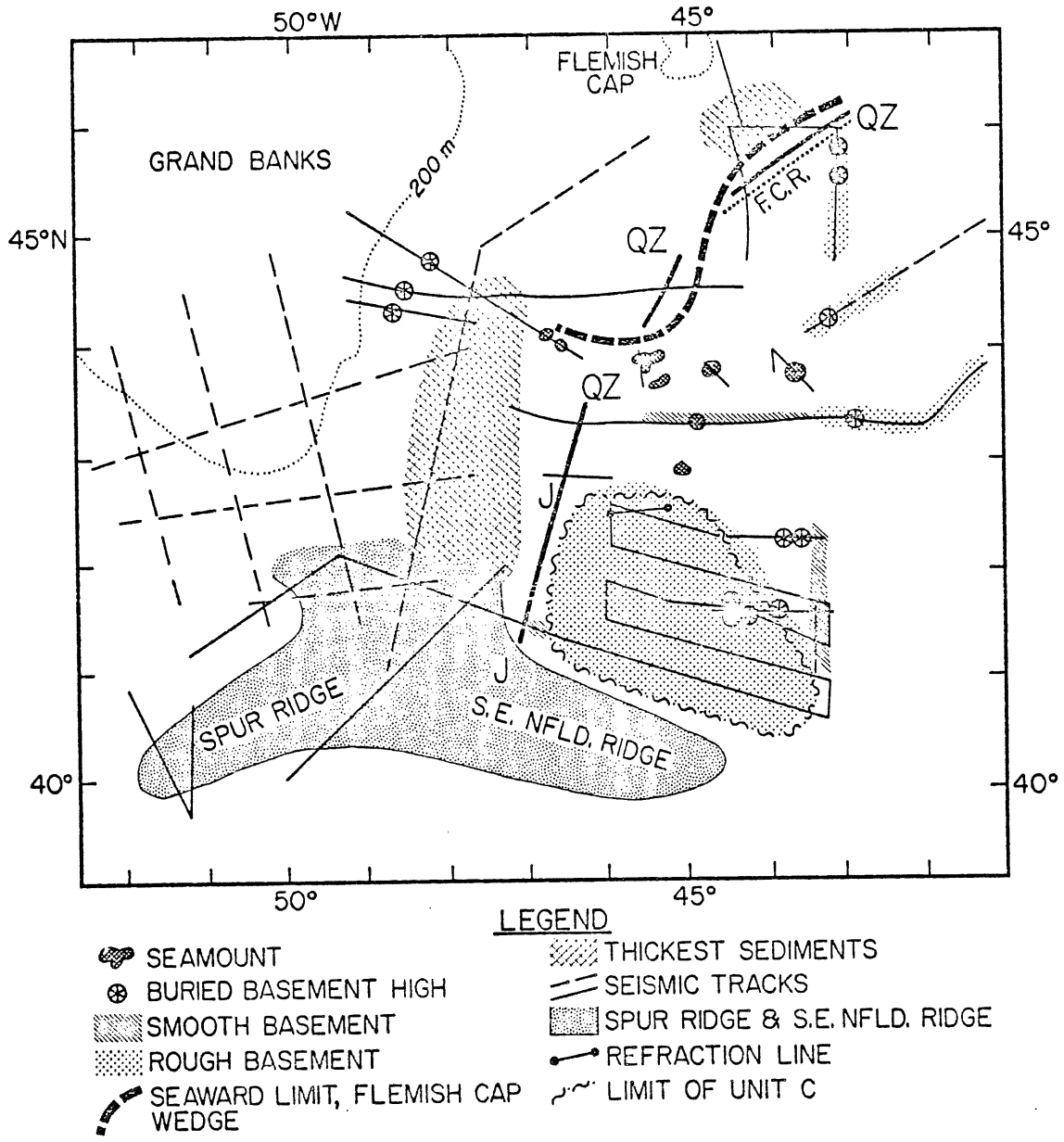

Figure 4.11

Synopsis of seismic reflection results.

tially flat-lying sediments that fill in basement relief; Unit A, the interval between the seafloor and R_1, thickens and grades into a wavy-laminated facies toward the continental margins and SENR.

Correlatives to these units have been tentatively identified on the continental margin seismic profiles. Particularly thick sections beneath the presumed R_2 reflector are observed in deep troughs beneath the upper rise on the Eastern Banks and Flemish Cap margins. The point at which these units and the presumed Unit B correlatives pinch out on basement highs to the east and south (75 km on Line 38C; 260 km on Line 43) is coincident with the change from a smooth to a disturbed magnetic field character. The two youngest units in the section along the margins are considered to be members of Unit A. The older unit (the Flemish Cap Wedge) displays a complex internal structure, with wavy-laminated or disturbed reflectors and numerous wedgeouts and angular discordances. Well-stratified sediments (distal turbidites) unconformably overlie the Flemish Cap wedge to the east and south.

On the SENR and Spur Ridge expendable sonobuoy results indicate that reflector R_2 is correlative with a strong, flat-lying reflector ponded between basement highs (reflector PR). No correlative to Unit B is observed on the ridges, presumably because of tectonism related to the formation of these structures and uplift of the southwestern Grand Banks in Early Cretaceous time (Chapter 2, Jansa and Wade, 1975).

4.4 Correlation of Acoustic Stratigraphy

The acoustic stratigraphy outlined above will be much more useful in clarifying the evolution of the Newfoundland Basin if some litho-

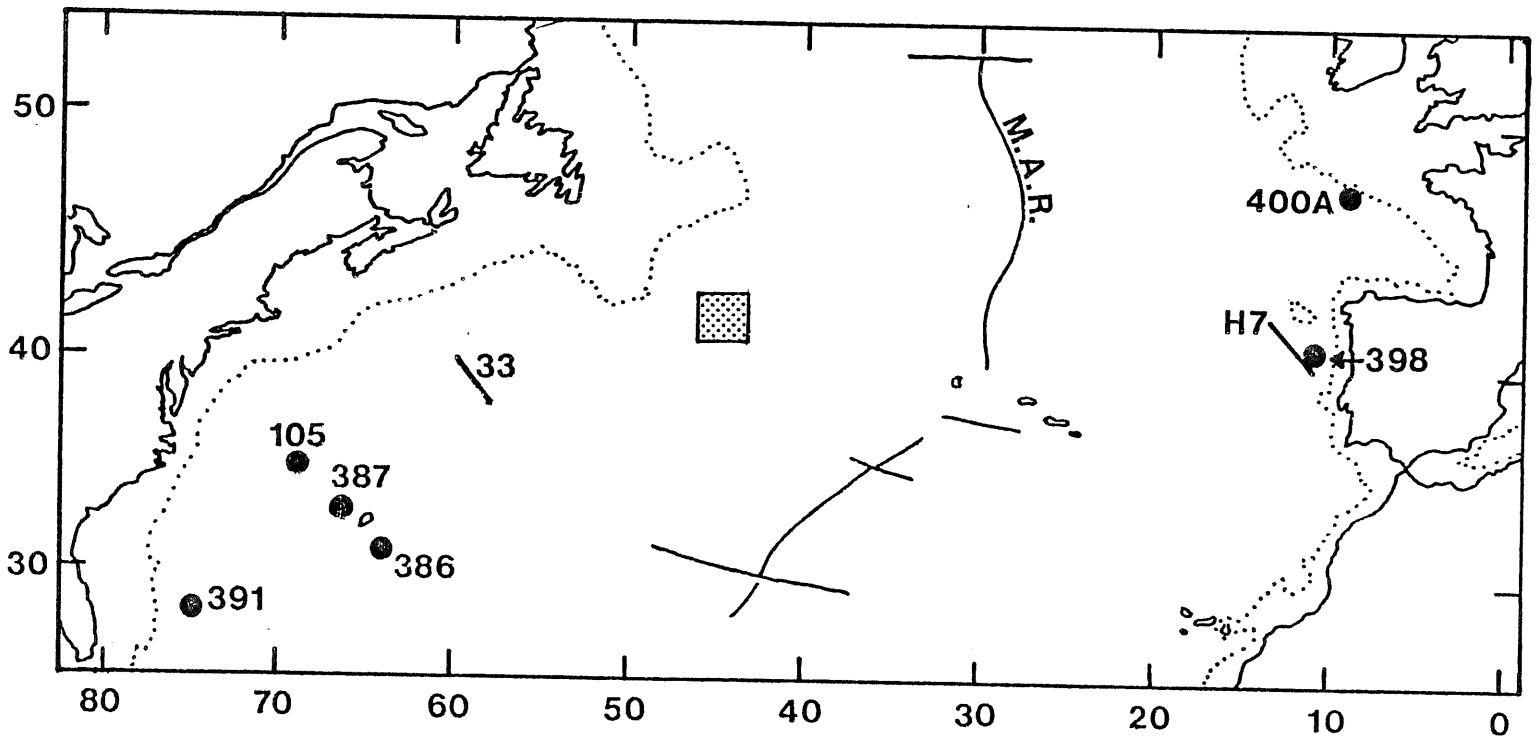

Figure 4.12

Location map, DSDP Sites and seismic profiles for acoustic stratigraphic correlation. Stippled square is type locality for Newfoundland Basin section (southern survey area). 2,000 m contour shown.

logic and chronologic identifications can be made. The only units in the succession which have been sampled thus far are acoustic basement, which dredge hauls show is basaltic in the area of the seamounts, and the sedimentary cap on Shredder Seamount. The age and nature of the other units in the succession and possible changes in the nature of basement near the continental margins must be inferred by analogy with related areas where both seismic and direct sample control are available. The areas examined in this section are the Bay of Biscay-Iberian margin and the Northwest Atlantic south of the SENR (Fig. 4.12). The implications of these correlations for the relationship between seismic horizons in the Newfoundland Basin and on the Grand Banks are also examined.

It is worthwhile to emphasize at the outset that this type of comparison between widely separated areas provides at best a general indication of possible ages and lithologies in the section. Lithologic correlations are particularly problematic since, even in the earliest stages of seafloor spreading, the Newfoundland Basin was physically separated from the two comparison areas by the ancient Mid-Atlantic Ridge and the Newfoundland Fracture Zone.

4.4.1 Iberia-Bay of Biscay

DSDP Sites 398 (Ryan, Sibuet et al., 1976) and 400 A (Montadert, Roberts et al., 1976) have been chosen as the points of comparison on the Iberian and Biscay margins (Fig. 4.12). Thick sections were drilled at both sites, with 398 bottoming in Hauterivian limestone and mudstone and 400A bottoming in carbonaceous mudstones of Aptian-

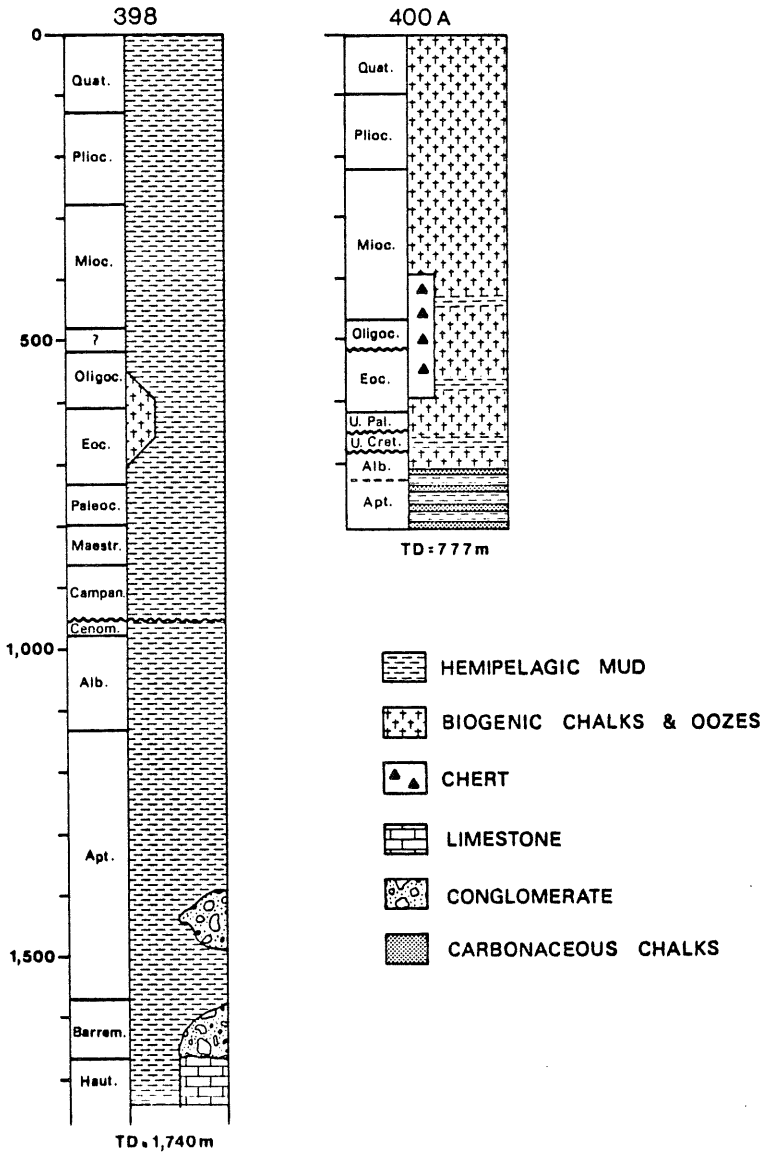

Figure 4.13

Stratigraphy at DSDP Sites 398 and 400A.

TABLE 4.4

Groupe Galice designation (velocity)	Acoustic Characteristics	Site 398 correlative	Newfoundland Basin correlative (velocity)
Acoustic basement (> 4.0 km/s)	- diffractant	none	Basement (> 4.8 km/s)
Formation 4 (2.5-3.5 km/s)	- strong upper reflector - fills in basement relief - relatively thin; hard to distinguish from basement - layering conformable with acoustic basement - some tectonic dips	Haut.-Apt. limestones and marls, passing upward into turbidites	Unit C (3.0-4.0 km/s)
Formation 3 (2.2-2.9 km/s)	- transparent to slightly stratified - fills relief; top nearly level - only depositional dips	Alb.-Cenom. "black shales" (claystones; below CCD)	Unit B (2.2-2.9 km/s)
Formation 2 (1.9-2.1 km/s)	- stratified with several internal reflectors - generally flat-lying, some inclined bedding (due to current activity?)	Maestr.-Olig. turbidites varying carbonate content	Unit A (1.9-2.1 km/s)
Formation 1 (1.9-2.1 km/s)	- inclined bedding common - 1a = upper transparent section - 1b = lower stratified section	Olig.-Present chalks and nanno ooze	

Albian age (Fig. 4.13). Correlation of seismic data in the vicinity of Site 398 with the drilled section, given by Groupe Galice (1977), provides the final element required for the present analysis.

Table 4.4 compares the acoustic stratigraphy of the Newfoundland Basin with that found west of Iberia. The correlation between the acoustic and drilled sections off Iberia, according to Groupe Galice (1977), is also shown. The similarities between the two acoustic stratigraphic sections (Fig. 4.14) are quite strong, so this comparison can be regarded as reasonably reliable. However, because of the increasing geographical separation of Iberia and the Newfoundland Basin through time, the lithological correlations become progressively less reliable toward the top of the section.

4.4.2 Northwest Atlantic

The acoustic and litho-stratigraphy of the Northwest Atlantic are now rather well known. Houtz and Ewing (1964) describe the velocity structure of the sedimentary succession on the basis of numerous expendable sonobuoy measurements at stations distributed throughout the North Atlantic. Two prominent reflectors, Horizons A and β, are nearly ubiquitous. The seafloor-Horizon A and Horizon A-Horizon β intervals are characterized by velocities of 1.6-2.2 km/sec and 1.7-2.9 km/sec, respectively, according to Houtz and Ewing (1964). Velocities below β are in the range 2.7-3.7 km/sec. H. R. Jackson *et al.* (1975) observe a similar velocity structure at sonobuoy stations on the Sohm Abyssal Plain.

The acoustic properties of the Northwest Atlantic and Newfoundland Basin sedimentary sequences are compared in Figure 4.15 and Table 4.5. The agreement between both the seismic profile and the sonobuoy data from each area is very good, indicating that R_1 and R_2 in the Newfoundland Basin likely do represent seismic Horizons A and B, respectively.

Deep Sea Drilling Project (DSDP) drilling in the western North Atlantic provides lithological identifications for these acoustic units and reflectors. However, drilling at numerous sites has shown that seismic Horizons A and β vary significantly in age and nature throughout the area. Tucholke and Mountain (1977) show that seismic "Horizon A" is actually one or more of a group of reflectors, which they term the Horizon-A Complex. The reflectors in this group range in age from Middle Eocene to Late Oligocene. Four consistently-observed and well-defined reflectors are identified and correlated with specific lithologies as follows (Tucholke and Mountain, 1977): Horizon A^v (Late Oligocene) is the top of a volcaniclastic turbidite sequence; Horizon A^t (Middle-Upper Eocene), observed west of Bermuda, marks the top of a siliceous turbidite unit; Horizon A^u (post-Middle Eocene) is an angular unconformity which truncates Horizons A^t and A^v and progressively older strata westward; Horizon A* (Late Maestrichtian) occurs well below the other reflectors in the complex and represents a thin calcareous unit. (The term "Horizon A", referring to the seismic horizon associated with one or all of these reflectors, will be retained in this section, since the concern here is with general identifications of acoustic horizons. It should be noted, however, that several distinct reflectors are often observed immediately below R_1 in the Newfoundland Basin and these may

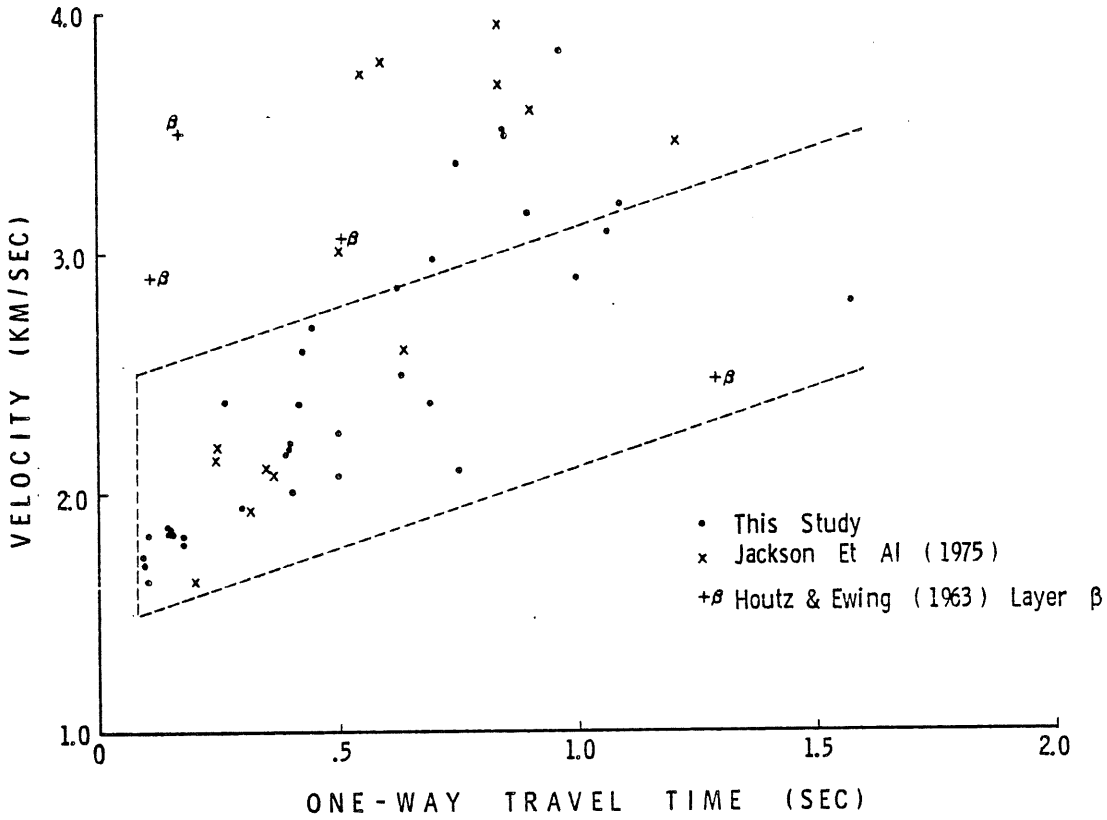

Figure 4.15

Comparison of velocity-depth relations in the Newfoundland Basin and Sohm Abyssal Plain. Dashed line indicates area in which interval solutions for units above Horizon β plot, after Houtz and Ewing, 1964.

TABLE 4.5

THIS STUDY

Unit	Velocity (km/sec) avg.	range	Thickness (km) avg.	range
A	1.77	1.6-2.0	0.9	0.5-1.5
B	2.4	2.1-2.5	1.5	0.6-2.3
C	3.25	3.0-3.5	1.0	0.4-2.2

HOUTZ & EWING (1964)

	Unit	Velocity
1.	Unconsolidated Tertiary sediments	1.6-2.2
2.	Semiconsolidated Upper Cretaceous sediments	1.7-2.9
3.	Lower Cretaceous and older consolidated sediments	2.7-3.7

be correlative with specific reflectors within the Horizon-A complex.)

The nature of Horizon β has also been clarified by DSDP drilling. Mountain and Tucholke (1977) show that β at most DSDP sites marks the change from Hauterivian limestones to Barremian black clays. At DSDP Site 4, however, this transition is significantly younger (Late Cretaceous). As additional evidence that Horizon β is diachronous, Mountain and Tucholke (1977) point out that the β reflector pinches out to the east against basement of approximately Hauterivian age (M11-M4) north of Bermuda and against younger basement of Barremian age (M4-M2) south of Bermuda.

The four Northwest Atlantic DSDP sections chosen for the present comparison (Figure 4.12; Ewing, Hollister et al., 1972; Benson, Sheridan et al., 1975; Tucholke, Vogt et al., 1975) illustrate the regional variability in Horizons A and β (Fig. 4.16). Except for the variation in the age of Horizon β, the lithology of the pre-Horizon A sections at all four sites is quite similar. Strong similarities also exist between the pre-Horizon A sediments at these Atlantic sites and those drilled at Sites 398 and 400A, described above. Very pronounced differences in lithology appear in the post-Horizon A units as local environmental factors (proximity to the shelf edge or volcanoes; local current regimes; glaciation) begin to dominate sedimentation.

In regard to the correlation with the Newfoundland Basin acoustic stratigraphic sequence, the above observations mean that a strong similarity can be expected between the lithology of the pre-R_1 section and the pre-Horizon A sections in the Northwest Atlantic. The younger, post-R_1 units may be chronologically equivalent to the post-

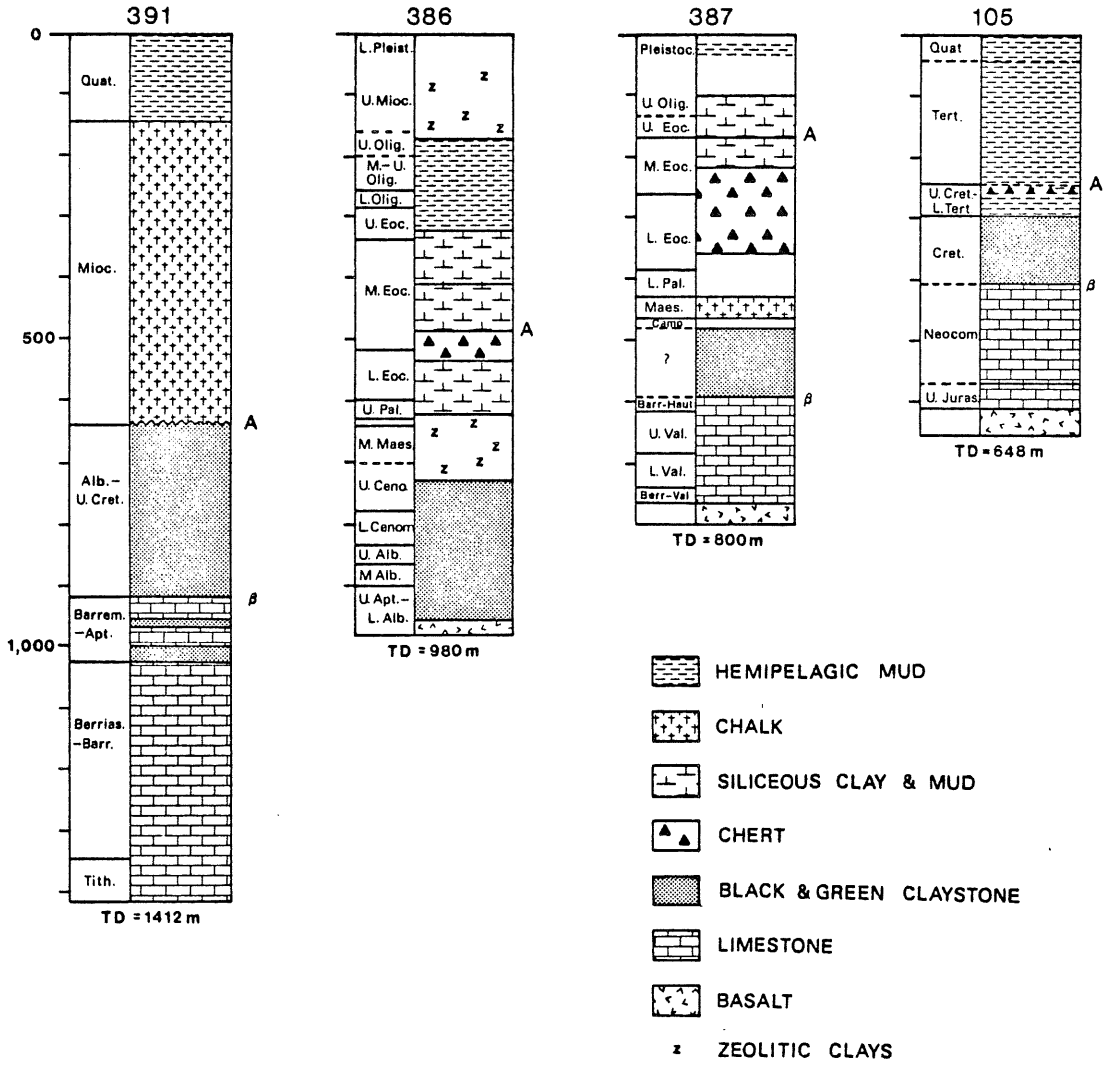

Figure 4.16

Stratigraphy at DSDP Sites 386, 387, 391, 105, Northwest Atlantic.

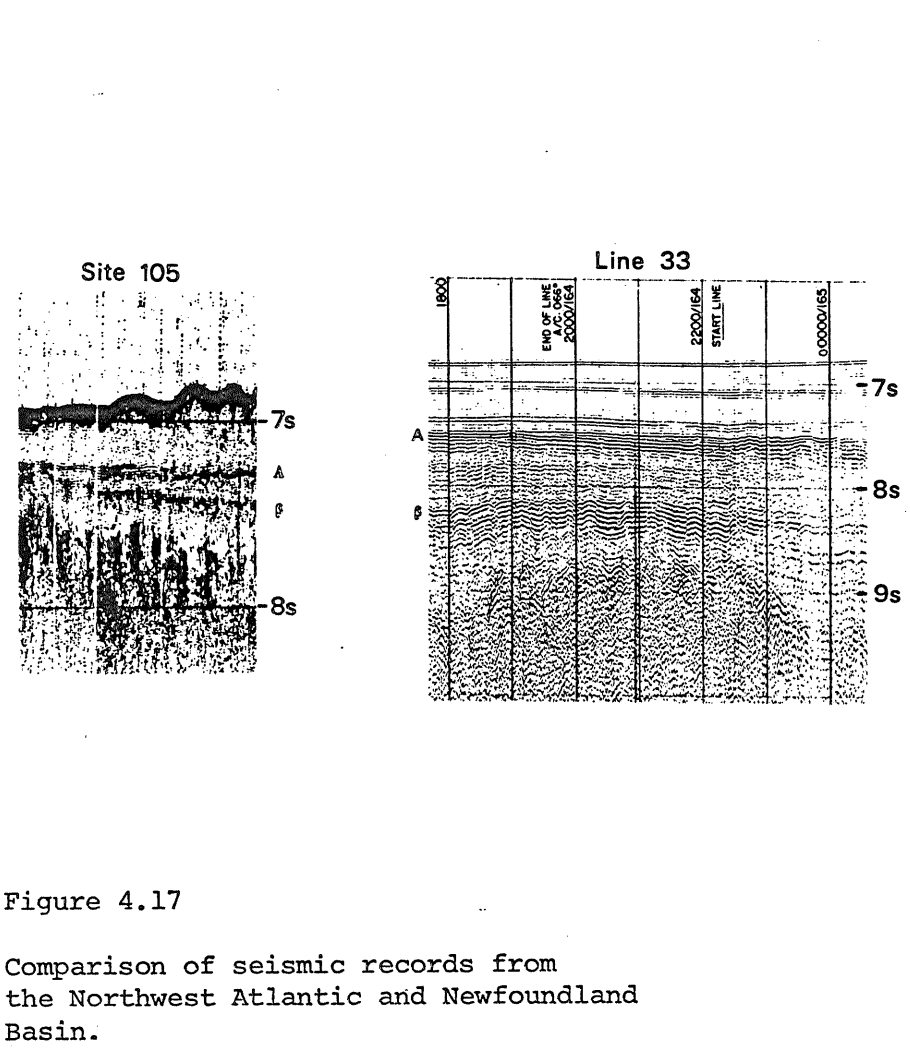

Figure 4.17

Comparison of seismic records from the Northwest Atlantic and Newfoundland Basin.

Horizon A units at these DSDP sites, but they probably comprise distinctly different lithologies.

The correlation of R_2 with Horizon β presents a problem. Chapter 5 of this thesis presents evidence that the oldest seafloor spreading isochron in the southern Newfoundland Basin is the J-anomaly, which correlates with anomalies M2-M4 of the Keathley sequence. Reflector R_2 in this area can be traced a considerable distance east of the J-anomaly, onto crust that is about 102 Ma old. On the other hand, the Horizon β reflector south of the SENR generally pinches out on crust that is J-anomaly age or <u>older</u>, although this horizon may be as young as Late Cretaceous in places (Mountain and Tucholke, 1977). This problem cannot be resolved until additional data on the nature of R_2 are obtained. Throughout the remainder of this thesis the correlation of Horison β with Newfoundland Basin reflector R_2 is accepted, and it is assumed that the inferred Late Cretaceous age of R_2 is further evidence for the diachronous nature of Horison β.

4.4.3 Conclusion

The two preceeding sections have briefly illustrated that very useful correlations between the acoustic stratigraphy in the Newfoundland Basin and the better-known stratigraphic sequences in the Northwest Atlantic and off western Iberia can be made with a fair amount of confidence. These comparative sketches lead to the postulated ages and lithologies for Units A, B and C shown in Figure 4.18. Two important points concerning the relationship between acoustic units or events in the Newfoundland Basin and stratigraphic elements on the Grand Banks can

be addressed using this proposed stratigraphy.

First, this provides a minimum age for the sediment fill in the grabens observed beneath the Eastern Banks and Flemish Cap margins (Profiles 36 and 43, Fig. 4.3b; 54-38; Fig. 4.3a). The sediments in the continental margin grabens are overlain by Units A and B, and thus are older than Early-Mid Cretaceous. The quiet magnetic character of the region in which the grabens lie may indicate that they occur within subsided continental crust (see Sections 5.2 and 8.1). The combination of structural setting and age of deposits leads to the inference that these grabens are rift-valley basins which, like the Grand Banks sub-basins (Chapter 2) formed during tensional phases early in the history of continental separation. By analogy with the Carson Sub-basin at the eastern edge of the Grand Banks (Fig. 2.4) these continental margin grabens may be expected to contain sediments as old as Upper Triassic.

The second point to consider is the seaward extent of the Avalon Unconformity. Workers in this region generally accept one of two very different interpretations on this topic. The problem is best considered in the Tail of the Bank region, where the same set of multichannel seismic records has been used as the basis for both interpretations (Lines 111-116, Fig. 4.2).

A. C. Grant (1977) and Gradstein et al. (1977) both trace the seismic event associated with the Avalon Unconformity on the Grand Banks (Grant's "Reflector U") from the shelf to the SENR as a continuous event. Reflectors below U on the SENR suggest to A. C. Grant (1977) that a considerable thickness (6-8 km) of Cretaceous and older

sediments underlie this horizon. The assumption that seismic event U on the SENR is strictly equivalent to U on the Grand Banks is a prime factor that leads A. C. Grant (1977) and Gradstein et al. (1977) to conclude that both areas are underlain by the same, continental basement.

The present author and King and Young (1977) have also examined these multi-channel records and do not consider reflector U to be continuous across the continental slope. King and Young (1977), who included similar records from the margins off Nova Scotia and Labrador in their analysis, consider the present day continental slope to be underlain by a succession of Mesozoic-Cenozoic paleo-slopes. In their view the Avalon Unconformity does not continue across the slope, but rather terminates near mid-slope in a zone of confused reflections and side-echoes which marks the paleo-slope succession. This does not rule out the possibility that the reflectors on the SENR and the Grand Banks may be genetically related events (i.e. contemporaneous unconformites, see Section 4.1.4). The main point is that the mid-slope region marks the boundary between two quite different regimes.

Further evidence that the U reflectors on the Grand Banks and on the SENR are not equivalent comes from the single-channel seismic and expendable sonobuoy data on Line 42M, which intersects multi-channel line 116 (Fig. 4.2, 4.3e). Reflector PR on Line 42M is identical with U and is believed to correlate with the other reflectors labelled PR in Fig. 4.2e. The correspondence between the measured 4.8-5.6 km/sec basement velocities and oceanic layer 2a velocities (Raitt, 1963) plus the high-amplitude magnetic anomaly signatures of the SENR and Spur Ridge are believed to be more consistent with the interpretation that

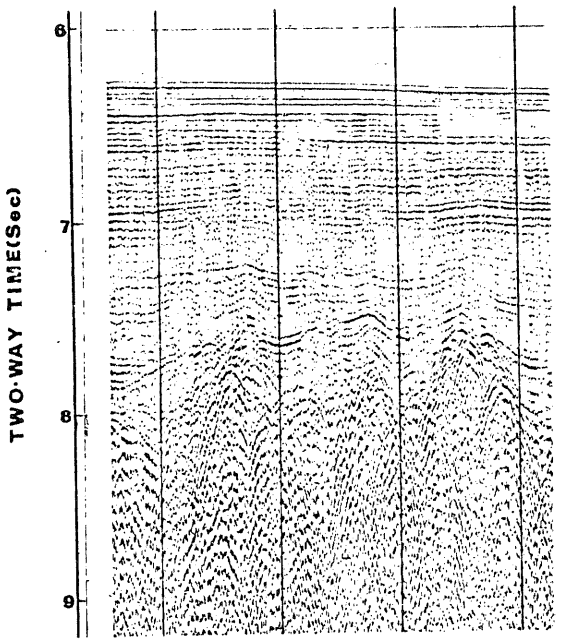

	Unit A	Upper Cret.-Lower Tert. to Recent	turbidites muds & oozes
R_1			
	Unit B	Mid-Upper Cretaceous	carbonaceous claystones
R_2	Unit C	Lower Cretaceous	limestones and marls

oceanic crust underlies this area. The velocity-depth data for these sections (Fig. 4.9) suggest that PR/U on the SENR and the Spur Ridge is the top (either depositional or erosional) of a relatively high-velocity sedimentary layer, 0.5-1.5 km thick. Velocities in the range 4.8-5.6 km/sec are measured beneath this interval. In some cases the latter velocities are clearly associated with the basement reflector beneath PR. In other cases no distinct reflector can be found below PR; it is assumed in these cases that the sedimentary layer below PR is masking the basement reflection. It is important to note that the multi-channel records consistently show U or PR as only a single event, whereas the single-channel profiles frequently indicate another reflector (basement) below this.

CHAPTER 5: MAGNETICS

B. R. Hall (1977; hereafter BRH) presents a compilation of magnetic data collected in the Newfoundland Basin up until 1975 and attempts to correlate the anomalies observed in this area with known oceanic anomaly sequences. The oldest and youngest anomalies in the southern Basin are identified as the J-anomaly (M2-M4) and Anomaly 31/32 (after Srivastava, 1978), respectively, giving age limits of 115 Ma and 73 Ma for the oceanic crust south of the seamounts. Identification of the anomalies observed between the J-anomaly and 31/32 and of the anomaly pattern in the northern part of the Basin poses much greater difficulties; BRH speculates as to the nature of these anomalies but proffers no definite interpretation. This study is summarized by C. E. Keen et al. (1977) and is discussed in greater detail in 5.4.

One task of the present study (Section 5.5) is to re-examine the results of BRH using additional data obtained in 1976 and taking into account recent studies of the initial fit and early spreading between Iberia and the Grand Banks (LePichon et al., 1977; Haworth, in prep.). Another important aim in this chapter (Section 5.3) is to examine magnetic evidence that bears on the relationship between the Newfoundland Basin and the surrounding continental areas or on boundaries between structural provinces within the Basin.

5.1 Data Collection and Reduction

The magnetic data which have been examined in this study were

collected during ten cruises conducted between 1965 and 1976 (Figure 5.1, Appendix IV). The detailed surveys over the Grand Banks and Flemish Cap have been compiled by Haworth and MacIntyre (1975) and are presented in simplified form in this report. All Bedford Institute profiles examined by BRH are included in the data base for the present study.

This chapter relies most heavily on results from four Bedford Institute cruises made since 1973. Ship's positions on these cruises were determined by navigational satellite and Loran C in the range-range mode; the estimated positioning accuracy for these tracks is ± 300 m at the 95% confidence limit (S. Grant, 1973).

The total magnetic field intensity was measured at 6-second intervals with a towed proton-precession magnetometer, and the values were recorded in both analog and digital form. The data have been corrected by removal of the International Geomagnetic Reference Field (IAGA, 1969) for the epoch appropriate to each cruise. This correction produces anomaly profiles with mean values (baselevels) significantly less than zero, and the discrepancy betwen the theoretical and actual regional fields appears to increase from 1965 to the present. Srivastava (1977) and Dawson and Newitt (1977) document large errors in the secular variation terms of the IGRF-65 and IGRF-75 fields which may well be responsible for the observed poor fit. Such errors presumably do not affect the shapes or relative amplitudes of the anomalies, so valid comparisons of these characteristics can be made without further correction. However, it is necessary to adjust the profiles to a zero-baselevel for two-dimensional modelling. The magnitude of the baselevel shift required for each cruise has been determined visually, and

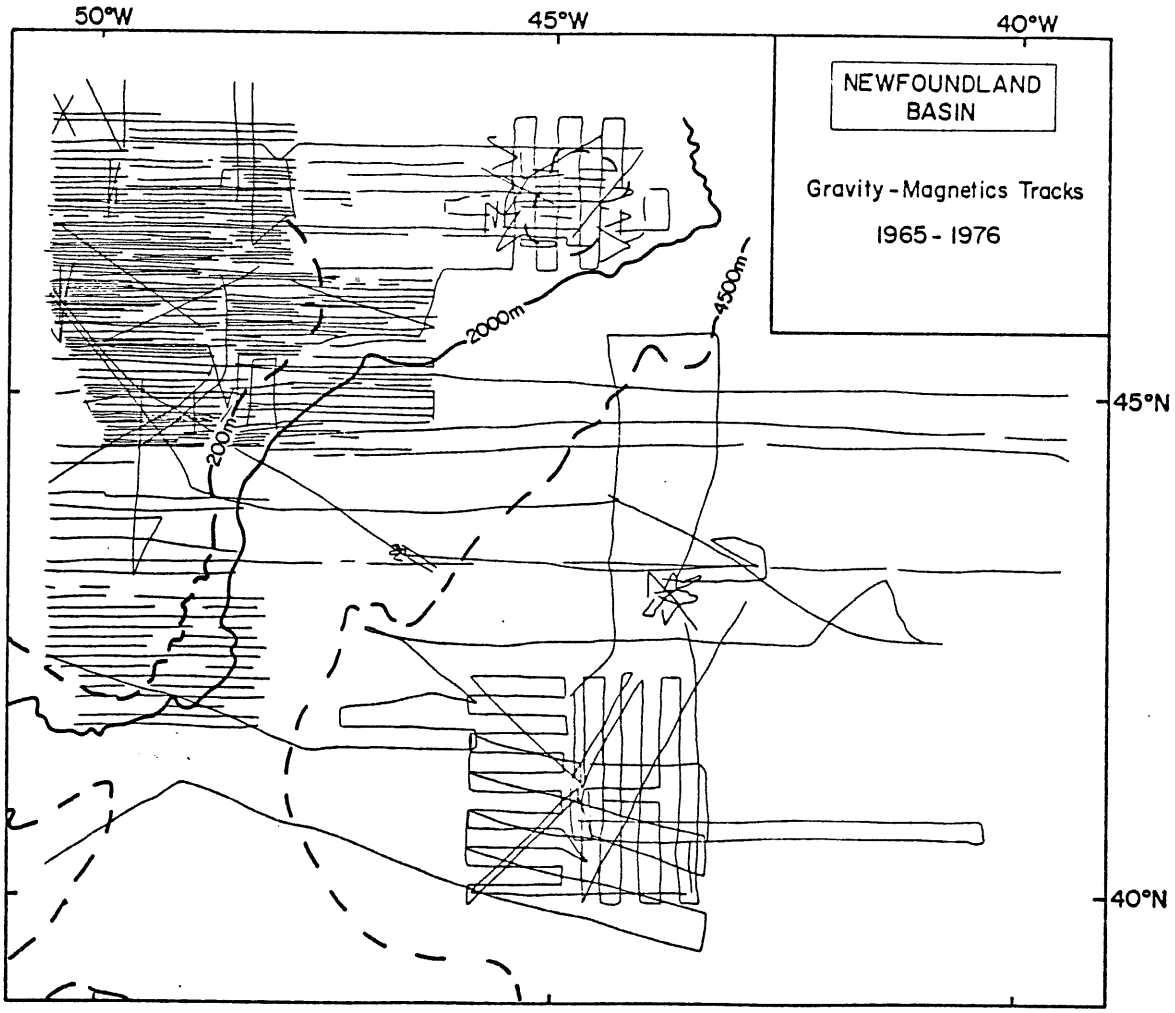
50°W
45°W
40°W
NEWFOUNDLAND
BASIN
Gravity - Magnetics Tracks
1965 - 1976
2000m
4500m
200m
45°N
40°N

Figure 5.1

the shift applied by hand. This adjustment effectively removes the errors due to the IGRF and, for the data collected during cruise MK76-031, the 20-50 nT errors caused by unusually close proximity of the magnetometer sensor to the ship (Appendix I).

5.2 Regional Anomaly Character

Figure 5.2 shows simplified contoured magnetic anomaly trends over the Grand Banks-Flemish Cap area (Haworth, 1975; Haworth and McIntyre, 1975) and the Newfoundland Basin survey areas (BRH; C. E. Keen et al., 1977), along with selected profiles which illustrate the character of the anomalies over the rest of the area. Seismic and gravity data accompanying the profiles shown are given in Figure 4.3.

On the Grand Banks and Flemish Cap Haworth (1975) and Haworth and Lefort (in prep.) show that the sinuous-shaped, roughly north-south trending positive anomalies reflect Hercynian structures developed in volcanic rocks of the Avalon Zone. These anomalies all merge at their southern ends with an ESE-trending magnetic high, referred to as the Collector Anomaly (Section 2.1). Haworth and Lefort (in prep.) tentatively indicate that the easternmost of the sinuous anomalies continues south onto the upper continental rise of the Newfoundland Basin (Fig. 5.2).

Magnetic slope anomalies, such as are observed along much of the eastern North American continental margin, are not observed on the profiles across the Eastern Banks margin (Fig. 5.2). This section of the Newfoundland Basin margin is characterized by a marginal smooth zone that extends from the shelf to the transition between the upper

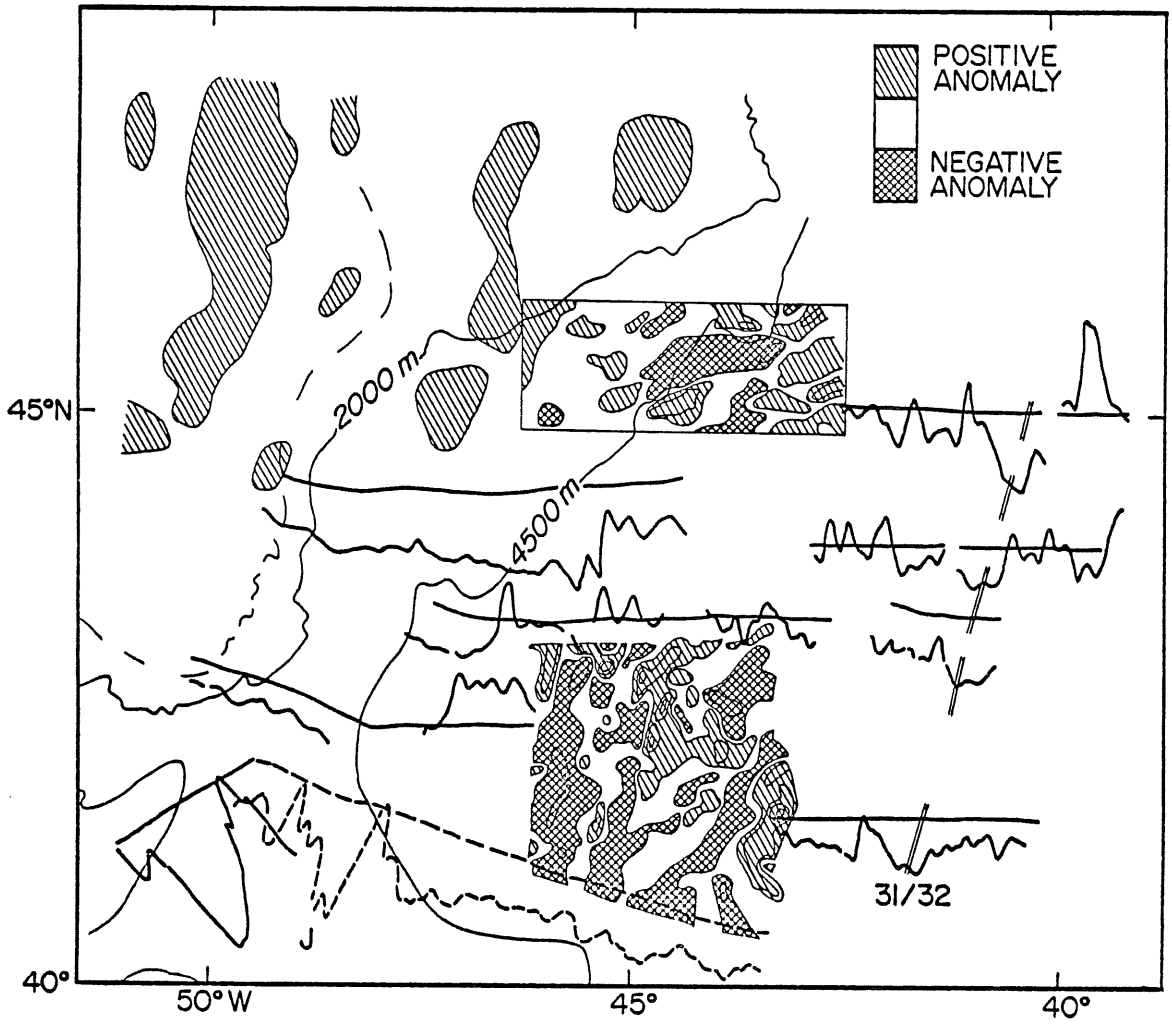

Figure 5.2

Magnetic anomaly trends.
Contours on the Grand Banks from Haworth (1975).
Newfoundland Basin survey areas contoured by B.R. Hall (1977).

and lower continental rise provinces. South of the seamounts the smooth zone is terminated abruptly on the seaward side by a 500-700 nT (peak-to-peak) anomaly which is on strike with the J-anomaly (BRH; C. E. Keen et al., 1977). North of the seamounts it appears that the seaward boundary of the smooth zone is somewhat less abrupt. The boundary here is marked by a series of short-wavelength anomalies which increase in amplitude eastward.

Anomalies in the magnetically disturbed region seaward of the smooth zone exhibit amplitudes and wavelengths comparable to those associated with oceanic crust generated by seafloor spreading. Anomaly 31/32 (Srivastava, 1978; BRH) of the Cretaceous reversal sequence occurs at the eastern limit of the area of interest here (Fig. 5.2). The roughly lineated anomalies between the J-anomaly/smooth zone boundary and anomaly 31/32 are discussed in sections 5.2 and 5.3.

One final distinctive region to be noted in Figure 5.2 is the zone of very high-amplitude anomalies over the SENR and Spur Ridge. The J-anomaly identification of BRH is indicated in the figure.

5.3 Previous Studies

BRH presents data collected in the Newfoundland Basin through 1975 by several agencies (Bedford Institute of Oceanography; Lamont-Doherty Geological Observatory; U. S. Naval Oceanographic Office; NAVADO Project) and attempts to correlate the anomalies observed in this area with established magnetic reversal sequences. His study focuses on two particularly well-surveyed areas within the Basin (Section 5.3).

The results in the northern survey area (Fig. 5.3) are subject to rather large errors from several sources. These data were collected during numerous cruises undertaken between 1965 and 1974, and navigational control was often poor. In particular, on some of the earlier cruises positions were determined solely by dead-reckoning and celestial fixes. Furthermore, study of land-station magnetometer records from St. John's, Newfoundland, and Halifax, Nova Scotia, reveals that large temporal variations (65-210 nT) occurred during some periods of data collection; BRH reports that it is impossible to correct for these variations. The poor quality of the data set for this region is indicated by the large (109 nT, rms) cross-over errors.

In spite of these difficulties, BRH presents a contoured magnetic anomaly map for the northern area (Fig. 5.4a). He describes the anomaly pattern here as confused, noting that suggestions of both north-south and roughly east-west trends are visible.

The detailed magnetic data in the southern area (Fig. 5.3) were obtained during a multi-parameter survey carried out by the C.S.S. Hudson in 1975. Diurnal variations in the area were measured and corrected for during the study and navigational control was consistently good (± 300 m). The cross-over error for this survey is 22 nT (rms).

Tie-lines run to the east and west of the southern survey area establish its location with respect to anomaly 31/32 and the continental margin (Fig. 5.3). On the western tie-line BRH identifies the J-anomaly as the oldest seafloor spreading anomaly in the southern Basin.

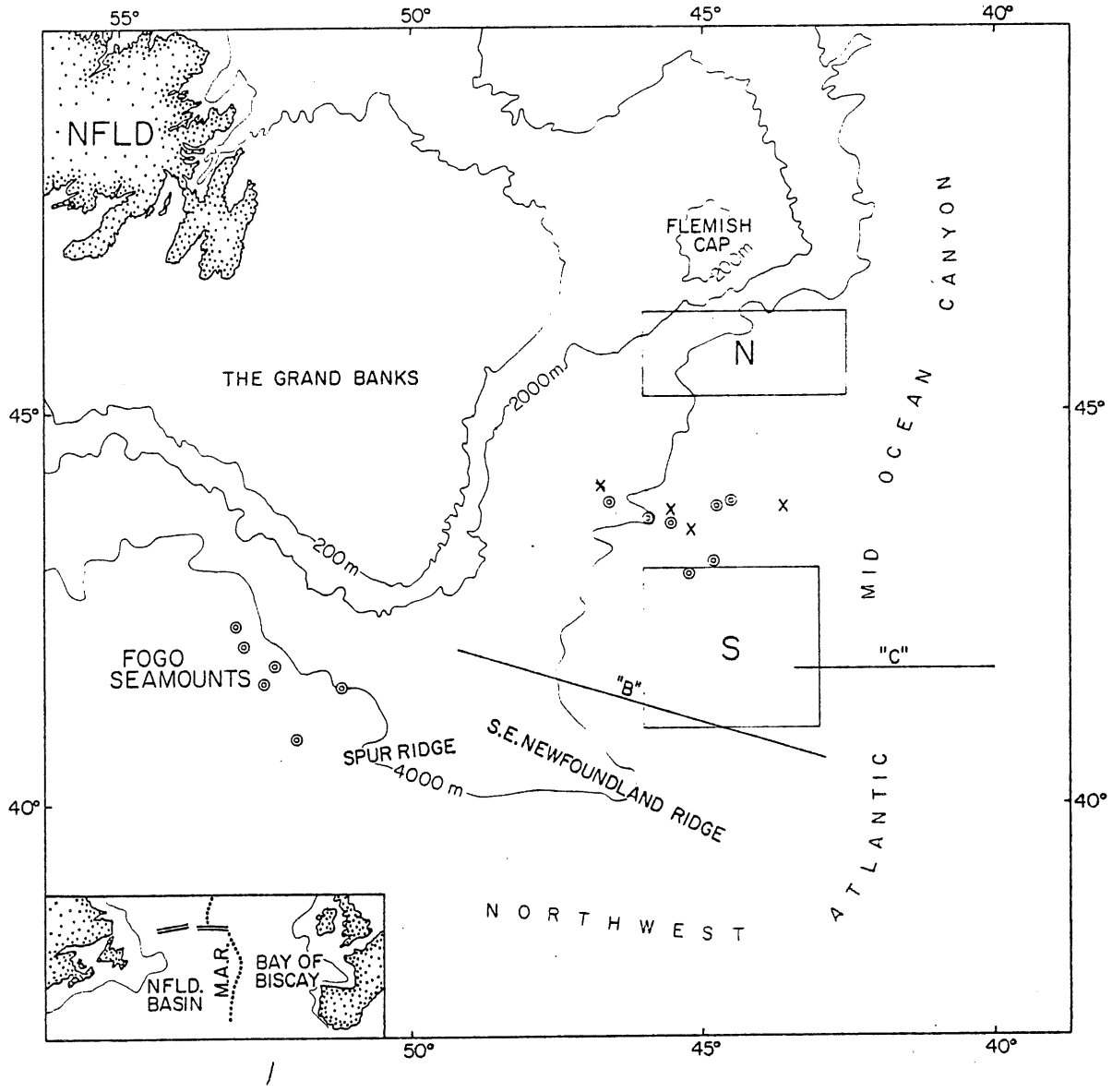

Figure 5.3

Location map: Survey areas and composite model profile ("B" and "C") studied by B.R. Hall (1977).

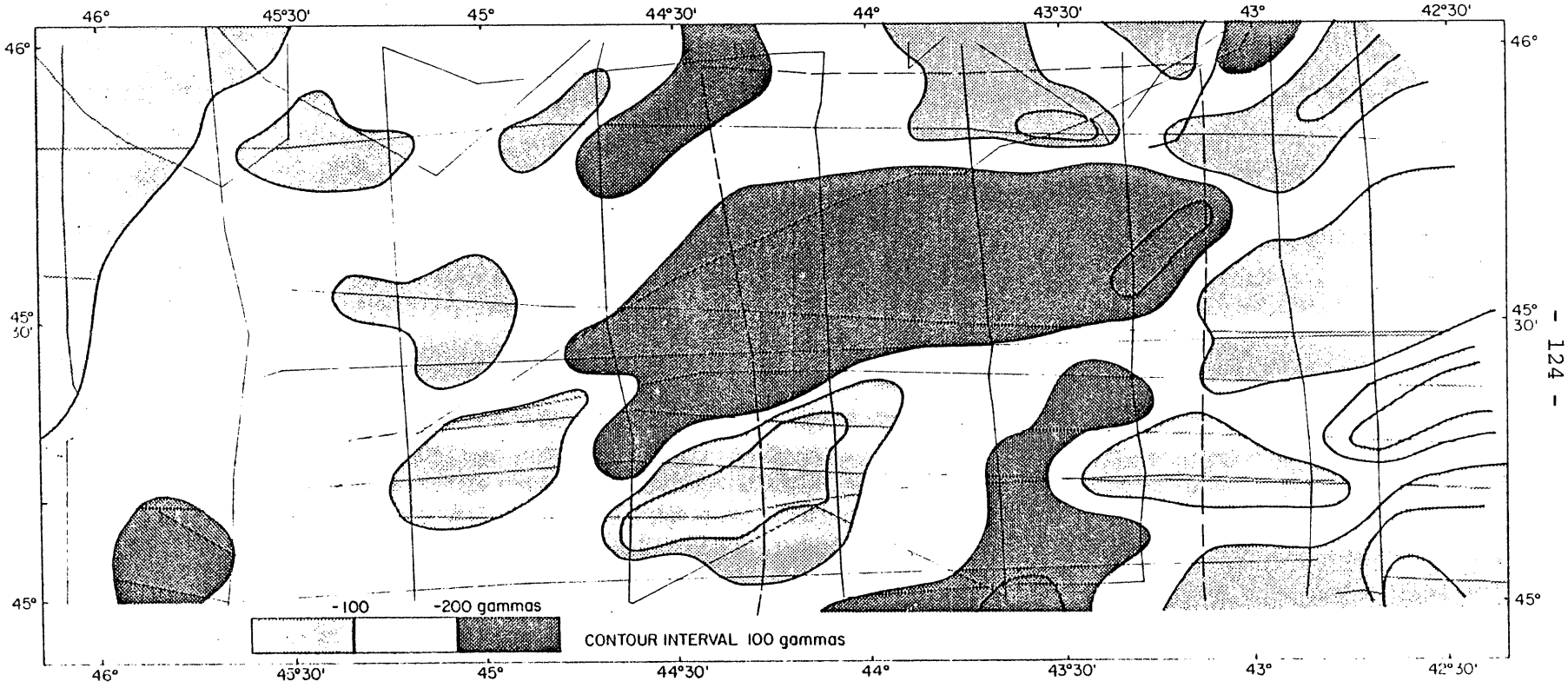

Figure 5.4a

Magnetic anomaly contours, northern survey area.
(after B.R. Hall, 1977).

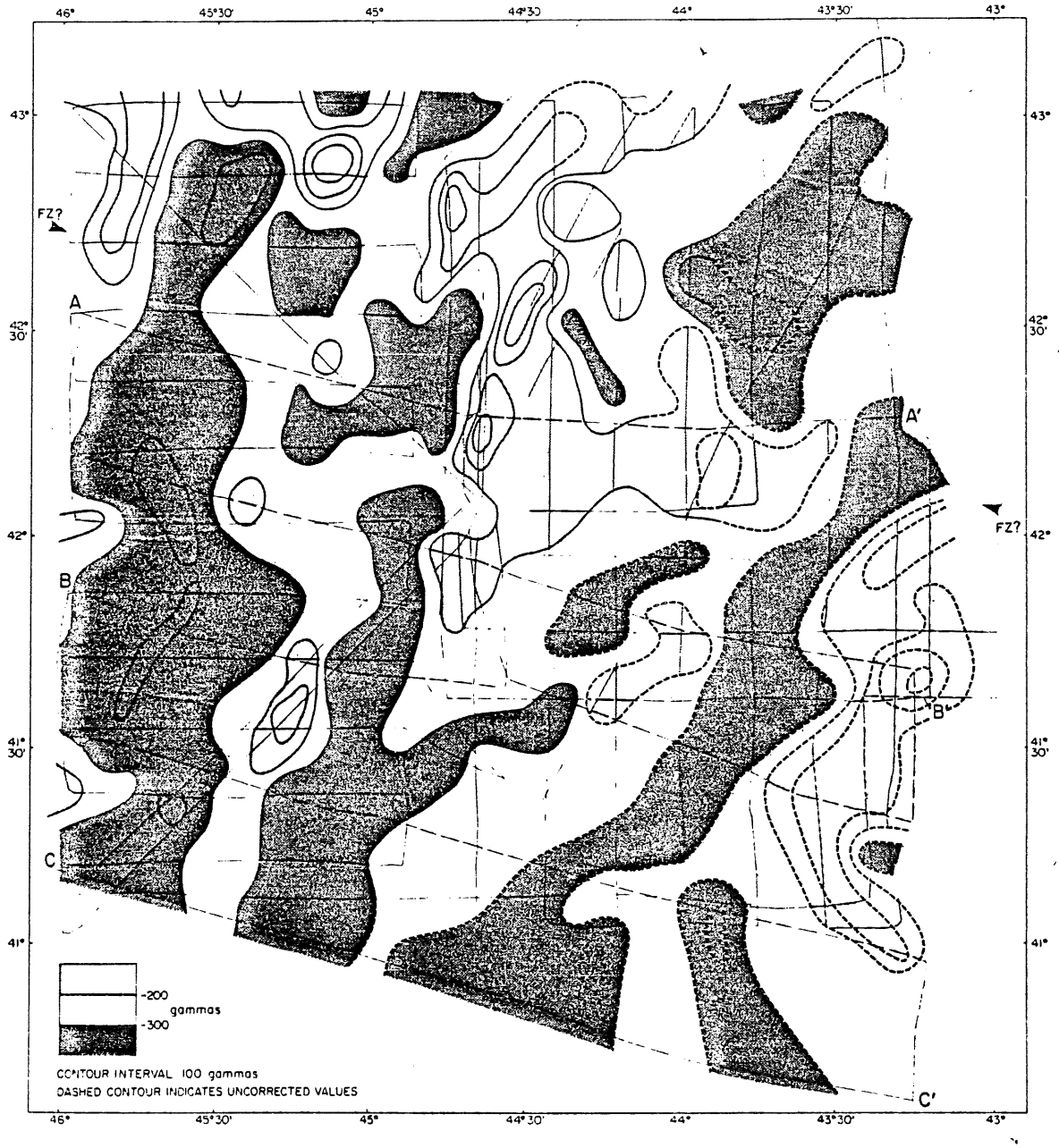

Figure 5.4b
Magnetic anomaly contours, southern survey area.
(after B.R. Hall, 1977).

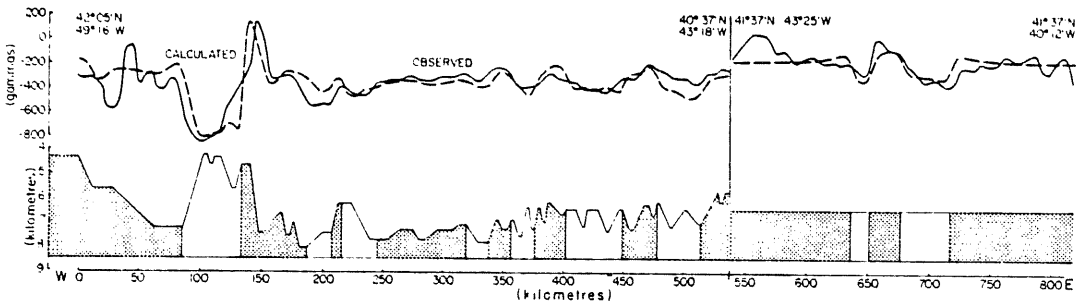

Figure 5.5a

Composite reversal model
(B.R. Hall, 1977).

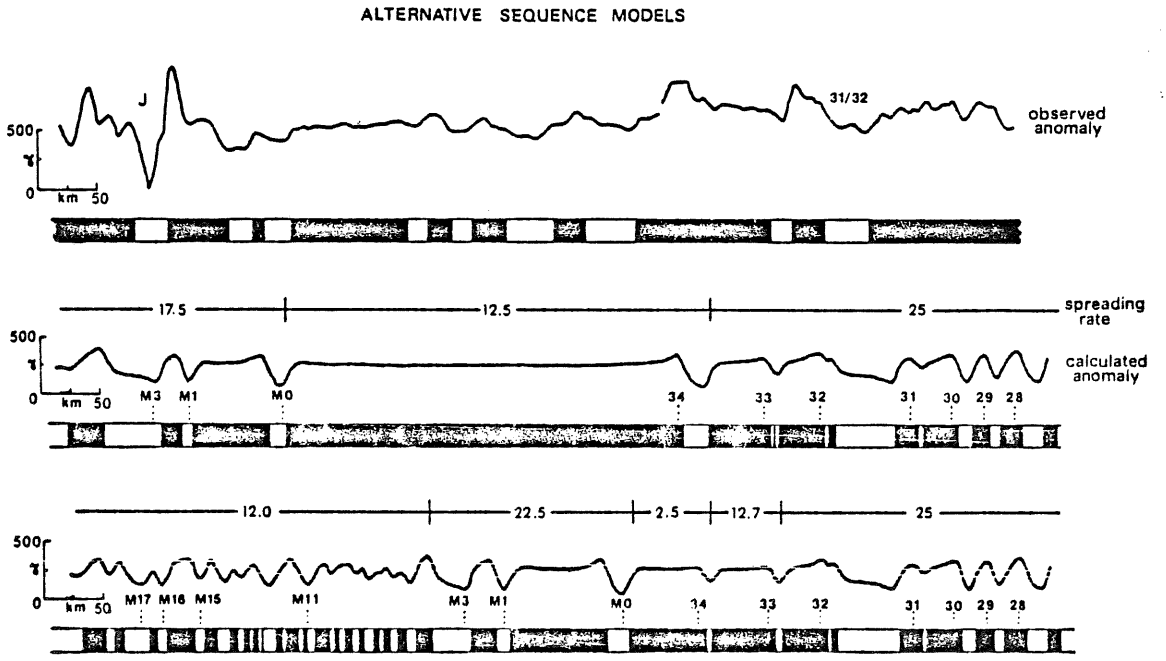

Figure 5.5b
Alternative anomaly correlations.
(B.R. Hall, 1977).

BRH's contoured magnetic map of the southern survey area (Fig. 5.4b) shows several prominent, roughly linear anomalies with a strike, at least in the western part of the area, of 015°. BRH presents two-dimensional block models, incorporating seismic reflection data on basement depth, which demonstrate that the contoured anomalies are not due solely to basement topography. These model results lead BRH to conclude that zones of reverse-polarity crust are required to satisfy the observations.

In order to correlate the contoured lineations with known reversal sequences, BRH gives a composite magnetic model profile which extends from anomaly 31/32 to the J-anomaly (Fig. 5.5a). The modelled reversal sequence for this line does not correlate well with published reversal sequences (Heirtzler et al., 1968; Larson and Pitman, 1972; LePichon et al., 1973; Larson and Hilde, 1975). More specifically, both of the published J-anomaly correlations with age (Tucholke, Vogt et al., 1975; Barrett and Keen, 1976; Rabinowitz et al., 1977) encounter serious problems (Fig. 5.5b).

If the J-anomaly correlation with M16-M17 is accepted, the model results require frequent and large changes in seafloor-spreading rates which are difficult to reconcile with other studies of North Atlantic spreading rates for this time (Vogt and Johnson, 1971; Pitman and Talwani, 1972; Larson and Pitman, 1972). On the other hand, accepting the M2-M4 (115 Ma) correlation for the J-anomaly requires that the modelled reverse-polarity zones in the southern survey area occur in crust that formed during the Cretaceous Normal Interval (KN; Helsley and Steiner, 1969; Irving and Pullaiah, 1976).

BRH favors this latter model for the Newfoundland Basin reversals, largely because it predicts more plausible spreading rates. The problem of KN reversals remains unresolved. BRH suggests that the modelled reversals might correlate with KN-age reversals reported from studies of Cretaceous sediments drilled by the Deep-Sea Drilling Project (Green and Brecher, 1974; Keating and Helsley, 1976, in press).

5.4 New Results and Observations

Additional data collected in the Newfoundland Basin in 1976 document the existence of a marginal magnetic smooth zone, the seaward boundary of which apparently is coincident with the continuation of the J-anomaly (BRH) north of the SENR (Section 5.1). Analysis of these new data prompted re-examination of the data presented by BRH for the northern and southern survey areas. This in turn has provided new insight into the two major paleomagnetic issues raised by the earlier work: The apparent occurrence of reverse polarity during KN (Section 5.5) and the origin of the J-anomaly (Section 5.4.1 and Chapter 8). The 1976 data do not conflict with or provide a basis for revision of the J-anomaly or anomaly 31/32 identifications of BRH; these anomaly identifications and the average spreading rates based on them are therefore retained.

5.4.1 The J-anomaly and the smooth zone boundary

Figure 5.6 compares the magnetic anomalies observed on four of the MK 76-031 profiles across the smooth zone boundary south of the

seamounts with the J-anomaly as observed over the SENR (BRH; C. E. Keen et al., 1977) and on the Spur Ridge (Renwick, 1973, Tucholke and Vogt et al., 1975). The peak-to-peak amplitude of the smooth-zone boundary anoamly in the southern Newfoundland Basin is comparable to that of the J-anomaly, and quite similar basement structures are associated with both anomalies (Tucholke and Vogt et al., 1975; Ballard et al., 1976; C. E. Keen et al., 1977; BRH, Ch. 4). However, the very different magnetic signature landward of the two anomalies casts doubt on their correlation. Is it possible that spatial association between the smooth zone boundary in the southern Newfoundland Basin and the J-anomaly is coincidental, and that there is no temporal or genetic link?

Magnetic model studies have been undertaken in attempting to resolve this question. A few limitations of such studies should be noted. First, all such models give inherently non-unique solutions. Secondly, the J-anomaly, because of its unique character, cannot be fitted using standard reversal-sequence block models and typical parameters (Rabinowitz et al., 1977; C. E. Keen et al., 1977); arbitrary variations in magnetic source-layer thickness or/and increases in magnetization contrasts must be invoked to match the unusually high amplitude of the J-anomaly. Nevertheless, two-dimensional models coupled with seismic reflection data may help to eliminate inappropriate combinations of structure and magnetization for the anomaly sources.

Models were constructed along three seismic profiles crossing the smooth-zone boundary, using the methods and source-layer parameters

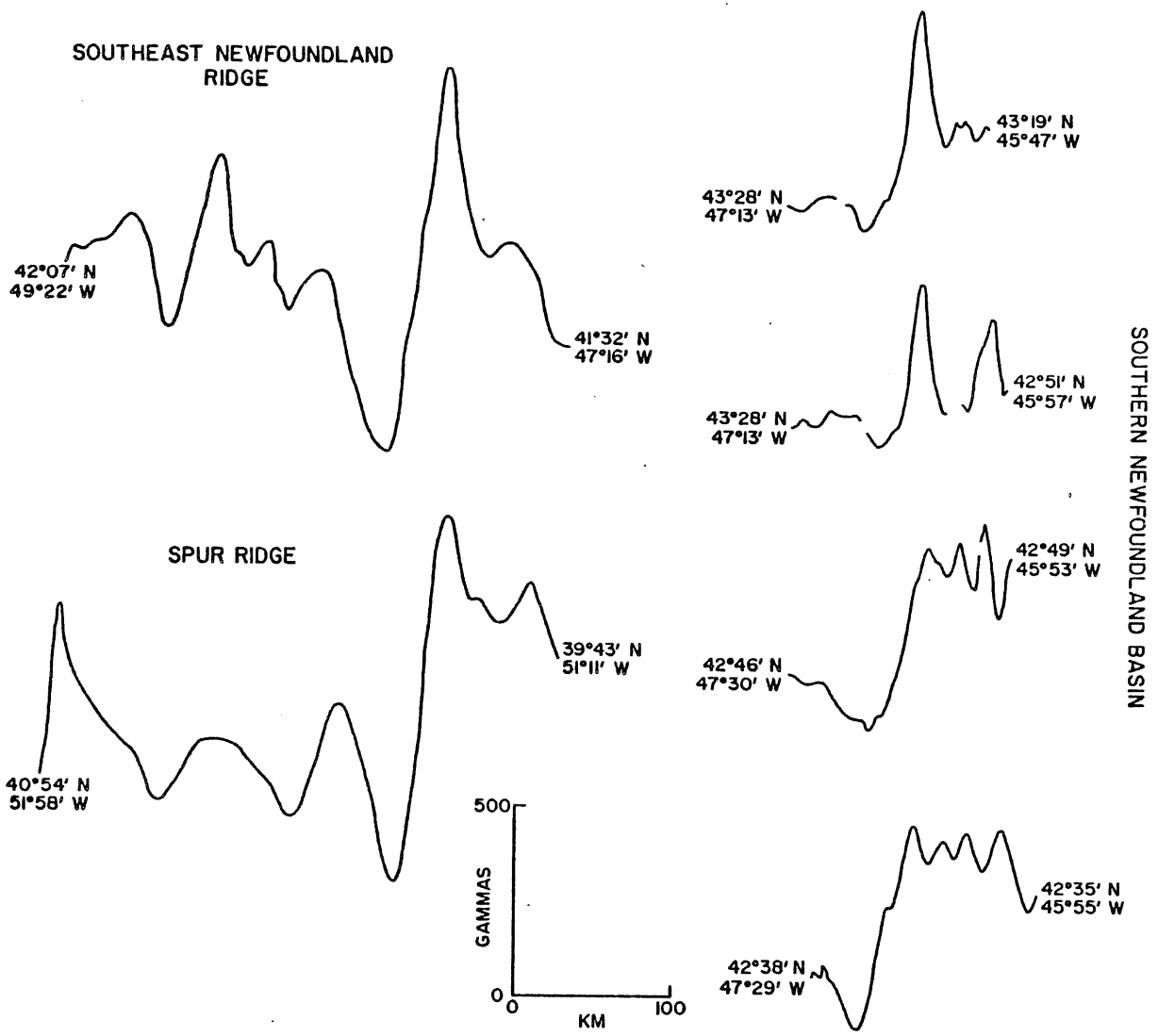

Figure 5.6: J-anomaly and smooth zone boundary comparison.

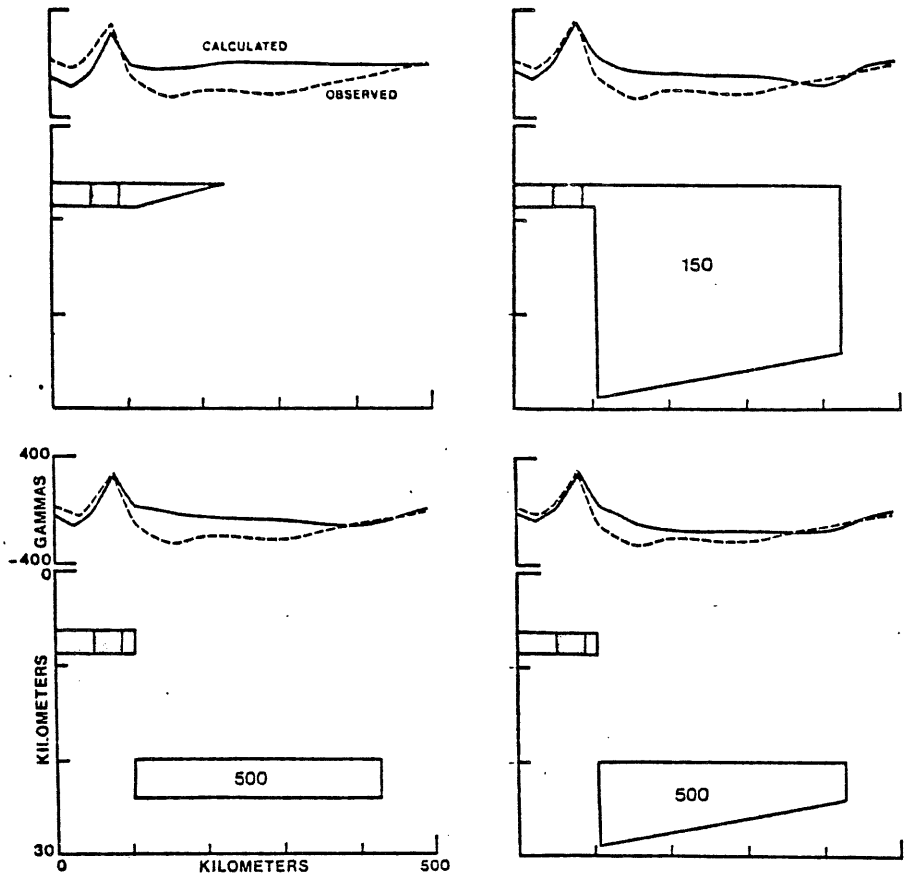

Figure 5.8

Summary of two-dimensional modelling results, southern Newfoundland Basin smooth zone boundary.

used by BRH for other southern Newfoundland Basin profiles. (Upper surface of source-layer determined from seismic profiles, lower surface planar at 8.5 km; intensity of magnetization .0025 emu/cc). These models produce satisfactory fits to the anomalies seaward of the smooth zone, but they do not reproduce the amplitude of the boundary anomaly or the long-wavelength low observed landward of the boundary.

Numerous models, employing a variety of source-layer geometries and parameters, were constructed in attempting to fit the latter features of the magnetic field. Figure 5.7 shows simplified versions (without topography on the upper surface) of several models for lines 43 and 44. No model was found which produced a truly satisfactory fit. The closest approximations to the observed field are obtained by postulating sharp changes in source-layer depth or thickness at the smooth zone boundary and constant polarity landward of the boundary. Equivalent fits result from using a very thick source layer of low remanent magnetization intensity (which could also represent a low susceptibility) or a thinner, deep layer of high intensity.

These results imply that the smooth zone boundary anomaly is due to an edge-effect. The models do not indicate the actual geology producing the edge-effect and they do not rule out the possibility that the boundary is an isochron. Thus, it is still conceivable that the J-anomaly in the Newfoundland Basin is coincident with the smooth zone boundary.

5.4.2 Newfoundland Basin anomaly pattern

The anomaly patterns mapped by BRH in the northern and southern

survey areas have been re-examined in this study with two questions in mind. First, whether there is in fact a correlation between the two sets of data; second, to clarify interpretation of the anomaly geometry.

Two profiles were run across the Basin during MK76-031 in order to check the northward continuity of the anomalies mapped by BRH in the southern survey area. Inspection of the anomalies and reversal models along these tracks and the tracks modelled by BRH (Fig. 5.8) has not revealed any correlation between the two sets of data. In light of the latter result, the data from the southern survey area were re-examined to determine whether the contoured anomaly pattern might be re-interpreted.

An interesting feature of the anomaly pattern in the southern Basin which was not mentioned by BRH is the branching of anomalies near the center of the survey area (Fig. 5.4b). The 015° trend observed in the western part of the area is replaced in the eastern half by short anomaly segments with a 055-060° trend with offsets at 145° (Fig. 5.9a). The age of the crust at the change in anomaly strike on the southern survey area is 102 Ma, calculated on the basis of a 1.75 cm/yr spreading rate (BRH) and a measured distance from the J-anomaly of 222 km.

The anomalies in the eastern part of the northern survey area can also be described in terms of this anomaly-fracture zone orientation (Fig. 5.9b). The magnetically different region west of 44°45'W in Fig. 5.9b is the marginal smooth zone.

LePichon et al. (1977) propose that the initial motion of Iberia with respect to the Grand Banks and the opening of the Bay of Biscay both occurred by rotation about a pole located northeast of Paris.

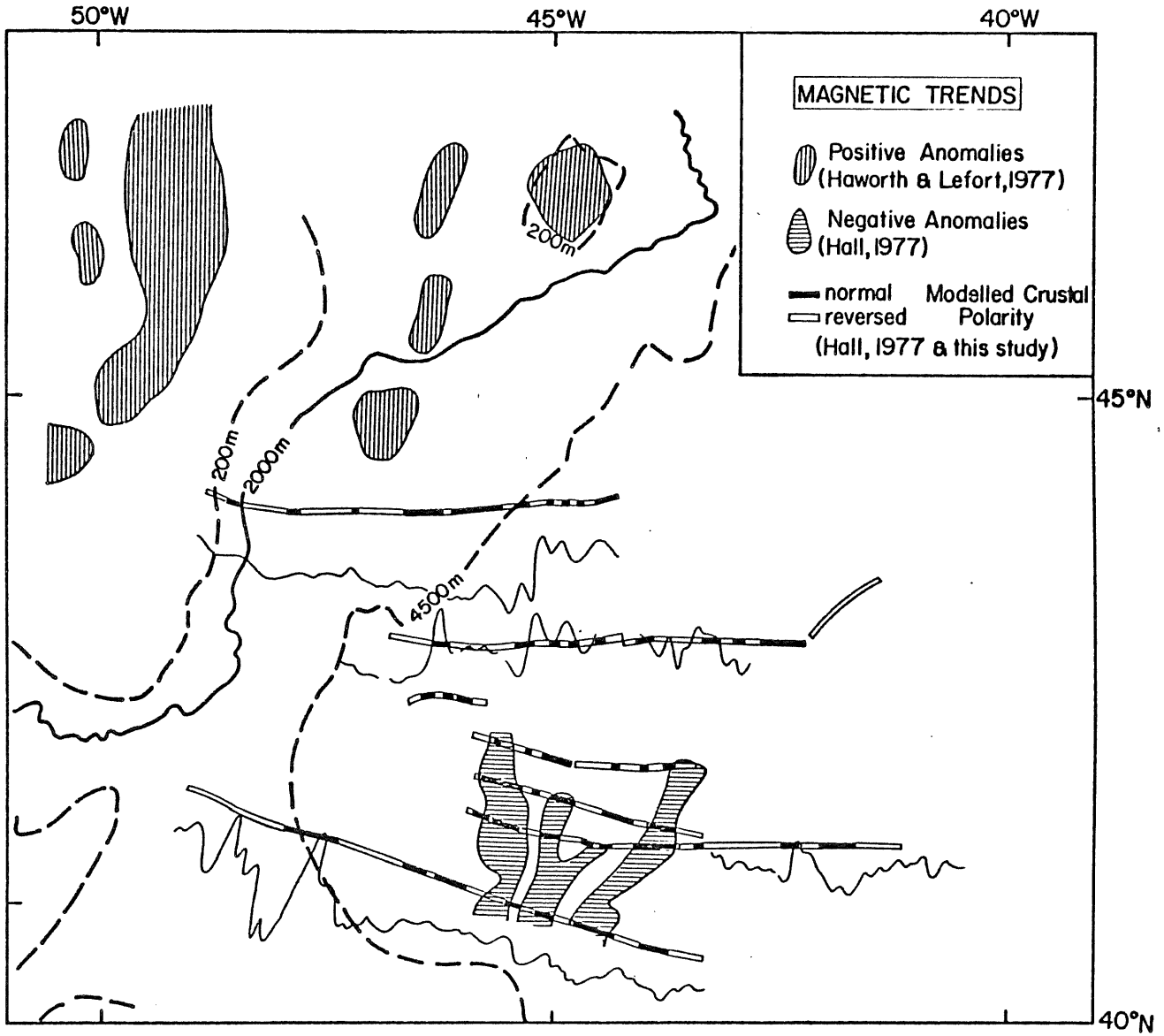

Figure 5.8

Two-dimensional modelling results and observed magnetic anomalies.

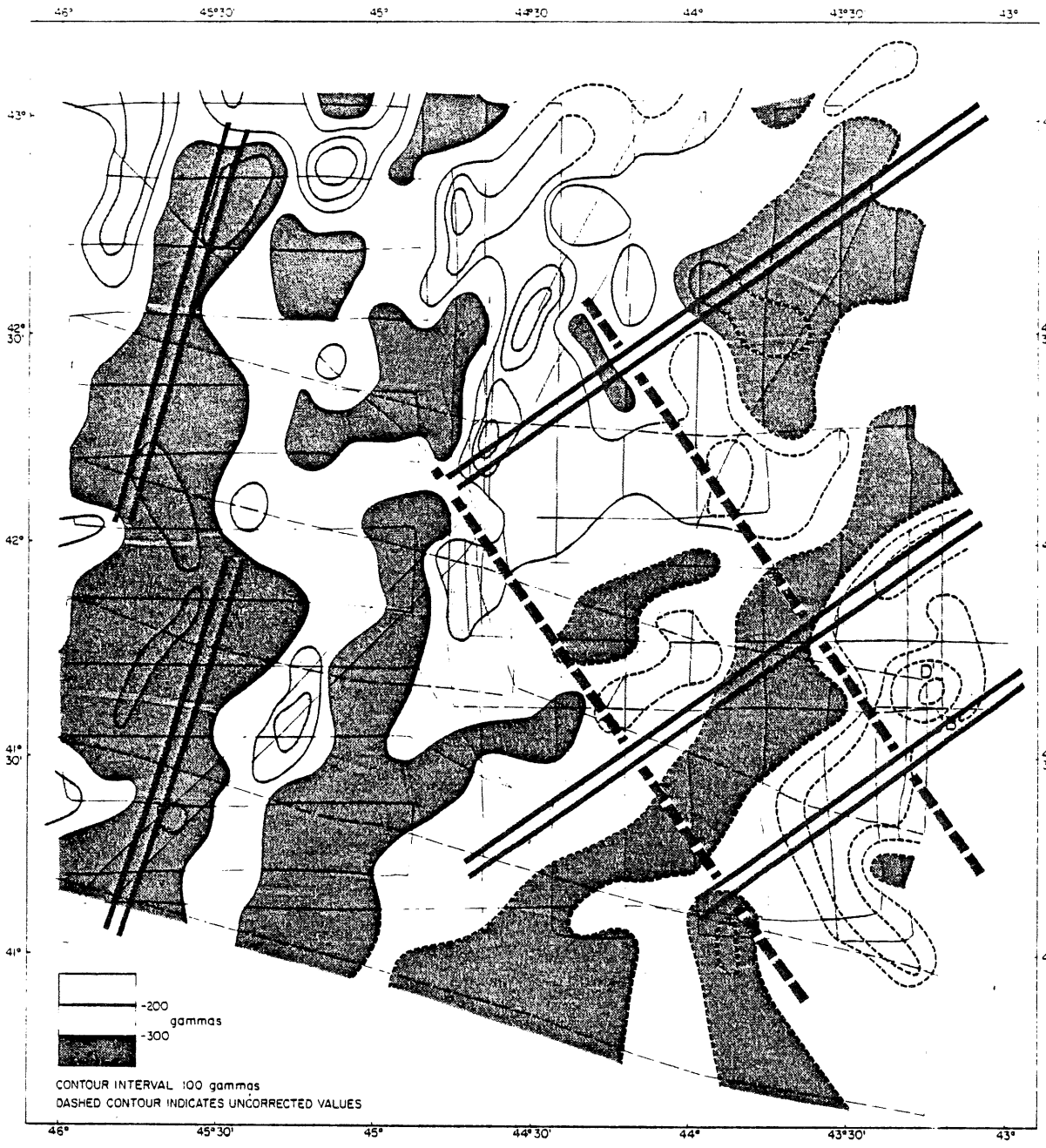

Figure 5.9a
Revised interpretation of magnetic anomaly trends, Southern Newfoundland Basin. Double solid lines are spreading axis; dashed lines are fracture zones. Contours from BRH.

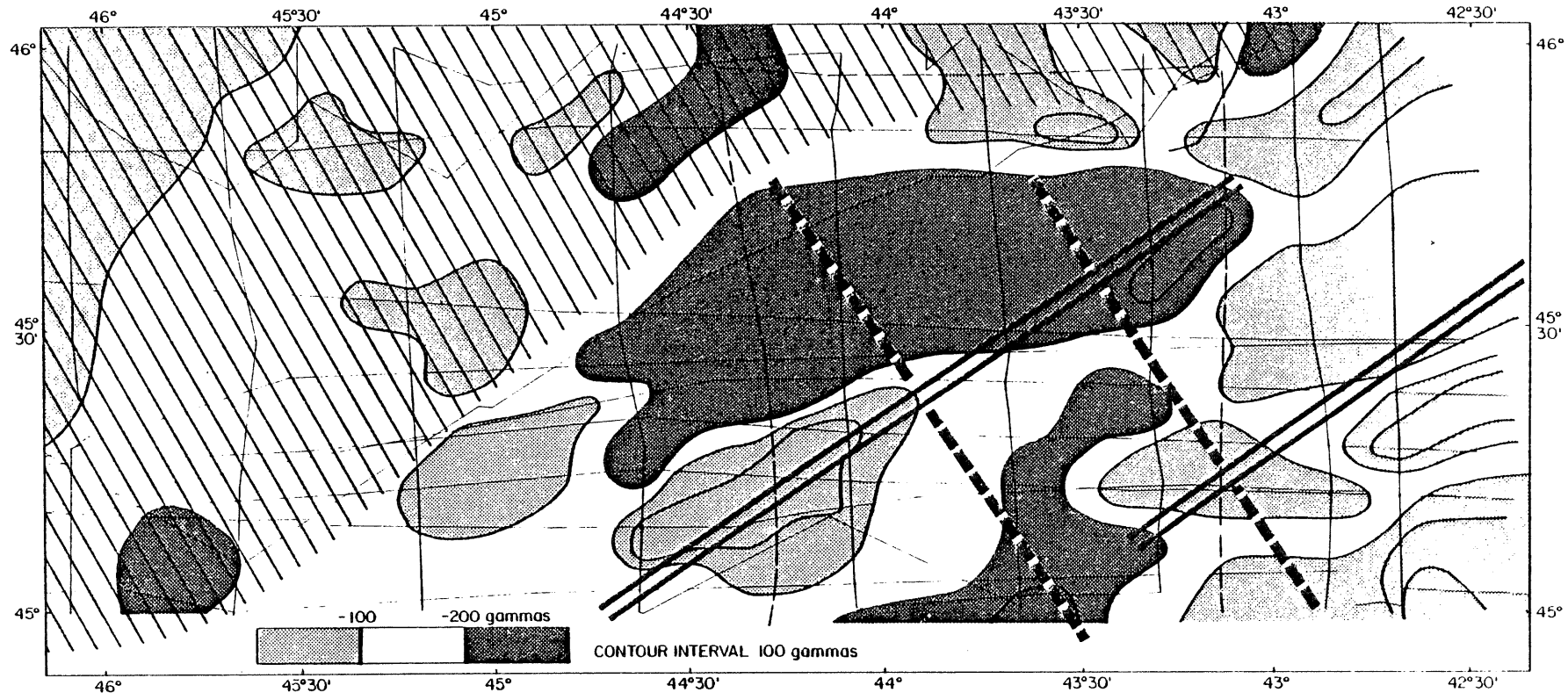

Figure 5.9b
Revised interpretation of magnetic anomaly trends, Northern Newfoundland Basin; symbols as in 5.9a. Diagonal ruling indicates smooth zone. Contours from BRH.

The pattern of 055° anomalies and 145° offsets in the Newfoundland Basin coincides almost exactly with the ridge and fracture zone trends required for this pole of rotation. The implications of this fact are discussed further in Chapter 8.

This re-interpretation of the Newfoundland Basin anomaly pattern offers at least one simple explanation for the confused reversal sequences and poor anomaly correlations described earlier: Most tracks and all model profiles currently available cross the area at rather low angles to the 055° lineations, intersecting both fracture zone and sea-floor-spreading anomalies. Correlation of the anomaly sequence between 31/32 and the J-anomaly with known Cretaceous anomaly sequences is not possible with the present coverage.

5.5 The problem of KN reversals

BRH points out that correlation of the J-anomaly with the younger Keathley sequence anomalies M2-M4 (Fig. 5.5b) requires that some of the modelled reversals east of the J-anomaly occurred during the Cretaceous Normal Interval (KN), which is supposedly a long, normal-polarity interval of Upper Cretaceous age (Irving and Pullaiah, 1976). If correct, this postulate has profound paleomagnetic implications. A review of the issue is presented below, followed by discussion of several possibly important processes affecting the oceanic magnetic layer.

The substantial terrestrial paleomagnetic evidence for constant normal polarity during KN was summarized by Irving and Pullaiah (1976). These authors also compare several Jurassic-Cretaceous time- and polarity-scales with marine reversal sequences. Terrestrial and marine

evidence for the limits of KN differ by several million years, but are in agreement on the existence of a long interval of normal polarity. Using the London time-scale (Harland et al., 1964) and the polarity scale of Larson and Pitman (1972), Irving and Pullaiah (1976) contend that 81 Ma and 110 Ma are the best estimates for the bounds of KN.

Recent detailed stratigraphic and paleomagnetic study of the limestone intervals in the Cretaceous and Paleocene pelagic sediments exposed at Gubbio, Italy (Alvarez and Lowrie, 1977), provide further evidence for the existence and age limits of KN. A younger limit of 76-82 Ma is given in this study.

However, there is also evidence which suggests that a number of field reversals occurred during KN. Green and Brecher (1974) randomly sampled 13 different sedimentary intervals in a 204 m section of the sequence cored at DSDP Site 263 (Leg 27) and found three of these to be of reverse polarity. Although "some paleontological evidence" suggested that these cores were of KN (Albian) age, Green and Becher (1974) interpret the presence of the reversals as evidence that the cores in fact pre-date KN.

According to Keating and Helsley (1976), "...at least four intervals of reversed polarity of Albian age have been found which have not been identified in the seafloor anomaly sequence." Additional work by Keating and Helsley (in press) on 44 sediment sequences, both outcrop and DSDP core samples, show that mixed polarity characterizes the entire Lower Cretaceous and the final stage of the Upper Cretaceous. Between 100 Ma and 70 Ma Keating and Helsley (in press) find normal polarity interrupted by three brief reversals.

Further terrestrial evidence for reversals during KN may come from Krumsiek's (1977) study of Cretaceous strata in the Haut-Atlas of southwestern Morocco. Preliminary results from the first of four sections to be studied show five reversals of Aptian to Cenomanian age.

In the North Atlantic south of the SENR several workers have reported the presence of roughly lineated anomalies over crust presumed to be of KN age (Vogt and Johnson, 1971; Hayes and Rabinowitz, 1975). Vogt finds (pers. comm.), as did BRH, that these anomalies are best modelled as zones of reverse-polarity crust. According to Hayes and Rabinowitz (1975), KN crust in the Pacific does not display this type of signature. However, the Cretaceous crust in the Pacific has not been studied in great detail, to this author's knowledge.

Obviously the magnetostratigraphy of the Cretaceous is yet rather unclear. The contradictions in the evidence thus far assembled might reflect conflicting biostratigraphic interpretations, errors in absolute age assignments of sediments, sampling or interpretational biases, or any number of other factors. Two interpretations of the existing data are possible, each of which raises interesting questions:

a. KN (81-110 Ma) was an interval of virtually constant normal polarity. What then, causes the apparent reversals in Atlantic oceanic crust and in some sediments of this age?

b. KN was an interval of mixed, perhaps predominantly normal polarity. Why, then, are reversals of this age not observed more consistently?

The former point raises issues most relevant to the present study, specifically the question as to what processes might affect an igneous

source-layer of uniform normal polarity in such a way as to produce apparent reversals. The remainder of this section considers, in a simplistic fashion two processes which might be involved. The essence of the discussion is that the KN oceanic crust may be a very obvious case in which geological complexity renders our current concepts of crustal magnetization, and hence our normal modelling and analytical methods, invalid.

The seafloor spreading hypothesis depends critically on the assumption that marine magnetic anomalies reflect the thermal remanent magnetization (TRM) acquired by the basalts of the oceanic crust during rapid post-eruptional cooling. It is now known that the processes involved in oceanic crustal magnetization are much more complex, on all scales from crustal to crystalline (see, for example, Harrison, 1976; Scientific Party, 1976; Kidd, 1977; Ryall et al., 1977); J. M. Hall (1977) questions whether any of the natural remanence in the oceanic crust is TRM. Alteration of the original TRM is thus the first mechanism to consider as a possible cause of the KN "reversals".

Either viscous remanent or chemical remanent components could overprint the original TRM. While it is unlikely that significant changes in magnetization direction could be produced by either of these effects (Merrill, 1975; J. M. Hall, 1977) there are certain conditions which could lead to changes in magnetization intensity by a factor of three or four (Johnson and Merrill, 1973; Merrill, 1975). The consequent magnetization contrast between juxtaposed blocks of altered and unaltered material would give rise to anomalies that could be modelled as normal and reverse polarity bodies, respectively (Fig. 5.10).

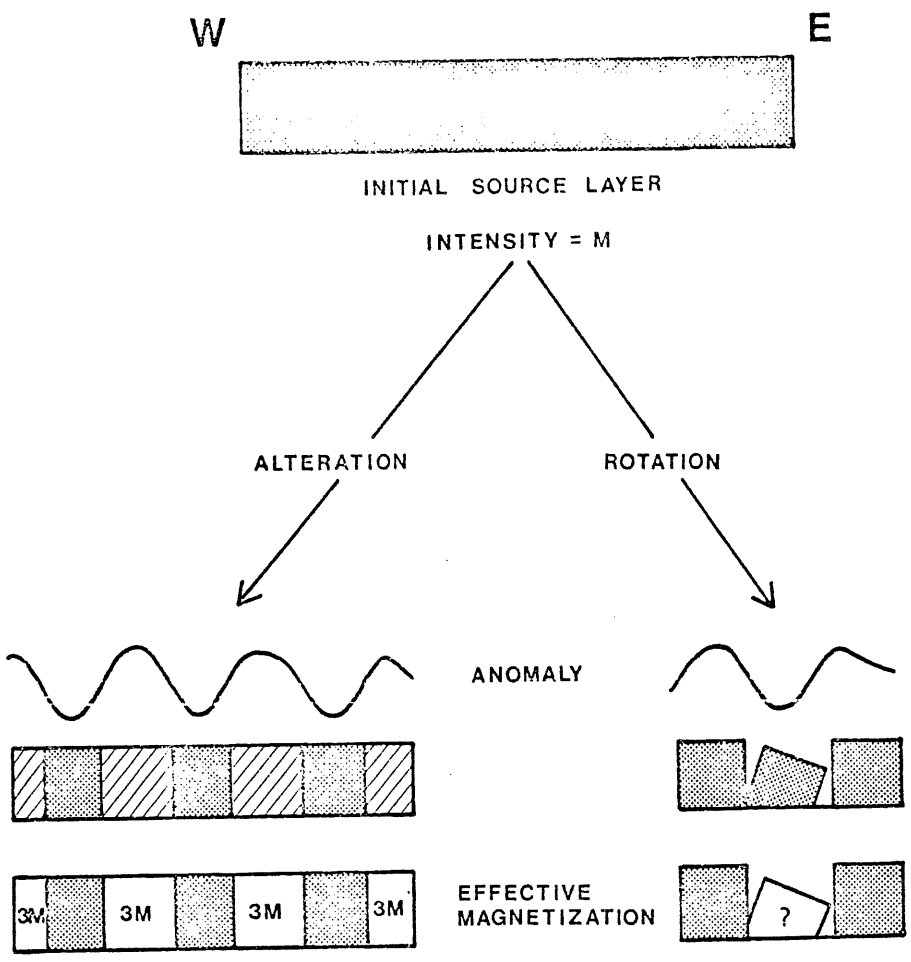

Figure 5.10
Possible mechanisms for formation of KN lineations.

This model clearly implies that the alteration (presumably related to hydrothermal processes) has selectively affected alternating elongated strips of crust.

Recent results from DSDP drilling in the Atlantic (e.g. Luyendyk, Cann et al., 1977; Donnelly, Francheteau et al., 1977) indicate that tectonic rotations of 10-30° are common in oceanic crustal blocks. Tectonic tilting of elongate crustal blocks could also produce effective magnetization contrasts that might be erroneously modelled as reversals (Fig. 5.10). The observed anomaly would probably be quite sensitive to the size of the blocks (both length and width), the amount and uniformity of rotation and the sharpness of the "edges" between blocks. Figure 5.10 illustrates this in a very schematic manner. In actuality, the interplay of these and other conceivable factors is undoubtedly very complex and development of a more explicit model must await detailed analysis of data from several areas in which KN lineations are observed.

The very possibility that either of the above models might account for the KN lineations has obvious and profound implications for paleomagnetism and ocean crust geology. The alternative point raised earlier, that mixed polarity characterizes KN but has generally not been detected, raises equally significant questions about paleontologic and radiometric age control, sampling biases, the fidelity of the terrestrial and oceanic crust as recorders of the earth's field, etc. There is clearly much work to be done on both of these fronts.

Clearly, then, there are several ways to explain apparent reversals in KN oceanic crust, and it is possible that one or more of these

could produce the observed anomaly character. Both of tbe models discussed above require that the crust has a well-developed tectonic fabric. Failure to develop such a fabric in the Pacific, perhaps because of higher spreading rates, could explain why KN anomaly lineations appear.

5.6 Summary

Qualitative examination of magnetic anomalies over the Newfoundland Basin shows that the distinctive signature of the surrounding continental areas (Haworth, 1975; Haworth and Lefort, in prep.) extends seaward onto the upper continental rise along the full length of the margin. The lack of a magnetic slope anomaly comparable to that observed along Atlantic margins south of the SENR reflects the fact that the physiographic continental margin in the Newfoundland Basin is not the locus of the ocean-continent edge.

The rather flat, generally negative field in the marginal smooth zone is abruptly terminated, near the transition from upper to lower continental rise, by a 500-700 nT positive anomaly. South of the seamounts this anomaly is coincident with the J-anomaly.

The disturbed area seaward of the magnetic smooth zone displays a pattern of roughly lineated anomalies. South of the seamounts the lineations display two azimuths (Fig. 5.9a): 015° (parallel to the smooth zone boundary) from the western limit of the disturbed zone to about 45°W; 055° east of 45°W. In the northern detailed survey area (Fig. 5.9b) only the 055° lineations are observed. The pattern of 055° anomaly lineations and 145° offsets is evidence supporting the hypothesis that the opening of the Bay of Biscay and early Iberia-North

America relative motions involved rotation about a pole located northeast of Paris (LeBorgne et al., 1971; LePichon et al., 1971; LePichon et al., 1977).

Two important points raised by these observations have been considered in some depth in this chapter. These are: a) The relationship, other than geometrical, between the J-anomaly and the smooth zone boundary; and b) The origin of apparent reversals within the crust east of the J-anomaly, which presumably formed during KN, the Cretaceous Quiet Interval (Irving and Pullaiah, 1976).

The data do not at present provide a definite solution to the first of these questions. Similar amplitudes and wavelengths characterize the J-anomaly and the smooth zone boundary anomaly (Fig. 5.6), and comparable basement structures are associated with both anomalies. In the southern Basin the boundary anomaly is on strike with the J-anomaly observed on the northern flank of the SENR (BRH); in the northern Basin the 055° lineations occur immediately seaward of the boundary. The weight of this circumstantial evidence supports the coincidence of the J-anomaly and the smooth zone boundary south of the seamounts and suggests that the boundary is younger north of the seamounts.

The question of apparent KN reversals is predicated upon correlation of the J-anomaly with the younger Keathley sequence anomalies. This correlation is favored for the Newfoundland Basin (BRH, C. E. Keen et al., 1977) and by most other studies in the North Atlantic (Rabinowitz et al., 1977). Most of the discussion in Section 5.5 further assumes that the magnetic field was normal between about 81 Ma and 110 Ma. Two

mechanisms are discussed which theoretically could modify oceanic crust of uniformly normal polarity so as to produce large magnetization contrasts (up to 0.05 emu/cm^3) which might be mis-interpreted as reversals. Both rock-magnetic and tectonic processes can produce sufficiently large magnetization contrasts, and in crust with a well-developed tectonic fabric, such as forms at present at slowly-spreading ridges, these processes might give rise to reasonably coherent anomaly lineations. The goal in this discussion has not been to provide definitive answers or detailed models, but rather to provoke fresh thinking and to urge renewed research on this very complex and important topic.

CHAPTER 6: GRAVITY

Bedford Institute has collected a considerable quantity of gravity data in the Newfoundland Basin and surrounding areas since 1965 (Figure 5.1; Appendix IV). The value of these data in the present study lies chiefly in their bearing on the following three points: the structure of the continental margin; the location of the ocean-continent transition; the delineation of major structural elements within the Newfoundland Basin and of relationships between these features and structures in the surrounding continental areas.

This chapter examines the gravity data and their correlation with shallow crustal structures and magnetic data with these points in mind. Sections 6.1 and 6.2 describe the salient features of the contoured free-air field and of isostatic and free-air profiles, respectively. The emphasis shifts, in the modelling studies described in Section 6.3, to the continental margin regime. The chapter concludes with a summary of the main points emerging from analysis of the gravity data (6.4) and a general discussion of some aspects of isostatic and free-air gravity anomalies at rifted continental margins (6.5).

All the data used in this study were measured with Graf Askania GSS-2 gravimeters mounted on gyro-stablized platforms. Cross-coupling errors were measured on some of the cruises, but no cross-coupling correction has been applied to the data.

6.1 Free-air Averages

Variations in navigational accuracy over twelve years of surveying and errors induced by ship motion in heavy seas render simple contouring of these data impossible. In order to smooth out these variations and obtain meaningful contours, the free-air data were averaged over square areas measuring 1/4° of latitude (27.7 km) on a side, using the GRIDITMS computer program described by Haworth and MacIntyre (1975). A second program, GPCP (Haworth and MacIntyre, 1975), was used to plot and contour the averaged values; the machine contouring was verified by hand.

Comparison of the 1/4° -average bathymetry shown in Figure 6.1 with the actual bathymetry (Fig. 3.1) gives a qualitative indication of the amount of fine detail lost through the averaging. Woollard (1969) shows that the amount of suppression produced by averaging data in this manner is a function of the anomaly wavelength and the size of the averaging area:

$$\theta = 120X - 20$$

where: θ = percent of suppression

X = percent of the wavelength used in averaging.

For 1/4° averaging areas, this gives zero suppression of wavelengths 167 km or greater, 50% suppression of 48 km wavelengths and, obviously, 100% suppression of 27.7 and shorter wavelengths. For present purposes, this suppression does not significantly reduce the information content of the data.

Figure 6.1 shows that the continental shelf to the north and west of the Newfoundland Basin is characterized by positive free-air anomalies which attain amplitudes of 70-100 mgal along the southeastern edge of Flemish Cap, over Beothuk Knoll and in a band extending eastward from the shelf into the Basin at the Tail of the Bank. The latter trend is coincident with the prolongation of the Collector Anomaly, the linear positive magnetic and gravity anomaly which is believed to mark the southern limit of the Precambrian Avalon Zone on the Grand Banks (Chapter 2; Haworth, 1975; Haworth and Lefort, in prep.). Low-amplitude positive anomalies (0-20 mgal) are observed over Flemish Pass and parts of the Grand Banks. The prominent negative anomaly at the northwestern limit of the map area has been shown to reflect the thick sedimentary accumulation in the Jeanne d'Arc Sub-basin (Haworth and MacIntyre, 1975).

Significant changes in the amplitude and average value of the shelf-edge anomalies occur along the strike of the continental margin. This apparent segmentation of the margin parallels the physiographic subdivision outlined in Chapter 3. The Flemish Cap and Eastern Banks margin segments exhibit typical shelf-edge free-air anomalies of which the negative regions labelled E and F in Fig. 6.1 mark the negative, seaward portions. The Flemish Pass segment of the margin displays an anomaly of similar shape, but with lower amplitude and a mean value greater than zero (see also Fig. 6.2, profile 36).

Gravity over most of the lower continental rise ranges from 0-20 mgal. The Newfoundland Seamounts and the northwestern part of the lower rise are characterized by somewhat higher gravity than the rest

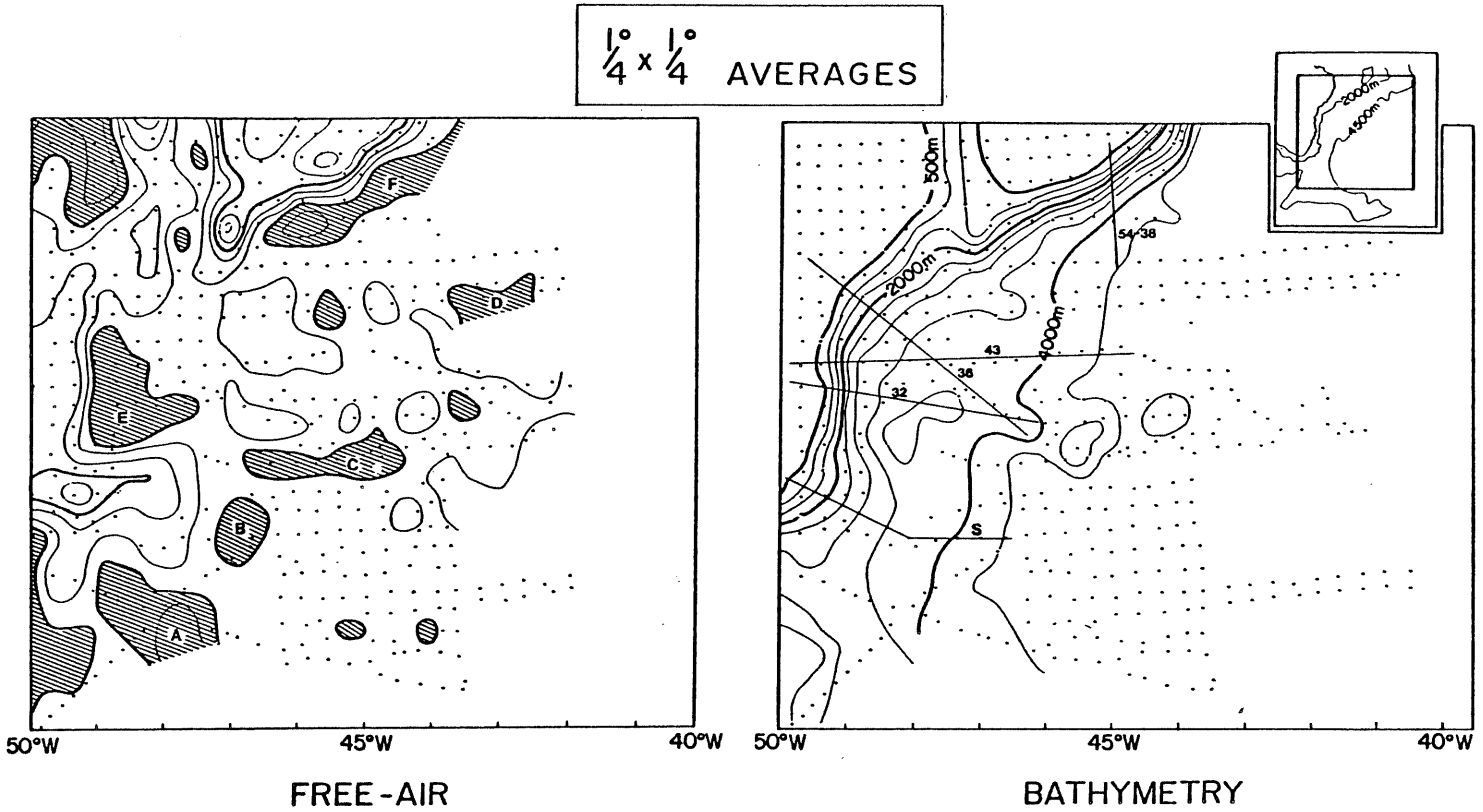

Figure 6.1

Average free-air gravity anomalies and bathymetry.
Negative anomalies shaded; contour intervals 20 mgal and 500μ.
Location of profiles in Fig. 6.2 also shown.

of the Newfoundland Basin (20-50 mgal).

Four regions of negative gravity are sufficiently well-controlled by the track coverage to be significant (A-D, Fig. 6.1). Negative region C, the east-west striking belt just south of the seamounts, is colinear with the prolongation of the Collector Anomaly, noted above. The western limits of negative anomalies B, C and D are colinear with the western limit of the -20 mgal contour in anomaly A; the line A-D (Fig. 6.1) is parallel to, and nearly coincident with, the boundary between the smooth and disturbed magnetic regions described in Section 5.3.

6.2 Profiled data

Bathymetric, magnetic and gravimetric data along the five profiles indicated in Figure 6.1 are presented in Figure 6.2. The isostatic gravity anomaly is shown along with the free-air anomaly for each profile, primarily to permit comparison with rifted margins elsewhere (Section 6.5). In view of the great emphasis placed on the significance of isostatic gravity anomalies at rifted margins in the recent literature (e.g. Talwani and Eldholm, 1972, 1973; Rabinowitz, 1973, 1974; Rabinowitz and LaBrecque, 1977) it is worthwhile to digress briefly in order to critically examine the assumptions involved in calculation of the isostatic corrections and the comparative significance of the isostatic and free-air anomalies.

The isostatic anomaly is the difference between the observed Bouguer anomaly (equivalent to the free-air anomaly at sea) and the

anomaly predicted by an isostatic model. The principle underlying the latter theoretical model is that hydrostatic equilibrium obtains at some depth (T, the depth of compensation) within the earth's crust, i.e. all crustal columns exert the same pressure at the depth of compensation. The most widely used model is that of Airy, in which areas of high elevation are compensated by deep crustal "roots", and vice versa. Where the gravity anomaly calculated for the isostatic model approximates the observed Bouguer gravity, the isostatic anomaly will be near zero, indicating that the area is essentially in isostatic equilibrium. Non-zero isostatic anomaly values thus indicate that the actual crustal section contains uncompensated mass excesses or deficiencies.

The great interest in isostatic gravity at rifted continental margins has arisen from the desire to obtain more information on structures beneath the continental slope and upper rise and to locate the ocean-continent boundary. As Worzel (1965) shows, free-air anomalies over the slope and rise are dominated by the effects of seafloor topography and compensating mantle topography (herein termed the "shelf-edge anomaly"). It is a simple procedure to calculate an isostatic correction which largely removes the components of the free-air anomaly arising from these layers (the effect of the sediment layer can be included in the correction, if desired) and so reveals more clearly the gravity signature of intra-crustal density distributions. For this limited purpose, the choice of a particular isostatic model is not crucial (Talwani and Eldholm, 1973; Konig and Talwani, 1977; Rabinowitz and LeBrecque, 1977).

Seaward of the physiographic margin the isostatic correction is usually small, and the free-air and isostatic anomalies are essentially

identical. It seems evident, then, that the isostatic anomaly should not contain any more significant information than the free-air anomaly, except perhaps in the slope region. More specifically, application of an isostatic correction to the observed data does not reduce the limitations imposed by the non-uniqueness of potential field data. This means that the isostatic anomalies, like the free-air, are best interpreted in conjunction with seismic and other potential field data wherever possible. The subject of isostatic gravity at rifted margins in general is taken up again in Section 6.5.

The isostatic anomalies along the Newfoundland Basin profiles shown in Figure 6.2 were calculated using two-dimensional Airy isostatic models and assuming point-wise isostatic equilibrium. The isostatic models consisted of three uniform layers (water, 1.03 gm/cm^3; crust, 2.67 gm/cm^3; mantle, 3.3 gm/cm^3) and the depth of compensation was assumed to be 30 km. Only the effect of the water layer and its compensation were taken into account in calculating the isostatic corrections for these profiles.

Profiles 54-38, 36, 43 and 32 cross the Flemish Cap and Eastern Banks margins north of the Newfoundland Seamounts (Fig. 6.1). Recall that the seismic data along these lines (Figs. 4.3a, b) show that there are thick accumulations of sediment in deep troughs beneath the slope and upper rise, and that these troughs are bounded to seaward by seamounts or by buried basement highs (the Flemish Cap Ridge); a prominent basement high is observed beneath the base of the slope on lines 36 and 43; and the continental rise sediment prism is particularly thick north of the seamounts.

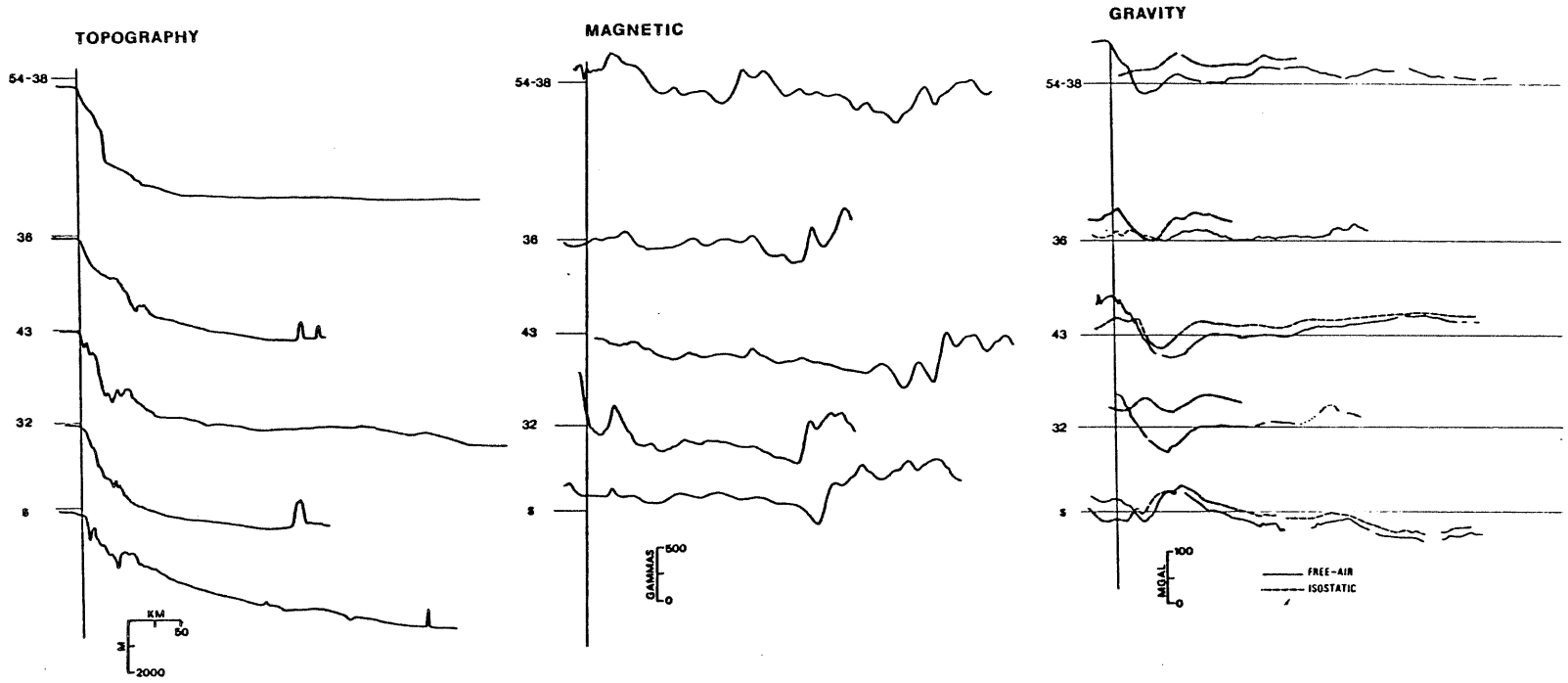

Figure 6.2

Bathymetry, magnetic and gravity profiles.
See Fig. 6.1 for location.

Free-air shelf-edge anomalies are prominent in the gravity data on all four of these profiles (Fig. 6.2). As noted in the $^{1}/_{4}°$ averages, changes in the amplitude and mean value of the shelf-edge anomalies are evident from south to north along the Eastern Banks margin (compare profiles 32 and 43 with profile 36) and between this area and the Flemish Cap margin (profile 54-38). On profiles 43 and 32 the free-air anomaly seaward of the low over the base of the slope remains at zero for a distance of about 100 km and then increases to about 50 mgal. A similar pattern is observed on profiles 54-38, and 36, but here small positive anomalies (20 mgal) are observed between the base of the slope and the region displaying the constant, near-zero free-air anomalies.

The isostatic anomalies on these four lines are very interesting, contrasting strongly with the anomalies observed across the Tail of the Bank margin (Line S) and on most other rifted continental margins (Section 6.5). The shelf-edge topographic effect has been substantially reduced by the isostatic correction, as expected, and Line 32 provides a good example of a case in which the isostatic correction reveals a significant gravity anomaly which was not visible in the free-air field. The isostatic anomalies are generally positive, and the difference between the isostatic and free-air values is rather large over most of the profile length. It has been verified that including the effect of the sediment layer in the isostatic correction lessens this difference appreciably.

Line S, crossing the continental margin near the Tail of the Bank, displays a rather different gravity signature. The shelf-edge free-air anomaly is quite subdued here, and the free-air and isostatic anomalies

are more nearly equal in value. Again, as on Line 32, the isostatic anomaly reveals a gravity high near the middle of the continental slope, coincident with a large positive magnetic anomaly, which was not visible in the free-air anomaly. A prominent gravity high (free-air and isostatic) is observed over the base of the slope, coincident with a broad magnetic anomaly minimum. The gravity anomalies decrease rather steadily seaward of this positive anomaly. A small gravity high is observed at the change in magnetic field character that marks the boundary of the marginal smooth zone (Chapter 5). Unfortunately, there are no seismic data available along this profile to clarify the relationship between these observations and shallow crustal structure.

6.3 Continental Margin Models

The gravity profiles described above and the physiography outlined in Chapter 3 both indicate clearly that the continental margin is structurally segmented. Two-dimensional models of the free-air gravity across the margin have been constructed along four profiles 54-38, 43, 36, 32, Figs. 6.1 and 6.2) to see what kinds of differences in crustal structure might exist between these segments.

The models were constructed in the following manner. The water, sediment, crust and mantle layers were considered as uniform layers and were assigned densities of 1.03, 2.20, 2.70 and 3.30 gm/cm^3, respectively. Initial model geometries incorporated the observed water depth and sediment thickness and the depth to Moho determined in calculating the isostatic anomalies in Figure 6.2. In the latter calculation it was assumed that the crust is homogeneous from seafloor to man-

tle, whereas the models include a layer of lower density (sediment) at the top of the crust. As a result, these initial model geometries produced gravity values that were consistently low. The depth to Moho was therefore adjusted upward (by trial-and-error) to compensate for the sediment layer. A check of the mass contained in oceanic and continental crustal columns shows that the adjusted mantle configurations are consistent with the assumption of isostatic equilibrium. Line S, for which no seismic reflection control exists, was modelled in essentially the same way, except that hypothetical rather than observed basement topography was put into the model and adjusted to account for as much as possible of the short-wavelength anomaly field.

The final models are shown in Figure 6.3. In general there is a strong similarity between all of the models. The results indicate that the change from continental to oceanic crustal thickness occurs over a relatively narrow region (70-100 km) and that uncompensated basement topography can account for most of the short-wavelength components of the free-air field. Several more specific points are worth noting.

Line 36 (Fig. 6.3b), which extends to the western limit of the Newfoundland Seamount province, incorporates a 2.5 km increase in crustal thickness beneath Screech and Number 3 seamounts; an intracrustal density low could equally well be postulated, but is felt to be less likely. The thick accumulation of sediments beneath the slope on this line is consistent with the fact that basement is too deep to be observed on the seismic record across the slope.

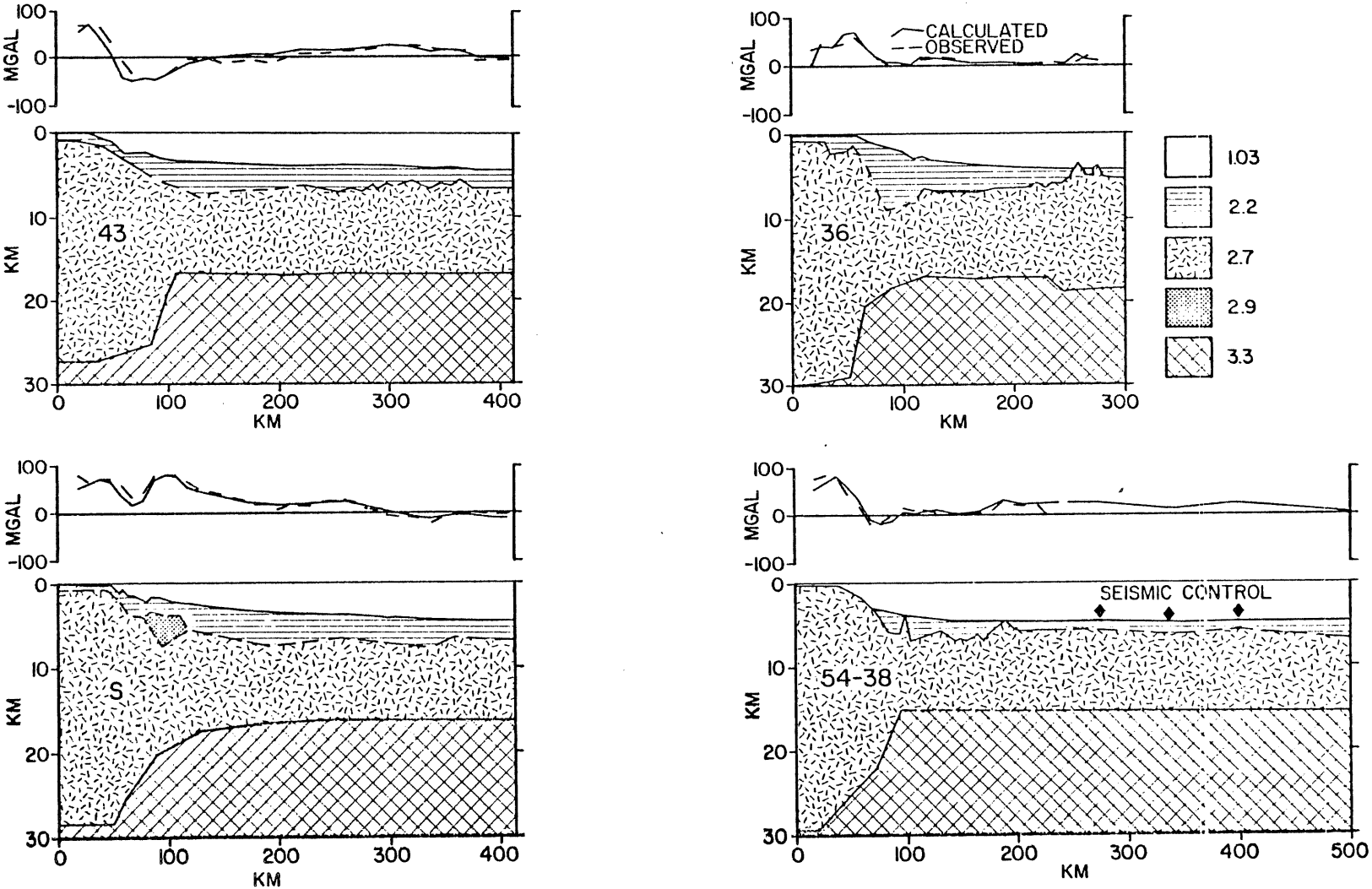

Figure 6.3: Free-air gravity models.

Line S crosses the positive anomaly that marks the prolongation of the Collector Anomaly (Chapter 2) into the southern Newfoundland Basin. The model for this line differs significantly from the others in Figure 6.3. First, the depth to mantle changes more smoothly from the continental to the oceanic sections of the model. Secondly, the amplitude of the gravity high over the base of the slope could not be accounted for by simply assuming that a basement high (ρ = 2.67 gm/cm^3) underlies the observed seafloor high. Consequently, the final model includes a high-density body (ρ = 2.9 gm/cm^3) beneath this point. If this is postulated to represent an igneous intrusive, then it must be a mass of reversed magnetic polarity, since the gravity maximum coincides with a broad magnetic anomaly minimum. For a density of 2.9 gm/cm^3, the velocity-density data given by Ludwig et al. (1970) predict a compressional wave velocity between 6.2 km/sec and 7.2 km/sec. Velocities in this range are appropriate for lithologies from both the continental and oceanic domain, such as schists, gabbros and metabasites (Sheridan and Drake, 1968; Mayhew, 1974; Christensen and Salisbury, 1975).

None of these models takes into account possible differences in the density of sub-continental and sub-oceanic mantle. C. E. Keen and Loncarevic (1966) obtain values of 3.42 gm/cm^3 and 3.32 gm/cm^3 for the density of the mantle beneath the shelf and lower rise, respectively, on the Nova Scotia margin. Similar models (essentially Pratt isostatic models) can be constructed for the Newfoundland Basin profiles, but seismic refraction data across the margin are necessary to determine whether this mechanism for isostatic compensation or the Airy type assumed above is actually operative.

6.4 Summary

The significant points of this section are:

1. Shelf-edge anomalies are well-developed along the Flemish Cap and Eastern Banks margins, with a high over the shelf edge and a low over the slope. Modelling suggests that both basement and mantle topography contribute to the high, while thick sediment accumulations beneath the slope appear to account for the low.

2. The Flemish Pass and Tail of the Bank margins display modifications of the typical shelf-edge anomaly. Simple differences in basement and mantle topography can account for the observations on Line 36. One Line S, a high-density body beneath the slope is required to fit the broad positive anomaly which marks the prolongation of the Collector Anomaly into the Newfoundland Basin.

3. If modelled crustal thickness were the sole criterion for distinguishing between oceanic and continental crust, the ocean-continent boundary would be placed in a rather narrow (tens of kilometers) zone near the base of the slope on profiles 43, 54-38 and 36 (excluding seamounts from consideration). The model for line S (Fig. 6-3b) indicates that the change from continental to oceanic crustal thickness at the Tail of the Bank occurs over a region about 100 km wide.

4. It is not possible at this time to determine with certainty the nature of the structural differences between the various segments of the continental margin. The schematic models presented here suggest that the degree of relative subsidence between adjacent margin segments and, possibly, volcanic or intrusive activity on some segments, are significant factors. Grow and Bowin (1977) attribute the segmented

nature of the eastern United States continental margin to similar factors.

5. Uncompensated basement topography, consistent with available seismic reflection data, can account for most of the short-wavelength features of the gravity anomaly.

6. The model of the westernmost Newfoundland Seamounts suggests that either lower density material within the crust or thicker crust underlie the seamounts; the latter is believed to be more plausible. However, the amount of data currently available here is quite marginal, so this result should be accepted with caution.

7. A linear gravity low strikes NNE across the Basin from the vicinity of the Tail of the Bank to Flemish Cap. Modelling of Line S, which crosses this low (350 km; Fig. 6.3b) suggests that the low reflects a narrow trough of sediment; the rough-smooth magnetic transition occurs over the seaward side of this feature.

6.5 Discussion: Gravity anomalies at rifted continental margins

The observation that linear belts of spatially-related gravity and magnetic anomalies characterize many rifted continental margins led Talwani and Eldholm (1973) to propose that distinctive anomaly associations and, in particular, isostatic gravity anomaly characteristics could be used to identify the location of the ocean-continent boundary. Examining data from the margins of Norway and Southwest Africa, Talwani and Eldholm (1973) noted that a distinctive isostatic gradient coincides with the seaward boundary of the marginal magnetic smooth zone, and they interpreted this gradient as a "diagnostic" indication of the change from continental to oceanic crust. This de-

scriptive model has been applied, with varying degrees of success, to many other rifted margins, although few studies have addressed the problem of determining the origin of the "diagnostic" isostatic anomalies (see Rabinowitz and LaBrecque, 1977).

It seems worthwhile to examine the applicability of this model in a variety of cases. This undertaking is prompted by the following observations and questions. First, it was stated earlier on in this chapter that isostatic anomalies are in fact only a little more useful, and no less non-unique, than free-air anomalies. This naturally leads one to wonder whether particular characteristics of the isostatic gravity anomaly can really provide a reliable indication of the ocean-continent boundary when free-air anomalies cannot. Secondly, the initial studies of Talwani and Eldholm (1972, 1973) and most subsequent studies in which the Talwani-Eldholm model has been shown to account very successfully for the observations (e.g. Rabinowitz, 1976; Konig and Talwani, 1977; Rabinowitz and LaBrecque, 1977) consider Cretaceous margins; do older rifted margins display the "diagnostic" isostatic anomalies? Finally, there is a significant difference between the gravity signature of the margins in the northern and southern Newfoundland Basin; how do these profiles compare with observations at other rifted margins, and with the Talwani-Eldholm model? This discussion is intended to be provocative rather than expository, pointing out areas for further study and offering some possible interpretations, but few definitive answers.

The gravity profiles that have been selected for this comparison are

shown in Figure 6.4. Newfoundland Basin profiles 54-38 (Flemish Cap margin) and S (Tail of the Bank margin) were chosen from among the profiles in Figure 6.2 because these crossings of the margin include continuous gravity measurements out to the magnetic smooth zone boundary and are not complicated by the presence of seamounts. The other profiles were included because they are representative of a) the margins upon which Talwani and Eldholm (1973) based their model (profiles 8 and 9) and other margins to which the model appears to be applicable (profile 7; Konig and Talwani, 1977); b) an older Atlantic margin (profiles 5 and 6; Rabinowitz, 1974); and c) a Cretaceous margin adjacent to the Newfoundland Basin (profiles 1 and 2; Srivastava, 1978; Folinsbee, in prep.). The location of prominent magnetic highs and of the ocean-continent boundary according to the original authors are indicated above each profile.

The characteristics of the isostatic gravity anomalies (hereafter called the '"ocean-continent" anomaly' for simplicity) upon which Talwani and Eldholm (1973) base their model are illustrated clearly by profiles 7 through 9. These profiles also illustrate the high degree of similarity in gravity signature which Cretaceous margins often display. On each line the "ocean-continent" isostatic anomaly coincides with a prominent magnetic anomaly (identified as anomaly 22 on profile 7; Konig and Talwani, 1977) and a basement high; its position landward of the shelf edge on profile 8 is attributed by Rabinowitz (1976) to seaward progradation of the shelf sediments onto oceanic crust. The "ocean-continent" anomaly is interpreted in each of these three studies as the effect of uncompensated oceanic basement relief.

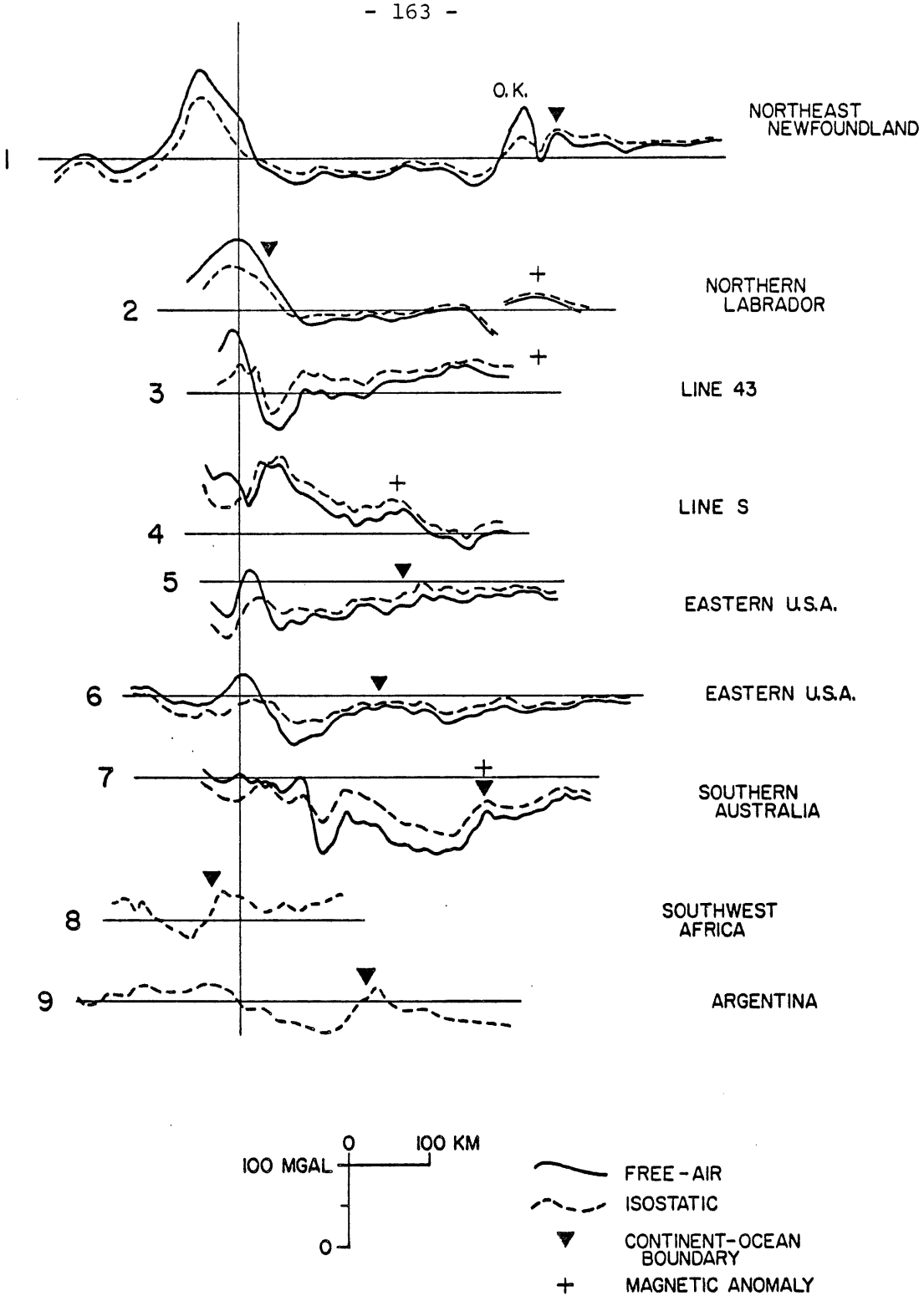

Figure 6.4

Comparison of free-air and isostatic gravity on Jurassic and Cretaceous rifted margins.

Rabinowitz (1974) interprets the gravity data across the eastern U.S. continental margin south of the New England Seamounts (profiles 5 and 6) in terms of the Talwani and Eldholm (1973) model and the hypothesis that all magnetic smooth zones bordering rifted continental margins reflect, at least in part, a zone of subsided continental crust. He identifies a magnetic anomaly (Anomaly E) which divides the Jurassic Quiet Zone into a smoother landward and rougher seaward section and models this anomaly as the landward termination of the oceanic magnetic anomaly source-layer. However, the isostatic gravity signature associated with Anomaly E bears little resemblance to the supposedly diagnostic "ocean-continent" anomalies in profiles 7-9. Possibly this reflects decay of isostatic anomalies with time. Alternatively, this margin may be fundamentally different from those described above, and the Talwani and Eldholm model may simply not apply here. Until the significance of the "ocean-continent" anomaly is understood more fully, it is not clear what the nature of these "fundamental" differences might be.

It is important to note that strongly conflicting interpretations have been proposed for the location of the ocean-continent boundary and the origin of Anomaly E north of the New England Seamounts. C. E. Keen et al. (1975) present seismic refraction data from the margin off Nova Scotia which show that the transition from oceanic to continental crustal thickness occurs near the base of the continental slope; this transition is about 100 km landward of Anomaly E. C. E. Keen et al. (1975) interpret the magnetic slope anomaly (East Coast Magnetic Anomaly of Rabinowitz, 1974) as an edge-effect due to magnetization con-

trasts at the boundary between oceanic and continental crust. Oceanic layer 2 is traced on seismic reflection profiles to within 90 km of the shelf edge. In a subsequent detailed magnetic and seismic study of the Jurassic Quiet Zone north of the New England Seamounts Barrett and Keen (1976) show that the location of Anomaly E coincides with the point where both sediment thickness and basement depth begin to increase rapidly landward. These authors also show that the correlation between positive oceanic basement topography and magnetic anomalies is very strong in this area. On the basis of these observations and the earlier studies of C. E. Keen et al. (1975) Barrett and Keen (1976) conclude that Anomaly E represents a basement topographic effect and the more subdued character of the anomalies to landward is due to increasing depth of burial of the oceanic crust.

Representative gravity profiles from the western Labrador Sea and northeastern Newfoundland continental margins are shown in profiles 1 and 2 (Srivastava, 1978; Folinsbee, in prep.). The most important point to note is the considerable variability in gravity signature at the presumed ocean-continent boundaries on these profiles. Profile 1 extends across the northeastern Newfoundland margin to Orphan Knoll, a sunken continental fragment (Ruffman and van Hinte, 1971). Continental structural trends from the shelf continue out into the region between the shelf edge and Orphan Knoll, confirming that this area is floored by subsided continental crust (A. C. Grant, 1972; Haworth, in prep). The ocean-continent transition thus lies seaward of Orphan Knoll; Folinsbee (in prep.) places it at the positive isostatic and free-

air anomaly 40 km to seaward of the Knoll. In interpreting the unusually high-amplitude isostatic and free-air anomalies observed over the shelf edge along the Newfoundland and Labrador margins, Folinsbee (in prep.) invokes lithospheric flexure induced by the accumulation of a large uncompensated load of sediments.

The gravity signature at the point designated as the ocean-continent boundary on profile 2 (Srivastava, 1978) bears virtually no resemblance to the supposedly typical signature, although Srivastava (1978) cites Talwani and Eldholm (1973) as the source for the principle followed in locating the boundary. Srivastava's interpretation is based on examination of a large amount of detailed geophysical data from the Labrador Sea and its margins, and it is consistent with the results of other studies to the north and south of the region included in his study, so it cannot be lightly dismissed; the disagreement with the proposed general model for gravity at continental margins must be regarded as significant.

Profiles 43 and S from the Newfoundland Basin were described in general terms in an earlier section (6.2). Only a few points need to be noted in the present context. The observations along Line S appear to be in fair agreement with the Talwani-Eldholm model. The free-air and isostatic high 250 km east of the shelf break is coincident with the J-anomaly, which marks the seaward limit of the marginal magnetic smooth zone in the southern Newfoundland Basin. The smooth zone boundary occurs about 25 km east of the end of profile 43, which crosses the Eastern Banks margin north of the Newfoundland Seamounts. Although

this profile does not extend quite as far as one would hope, it does serve to illustrate the unique character of gravity across the northern Newfoundland Basin margins. The progressive increase in the free-air gravity to seaward appears to be largely due to a decreasing sediment thickness and depth to basement (Fig. 6.3).

What do all of these observations mean in terms of present knowledge of gravity at rifted margins and ocean-continent boundaries?

First, the data presented in Figure 6.4 confirm the point made above concerning free-air versus isostatic anomalies: both anomalies display very similar characteristics at the presumed ocean-continent boundary, and both can be attributed to uncompensated basement highs. What makes these gravity anomalies diagnostic of the ocean-continent boundary is not a particular aspect of their shape but rather their association with a pronounced change in magnetic field character and seismic structure.

The profiles in Figure 6.4 also illustrate that the gravity model described by Talwani and Eldholm (1973) successfully accounts for the observations on certain Cretaceous rifted margins but is apparently not valid for a number of other Cretaceous margins and for the Jurassic margin off the eastern United States. The possibility that the initial gravity signature of the ocean-continent boundary varies from margin to margin as a function of temporal changes in the rifting process or regional changes in the geology (e.g. the complexity of pre-rift structures and their orientation to the prevailing stresses; Arthaud and Matte, 1977) must be considered in attempting to account for these differences. The history of the margin subsequent to rifting will also involve a

variety of processes which may vary significantly from one margin to another, and the possibility that their effects might mask or mimic the gravity signature of the ocean-continent boundary cannot be ignored.

In summary, it seems evident that present knowledge of the factors controlling gravity at rifted margins is insufficient to justify formulation of generalized models, especially models which consider gravity data separately from other geophysical data. The utility of the Talwani-Eldholm model in many cases must not obscure the fact that there are many fundamental questions yet to be answered.

CHAPTER 7: THE NEWFOUNDLAND SEAMOUNTS

The Newfoundland Seamounts were discussed briefly in Section 3.1. The present chapter reviews the seamount morphology and structure (7.1) and presents petrographic, geochemical and chronological data (7.2, 7.3). This discussion is not oriented towards development of a detailed petrogenetic model, but rather towards assembling all the evidence that bears on the significance of the seamount volcanism in the evolution of the Newfoundland Basin (7.4).

The morphological and geochemical data from Scruncheon and Dipper Seamounts presented by Sullivan and Keen (1977) are included in this report, supplemented by results from subsequent studies of Screech and Shredder Seamounts. Many of the data are presented within the text in the form of summary diagrams. Appendix II gives additional details, including cruise lists and dredge station locations, a discussion of geochemical analytical methods and accuracy, a complete listing of geochemical data and photomicrographs (reflected and transmitted light).

7.1 Morphology and Structure

The thirteen peaks which comprise the Newfoundland Seamounts lie in a roughly triangular area near the center of the Newfoundland Basin (Fig. 7.1). Most of the seamounts lie within a relatively narrow east-west zone between 43°30'N and 44°N. The tops of the seamounts lie at depths of 2,500m-3,100 n (Table 3.1), but the total relief of the seamounts (including the buried bases of the structures) is fairly constant between 3.1 km and 3.2 km, where known. There appears to be an increase in seamount volume from west to east; the direction of elongation is

increase in seamount volume from west to east; the direction of elongation is variable throughout the group (Table 3.1).

As discussed in Chapter 4, the present seismic coverage in the seamount area is sparse. No tracks have been run across the seamount province in a north-south direction, and only one line is available crossing the entire region from east to west. Basement along the latter line is up to 1 second shallower, and generally smoother than that observed elsewhere in the Basin. The four seismic profiles across seamount peaks (Figs. 3.8 and 4.2) all terminate too near the junction between the seamount flank and the adjacent acoustic basement to provide much information on fractures or other basement structures associated with the seamounts. In spite of these limitations, several significant observations can be made.

The flanks of the seamounts are acoustically continuous with adjacent seismic basement, which is inferred, by correlation with a nearby crustal refraction section (H. R. Jackson et al., 1975), to be the top of oceanic layer 2. The sediment cover post-dates seamount formation, and deposition throughout most of the section appears to have been influenced by proximity to the seamount structures.

Deep troughs (faults?) occur near the true, sub-seafloor base of at least two seamounts. Each of these fractures is only observed on a single track, so their strike and extent are unknown.

Up to 0.3 seconds of strongly reflective sediment forms the rather flat top of Shredder Seamount; dredging has shown that this sedimentary cap consists of shallow-water bioclastic limestone. Little or no sediment cover is evident on the other seamounts profiled.

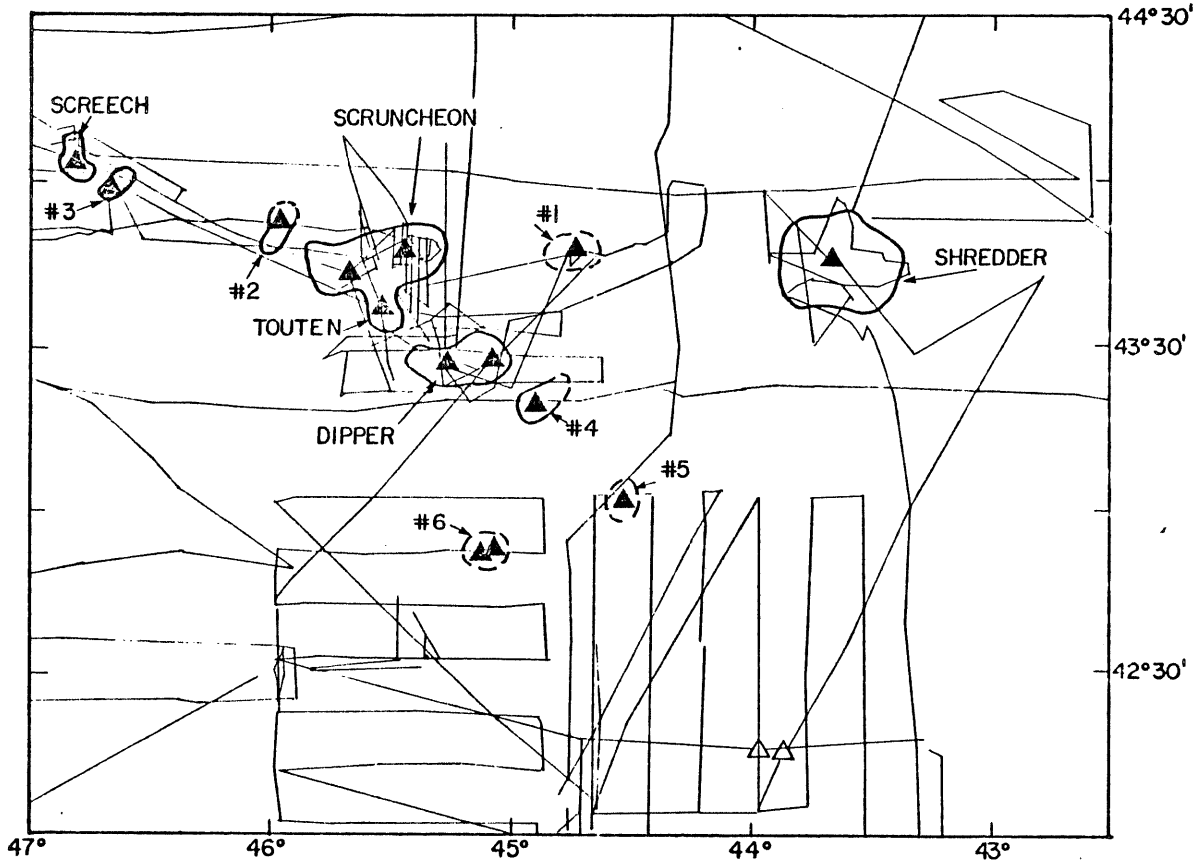

Figure 7.1

Ship's tracks and seamount locations. Solid traingles=seamount peaks; outlines of seamounts at seafloor shown as heavy solid lines.

7.2 Petrography and Geochemistry

A comprehensive account of the first studies on samples dredged from the Newfoundland Seamounts is given by Sullivan and Keen (1977). Their study of Scruncheon and Dipper Seamounts has subsequently been extended to include Screech and Shredder Seamounts.

Highly-altered basalts were recovered from all of the seamounts dredged. The Screech, Scruncheon and Dipper samples are most commonly vesiculated and porphyritic, with clinopyroxene, feldspar and iron-titanium oxide phenocrysts. The groundmass consists of highly-oxidized iron-titanium oxides and altered plagioclase microlites or laths in a matrix of green, yellow and orange-brown clays and alteration products; zeolites are absent, and calcite is very rare. The basaltic material recovered from Shredder Seamount, in the form of 0.5-1.5 cm diameter pebbles in a limestone pavement (see below), is petrographically identical. These petrographic and mineralogic characteristics suggest that the seamounts consist of alkali basalts which have undergone extensive low-temperature seafloor alteration (Hart et al., 1974; Bass, 1976; Vallance, 1976).

The occurrence of sodic trachytes on at least two seamounts (Scruncheon and Dipper) confirms the alkaline affinity of the basalts. The trachytes are very fresh and contain phenocrysts and glomerophenocrysts of plagioclase, amphibole, biotite and iron-titanium oxides set in a very fine-grained fluidal matrix of plagioclase and potash feldspar.

Thirty-eight samples were selected for major and trace element geochemical analysis, and twenty-two for rare-earth element (REE) analysis (Appendix II). The geochemical data must be interpreted with some caution, in view of the highly altered state of the samples (except the trachytes). Most major elements (and hence the normative compositions) are particularly unreliable as petrogenetic indicators in these circumstances and have not been used for this purpose in the present study. Certain major and trace elements (e.g. Ti, P, Zr, Y, Nb), the REE and the compositions of unaltered pyroxene phenocrysts, on the other hand, are believed to be relatively unaffected by sea-floor weathering (Hart et al., 1974; Frey et al., 1974; Vallance, 1974), and are commonly relied upon as sources of meaningful petrogenetic information for altered basalts. A variety of models have been advanced which attempt to define basalt type or the tectonic setting of the eruption on the basis of these parameters (Pearce and Cann, 1973; Rhodes, 1973; Ridley et al., 1974; Nisbet and Pearce, 1977). If valid, such geochemical discriminants would be very useful in interpreting the significance of ancient basic volcanic rocks. The data presented here have been used to test several of these models.

The REE abundances (Fig. 7.2) confirm the alkaline character of the basalts. Such steeply-sloping, uninflected patterns are characteristic of oceanic islands and seamounts (Flower, 1971; Hughes and Brown, 1972; Kempe and Schilling, 1974; Zielinski, 1975; Buckley, 1976; Bonatti et al., 1977; Batiza, 1977b; Houghton, in prep.). In general terms, oceanic island and seamount volcanism is the main

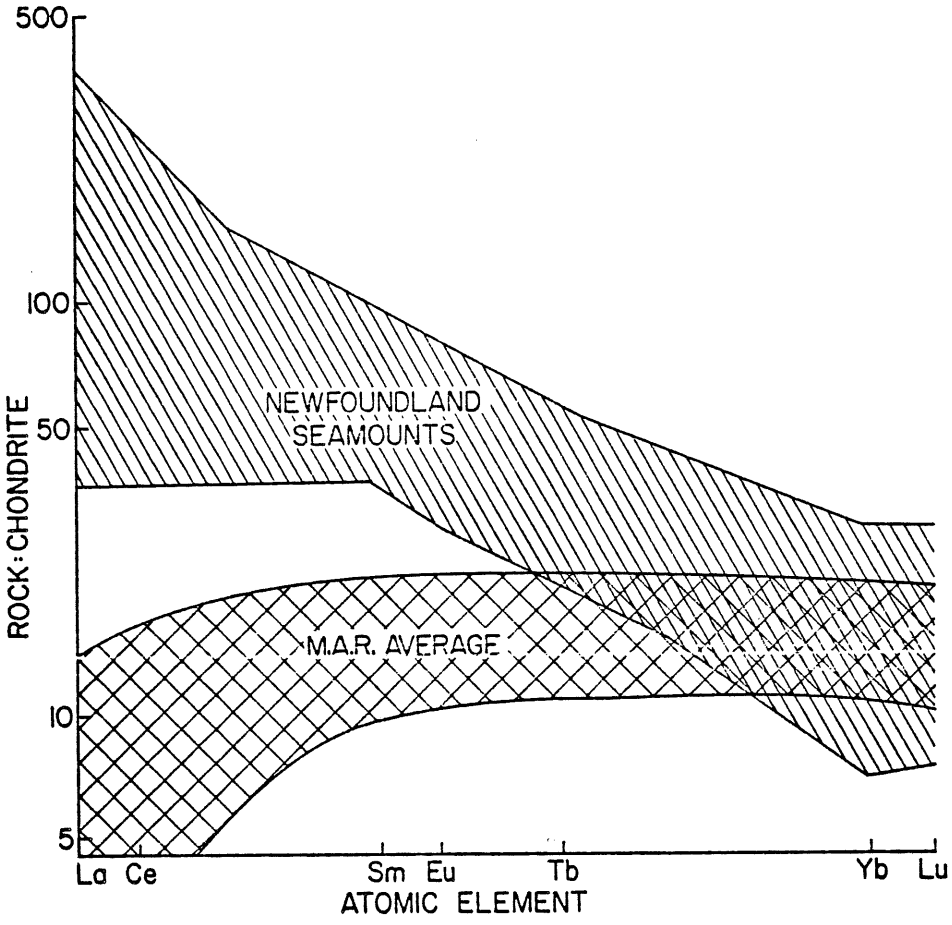

Figure 7.2

Summary of REE abundances, Newfoundland Seamounts.
(see also Appendix II).

element in the "mid-plate" (as opposed to ocean ridge or island arc) basic volcanic regime. A variety of more specific mechanisms have been proposed to account for this activity, including thermal plumes (Morgan, 1972; Schilling, 1971, 1973; Kempe and Schilling, 1974) volcanism along transform faults (Erickson et al., 1970; Handschumacher, 1973) or propagating fractures (Walcott, 1976) and shear melting (Shaw and Jackson, 1973).

The geochemical discriminants examined here (Figs. 7.3, 7.4) are not particularly successful in classifying the Newfoundland Seamount basalts correctly. In one case (Fig. 7.3a) the analyses fall in several composition fields, while in another (Fig. 7.3b) they plot outside of all defined fields. This behavior may indicate that the elements involved were in fact mobile to a significant degree under the conditions of alteration. However, it seems that the failure of the Ti-Zr discriminant (Pearce and Cann, 1973) is also related to a deficiency in the original definition of the composition fields. Published values of Ti and Zr for a number of seamounts and oceanic islands are shown along with the Newfoundland Seamount data in Figure 7.3b to demonstrate that the "within-plate basalt" field as originally defined fails to encompass a significant group of known within-plate basalt compositions.

The discriminants which only attempt to distinguish between alkaline and sub-alkaline (ocean-ridge) basalts are somewhat more successful (Fig. 7.4), although there is considerable scattering of the data on these plots, too. Again, the scattering across composi-

Figures 7.3 and 7.4: Geochemical discriminants.

7.3a: Ti-Zr-Y, Pearce and Cann (1973).

7.3b: Ti-Zr, Pearce and Cann (1973). Numbers indicate published analyses: 1-4 = Reunion, Galapagos, Madeira, Azores, from Pearce and Cann (1973); 5 = Marquesas (Bishop and Woolley, 1973); 6 = Red Sea islands (Gass et al., 1971); 7 = Easter line seamounts (Bonatti et al., 1977); 8 = Hawaii (Pearce and Cann, 1973); 9 = Guadalupe Island (Batiza, 1977b).

7.3c: Pyroxene compositions, Nisbet and Pearce (1977).

7.3d: Pyroxene compositions, Nisbet and Pearce (1977).

7.4a: Zr-Nb, Rhodes (1973).

7.4b: P_2O_5-TiO_2, Ridley et al. (1974)-

7.4c: Pyroxene compositions, Nisbet and Pearce (1977). s, a and ρ denote sub-alkaline, and peralkaline composition fields, respectively.

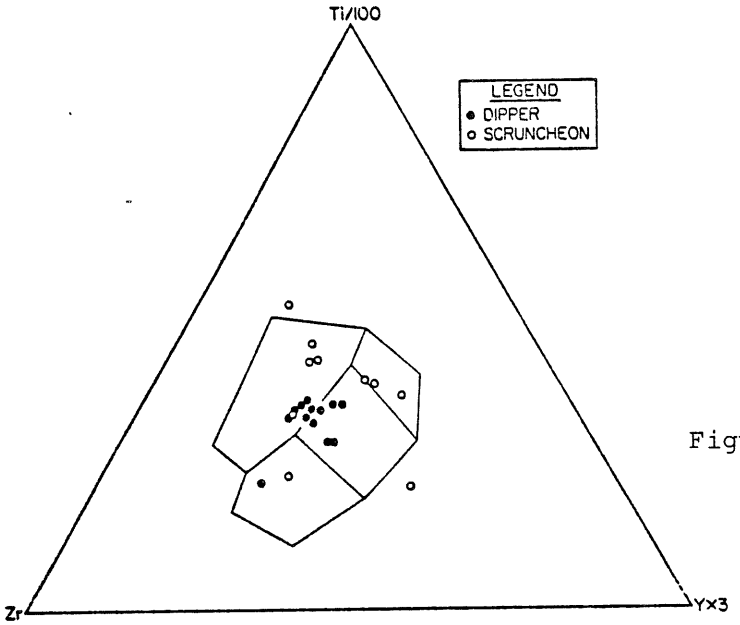

Figure 7.3a

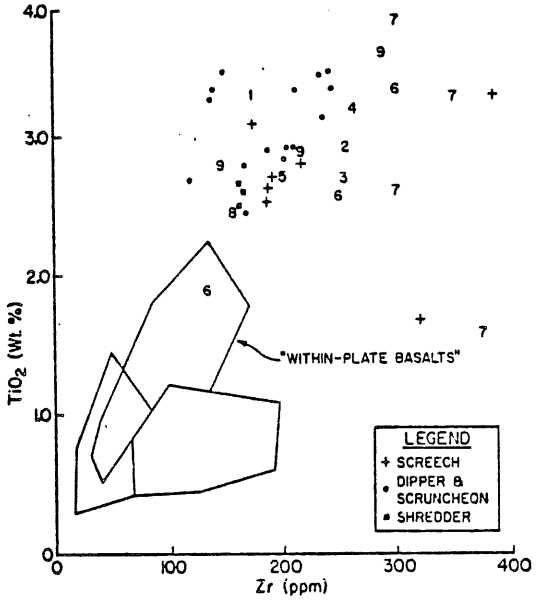

Figure 7.3b

Figure 7.3c

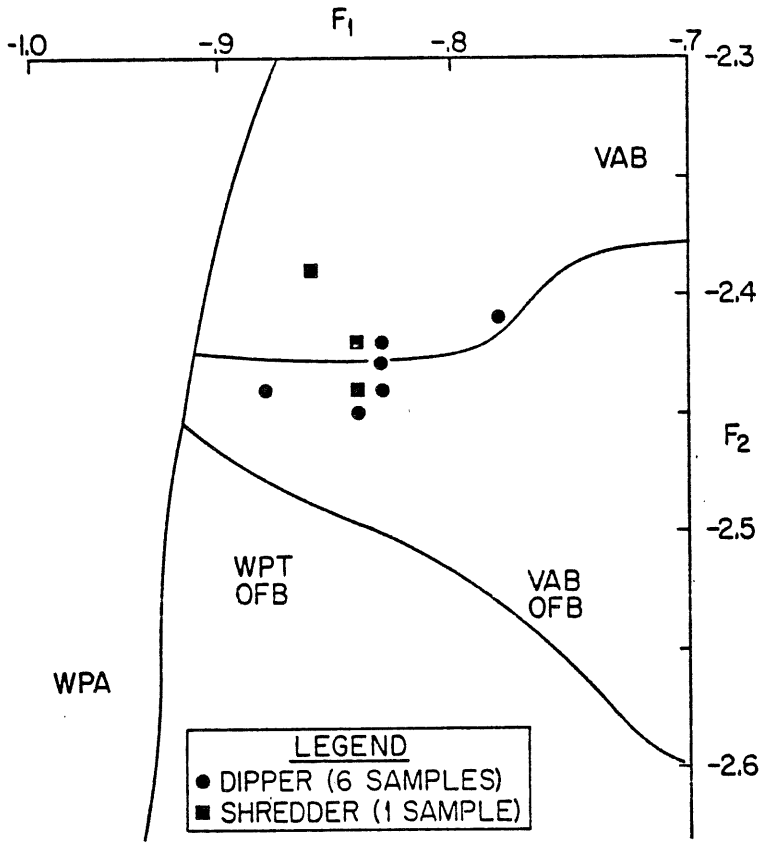

$F_1 = -0.012(SiO_2) - 0.0807(TiO_2) + 0.0026(Al_2O_3) - 0.0012(FeO^*) - 0.0026(MnO) + 0.0087(MgO) - 0.0128(CaO) + 0.0419(Na_2O)$.

$F_2 = -0.0469(SiO_2) - 0.0818(TiO_2) - 0.0212(Al_2O_3) - 0.0041(FeO^*) - 0.1435(MnO) - 0.0029(MgO) + 0.0085(CaO) + 0.0160(Na_2O)$.

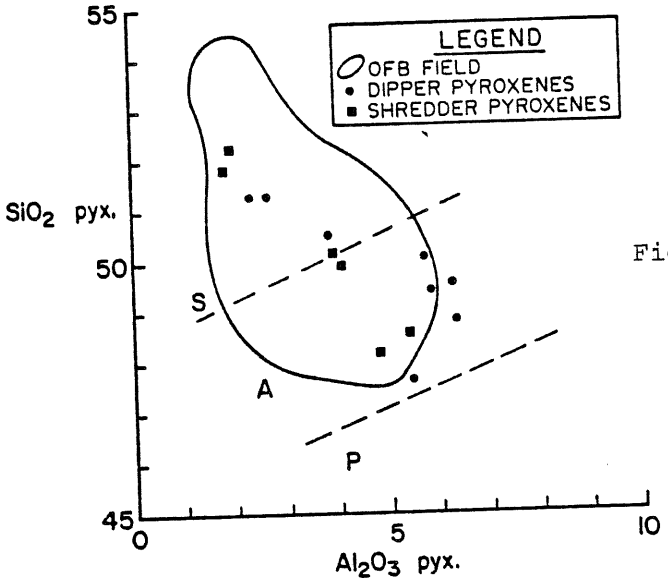

Figure 7.4c

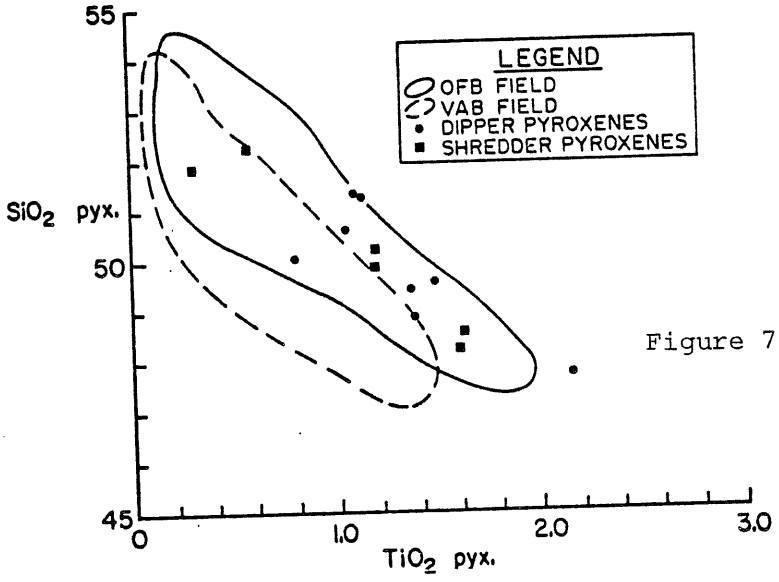

Figure 7.3d

Figure 7.4

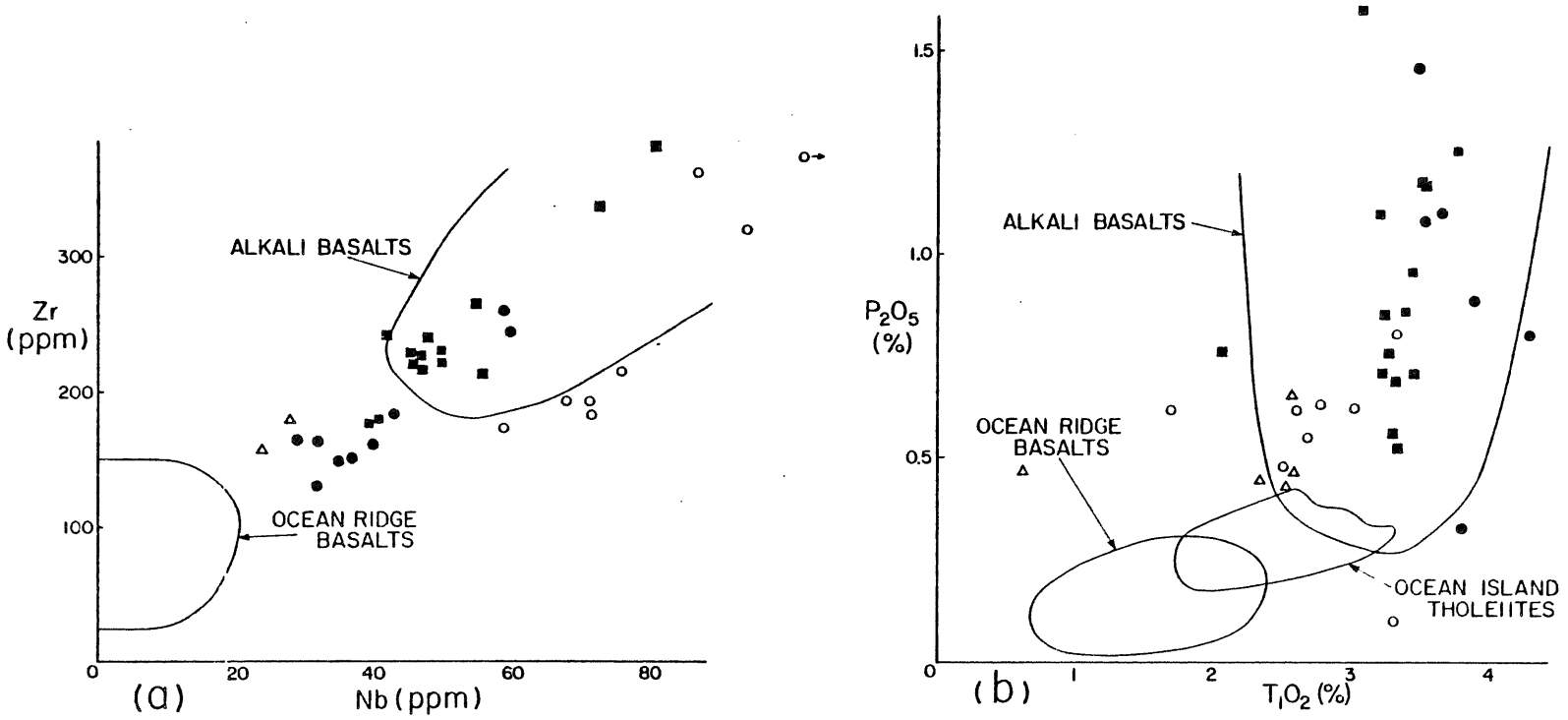

● SCRUNCHEON
■ DIPPER
o SCREECH
Δ SHREDDER

tion field boundaries might reflect element mobility during alteration, inaccuracies or omissions in the definitions of the fields or real trends in the original chemistry.

It is often assumed that these geochemical discriminants can be applied to ancient, metamorphosed basalts because the elements involved are immobile during the tectonic and (supposedly isochemical) metamorphic history of these rocks. However, this assumption is invalidated if seafloor weathering or oceanic hydrothermal processes produce non-isochemical changes in the original chemistry prior to the metamorphism and tectonic activity. The results presented above indicate that this blurring of the geochemical signature does occur, and they also show that significant members of the oceanic basalt association are not encompassed by some discriminants. Therefore, the validity of these models for ancient rocks should still be considered an open question.

7.3 Seamount and Crustal Ages

The hot spot, propagating fracture and shear-melting models for the formation of linear groups of islands or seamounts (see above) predict that the locus of active volcanism migrates in a single direction through time. Determination of the spatio-temporal pattern of volcanism thus constitutes a critical test of these hypotheses.

Unfortunately, chronological data from the Newfoundland Seamounts are quite limited at present. Sullivan and Keen (1977) report the results of $^{40}Ar/^{39}Ar$ stepwise-heating experiments on plagioclases from

two Scruncheon Seamount trachytes (Fig. 7.5). These measurements were made by V. Stukas at Dalhousie University (Stukas, 1977). Sample 25/1a (Fig. 7.5a) shows a nearly classical gas-release pattern with a good apparent-age plateau at about 97 Ma. The age spectrum for sample 25/4 (Fig. 7.5b) is disturbed, with several intermediate heating steps (<1000°C; 80% of the gas released) giving lower apparent ages than the other heating steps. This type of behavior has been widely observed (Turner and Cadogan, 1974; Seidemann, 1976; cited in Stukas, 1977) but the origin of the phenomenon is not clear. Stukas (1977) finds, as do numerous other investigators, that the isotopic ratios from the high-temperature (> 1000°) steps give a well-defined correlation plot despite the disturbance in the release pattern. The correlation plot in Figure 7.5c combines the data from 25/1a with the three high-temperature steps in 25/4 to obtain an age of 97.7 ± 1.5 Ma. This is accepted as a valid result, with the reservation that the origin of disturbed $^{40}Ar/^{39}Ar$ release patterns needs further clarification.

Only one other chronological datum has been obtained at the time of this writing. A slab of shallow-water bioclastic limestone measuring 70 cm x 50 cm x 10 cm was dredged from Shredder Seamount during the 1975 Hudson Cruise (Station 110; Appendix II, Table 1). The fossils in this sample have been examined by Dr. L. F. Jansa and F. M. Gradstein of the Geological Survey of Canada. Although the microfauna is rather sparse and very poorly preserved, it indicates a probable Early Cretaceous age for this deposit (Jansa and Gradstein,

Figure 7.5: $^{40}Ar/^{39}Ar$ age spectra and correlation plot, Scruncheon Seamount trachytes 25/1 and 25/4. Shaded bars on release patterns indicate 1σ errors.

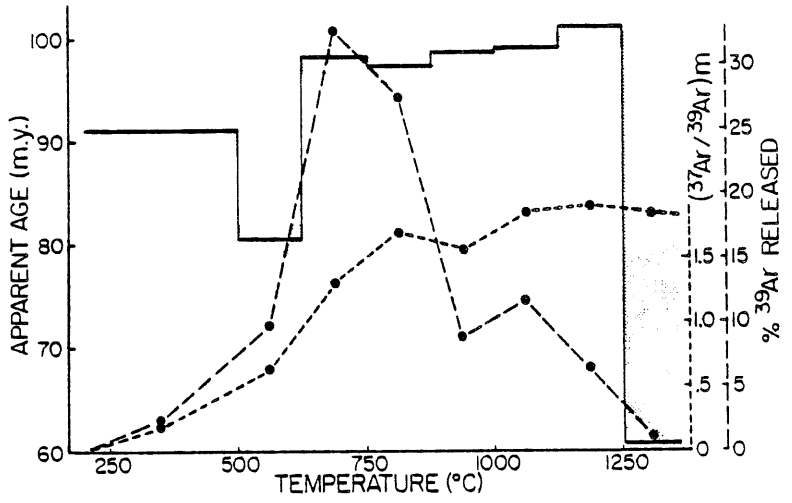
APPARENT AGE (m.y.)
100
90
80
70
60
250
500
750
1000
1250
TEMPERATURE (°C)
$(^{37}Ar/^{39}Ar)m$
30
25
20
15
10
5
0
1.5
1.0
.5
% ^{39}Ar RELEASED

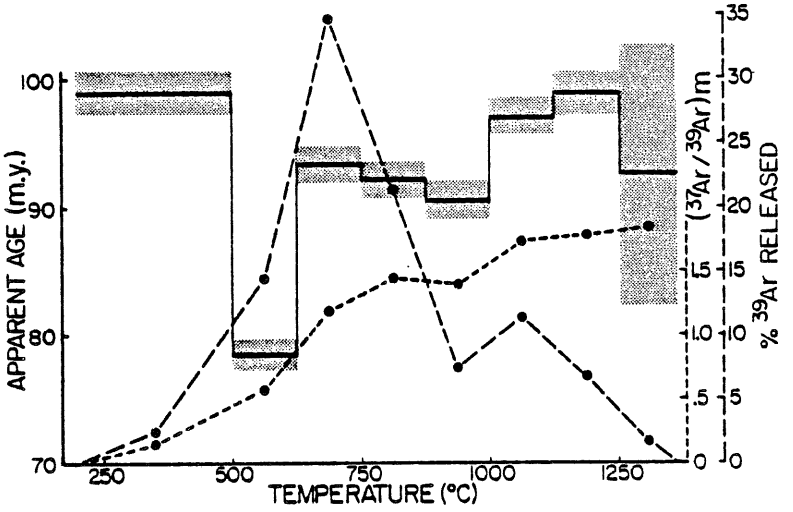
APPARENT AGE (m.y.)
100
90
80
70
250
500
750
1000
1250
TEMPERATURE (°C)
$(^{37}Ar/^{39}Ar)m$
35
30
25
20
15
10
5
0
1.5
1.0
.5
% ^{39}Ar RELEASED

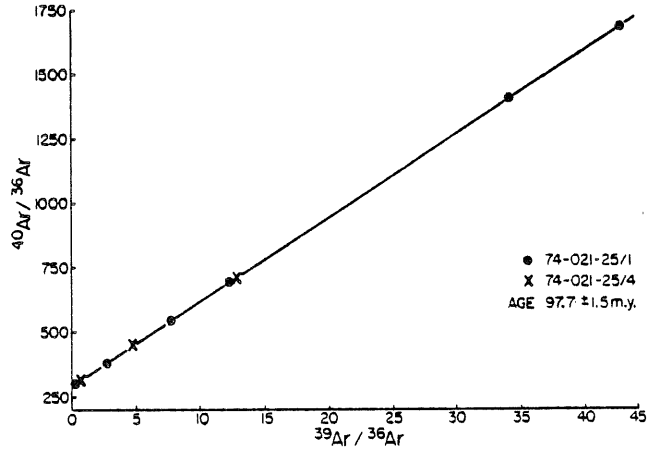
$^{40}Ar/^{36}Ar$
1750
1500
1250
1000
750
500
250
0
5
10
15
20
25
30
35
40
45
$^{39}Ar/^{36}Ar$
● 74-021-25/1
X 74-021-25/4
AGE 97.7 ±1.5 m.y.

pers. comm.; Gradstein et al., 1977). This gives a rough minimum age for Shredder Seamount but provides no indication of the time when the volcanic activity began.

The currently-available chronological data are clearly insufficient to define the spatio-temporal pattern of volcanism in the Newfoundland Seamount province. However, the magnetic anomaly evidence that the age of the Newfoundland Basin crust is 73-115 Ma (anomaly 31/32 - J-anomaly, Chapter 5), in conjunction with the chronological evidence that late-stage trachytic volcanism and shallow-water sedimentation were occurring about 100 Ma and the seismic evidence that little sediment accumulated between the time of crustal formation and seamount volcanism, indicates that the seamounts formed on very young crust near the ridge crest.

It might be useful to know the age difference between the seamounts and the surrounding crust more precisely and to have some indication as to the amount of time involved in construction of the volcanos. However, the position of the spreading center at specific times between 110 Ma (J-anomaly) and 73 Ma (anomaly 31/32) cannot be determined because of the confused magnetic anomaly pattern in this region (Section 5.4, 5.5). Therefore, estimates of crustal ages adjacent to the seamounts and of times of formation must be made indirectly.

One way to estimate the crustal age near the seamounts is to make a linear extrapolation of crustal ages between the two well-known magnetic anomalies that bound the oceanic Newfoundland Basin

to the east and west. Spreading rates north of the SENR during this period are not accurately known but likely were not constant, so this procedure at best gives a very general indication of the crustal ages. The results of this exercise indicate that Scruncheon Seamount is built on crust that is about 112 Ma old. If the 97.7 Ma trachytes represent a rather late volcanic event, and their composition suggests this is so, then a maximum period of 14.3 Ma is obtained for the construction of this seamount. Shredder Seamount presents some problems in this analysis, since the crustal age obtained (about 100 Ma) is equal to or younger than the age of the limestone cap. This apparent discrepancy probably signifies the failure of the assumption that the age of the crust varies in a simple linear fashion with distance between the J-anomaly and anomaly 31/32.

Vogt (1974) proposes a model relating volcano height to the thickness of the lithospheric plate which offers a second approach to the question of seamount and crustal ages. This model assumes that magma generation occurs at the base of the lithosphere and that the major factor controlling volcano height is the isostatic balance between the lithospheric plate and the magma column. Given these assumptions and the fact that the thickness of the lithosphere varies as a function of crustal age (as $T(t) = Kt^{\frac{1}{2}}$; Parker and Oldenburg, 1973; Sclater et al., 1975), volcano height can be used to determine crustal age. Vogt (1974) defines an adjusted volcano height (H*) which takes into account the density differences between magma and the lithosphere, sediment, water and air and attempts to use the observed values of H*-age for 24 oceanic islands to evaluate the constant 'K' in the plate thickness law.

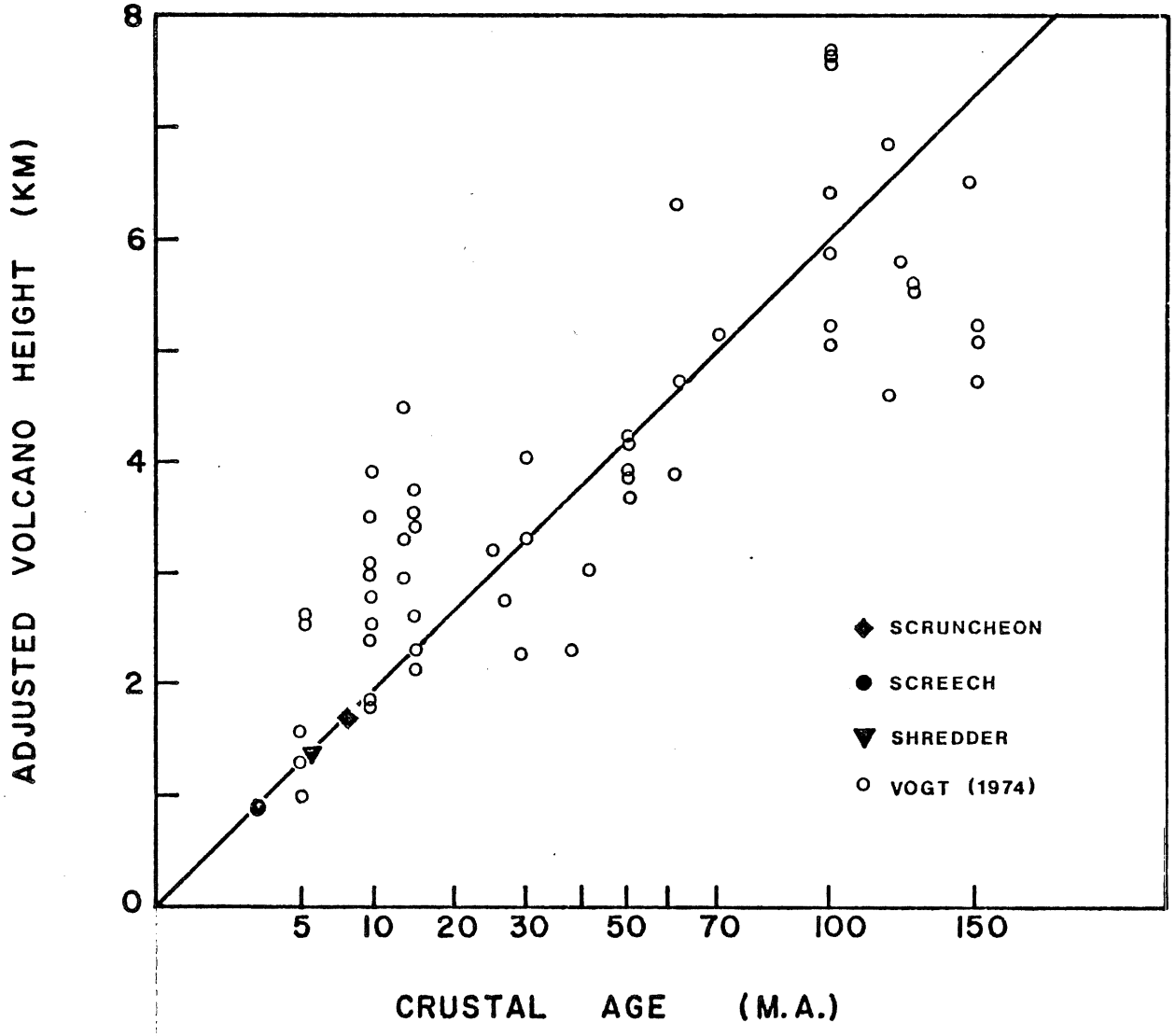

Figure 7.6: Isostatically-adjusted volcano height as a function of crustal age. (after Vogt, 1974).

TABLE 7.1

$$H^* = h_w \frac{\rho\ell - w}{\rho\ell} + h_s \frac{\rho\ell - \rho s}{\rho\ell} + h_T$$

where H^* = adjusted volcano height

h_w = water layer thickness (to top of seamount)

h_s = sediment thickness

h_T = volcano height about sealevel

ρ = density: $\rho\ell$ = magma 2.85 g/cc
ρs = sediment 2.2 g/cc
ρw = water 1.03 g/cc

	SCREECH	SCRUNCHEON	SHREDDER
h_s	∿2.0 km	1.8 km	1.7 km
h_w	0.7 km	2.0 km	1.3 km
h_T	0	0	0
H^*	0.9 km	1.69 km	1.38 km

The main premise of Vogt's analysis - that volcano height is limited isostatically - overlooks many local structural and physico-chemical factors that affect volcanism and also assumes that there is an unlimited magma supply. The isostatic limit does, however, clearly provide the maximum height a volcano can attain (Yoder, 1976). The rather uniform total relief (Table 3.1) of the Newfoundland Seamounts may indicate that a general constraint of this type controlled volcano height in this case. If so, adaptation of Vogt's analysis to the Newfoundland Basin may provide useful data on the age of the crust upon which the seamounts were constructed.

The constants and seamount data used in this calculation are given in Table 7.1, along with the formula for H* according to Vogt (1974). The h_t term is zero in the present case, since none of the volcanoes rises above sealevel. The resulting values for H* are plotted in Figure 7.6.

The straight line in Figure 7.6 shows plate thickness as a function of the square-root of crustal age. Sclater et al. (1975) show that this $t^{\frac{1}{2}}$ law is valid for lithosphere less than 80 Ma old. As stated earlier, the seismic and chronological data from the Newfoundland Seamounts show that much less than 80 Ma elapsed between crustal formation and seamount formation, so the $t^{\frac{1}{2}}$ law can be assumed to apply to the Newfoundland Basin at the time of seamount volcanism. Different values for the constant K in the plate thickness law (e.g. K = 9.4, Parker and Oldenburg, 1973) produce convex-upward curves in Figure 7.6 which to some extent fit the data points

of Vogt (1974) more successfully, but these do not give significantly different results for the range of adjusted heights under consideration here.

Within the limits of these assumptions, the model suggests (Fig. 7.6) that Screech Seamount, which is located at or just seaward of the magnetic smooth zone boundary, formed on crust that was less than 5 Ma old. It was shown in Chapter 5 that the smooth zone boundary between the SENR and the seamounts is probably coincident with the J-anomaly and so is a 115 Ma isochron. Therefore, Screech Seamount probably formed between 115 Ma and 110 Ma. Scruncheon Seamount formed on 9 Ma crust and Shredder Seamount formed on 7 Ma crust, according to this model. Assuming that the Scruncheon trachytes, dated at 97.7 ± 1.5 Ma, represent a late stage in the volcanism, then the crust surrounding Scruncheon must be at least 105-107 Ma old. Further, if the correct absolute age for the Shredder limestone is 100 Ma (end of the Early Cretaceous), then Shredder formed on 107-109 Ma crust.

These results appear to indicate that the volcanic activity producing Shredder and Scruncheon Seamounts occurred several million years (2-5 Ma?) after the Screech Seamount volcanism. The significance of such a small difference in age can certainly be questioned, so this indication must be considered as tentative.

7.4 Discussion

The main points brought out in the preceeding sections are: a) that the Newfoundland Seamount province comprises 13 peaks lying in a

triangular area near the center of the Newfoundland Basin; b) that the seamounts consist of alkali basalt and differentiates thereof that might represent a variety of thermal and tectonic regimes; c) that the seamounts post-date the surrounding crust by only a short period of time and were probably fully formed by about 97 Ma; d) that the eastern seamounts may have formed several million years after the western ones.

These data must now be incorporated into a model that explains the significance of the seamount volcanism in the evolution of the Newfoundland Basin. The position of the seamounts in relation to the major structural and geophysical elements in the Newfoundland Basin and surrounding continental shelf areas is shown in Figure 7.7. The geometry of the seamounts can be interpreted in terms of two linear trends: The western seamounts (Screech to Scruncheon) define a trend of 105°; the majority of the seamounts east and south of Scruncheon and two of the large buried basement highs in the southern survey area define a 145° trend. As indicated in Figure 7.7, these azimuths are those required for fracture zones formed during the phases of seafloor spreading marked by the J-anomaly (015°) and the younger 055° anomaly lineations, respectively (see Chapter 5). At its landward end, the 105° trend of the western seamounts correlates well with the southern limits of the Carson and Jeanne d'Arc Sub-basins (Chapter 2) and with a number of potential field anomaly offsets and gradients that reflect continental basement structures (Lefort and Haworth, in prep.). Shredder and Number 1 Seamounts lie northeast of the seamounts comprising the 145° group and are not obviously related to either trend.

It is proposed here that this spatial distribution of seamounts

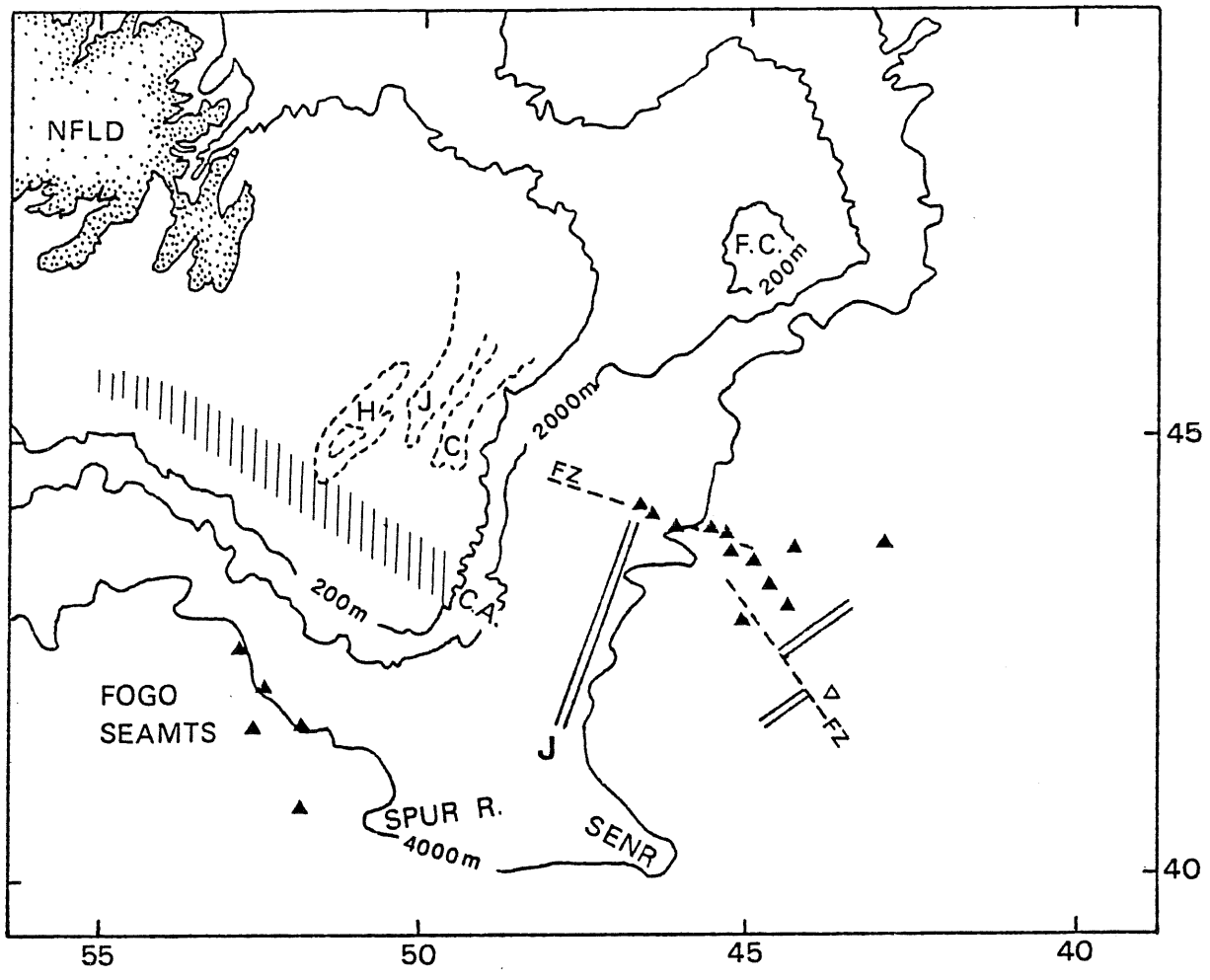

Figure 7.7

Newfoundland Seamounts in relation to structural elements on the Grand Banks (Haworth, 1975; Jansa and Wade, 1975) and in the Newfoundland Basin. H=Horseshoe Sub-basin; J=Jeanne d'Arc Sub-basin; C=Carson Sub-basin; C.A.=Collector Anomaly.

reflects initial localization of volcanism along the seaward extension of Grand Banks basement structures and subsequent control by transform faults associated with early spreading between Iberia and North America. The close correlation between the seamount trends and fracture zone trends leads to the inference that the seamounts represent a "leaky" transform fault (Menard and Atwater, 1968) or "transverse volcanic lineament" (Barberi and Varet, 1977) regime. Activity on both trends was probably episodic and is postulated to have been caused by changes in intraplate stresses due to changes in spreading rate or/and direction (Menard and Atwater, 1968; E. D. Jackson and Shaw, 1975). The tentative conclusion that the eastern seamounts post-date the western seamounts (Section 7.3) may be further evidence in favor of episodic activity.

The Red Sea-Afar Depression region of Africa is a good present-day analogue for the tectonic regime postulated for the Newfoundland Seamounts. Barberi et al. (1974) and Barberi and Varet (1977) have studied the relationship between continental structures, transverse volcanic lineaments and spreading directions in detail. The transverse volcanic lineaments are closely analogous to transform faults and "leaky" fracture zones in oceanic regimes; they are the loci of central (as opposed to fissural) volcanic activity and are characterized by alkalic basaltic compositions. These authors also note that the transverse volcanic zones tend to be aligned with offsets in both the axial volcanic ranges and the continental margins. The Hanish-Zukur group of volcanic islands in the southern Red Sea (Gass et al., 1973), which are geochemically similar to the Newfoundland Seamounts, lie along

thses transverse lineaments and have formed very near the active ridge crest.

CHAPTER 8: EVOLUTION OF THE NEWFOUNDLAND BASIN

This chapter draws on the material presented in the preceeding sections of the thesis to develop a plate tectonic model for the evolution of the Newfoundland Basin prior to anomaly 31/32 (73 Ma). The location of the ocean-continent boundary and the pre-drift positions of the continents must be established before proceeding to discuss plate motions. The evidence bearing on the nature and location of the ocean-continent boundary in the Newfoundland Basin is reviewed in Section 8.1, and a model for the present continental margin and ocean-continent boundary structures is presented. Two recent paleogeographic reconstructions of the North Atlantic region (LePichon et al., 1977; Haworth, in prep.) are reviewed in Section 8.2. The plate model presented in Section 8.3 uses the Haworth (in prep.) reconstruction, with the ocean-continent boundary as given in Section 8.1, as the initial configuration.

8.1 The Ocean-Continent Boundary

The ocean-continent boundary is a complex geological structure that forms during the final splitting of a continent. The preceeding stage of continental rifting and the transition from rifting to active seafloor spreading involve a variety of processes, many of which are not well understood, operating over several tens of millions of years. Locating the ocean-continent boundary on ancient continental margins, which have also undergone millions of years of subsidence and sedi-

mentation, is very difficult. Yet some knowledge of where the final split of the continent occurred is essential for paleogeographic reconstructions. An assumption commonly adopted in cases where the location of the ocean-continent boundary is not accurately know is that a partucular isobath marks the seaward limit of continental crust along the entire margin. LePichon et al. (1977) emphasize the fallacy of this assumption and also point out that locating the ocean-continent boundary along the Iberian and Grand Banks margins is exceptionally difficult because of the extremely complex pre-rift structures in these regions (Arthaud and Matte, 1977).

Seismic, magnetic and gravity data presented in Chapters 4, 5 and 6 of this thesis indicate that the ocean-continent boundary in the Newfoundland Basin is associated with the seaward boundary of the continental margin magnetic smooth zone. The data supporting this conclusion are summarized below (Fig. 8.1).

a) The marginal magnetic smooth zone in the Newfoundland Basin extends from just north of the SENR to Flemish Cap. The seaward limit of the smooth zone appears to be a diachronous boundary, coinciding with the J-anomaly (115 Ma) south of the seamounts and truncating younger (post-102 Ma) anomalies south of Flemish Cap.

b) One seismic refraction line is available on the lower continental rise south of the seamounts, and this shows that the crust seaward of the smooth zone is oceanic (H. R. Jackson et al., 1975). Magnetic anomalies seaward of the smooth zone display wavelengths and amplitudes typical of seafloor spreading anomaly lineations.

c) Seismic reflection data suggest that the smooth zone boundary separates the oceanic Newfoundland Basin from a significantly different structural and sedimentary regime, one perhaps closely allied with the early Mesozoic of the Grand Banks. Both basement and the overlying sedimentary sequence change character markedly in the vicinity of the smooth zone boundary. In particular, deep grabens immediately landward of the boundary contain thick accumulations of sediment which may be as old as Triassic (Section 4.4).

d) The seaward boundary of the smooth zone is not associated with any particularly prominent isostatic or free-air gravity anomalies (Fig. 6.2); the maximum anomaly observed at the boundary is about +20 mgal. Higher anomaly amplitudes and steeper gradients are observed over the continental slope, 50-25 km landward of the smooth zone boundary. This contrasts markedly with observations from many other Cretaceous rifted margins (Talwani and Eldholm, 1972, 1973; Konig and Talwani, 1977; Rabinowitz and LaBrecque, 1977) where steep isostatic gravity gradients and anomalies with amplitudes or 50 mgal and greater are consistently associated with the boundary of the marginal magnetic smooth zone (see Section 6.5).

e) Gravity and magnetic models do not provide strong constraints on interpretation of the actual geology at the ocean-continent boundary or the nature of the crust within the smooth zone. The gravity observations can be satisfied by incorporating minor topographic relief (observed or hypothetical) on the crust-sediment interface, without changing the depth to the crust-mantle interface. The magnetic observations require substantial changes in magnetic source-layer

depth or/and thickness and magnetization at the boundary but many combinations of parameters can be found which fit the observations.

Figure 8.2 presents a model for the Newfoundland Basin continental margin and ocean-continent boundary that is consistent with the above observations. The transition from continental to oceanic crust is postulated to occur between two major boundaries: one beneath the slope which, on the basis of seismic and gravity data, separates shallow continental basement from oceanic or subsided "modified" continental crust, and one near the upper-lower continental rise junction which, on the basis of seismic and magnetic data, marks the landward limit of a shallow, "typical" oceanic magnetic anomaly source-layer.

The crust in the transitional region between the continental slope and the magnetic smooth zone boundary is presumed to consist of a mixture of continental material, mafic intrusives rift-valley sediments. However, it is also possible that subsided oceanic crust representing perhaps 10 Ma of seafloor spreading lies within this transition zone. Schouten (pers. comm.) has identified changes in magnetic anomaly strike and spacing south of the SENR which imply that major changes occurred in the seafloor spreading regime at anomaly M10N time (124 Ma), and he suggests that this marks the initiation of spreading in the Newfoundland Basin. However, B. R. Hall (1977) and C. E. Keen et al. (1977) identify the J-anomaly as the oldest seafloor spreading anomaly in the Newfoundland Basin, suggesting 115 Ma for the initiation of active spreading. The interpretations of Schouten and of C. E. Keen et al. (1977) are not mutually exclusive. If oceanic crust older than

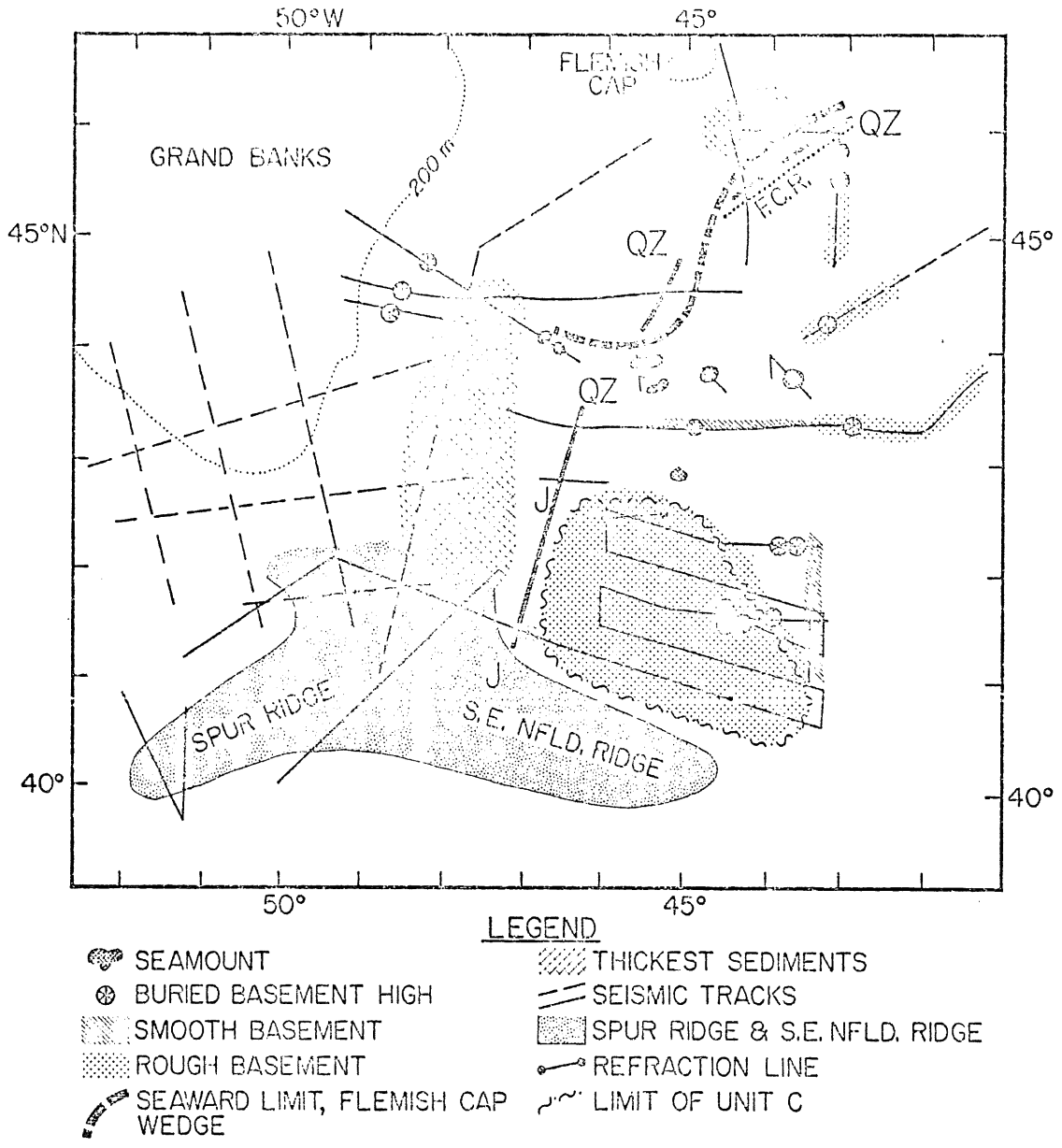

Figure 8.1
Summary of seismic and geophysical features.

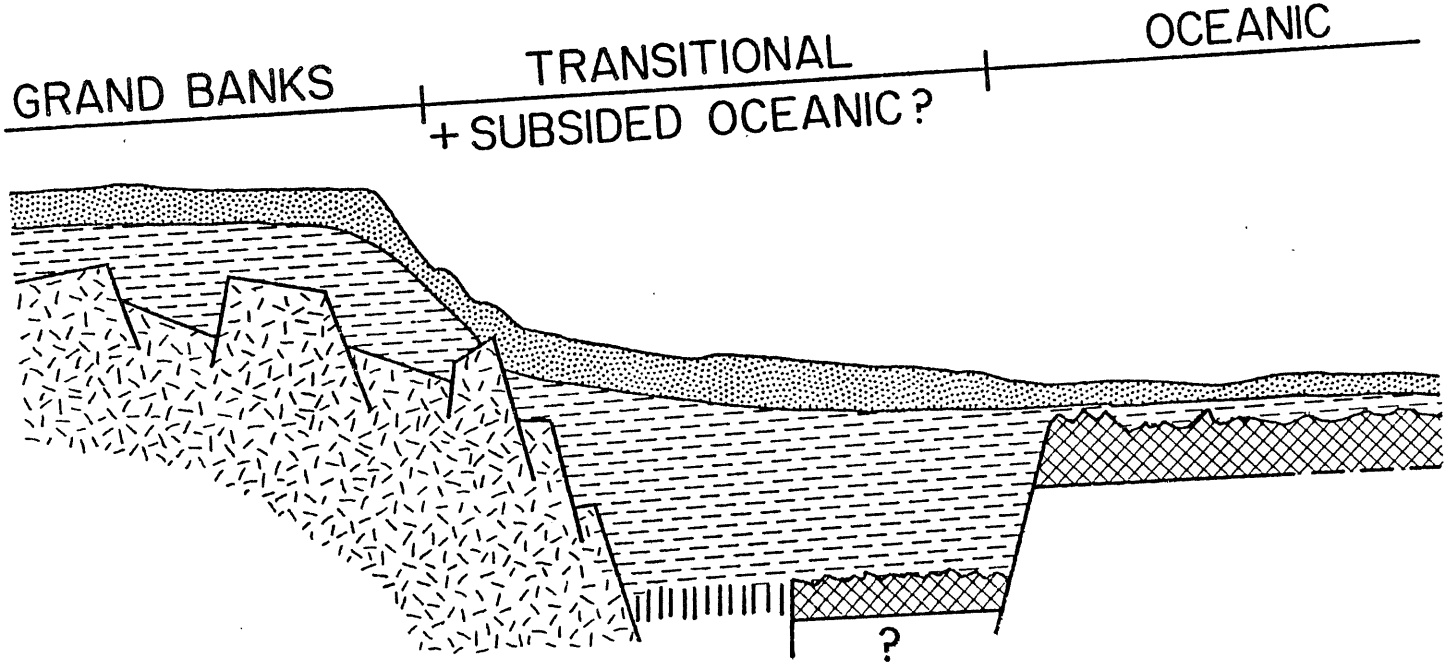

Figure 8.2: Postulated continental margin and ocean-continent boundary structure. Sediments are indicated by stippled and dashed pattern; oceanic crust by diamond grid; continental crust by random dashes, "transitional" crust by vertical ruling.

the J-anomaly is present, it may underlie the deep sedimentary basins observed just landward of the smooth zone boundary. This possibility is indicated in Figure 8.2.

The structures and geophysics of the continental margin in the vicinity of the Tail of the Bank are quite different from those described above. Rifting here may have involved very different processes than elsewhere in the Newfoundland Basin, owing to the proximity of the area to the Newfoundland Fracture Zone. In addition, the original margin structures may have been modified during subsequent stages of seafloor spreading, when this region was the focal point for the interactions of the North American, African and European plates (see Section 8.3). The location of the ocean-continent boundary in the vicinity of the Tail of the Bank was discussed in some detail in Chapter 4, where it was shown that the seismic and magnetic data presented in the present report are not consistent with recent hypotheses that the Spur Ridge and SENR are underlain by continental crust (A. C. Grant, 1977; Gradstein et al., 1977). Specifying a position for the ocean-continent boundary off the Tail of the Bank is difficult because there is a crucial gap in magnetic and gravity coverage here, with virtually no overlap between primarily shelf-based and primarily deep-water geophysical surveys. The center-line of the bathymetric depression separating the ridge structures from the Grand Banks shelf is therefore taken as the best estimate of the seaward limit of continental crust.

Figure 8.3 shows the postulated location of the ocean-continent boundary in the Newfoundland Basin and Tail of the Bank area based on

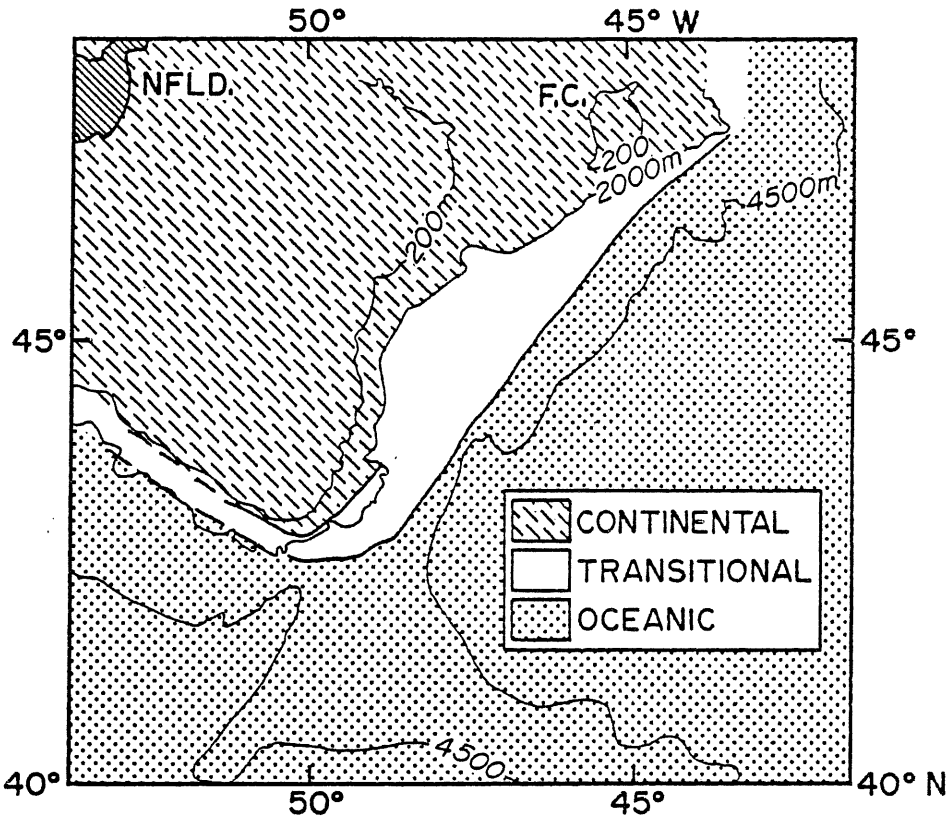

Figure 8.3

Postulated location of the ocean-continent boundary. Location southwest of the Grand Banks based on data in H. R. Jackson et al. (1975).

the foregoing discussions. The transitional zone is shown extending from the base of the slope (2,000 m) to the ocean-continent boundary (roughly coincident with the 4,000 m isobath).

8.2 Pre-drift Reconstructions

The pre-drift positions of the continents in this part of the North Atlantic have proved very difficult to determine, primarily because of the complexity of the pre-rifting continental structures (Chapter 1). Most reconstructions proposed to date assume that the Bay of Biscay must be closed in order to fit Iberia into the space between North Africa and the British continental margin. LePichon et al. (1971, 1977), LePichon and Sibuet (1971), LeBorgne et al. (1972) and Choukroune et al. (1973) argue that the Eulerian pole for the Iberian rotation lies northeast of Paris rather than along the axis of the Pyrenees (e.g. Bullard et al., 1965; Montadert and Winnock, 1971), and the magnetic anomaly pattern in the Newfoundland Basin (Section 5.4) supports this postulate.

To date, no model has been proposed which successfully closes the gap between Iberia and the Grand Banks and determines the pre-drift positions of continental fragments such as Flemish Cap and Galicia Bank. Most reconstructions leave a gap of several hundred kilometers between the presumed limits of continental crust in Iberia and on the Grand Banks (especially between the SENR and the Newfoundland Seamounts) and produce overlaps between other known continental regions (e.g. Bullard et al., 1965; Laughton, 1972, 1975).

Two reconstructions of the North Atlantic have recently been published which improve significantly upon these earlier attempts (Fig. 8.4). LePichon et al. (1977) base their re-assembly of the North Atlantic (Fig. 8.4a) on the identification of the structural framework of the opening (i.e. marginal fracture zones generated by offsets in the initial rift), the correlation of linear structures which cross the present continental margins at high angles and the fits of the oldest seafloor spreading isochrons. The final fit is made at the 3,000 m isobath on the African and North American margins and at the 2,000 m isobath on the younger margins; this difference is attributed to subsidence and modification of the continental margins with time. Except for a slight overlap between the northernmost tip of Africa (the Rif) and the Tail of the Banks, the Iberia-Africa overlap that has plagued so many reconstructions is resolved by the LePichon fit. However, several problems remain, particularly in the area of the present study. The gap between Europe and North America south of Rockall Bank and the overlap of Galicia Bank and Flemish Cap are unacceptable. The former problem can be partly solved by placing the ocean-continent boundary northeast of Newfoundland seaward of Orphan Knoll (A. C. Grant, 1972). LePichon et al. (1977) choose to resolve the latter problem by moving Galicia Bank 110 km closer to the Portugese margin along flow-lines for the Iberia-Europe rotation. The large gap between the Grand Banks and southwestern Portugal cannot be closed, for reasons which will be discussed below.

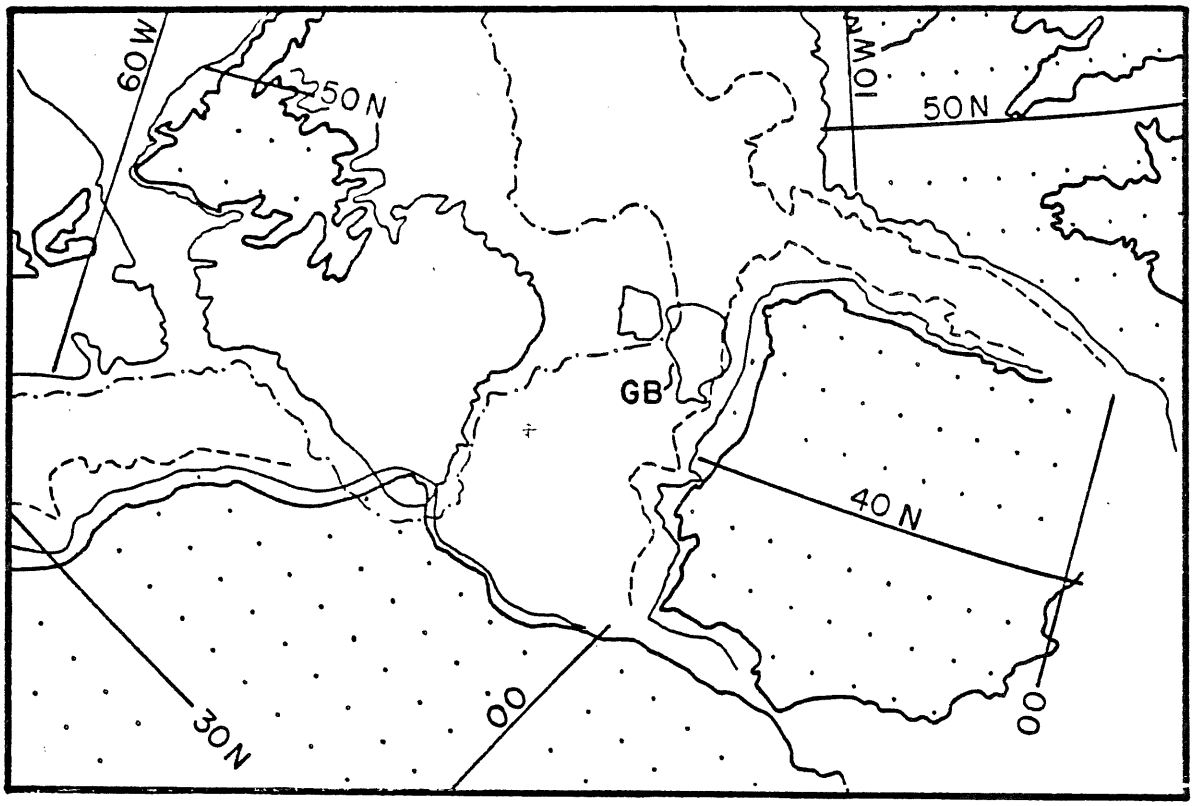

Figure 8.4a: LePichon et al. (1977) reconstruction.

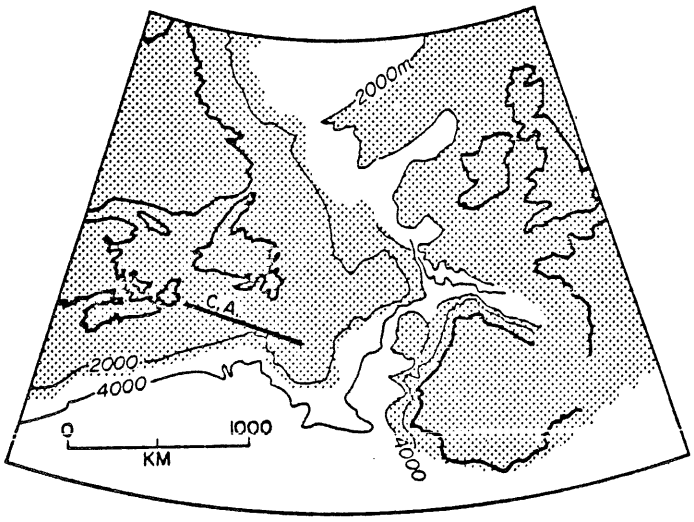

Figure 8.4b: Haworth (in prep.) reconstruction.

Haworth (in prep.) bases his model (Fig. 8.4b) on a substantial quantity of recent geophysical data on the Canadian shelf and continental margin, and on Srivastava's (1978) detailed study of seafloor spreading in the Labrador Sea and North Atlantic north of 45°N. Haworth modifies the reconstruction proposed by Srivastava (1978) (which does not define the closure of the Bay of Biscay) in light of detailed structural and stratigraphic correlations between North America and Europe. Similar correlations (Lefort, 1975; Lefort and Haworth, in press) between Iberia and the Grand Banks are then used to determine the original positions of these continents.

The main difference between the Haworth and the LePichon reconstructions lies in the pre-drift position of Greenland with respect to North America. Haworth accepts Srivastava's (1978) position for Greenland (Fig. 8.5a), which is several hundred kilometers closer to North America than the position used in the LePichon model (Fig. 8.5b). Srivastava's (1978) model for the separation of Greenland from North America includes a stage in which 250 km of strike-slip motion occurs along the Nares Strait (Wegener Fault, J. T. Wilson, 1963). LePichon et al. (1977) reject the hypothesis of decoupling across Nares Strait and so can not close Baffin Bay and the Labrador Sea entirely. The end result is a difference of approximately 200 km in the position of Europe-Iberia with respect to North America. The Haworth-Srivastava model places Europe several hundred kilometers further south than the LePichon fit, thereby removing the overlap between Flemish Cap and Galicia Banks, closing the gap south of Rockall and permitting a closer fit between Portugal and the Grand Banks.

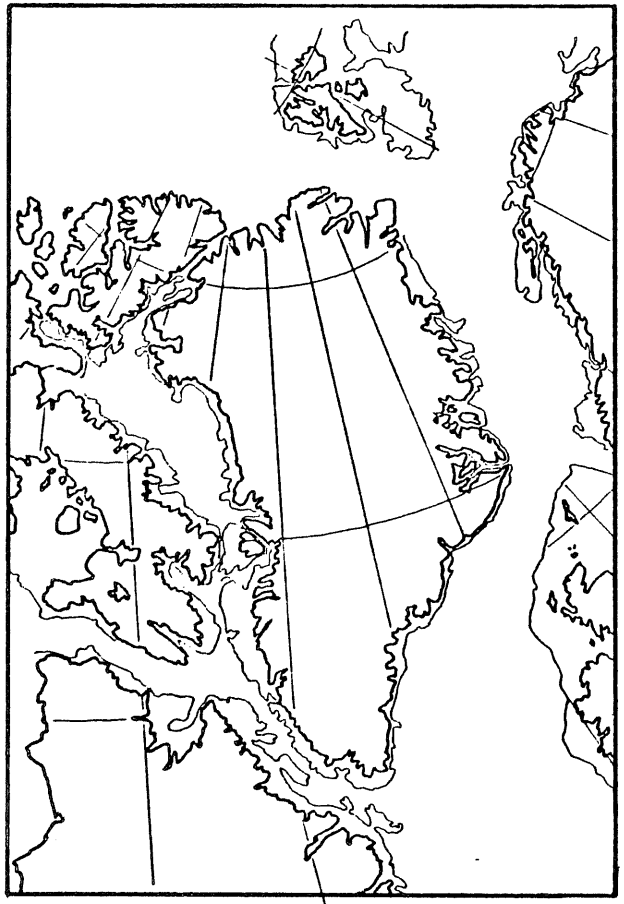

Figure 8.5a

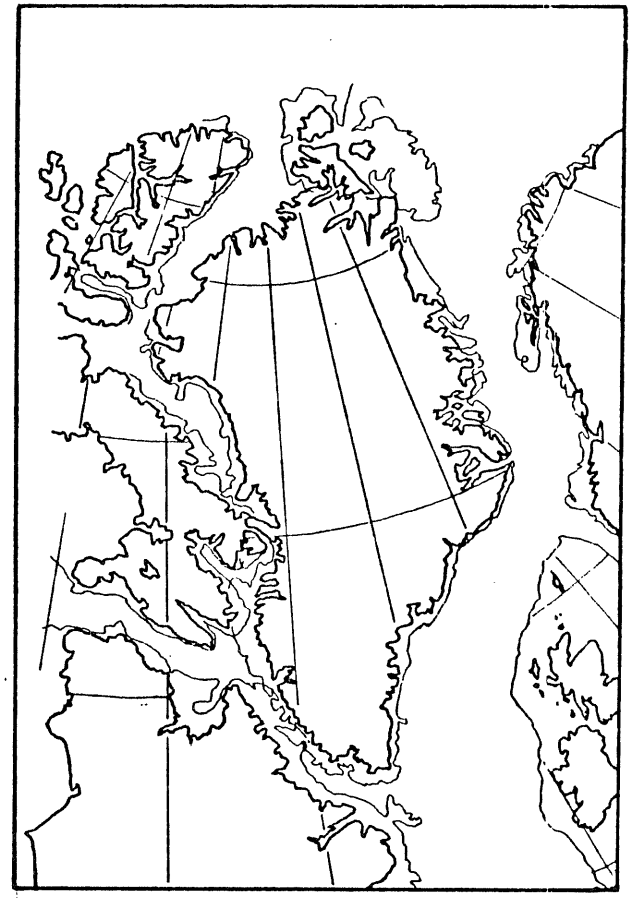

Figure 8.5b

Greenland-North America pre-drift fits
a) LePichon et al. (1977)
b) Srivastava (1978)

The conflicting interpretations of the pre-drift positions of Arctic continents is beyond the scope of the present study. The Haworth-Srivastava model is preferred here on the grounds that a) it takes into account significantly more detailed geological data from the very complex Iberia-Grand Banks regions and b) it produces a substantially closer fit between these continental areas than does the LePichon model. It will be shown in the next section that incorporation of the ocean-continent boundary determined in the present study (Section 8.1) into Haworth's model resolves the problem of the gap between Iberia and the Grand Banks.

8.3 Seafloor Spreading Model

In order to be acceptable, any model proposed for the seafloor spreading history of the Newfoundland Basin must a) be consistent with data from the North Atlantic and Labrador Sea; b) account for contemporaneous spreading in the Bay of Biscay (C. A. Williams, 1975); c) account for the origins of the SENR and the Newfoundland Seamounts; and d) be consistent with available data from the Portugese continental margin and adjacent oceanic areas (Groupe Galice, 1977).

Several observations made in the present study must also be incorporated into the model:

1) Deep grabens underlie the continental slope along the Flemish Cap and Eastern Banks margins which, by analogy with the Grand Banks sub-basins and grabens on the Portugese margin (Jansa and Wade, 1975; Groupe Galice, 1977) may contain sediments as old as Upper Triassic (Section 4.4).

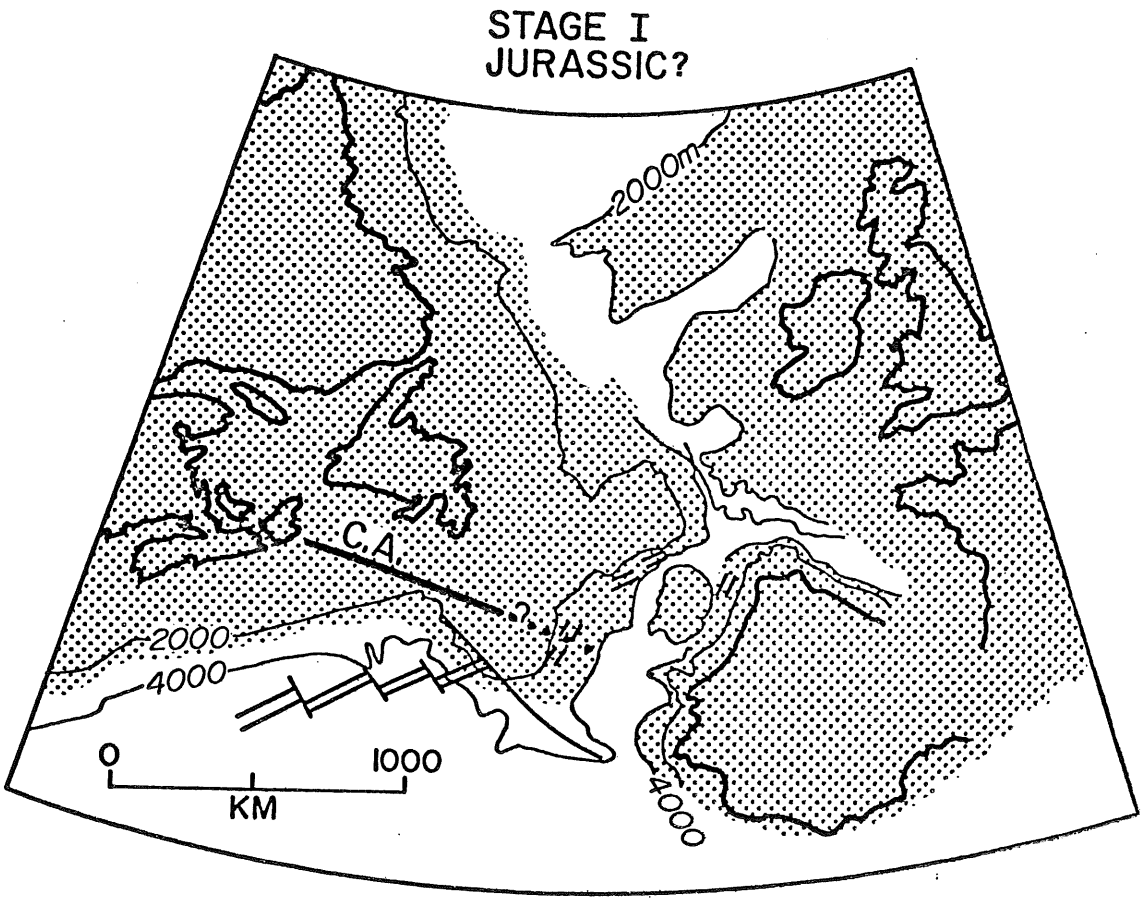

Figure 8.6a

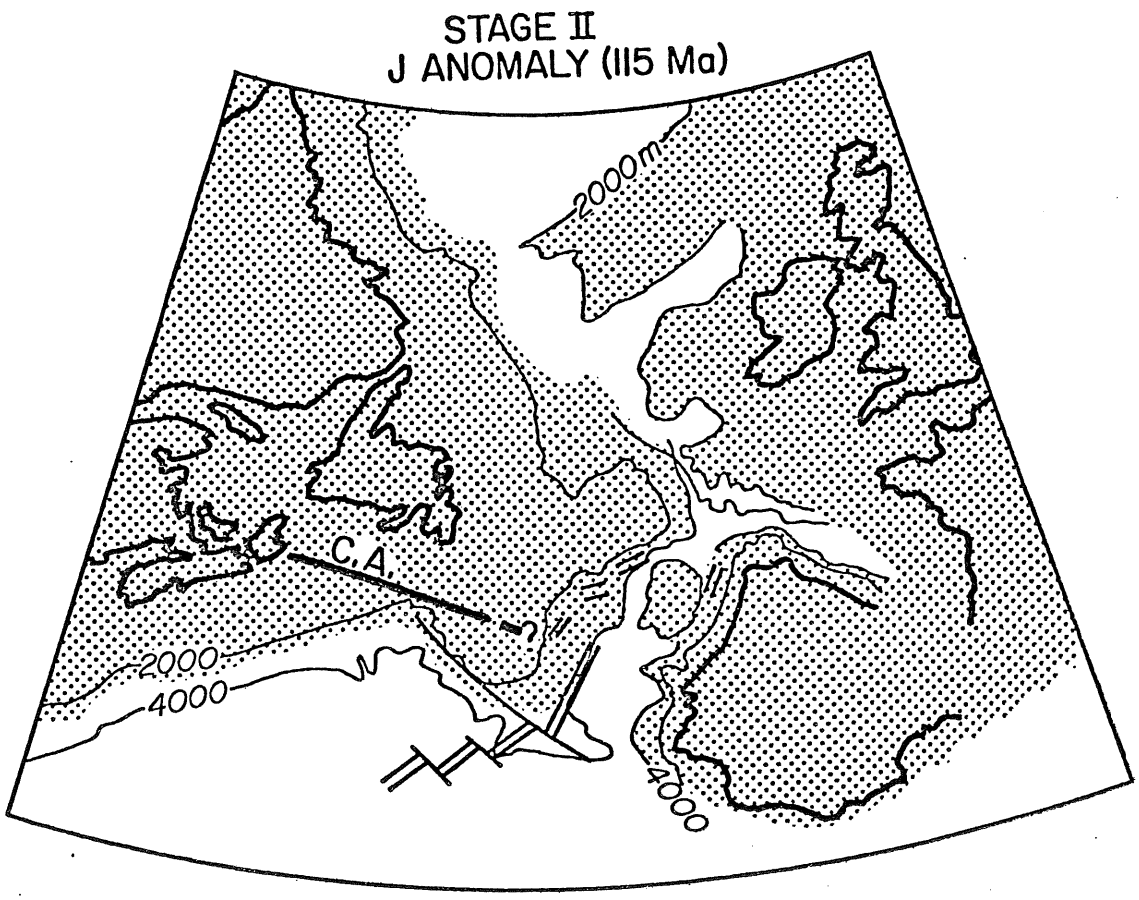

Figure 8.6b

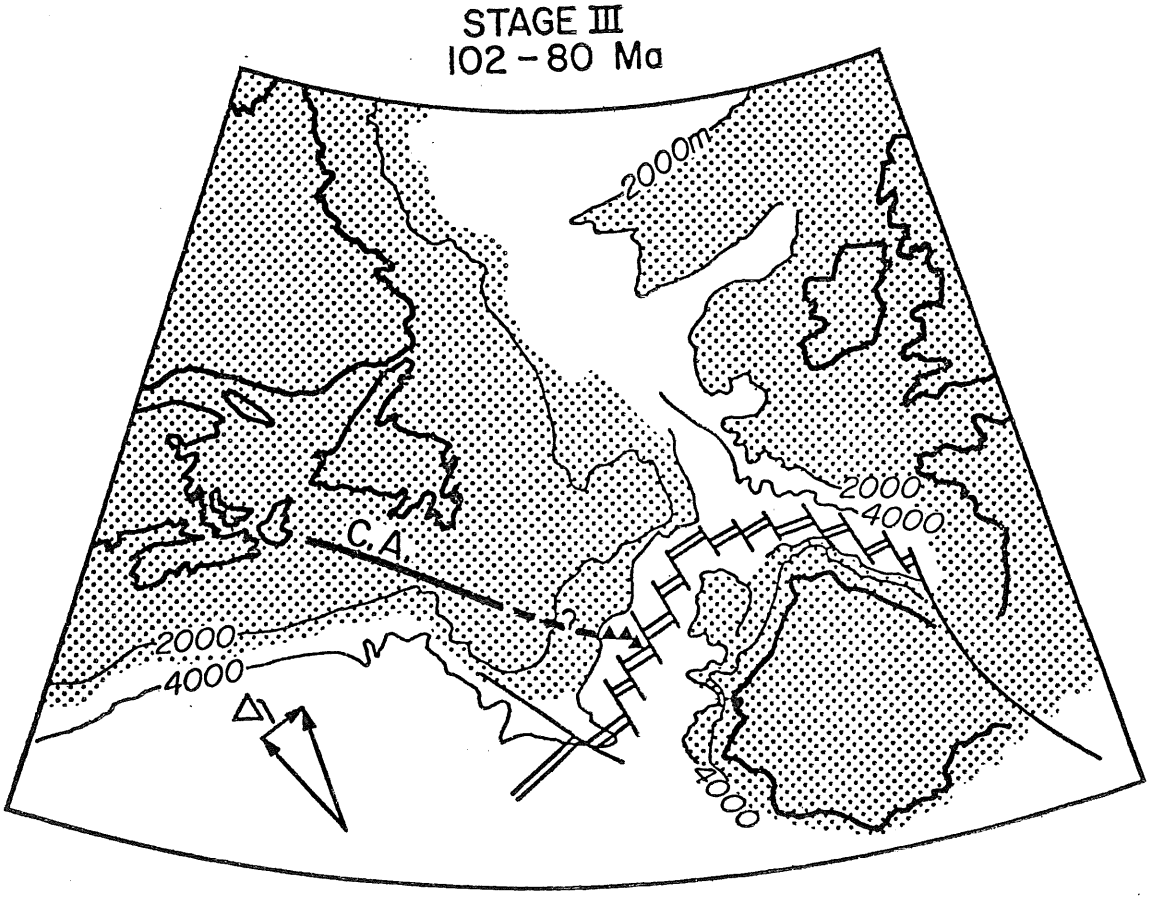

Figure 8.6c

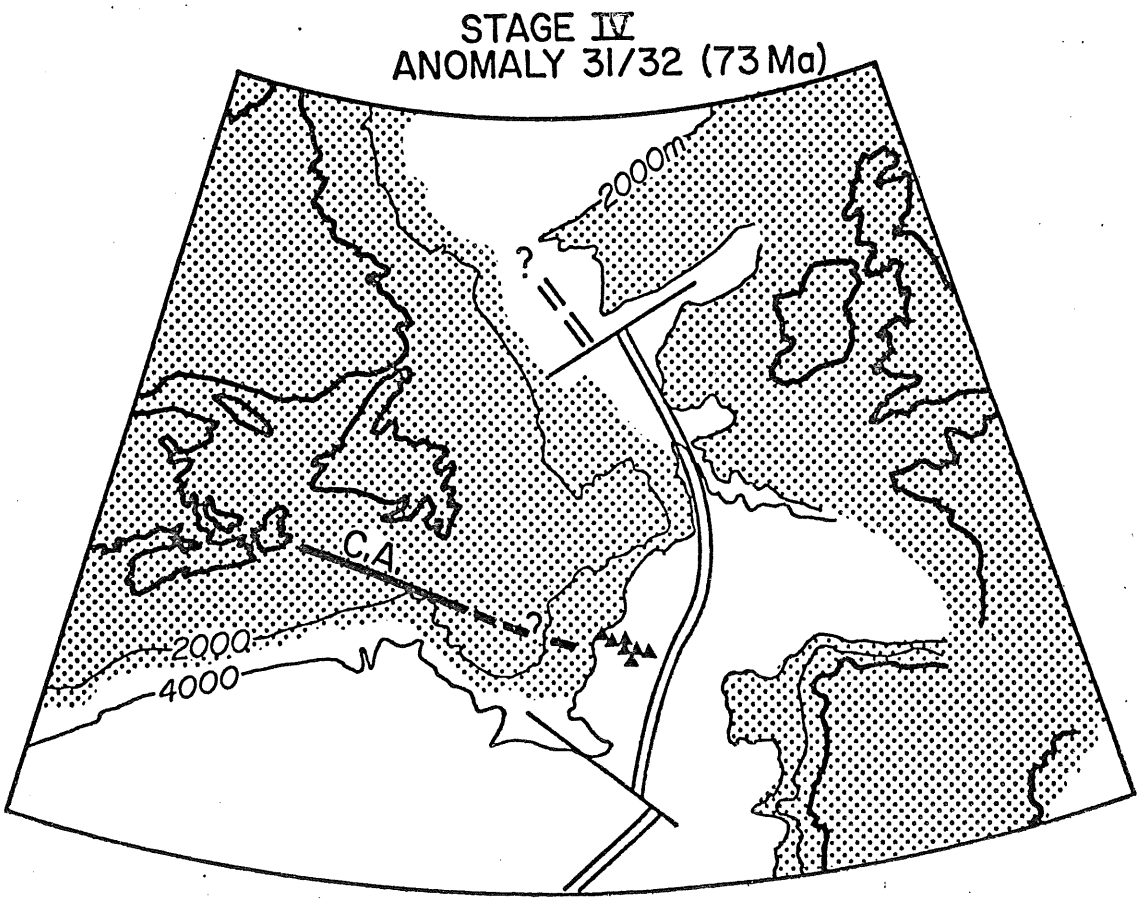

Figure 8.6d

2) Magnetic anomaly trends in the Newfoundland Basin indicate that the spreading center underwent a major change in trend from 015° (J-anomaly) to 055° approximately 12 Ma after spreading began.

3) The Newfoundland Seamounts appear to represent two episodes of volcanic activity along fracture zones formed during the J-anomaly and the 055° phases of spreading. The earlier fracture zone trend, and hence the initial locus of seamount volcanism, is related to the seaward prolongation of basement structures on the Grand Banks. Several lines of evidence (Chapter 7) indicate that the seamounts postdate the surrounding crust by only a short period of time, probably 10 Ma of less.

The model presented in Figure 8.6 succeeds reasonably well on most of these points. North Africa has been omitted from the diagrams for clarity, but this does not affect the present discussion.

Stage I: Pre-drift

Figure 8.6a shows the pre-drift positions of North America, Europe and Iberia according to the Haworth-Srivastava model described above. The seaward limit of continental crust (stippling) in the Newfoundland Basin is based on results presented in this study. West of Portugal, the limit indicated is the position of the J-anomaly as mapped by Groupe Galice (1977). With the addition of the Newfoundland Basin data and the inference that the J-anomaly west of Portugal also marks the ocean-continent boundary, the gap between southwestern Portugal and the southern Grand Banks is essentially closed. The Collector Anomaly (Haworth, 1975; Chapter 2) is shown extending east-

ward into the Newfoundland Basin. Haworth (in prep.) points out that a plausible further continuation of the Collector eastward into southern Portugal and Spain is not evident. However, the Collector Anomaly trend indicated in Figure 8.6a correlates well with a pronounced bathymetric offset of the Portugese margin near Lisbon, and with a sharp magnetic gradient and J-anomaly offset (Groupe Galice, 1977).

Active seafloor spreading was occurring south of the Newfoundland Fracture Zone (predecessor of the SENR) at this time. Pitman and Talwani (1972) suggest that rifting between North America and Africa began about 200 Ma and was followed at about 190 Ma by active drift, and most subsequent studies are in basic agreement with this timing. The formation of the Grand Banks sub-basins and of the grabens along the Newfoundland Basin and Portugese margins occurred during this phase (schematically indicated in Fig. 8.6a as short double lines).

Stage II: J-anomaly time (115 Ma)

The second stage of the model (Fig. 8.6b) shows the geometry at J-anomaly time (115 Ma). The Africa-North America spreading center is coincident with the present position of the Spur Ridge now, and active spreading has begun in the area between the Newfoundland Fracture Zone and the southern edge of Galicia Bank. The nature of the northern termination of this spreading center is not known. It is possible that there was a transform fault along the projected eastward extension of the Collector Anomaly, but there are at present no data to support this idea. It seems more likely that spreading simply died

out northward along the ridge, such that the active spreading regime gave way to incipient spreading between Galicia Bank and the northern Grand Banks. The result of this would be anticlockwise rotation of Iberia with respect to North America and of Galicia Bank with respect to Iberia, thus perhaps explaining how Galicia Bank came to its present position on the Iberian margin.

Stage III: 102 Ma to 73 Ma (anomaly 31/32)

Approximately 12 Ma after the formation of the J-anomaly, the spreading geometry underwent a major change north of the Newfoundland Fracture Zone. Figure 8.6c depicts the spreading geometry for the time interval between the shift in the North America-Iberia pole of rotation (102 Ma) and anomaly 31/32 (73 Ma). Spreading occurs simultaneously and about the same pole in the Bay of Biscay and the Newfoundland Basin throughout most of this stage. The relative motion between Iberia and Europe is taken up on the North Pyrenean Fault (LePichon et al., 1970; Choukroune et al., 1972). Spreading between Rockall and Europe, schematically indicated in Figure 8.6c, began about 90 Ma (Roberts, 1974; Srivastava, 1978).

The vector triangle shown in Figure 8.6c indicates that the ridge geometry proposed for this stage requires that a component of extension act across the Newfoundland Fracture zone. Consequently, the transform fault joining the ridge segments at the Tail of the Bank will be "leaky" (Menard and Atwater, 1968). The migration of this leaky transform to the southeast during this period of time is believed to be an important factor in the formation of the SENR.

The formation of the Newfoundland Seamounts was completed by about 100 Ma. Screech, Number 3, Number 2 and Scruncheon Seamounts formed along a fracture zone trend related to the first phase of Iberia-North America spreading. Volcanic activity on this trend is believed to be related to the shift in the pole of spreading at 102 Ma. Mafic extrusives of approximately Cenomanian age encountered in an exploratory well drilled just south of the Collector Anomaly on the Grand Banks (Gradstein et al., 1977) may indicate that this structure was also reactivated by the event. The seamounts east and south of Scruncheon and several of the large buried basement highs in the southern Newfoundland Basin are also believed to have formed by volcanism along "leaky" transform faults during the second phase of spreading (055° lineations).

Stage IV: 73 Ma (anomaly 31/32)

The final frame in the spreading model (Fig. 8.6d) shows the positions of the continents and the spreading geometry at anomaly 31/32 time. The cessation of spreading in the Bay of Biscay and the change in spreading direction in the Atlantic to that of the Cenozoic anomalies occurred prior to anomaly 31/32. Srivastava (1978) identifies anomaly 34 (80 Ma) as the oldest isochron adjacent to the Newfoundland continental margin between Flemish Cap and the Charlie Fracture Zone, and the topographic expression of the SENR terminates at about the position of the 80 Ma isochron according to Pitman and Talwani (1972). On the other hand, C. A. Williams (1975) and Pitman and Talwani (1972) identify anomaly 31/32 as the oldest anomaly west of Rockall and

Porcupine Bank, and C. A. Williams (1975) believes that anomalies 32-34 are present in the Bay of Biscay. If these identifications are correct, then the model in Figure 8.6 should include an additional stage between Stages III and IV during which an RRR triple junction existed off the northwestern corner of Iberia.

CHAPTER 9: SUMMARY AND SUGGESTIONS FOR FURTHER RESEARCH

The objectives of this study, stated in Chapter 1, were a) to investigate the structure of the Newfoundland Basin and adjacent continental margins and b) to use the knowledge gained through these investigations to clarify the pre-73 Ma plate tectonic history of the North Atlantic north of the Grand Banks and Azores-Gibraltar line. As with most such undertakings, this study has fulfilled some of its objectives and also brought to light problems requiring further research.

9.1 Summary

This study has shown that the ocean-continent boundary in the Newfoundland Basin north of the SENR is defined by a) a prominent magnetic anomaly at the seaward boundary of a continental margin magnetic smooth zone; b) basement highs separating the landward region of deep basement from the shallower basement to seaward; and c) low-amplitude (20-30 mgal) isostatic and free-air gravity highs. The 4,000 m isobath is approximately coincident with the ocean-continent boundary. Between the seamounts and the SENR the boundary appears to be coincident with the J-anomaly and is thus dated as 115 Ma. North of the seamounts the boundary truncates magnetic anomalies that formed between about 102 Ma and 80 Ma; it is not precisely dated here.

Complex basement structures along the seaward extension of the Grand Banks marginal fracture zone make definition of the ocean-continent boundary off the Tail of the Bank more difficult. Several

authors (Gradstein et al., 1977; A. C. Grant, 1977) have postulated that continental crust extends quite far to seaward beneath the Spur Ridge and SENR, but the geophysical data presented in this thesis clearly indicate that both of these structures are oceanic. The ocean-continent boundary is therefore placed at the morphological boundary between the Grand Banks and the SENR-Spur Ridge structures in this study.

It has been shown that the structural characteristics and stratigraphy of the marginal area between the ocean-continent boundary and the edge of the continental shelf correlate well with the Triassic-Jurassic of the Grand Banks and western Iberia. This supports and extends the results of the many land-based and shelf-based comparative studies that have been undertaken in these regions (R.C.L. Wilson, 1975; Lefort, 1975; Haworth and Lefort, in prep.).

The Newfoundland Basin seaward of the ocean-continent boundary is underlain by oceanic crust ranging in age from 115 Ma (J-anomaly) to 73 Ma (anomaly 31/32). The magnetic anomaly pattern in this region indicates that at least two major changes in plate motions occurred during the evolution of the seafloor here. At about 102 Ma the strike of the spreading axis changed from 015° (J-anomaly trend) to 055°; this is believed to be concomitant with the initiation of active spreading about the same pole (northeast of Paris) between Iberia and Europe. At about 80 Ma (anomaly 33) the locus of spreading shifted to the Cenozoic trend evident in the pattern of magnetic anomalies 33 through 1. The SENR is postulated to have formed by the southeastward migration of a 'leaky' ridge-ridge transform fault during the inter-

val of time between these two pole changes and by subsequent differential subsidence of the Newfoundland Basin and Sohm Abyssal Plain. The Newfoundland Seamounts appear to have formed in two stages during the time interval 115-97 Ma. The first stage of activity, which produced the smaller, westernmost seamounts, occurred along fracture zones formed along the seaward prolongation of continental structures. The seamounts east and south of Scruncheon Seamount follow the trends of fracture zones formed during the 102-80 Ma spreading phase. Both of these trends are believed to represent "leaky" transform fault volcanism (Menard and Atwater, 1968).

This study has also established that the sedimentary sequence in the oceanic Newfoundland Basin correlates well with that of the Northwest Atlantic south of the SENR and of the continental margins of Iberia and the Bay of Biscay. This correlation with areas in which Deep Sea Drilling results are available provides a basis for assigning some preliminary ages and lithologies to the units in the Newfoundland Basin stratigraphic sequence, which is at present known only from seismic reflection studies.

In the preceeding chapter the above findings were integrated with other data from the Grand Banks, western Iberia and the Bay of Biscay and used to evaluate two recently-proposed models for Iberia-North America pre-drift paleogeography. The reconstruction of Haworth (in prep.), supplemented by these marine data, is quite successful in resolving most of the gaps and overlaps that have plagued so many previous models. This paleogeography is therefore taken as the initial configuration for the plate model derived from the data collected during

this study. The consistency of this model with data from Iberia and the Bay of Biscay is quite good, so it can be accepted with confidence as a meaningful working model for early Iberia-North America spreading.

Two sections of this thesis addressed topics of very much broader interest. In Chapter 5 the significance of roughly lineated magnetic anomalies in oceanic areas that presumably formed during the Cretaceous Normal Polarity Interval (81-110 Ma) was discussed. At present, evidence for reversals during this period comes only from paleomagnetic studies on DSDP sediment cores (Keating and Helsley, 1976, 1977, in press) and from modelling of roughly-lineated anomalies over crust of this age in the Atlantic (Vogt and Johnson, 1971; Hayes and Rabinowitz, 1975; B. R. Hall, 1977; C. E. Keen et al., 1977). The present study considered the latter observations. It was shown that at least two reasonably plausible mechanisms exist which could modify a simple normal-polarity magnetic source-layer in such a way that roughly lineated anomalies would be produced. Both of the models discussed require that the oceanic crust have a strong tectonic fabric, such as forms at present at slowly-spreading ridges. This is not compatible with Larson and Pitman's (1972) conclusion that a worldwide pulse of rapid spreading occurred from 110-81 Ma.

Some aspects of recent studies of gravity anomalies at rifted margins were discussed in Chapter 6, with particular reference to the signature of the ocean-continent boundary. On the basis of the comparison of gravity profiles from a number of Jurassic and Cretaceous rifted margins that was made in Section 6.5 the hypothesis that iso-

static gravity anomalies can be "diagnostic" of the ocean-continent boundary was discounted. Isostatic and free-air anomalies provide essentially the same information (except in the immediate vicinity of the shelf-break and slope), and combined use of seismic, magnetic and gravity data is still essential to determination of the ocean-continent boundary.

9.2 Suggestions for further research

This thesis has intentionally focused on the Cretaceous structural and plate tectonic history of the Newfoundland Basin. As a result of this choice, several very intriguing aspects of the data have gone unexplored. In addition to investigating topics of this nature, future research can be directed towards testing the evolutionary model presented in Chapter 8. A number of interesting avenues for further study are outlined below; this is by no means an exhaustive list, and the selection of topics mentioned is strongly biased by the author's personal interests.

In terms of testing the interpretations presented in Chapter 8, there are several points which come readily to mind:

a) If the SENR formed by the southeastward migration of a "leaky" fracture zone, as postulated, it should be composed in part of alkali basalts and these should become younger to the southeast. This might be verified by dredging or shallow drilling, if appropriate sites can be found.

b) The postulated genetic link between the seamounts and Grand Banks basement structures and the proposed two-stage evolution of the seamounts

could be checked by collection of additional seismic data and dredge samples. The seamount model in Chapter 7 neither explains the observed variation in seamount size and shape nor predicts a different pattern; might the significance of these variations be clarified if more detailed data were available on the basement structures associated with the seamounts?

c) The J-anomaly/smooth zone boundary is not as well documented as it should be. What kind of transition occurs between Line 42 on the northern flank of the SENR (where high-amplitude anomalies are observed west of the J-anomaly) and Line S (where the J-anomaly marks the seaward boundary of the marginal smooth zone)? What happens where the trend of the smooth zone boundary in the southern Newfoundland Basin intersects the Flemish Cap smooth zone boundary?

d) Seismic refraction data within the smooth zone would provide useful information on the nature of the crust in this area. Is the smooth zone underlain by foundered or "oceanized" (Beloussøv, 1968) continental crust, by oceanic crust, or by a combination of the two?

Investigations along these lines would require additional ship time dedicated to the Newfoundland Basin, and the present outlook for meeting this requirement is very bleak. Given this situation, what further projects should be pursued with the data in hand?

The deep-penetration seismics available in the Newfoundland Basin provide an excellent data base for study of post-Cretaceous sedimentation in this area. This topic has great potential and should be given a very high priority.

Continuing investigation of the apparent magnetic reversals in oceanic crust formed during the Cretaceous Normal Polarity Interval is another high-priority item. Roughly lineated anomalies have been observed in crust of this age in several parts of the North Atlantic (Vogt and Johnson, 1971; Hayes and Rabinowitz, 1975; B. R. Hall, 1977); KN-age crust in the Pacific is apparently not lineated (Larson and Pitman, 1972; Rabinowitz and Hayes, 1975). The magnetic data base in the Newfoundland Basin (compiled by B. R. Hall, 1977) is perhaps the best that is currently available for study of this problem, and it should be put to full use. Two obvious ways to proceed are a) application of time-series analyses to the data and b) detailed comparative studies with related regions in both the Atlantic and the Pacific.

The Newfoundland Seamount study can also be extended. This thesis considered the seamounts in the context of the evolution of the Newfoundland Basin; one might consider their significance in several broader contexts, such as North Atlantic seamount volcanism; Cretaceous seamounts worldwide; primary and secondary mineralogical and chemical features of oceanic central (as opposed to fissural) volcanoes.

Finally, a topic requiring further study that was pointed out in Chapter 6: the factors contributing to the gravity signatures of rifted margins and the variations of these factors in space and time. There are a number of questions here which need to be resolved before reliable general models can be formulated; these are discussed in Section 6.5.

9.3 Conclusion

The eye is the first circle; the horizon which it forms is the second; and throughout nature this primary figure is repeated without end. It is the highest emblem in the cipher of the world... We are all out lifetime reading the copious sense of this first of forms... Our life is an apprenticeship to the truth that around every circle another can be drawn; that there is no end in nature, but every end is a beginning; that there is always another dawn risen on mid-noon and under every deep a lower deep opens.

Emerson

References

Alvarez, W. and W. Lowrie, 1977: Upper Cretaceous-Paleocene magnetic stratigraphy at Gubbio, Italy, III: Upper Cretaceous magnetic stratigraphy; Geol. Soc. Amer. Bull. 88, 374-377.

Amoco Canada Petrol. Co. Ltd. and Imperial Oil Limited, 1973: Regional geology of the Grand Banks; Bull. Can. Petrol. Geol. 21(4), 479-503.

Arthaud, F. and P. Matte, 1975: Late Hercynian wrench faults in southwestern Europe: Geometry and nature of deformation; Tectonophysics 25, 139-171.

Arthaud, F. and P. Matte, 1977: Late Paleozoic strike-slip faulting in Southern Europe and Northern Africa: Result of a right-lateral shear zone between the Appalachians and the Urals; Bull. Geol. Soc. Am. 88, 1305-1320.

Auzende, J., J. Olivet, and J. Bonnin, 1970: La marge du Grand Banc et la fracture de Terre-Neuve; C. R. Acad. Sc. Paris Ser. D., 271, 1063-1066.

Bailey, R. J. 1975: Sub-Cenozoic geology of the British continental margin (Lat. 50°N to 57°N) and the re-assembly of the North Atlantic late Paleozoic supercontinent; Geology 3, 591-594.

Baldwin, B., P. J. Coney and W. R. Dickinson, 1974: Dilemma of a Cretaceous time-scale and rates of seafloor spreading; Geology 2, 267-270.

Ballard, J. A., P. R. Vogt and G. Egloff, 1976: The magnetic "J-anomaly" and associated structures in the North Atlantic [abs]; EOS, Trans. Amer. Geophys. Union 57, 264.

Barberi, F., H. Tazieff and J. Varet, 1972: Volcanism in the Afar depression: Its tectonic and magmatic significance; Tectonophysics 15(1/2), 19-29.

Barberi, F. and J. Varet, 1977: Volcanism of Afar: Small-scale plate tectonics implications; Geol. Soc. Am. Bull. 88, 1251-1266.

Barrett, D. L. and C. L. Keen, 1976: Mesozoic magnetic lineations, the magnetic Quiet Zone and seafloor spreading in the Northwest Atlantic; Jour. Geophys. Res. 81(26), 4875-4884.

Bass, M. N., 1976: Secondary minerals in oceanic basalt, with special reference to Leg 34, Deep Sea Drilling Project; Initial Reports of the Deep Sea Drilling Project 34, U.S. Gov't. Printing Office, Washington, 393-432.

Batiza, R., 1977a: Age, volume, compositional and spatial relations of small isolated oceanic central volcanoes; Mar. Geol. 24, 169-183.

Batiza, R., 1977b: Petrology and chemistry of Guadalupe Island: An alkalic seamount on a fossil ridge crest; Geology 5, 760-764.

Beloussov, V. V., 1968: Some problems of development of the earth's crust and upper mantle of oceans; in: "The Crust and Upper Mantle of the Pacific Area, L. Knopoff, C. L. Drake and P. J. Hart (eds.) Amer. Geophys. Union Monogr. 12, Washington, D. C., 449-459.

Benson, W., Sheridan, R. E. and Scientific Party, 1976: In the North Atlantic: Deep-sea drilling; Geotimes 21(2), 23-25.

Berggren, W. A., D. P. McKenzie, J. G. Sclater and J. E. van Hinte, 1975: World-wide correlation of Mesozoic magnetic anomalies and its implications: Discussion and reply; Geol. Soc. Amer. Bull. 86, 267-272.

Bishop, A. C. and A. R. Woolley, 1973: A basalt-trachyte-phonolite series from Ua Pu, Marquesas Islands, Pacific Ocean; Contrib. Mineral. Petrol. 39, 309-326.

Bonatti, E., C. G. A. Harrison, D. E. Fisher, J. Honnorez, J. G. Schilling, J. J. Stipp and M. Zentilli, 1977: Easter Volcanic chain (Southwest Pacific): A mantle hot line; Jour. Geophys. Res. 82(17), 2457-2578.

Buckley, H. A., 1976: The Discovery Tablemount Chain; Deep-Sea Res. 23, 937-948.

Bullard, E. C., and R. G. Mason, 1961: The magnetic field astern of a ship; Deep-Sea Res. 8, 520-527.

Bullard, E. C., J. E. Everett and A. G. Smith, 1965: The fit of the continents around the Atlantic; in: Symposium on Continental Drift, Phil. Trans. Roy. Soc. London, Ser. A, 258, 41-51.

Cande, S. C. and Y. Kristofferson, 1977: Late Cretaceous magnetic anomalies in the North Atlantic; Earth Planet. Sci. Lett. 35, 215-224.

Carey, S. W., 1958: A tectonic approach to continental drift; in: Continental Drift, a symposium, S. W. Carey (ed.), Univ. of Tasmania Press, Hobart, 177-355.

Chase, R. L., 1977: J. Tuzo Wilson Knolls: Canadian hotspot; Nature 266, 345-347.

Choubert, B., 1935: Recherche sur la genèse des chaînes paleozoiques et anté cambriennes; Rev. Géogr. Phys. Dyn. 8, 5-50.

Choukroune, P., X. LePichon, M. Seguret and J-C. Sibuet, 1973: Bay of Biscay and Pyrenees; Earth Planet. Sci. Lett. 18, 109-118.

Christensen, N. I. and M. H. Salisbury, 1975: Structure and constitution of the lower oceanic crust; Rev. Geophys. Space Phys. 13(1), 57-85.

Clague, D. A., G. B. Dalrymple and R. Moberley, 1975: Petrography and K-Ar ages of dredged volcanic rocks from the western Hawaiian Ridge and the southern Emperor Seamount chain; Geol. Soc. Am. Bull. 86, 991-998.

Dainty, A. M., C. E. Keen, M. J. Keen and J. E. Blanchard, 1966: Review of geophysical evidence on crust and upper mantle structure on the eastern seaboard of Canada; in The Earth Beneath the Continents, J. S. Steinhart and J. T. Smith (eds.), 349-369.

Davies, T. A. and A. S. Laughton, 1972: Sedimentary Processes in the North Atlantic; Initial Reports, Deep-Sea Drilling Project 12, U. S. Gov't Printing Office, Washington, 905-934.

Dawson, E. and L. R. Newitt, 1977: I.G.R.F. comparisons [abs]; EOS, Trans. Amer. Geophys. Union 58(8), 748.

Dewey, J. F., W. C. Pitman III, W. B. F. Ryan and J. Bonnin, 1973: Plate tectonics and the evolution of the Alpine system; Geol. Soc. Am. Bull. 84, 3137-3180.

Donnelly, T. W., Francheteau, J. and Scientific Party, 1977: Mid-ocean ridge in the Cretaceous; Geotimes 22(6), 21-23.

Emery, K. O. and E. Uchupi, 1972: Western North Atlantic Ocean: Topography, Rocks, Structure, Water, Life and Sediments; Amer. Assoc. Petrol. Geol. Memoir 17, Tulsa, Oklahoma, 532 pp.

Engel, A. E. J., C. G. Engel and R. G. Havens, 1965: Chemical characteristics of oceanic basalts and the upper mantle; Geol. Soc. Am. Bull. 76, 719-734.

Erickson, B. H., F. P. Naugler and W. H. Lucas, 1970: Emperor fracture zone: a newly discovered feature in the central north Pacific; Nature 225, 53-54.

Ewing, G. N., A. M. Dainty, J. E. Blanchard and M. J. Keen, 1966: Seismic studies on the eastern seaboard of Canada: The Appalachian System I; Can. Jour. Earth Sci. 3(1), 89-109.

Ewing, J. I. and C. D. Hollister, 1972: Regional aspects of deep-sea drilling in the western North Atlantic; Initial Reports of the Deep Sea Drilling Project 11, U. S. Gov't Printing Office, Washington, 951-973.

Fenwick, D. K. B., M. J. Keen, C. E. Keen and A. Lambert, 1968: Geophysical studies of the continental margin northeast of Newfoundland; Can. Jour. Earth Sci. 5, 483-500.

Flood, R. and C. D. Hollister, 1974: Current-controlled topography on the continental margin off the eastern United States; in Geology of Continental Margins, C. A. Burk and C. L. Drake (eds), Springer Verlag, New York, 197-206.

Flower, M. F. J., 1971: REE distribution in lavas and ultramafic xenoliths from the Comores Archipelago, W. Indian Ocean; Contrib. Mineral. Petrol. 31, 335-346.

Folinsbee, R. A., in prep.: The deep crustal structure of the continental margin northeast of Newfoundland: Sediment loading and subsidence.

Fox, P. J., E. Schreiber and J. J. Peterson, 1973: The geology of the oceanic crust: Compressional wave velocities of oceanic rocks; Jour. Geophys. Res. 78(23), 5155-5172.

Francheteau, J. and X. LePichon, 1972: Marginal fracture zones as structural framework of continental margins of S. Atlantic ocean; Bull. Amer. Assoc. Petrol. Geol. 56. 991-1007.

Frey, F. A., W. B. Bryan and G. Thompson, 1974: Atlantic ocean floor: Geochemistry of basalts from Legs 2 and 3 of the Deep-Sea Drilling Project; Jour. Geophys. Res. 79, 5507-5527.

Gass, I. G., D. I. J. Mallick and K. G. Cox, 1973: Volcanic islands of the Red Sea; Jour. Geol. Soc. Lond 129, 275-310.

Gradstein, F. M., G. L. Williams, W. A. M. Jenkins, and P. Ascoli, 1975: Mesozoic and Cenozoic stratigraphy of the Atlantic continental margin, Eastern Canada; in Canada's Continental Margins and Offshore Petroleum Exploration, C. J. Yorath, E. R. Parker and D. J. Glass (eds.), Can. Soc. Petroleum Geologists, Memoir 4, 103-131.

Gradstein, F. M., A. C.Grant and L. F. Jansa, 1977: Grand Banks and J-Anomaly Ridge: A geological comparison; Science 197, 1074-1076.

Grant, A. C., 1971: Geological and geophysical results bearing on the structural history of the Flemish Cap region; in Earth Science Symposium on Offshore Eastern Canada, P. J. Hood (ed), Geol. Surv. Can., Paper 71-23, 373-388.

Grant, A. C., 1972: The continental margin off Labrador and eastern Newfoundland--morphology and geology; Can. Jour. Earth Sci. 9, 1394-1430.

Grant, A. C., 1977: Continental crust beneath the Newfoundland Ridge: Evidence from multi-channel seismic reflection data; Nature 270, 22-25.

Grant, S., 1973: Rho-rho Loran-C combined with satellite navigation for offshore surveys; Int'l Hydrographic Rev. L(2).

Green, K. E. and A. Brecher, 1974: Preliminary paleomagnetic results for sediments from Site 263, Leg 27; Initial Reports of the Deep Sea Drilling Project 27, U. S. Gov't Printing Office, Washington, 405-413.

Groupe Galice, 1977: The continental margin off Galicia and Portugal-Acoustical stratigraphy, dredge stratigraphy and structural evolution; Inst. Francais du Petrole, Div. Géologie, Ref. 25 451.

Grow, J. A., and C. O. Bowin, 1977: Free-air gravity anomalies over the U. S. Atlantic continental margin [abs]. Geol. Soc. Amer. Abstracts with Programs 9(7), 999.

Hall, B. R., 1977: Collection, reduction and interpretation of magnetic data from the Newfoundland Basin; M.Sc. thesis (unpubl.), Dalhousie University, Halifax, Nova Scotia, 107 pp.

Hall, J. M., 1976: Major problems regarding the magnetization of oceanic crustal Layer 2. Jour. Geophys. Res. 81(23), 4223-4230.

Hall, J. M., 1977: Does TRM occur in oceanic layer 2 basalts?; J. Geomag. Geoelectr. 29, 411-419.

Hall, J. M., D. L. Barrett and C. E. Keen, 1977: The volcanic layer of the ocean crust adjacent to Canada--a review; in: Volcanic Regimes in Canada, W. R. A. Baragar, L. C. Coleman and J. M. Hall (eds.), Geol. Assoc. Canada Special Paper 16, 425-444.

Handschumacher, D., 1973: Formation of the Emperor Seamount chain; Nature 244, 150-152.

Harland, W., A. Smith and B. Wilcock, 1964: The Phanerozoic time-scale; Quat. Jour. Geol. Soc. Lond. 120, 260-262.

Harrison, C. G. A., 1976: Magnetization of the oceanic crust; Geophys. Jour. Roy. Astr. Soc. 47, 257-283.

Hart, S. R., A. J. Erlank, and E. J. D. Kable, 1974: Seafloor basalt alteration: Some chemical and Sr-isotopic effects; Contrib. Min. and Pet. 44, 219-230.

Haworth, R. T., 1975: The development of Atlantic Canada as a result of continental collision--Evidence from offshore gravity and magnetic data; in Canada's Continental Margins and Offshore Petroleum Exploration, C. J. Yorath, E. R. Parker and D. J. Glass (eds.), Can. Soc. Petrol. Geol., Memoir 4, 59-77.

Haworth, R. T. (in prep.): Appalachian structural trends northeast of Newfoundland and their trans-Atlantic correlation; submitted to Tectonophysics.

Haworth, R. T., and J. B. MacIntyre, 1975: The gravity and magnetic fields of Atlantic offshore Canada; Marine Sci. Paper 16, Geol. Survey Canada Paper 75-9, 22 pp.

Haworth, R. T. and J.-P. Lefort, in prep.: Geophysical evidence for the extent of the Avalon Zone in Atlantic Canada and its plate tectonic implications; Can. Jour. Earth Sci.

Hayes, D. E. and P. D. Rabinowitz, 1975: Mesozoic magnetic lineations and the magnetic quiet zone off Northwest Africa; Earth Planet. Sci. Lett. 28, 105-114.

Hays, J. D. and Pitman, W. C. III, 1973: Lithospheric plate motion, sealevel changes and climatic and ecological consequences; Nature 246 (5427), 18-22.

Heezen, B. C., Hollister, C. D. and Ruddiman, W. F., 1966: Shaping of the continental rise by deep geostrophic contour currents, Science 152, 502-508.

Heirtzler, J. R., G. Peter, M. Talwani and E. G. Zurflueh, 1962: Magnetic anomalies caused by two-dimensional structure: Their computation by digital computers and their interpretation; Technical Rept. No. 6, Lamont-Doherty Geological Observatory, Columbia University, New York.

Heirtzler, J. R., S. O. Dickson, E. M. Herron, W. C. Pitman III, and X. LePichon, 1968: Marine magnetic anomalies, geomagnetic field reversals, and motion of the ocean floor and continents; Jour. Geophys. Res. 73, 2119-2136.

Hekinian, R., H. Bougault and G. Pautot, 1973: The northern Atlantic Ocean: Preliminary study of the rocks of the Gibbs Fracture (53°N) and the Azores-Gibraltar Fracture Zone; Acad. Sci. C. R. Sér. D., 276(25), 3281-3284.

Hekinian, R. and G. Thompson, 1976: Comparative geochemistry of volcanics from rift valleys, transform faults and aseismic ridges; Contrib. Mineral. and Petrol. 57, 145-162.

Helsley, C. E. and M. B. Steiner, 1969: Evidence for long intervals of normal polarity during the Cretaceous period; Earth Planet. Sci. Lett. 5, 325-332.

Herrmann, A. G., M. J. Potts, and D. Knacke, 1974: Geochemistry of the rare earth elements in spilites from the oceanic and continental crust; Contrib. Mineral. and Petrol. 44, 1-16.

Herron, E. M., 1972: Seafloor spreading and the Cenozoic history of the East-Central Pacific; Geol. Soc. Am. Bull. 83, 1671-1692.

Hollister, C. D., 1967: Sediment distribution and deep circulation in the western North Atlantic; Ph.D. thesis (unpubl.), Columbia University, New York, 467 pp.

Hollister, C. D. and B. C. Heezen, 1972: Geological effects of ocean bottom currents: Western North Atlantic; in: Studies in Physical Oceanography, vol. 2, A. L. Gordon (ed.), Gordon and Breach, New York, 37-66.

Houghton, R. L., in prep.: The Petrology and Geochemistry of the New England Seamount Chain; Ph.D. thesis, Wood's Hole Oceanographic Institution, Wood's Hole, Massachusetts.

Houtz, R. and J. Ewing, 1964: Sedimentary volocities of the western North Atlantic margin; Bull. Seis. Soc. Am. 54, 867-895.

Houtz, R., J. Ewing and X. LePichon, 1968: Velocity of deep sea sediments from sonobuoy data; Jour. Geophys. Res. 73, 2615-2641.

Hughes, D. J. and C. G. Brown, 1972: Basalts from Madeira: A petrochemical contribution to the genesis of oceanic alkali rock series; Contrib. Mineral. Petrol. 37, 91-109.

IAGA Commission 2, Working Group 4, 1969: International Geomagnetic Reference Field 1965.0; Jour. Geophys. Res. 74, 4407-4408.

Irving, E., and G. Pullaiah, 1976: Reversals of the geomagnetic field, magnetostratigraphy, and relative magnitude of paleosecular variation in the Phanerozoic; Earth Sci. Reviews 12, 35-64.

Jackson, E. D. and H. R. Shaw, 1975: Stress fields in central portions of the Pacific Plate: Delineated in time by linear volcanic chains; Jour. Geophys. Res. 80(14), 1861-1874.

Jackson, H. R., C. E. Keen and M. J. Keen, 1975: Seismic structure of the continental margins and ocean basins of southeastern Canada; Geol. Surv. Can., Paper 74-51, 13 pp.

Jansa, L. F. and J. A. Wade, 1975: Geology of the continental margin off Nova Scotia and Newfoundland; in Offshore Geology of Eastern Canada, vol. 2, W. J. M. van der Linden and J. A. Wade (eds.), Geol. Surv. Can., Paper 74-30, 51-105.

Jansa, L. F., F. M. Gradstein, G. L. Williams, and W. A. M. Jenkins, 1977: Geology of the Amoco Imp. Skelly A-1 Osprey H-84 well, Grand Banks, Newfoundland; Geol. Surv. Can., Paper 77-21, 17 pp.

Jansa, L. F., P. Enos, B. E. Tucholke, F. M. Gradstein and R. E. Sheridan, in press: Mesozoic-Cenozoic sedimentary formations of the North American Basin; western North Atlantic.

Johnson, G. L. and E. D. Schneider, 1969: Depositional ridges in the North Atlantic; Earth and Planet. Sci. Lett. 6, 416-422.

Johnson, G. L., P. R. Vogt, and E. D. Schneider, 1971: Morphology of the Northeastern Atlantic and Labrador Sea; Deut. Hydrog. Zeits. 24, 49-73.

Johnson, H. P. and R. T. Merrill, 1973: Low temperature oxidation of a titanomagnetite and the implications for paleomagnetism; Jour. Geophys. Res. 78, 4938-4949.

Jones, E. J. W., J. I. Ewing, and M. Ewing, 1969: The influence of Norwegian Sea overflow water on sedimentation in the northern North Atlantic and Labrador Sea [abs]; EOS, Trans. Amer. Geophys. Union 50, 198.

Keating, B. H. and C. E. Helsley, 1977: Nature of the "Cretaceous Quiet Interval" [abs]; EOS Trans. Amer. Geophys. Union 58(8), 740.

Keating, B. H. and C. E. Helsley, 1976: Magnetostratigraphy of the Cretaceous, [abs]; Geol. Soc. Amer., Abstracts with Programs 8, 948.

Keating, B. H. and C. E. Helsley, in press: Paleomagnetic results from DSDP Site 391C and the magnetostratigraphy of Cretaceous sediments from the Atlantic Ocean floor; Initial Reports of the Deep Sea Drilling Project 44, U. S. Gov't Printing Office, Washington.

Keating, B. H. and C. E. Helsley, in press: Magnetostratigraphy of Cretaceous sediments from DSDP Site 386; Initial Reports of the Deep Sea Drilling Project 43, U. S. Gov't Printing Office, Washington.

Keating, B. H. and C. E. Helsley, in press: Magnetostratigraphic studies of Cretaceous sediments from DSDP Site 369; Initial Reports of the Deep Sea Drilling Project 41, U. S. Gov't Printing Office, Washington.

Keen, C. E., and B. D. Loncarevic, 1966: Crustal structure on the eastern seaboard of Canada: Studies on the continental margin; Can. Jour. Earth Sci. 3, 65-76.

Keen, C. E., M. J. Keen, D. L. Barrett, and D. E. Heffler, 1975: Some aspects of the ocean-continent transition of the continental margin of eastern North America; in: Offshore Geology of Eastern Canada, W. J. M. van der Linden and J. A. Wade (eds.), Geol. Surv. Can., Paper 74-30, 189-198.

Keen, C. E., B. R. Hall and K. D. Sullivan, 1977: Mesozoic evolution of the Newfoundland Basin; Earth Planet. Sci. Lett. 37, 307-320.

Keen, M. J., 1976: A Sonobuoy Manual, Parts I-V; Unpub. Report, Dalhousie University.

Keen, M. J. and C. E. Keen, 1971: Subsidence and fracturing of the continental margin of eastern Canada; in: Earth Science Symposium on Offshore Eastern Canada, P. J. Hood (ed), Geol. Survey Canada, Paper 71-23, 23-42.

Kempe, D. R. C. and J-G. Schilling, 1974: Discovery Tablemount basalt: Petrology and geochemistry; Contrib. Mineral. Petrol. 44, 101-115.

Kidd, R. G. W., 1977: A model for the process of formation of the upper oceanic crust; Geophys. J. Roy. Astron. Soc. 50, 149-183.

King, L. H. and I. F. Young, 1977: Paleocontinental slopes of East Coast Geosyncline (Canadian Atlantic Margin); Can. Jour. Earth Sci. 14(11), 2553-2564.

König, M. and M. Talwani, 1977: A geophysical study of the southern continental margin of Australia: Great Australian Bight and western sections; Geol. Soc. Amer. Bull. 88, 1000-1014.

Krumsiek, K., 1977: Cretaceous magnetostratigraphy of SW Morocco (abs); Abstr. of the European Geophy. Soc., EOS, Trans. Amer. Geophys. Union 58, 898.

Larson, R. L. and W. C. Pitman III, 1972: World-wide correlation of Mesozoic magnetic anomalies and its implications; Geol. Soc. Amer. Bull. 83, 3645-3662.

Larson, R. L. and T. W. C. Hilde, 1975: A revised time scale of magnetic reversals for the Early Cretaceous and Late Jurassic; Jour. Geophys. Res. 80, 2586-2594.

Laughton, A. S., 1972: The southern Labrador Sea--A key to Mesozoi and Early Tertiary evolution of the North Atlantic; in: Initial

Reports of the Deep Sea Drilling Project, 12, U. S. Gov't Printing Office, Washington, 1155-1179.

Laughton, A. S., 1975: Tectonic evolution of the Northeast Atlantic - A review; Norges Geologiske Undersok. 316, 169-193.

Laughton, A. S., Berggren, W. A. and Scientific Party, 1972: Initial Reports of the Deep Sea Drilling Project 12, U. S. Gov't Printing Office, Washington.

Laughton, A. S. and B. R. Whitmarsh, 1974: The Azores-Gibraltar plate boundary; in Geodynamics of Iceland and the North Atlantic Area, L. Kristjansson (ed.), D. Reidel Publ. Co., Dordrecht, Holland, 63-81.

LeBorgne, E., J.-L. Mouel, and X. LePichon, 1971: Aeromagnetic survey of South-western Europe; Earth Planet. Sci. Lett. 12, 287-299.

Lefort, J.-P. and R. T. Haworth, in press: Geophysical study of basement fractures on the western European and eastern Canadian shelves: Transatlantic correlations and Late Hercynian movements; in preparation.

LePichon, X., J. Ewing and R. Houtz, 1968: Deep-sea sediment velocity determination made while reflection profiling; Jour. Geophys. Res. 73, 2597-2614.

LePichon, X., J. Bonnin, and J.-C. Sibuet, 1970: Le faille nord-pyrénéen: faille transformante liée à l'ouverture du golfe de Gascogne; C. R. Hebd. Seanc. Acad. Sci. Paris 271, 1941-1944.

LePichon, X. and P. J. Fox, 1971: Marginal offsets, fracture zones and the opening of the North Atlantic; Jour. Geophys. Res. 76, 6294-6308.

LePichon, X., and D. E. Hayes, 1971: Marginal offsets, fracture zones and the early opening of the South Atlantic; Jour. Geophys. Res. 76, 6283-6293.

LePichon, X., J. Bonnin, J. Francheteau and J.-C. Sibuet, 1971: Une hypothèse d'évolution tectonique du Golfe de Gascogne; in: Histoire structurale du Golfe de Gascogne, Editions Technip, Paris, 22, VI.11-1 to 11.44.

LePichon, X. and J.-C. Sibuet, 1971: Comments on the evolution of the North-East Atlantic; Nature 233, 257-258.

LePichon, X., J. Francheteau and J. Bonnin, 1973: Plate Tectonics; Elsevier, Amsterdam, 300 pp.

LePichon, X., J.-C. Sibuet, and J. Francheteau, 1977: The fit of the continents around the North Atlantic Ocean; Tectonophysics 38, 169-209.

Lilly, H. D., 1966: Late Precambrian and Appalachian tectonics in the light of submarine exploration of the Grand Banks of Newfoundland and in the Gulf of St. Lawrence. Preliminary views; Am. Jour. Sci. 264, 569-574.

Ludwig, W. J., J. E. Nafe and C. L. Drake, 1970: Seismic refraction; in" The Sea, vol. 4, part 1, E. C. Bullard and A. E. Maxwell (eds.), Wiley-Interscience, New York, 53-84.

Luyendyk, B. P. and E. T. Bunce, 1973: Geophysical study of the northwest African margin off Morocco; Deep-Sea Research 20, 537-549.

Luyendyk, B. P., Cann. J. R. and Scientific Party, 1977: Young and hot drilling; Geotimes 22(3), 25-27.

Mayhew, M. A., C. L. Drake and J. E. Nafe, 1970: Marine geophysical measurements on the continental margins of the Labrador Sea; Can. Jour. Earth Sci. 7, 199-214.

Menard, H. W. and T. Atwater, 1968: Changes in direction of seafloor spreading; Nature 219, 463-467.

Merrill, R. T., 1975: Magnetic effects associated with chemical changes in igneous rocks; Geophysical Surveys 2, 277-311.

Monahan, D. and R. F. McNab, 1975: Macro- and meso-morphology of Flemish Cap, Flemish Pass, and the northeastern Grand Banks of Newfoundland; in; Offshore Geology of Eastern Canada, Vol. 2, J. M. van der Linden and J. A. Wade (eds.), Geol. Survey Canada Paper 74-30, 207-216.

Montadert, L. and E. Winock, 1971: L'histoire structurale du golfe de Gascogne; in: Histoire Structurale du Golfe de Gasgone, Editions Technip, Paris, VI.16-1 to VI.16-18.

Montadert, L., E. Winnock, J.-R. Delteil, and G. Grau, 1974: Continental margins of Galicia-Portugal and Bay of Biscay; in: The Geology of Continental Margins, C. A. Burk and C. L. Drake (eds), Springer-Verlag, New York, 323-342.

Montadert, L., Roberts, D. G. et al., 1976: Glomar Challenger sails on Leg 48; Geotimes 21(12), 19-22.

Montadert, L., D. G. Roberts, G. A. Auffret, W. Bock, P. A. du Peuble, E. A. Hailwood, W. Harrison, H. Kagami, D. N. Lumsden, C. Muller, D. Schnitker, R. W. Thompson, T. L. Thompson and P. P. Timofeev, 1977: Rifting and subsidence on passive continental margins in the North East Atlantic; Nature 268, 305-309.

Morgan, W. J., 1972: Plate motions and deep mantle convection; Geol. Soc. Amer., Memoir 132 (Hess Volume), 7-21.

Mountain, G. and B. E. Tucholke, 1977: Horizon β: Acoustic character and distribution in the western North Atlantic [abs.]; EOS, Trans. Amer. Geophys. Union 58(6), 406.

Nisbet, E. G. and J. A. Pearce, 1977: Clinopyroxene composition in mafic lavas from different tectonic settings; Contrib. Mineral. Petrol. 63, 149-160.

Parker, R. L. and D. W. Oldenburg, 1973: A thermal model for oceanic ridges; Nature 242, 137-139.

Pearce, T. H. and J. R. Cann, 1973: Tectonic setting of basic volcanic rocks determined using trace element analysis; Earth Planet Sci. Lett. 19, 290-300.

Pitman, W. C. III and M. Talwani, 1972: Sea-floor spreading in the North Atlantic; Geol. Soc. Amer. Bull. 83, 619-646.

Press, F. and W. C. Beckmann, 1954: Geophysical investigations of the emerged and submerged Atlantic coastal plain, Part VIII: Grand Banks and adjacent shelves; Geol. Soc. Amer. Bull. 65, 299-313.

Rabinowitz, P. D., The continental margin of the western N. Atlantic Ocean: a geophysical study; Ph.D. thesis (unpublished), Columbia University, New York, 181 pp.

Rabinowitz, P. D., 1974: The boundary between oceanic and continental crust in the western North Atlantic; in Geology of Continental Margins, C. A. Burk and C. L. Drake (eds.), Springer Verlag, New York, 67-83.

Rabinowitz, P. D. and J. L. LaBrecque, 1977: The isostatic gravity anomaly: Key to the evolution of the ocean-continent boundary at passive continental margins; Earth Planet. Sci. Lett. 35, 145-150.

Rabinowitz, P. D., S. C. Cande and D. E. Hayes, in Press: The J-Anomaly in the central North Atlantic Ocean; Initial Reports of the Deep-Sea Drilling Project 43, U. S. Gov't Printing Office, Washington.

Raitt, T. W., 1963: The Crustal Rocks, in: The Sea, 3, M. N. Hill (ed), Interscience, N. Y., 85-100.

Renwick, G. K., 1973: Sea-floor spreading and the evolution of the continental margins of Atlantic Canada; M.Sc. thesis (unpublished) Dalhousie University, Halifax, Nova Scotia, 96 pp.

Rhodes, J. M., 1973: Major and trace element chemistry of basalts from Leg 9 of Deep Sea Drilling Project (abs); EOS Trans. Am. Geophys. Union 54, 1014-1015.

Riddihough, R. P. and M. D. Max, 1976: A geological framework for the continental margin to the west of Ireland; Geol. Jour. 11, 109-120.

Ridley, W. I., J. M. Rhodes, A. M. Reid, P. Jakes, C. Shih, and M. N. Bass, 1974: Basalts from Leg 6 of the Deep Sea Drilling Project; Jour. Pet. 15, Part 1, 140-159.

Roberts, D. G., 1974: Structural development of the British Isles, the continental margin and the Rockall Plateau; in: The Geology of Continental Margins, C. A. Burk and C. L. Drake (eds), Springer Verlag, New York, 343-358.

Roberts, D. G., 1975: Marine geology of the Rockall Plateau and Trough; Phil. Trans. Roy. Soc. London 278, Ser. A., 447-509.

Ryall, P. J. C., J. M. Hall, J. Clark, and T. Milligan, 1977: Magnetization of oceanic crustal layer 2--results and thoughts after DSDP Leg 37; Can. Jour. Earth Sci. 14, 684-706.

Ryan, W. B. F., Sibuet, J. C. and Scientific Party, 1976: Drilling into passive continental margin; Geotimes 21(10), 21-24.

Ryan, W. B. F. and U. von Rad, 1976: Passive continental margin; Geotimes 21(10), 21-24.

Schilling, J.-G., 1971: Seafloor evolution: Rare earth evidence; Phil. Trans. Roy. Soc. London 268, Ser. A., 663-706.

Schilling, J.-G., 1973: Iceland mantle plume: Geochemical study of Reykjanes Ridge; Nature 242, 565-571.

Schneider, E. D., P. J. Fox, C. D. Hollister, N. D. Needham, and B. C. Heezen, 1967: Further evidence of bottom currents in the western North Atlantic; Earth Planet. Sci. Lett. 2, 351-359.

Scientific Party, Leg 37, 1975: Sources of magnetic anomalies on the Mid-Atlantic Ridge; Nature 255, 389-390.

Sclater, J. G., L. A. Lawver, and B. Parsons, 1975: Comparison of long-wavelength residual elevation and gravity anomalies in the North Atlantic and possible implications for the thickness of the lithospheric plate; Jour. Geophys. Res. 801 ;031-1052.

Scrutton, R. A., 1976: Crustal structure at the continental margin south of S. Africa; Geophys. Jour. Roy. Astron. Soc. 44, 601-623.

Seidemann, D. E., 1976: K-Ar and Ar^{40}/Ar^{39} dating of deep sea rocks; Ph.D. thesis (unpubl.), Yale University, New Haven, Connecticut.

Sen Gupta, B. K. and A. C. Grant, 1971: Orbitulina, a Cretaceous large foraminifera from Flemish Cap: Paleo-oceanographic implications; Science 173, 934-936.

Shaw, H. R. and E. D. Jackson, 1973: Linear island chains in the Pacific: result of thermal plumes or gravitational anchors?; Jour. Geophys. Res., 78, 8634-8652.

Sheridan, R. E. and C. L. Drake, 1968: Seaward extension of the Canadian Appalachians; Can. Jour. Earth Sci., 5, 337-373.

Sleep, N. H., 1971: Thermal effects of the formation of Atlantic continental margins by continental break-up; Geophys. Jour. Roy. Astron. Soc. 24, 325-350.

Srivastava, S. P., 1977: Goodness of fit of IGRF to the high-density magnetic survey data in the offshore regions of eastern Canada [abs]; EOS, Trans. Amer. Geophys. Union 58(8), 748.

Srivastava, S. P., 1978: Evolution of the Labrador Sea and its bearing on the early evolution of the North Atlantic; Geophys. Jour. Roy. Astron. Soc.

Stow, D. A. V., 1977: Late Quaternary stratigraphy and sedimentation on the Nova Scotian outer continental margin; Ph.D. thesis (unpubl.), Dalhousie University, Halifax, Nova Scotia, 360 pp.

Stukas, V., 1977: Plagioclase release patterns: A high-resolution ^{40}Ar-^{39}Ar study; Ph.D. thesis (unpubl), Dalhousie University, Halifax, Nova Scotia, 160 pp.

Sullivan, K. D. and C. E. Keen, 1977: Newfoundland Seamounts: Petrology and Geochemistry; in: Volcanic Regimes of Canada, W. R. A. Baragar, L. C. Coleman and J. M. Hall (eds.), Geol. Assoc. Canada, Special Paper 16, 461-476.

Talwani, M. and O. Eldholm, 1972: Continental margin off Norway: A geophysical study; Geol. Soc. Amer. Bull. 83, 3575-3606.

Talwani, M. and O. Eldholm, 1973: The boundary between continental and oceanic crust at the margins of rifted continents; Nature 241, 325-330.

Tucholke, B. E. and G. Mountain, 1977: The Horizon-A Complex: Lithostratigraphic correlation and paleoceanographic significance of reflectors in the western North Atlantic (abs); EOS, Trans. Amer. Geophys. Union 58, 406.

Tucholke, B., P. R. Vogt and Scientific Party, 1975: Glomar Challenger drills in the North Atlantic; Geotimes 20, 18-21.

Turner, G., and P. H. Cadogan, 1974: Possible effects of ^{39}Ar recoil in ^{40}Ar-^{39}Ar dating; Proc. Fifth Lunar Sci. Conf., Geochim. Cosmochim. Acta, Suppl. 5, Vol. 2, 1601-1615.

Uchupi, E., 1971: Bathymetric Atlas of the Atlantic, Caribbean, and Gulf of Mexico; Wood's Hole Oceanogr. Inst., Ref. 71-72.

Vallance, T. G., 1974: Spilitic degradation of a tholeiitic basalt; Jour. Petrol. 15, 79-96.

Vogt, P. R., 1971: Episodes of seafloor spreading recorded by the North Atlantic basement; Tectonophysics 12, 211-234.

Vogt, P. R., 1974: Volcano height and plate thickness; Earth Planet. Sci. Lett. 23, 337-348.

Vogt, P. R. and G. L. Johnson, 1971: Cretaceous seafloor spreading in the western North Atlantic; Nature 234, 22-25.

Walcott, R. I., 1976: Lithospheric flexure, analysis of gravity anomalies and the propagation of seamount chains; in: The Geophysics of the Pacific Ocean Basin and its Margin, G. H. Sutton, M. H. Manghnani and R. Moberly (eds), Amer. Geophys. Union Monogr. 19, 431-438.

Watson, J. A. and G. L. Johnson, 1970: Seismic studies in the region adjacent to the Grand Banks of Newfoundland; Can. Jour. Earth Sci. 7, 306-316.

Wegener, A., 1924: The Origin of Continents and Oceans; transl. of 4th (1929) edition, Methuen and Co., Ltd., London, 248 pp.

Williams, C. A., 1975: Seafloor spreading in the Bay of Biscay and its relationship to the North Atlantic; Earth Planet. Sci. Lett. 24, 440-456.

Williams, C. A. and D. P. McKenzie, 1971: The evolution of the North-East Atlantic; Nature 232, 168-173.

Williams, H., 1964: The Appalachians in northeastern Newfoundland: A two-sided symmetrical system; Am. J. Sci. 262, 1137-1158.

Williams, H., M. J. Kennedy, and E. R. W. Neale, 1972: The Appalachian structural province; in: Variations in Tectonic Styles in Canada, R. A. Price and R. J. W. Douglas (eds.), Geol. Assoc. Canada, Spec. Paper 11, 181-262.

Wilson, J. T , 1963: A possible origin of the Hawaiian Islands; Can. J. Phys. 41, 863-870.

Wilson, J. T., 1963: Evidence from islands on the spreading of the ocean floors; Nature 197, 536-538.

Wilson, R. C. L., 1975: Atlantic opening and Mesozoic continental margin basins of Iberia; Earth Planet. Sci. Lett. 25, 33-43.

Woollard, G. P., 1969: Regional variations in gravity; in: The Earth's Crust and Upper Mantle, P. J. Hart (ed), Amer. Geophys. Union Monogr. 13, 320-340.

Yoder, H. S. Jr., 1976: Generation of Basaltic Magma; Nat'l. Acad. Sciences, Washington, D. C., 265 pp.

Zielinski, R. A., 1975: Trace element evaluation of a suite of rocks from Réunion Island, Indian Ocean; Geochim. Cosmochim. Acta 39, 713-734.

APPENDIX I: MAGNETIC HEADING CORRECTIONS, MK76-031

The magnetometer sensors carried on this cruise were found to have serious leakage problems and seemed to operate only when towed about 70 m astern of the ship. This proximity of the ship and the sensor introduces a variation in the measured total field values that is dependent upon the ship's heading. It is not necessary to correct for this error if one is interested in relative anomaly amplitudes along tracks of constant azimuth (as in Section 5.2), or if one wishes to model long, constant-azimuth profiles (in which case the anomalies are visually adjusted to a zero-mean).

This appendix describes the procedure followed in measuring the azimuthal variation on board ship and in subsequent calculation of the heading correction (following Bullard and Mason, 1961).

The following procedure was followed in measuring the heading effect at sea: An unanchored marker buoy was laid in calm water (less than 5 kts of wind) just south of Sable Island on Day 288. The ship steamed past this marker on nine different courses, first with the magnetometer cable at its short (70 m) length and then at its full (150 m) length. Course changes, log mileage and magnetic field values were recorded at both ends of each track and at each passage of the buoy.

The measured total field with long and short cables are plotted as a function of azimuth in Figure I.1. The short cable gives an approximately cosine-form variation with 50 nT peak-to-peak amplitude.

The method used to calculate the correction for this error follows Bullard & Mason (1961). The azimuthal variation can be expressed as:

$$F(\theta) = a_0 + a_1 \cos \theta + a_2 \cos 2\theta + a_3 \sin \theta + a_4 \sin 2\theta$$

where $F(\theta)$ is the magnetic field as a function of azimuth (θ), a_0 is the mean value of $F(\theta)$ and a_1, a_2, a_3, a_4 are constants.

Fourier analysis of the coefficients gave:

$a_1 = -19.42$

$a_2 = 10.92$

$a_3 = 5.10$

$a_4 = -1.72$

The value of a_0 was determined by taking the difference between an arbitrarily-defined zero value and the mean value of $F(\theta)$. Several trials showed that setting 54170 nT = 0 gave the best fit to the observations (Fig. I.2).

The heading correction Δ is given as the difference between the true total field at the buoy (F_T) and the calculated cosine curve ($F(\theta)_c$). Representative values are given in Table I.1.

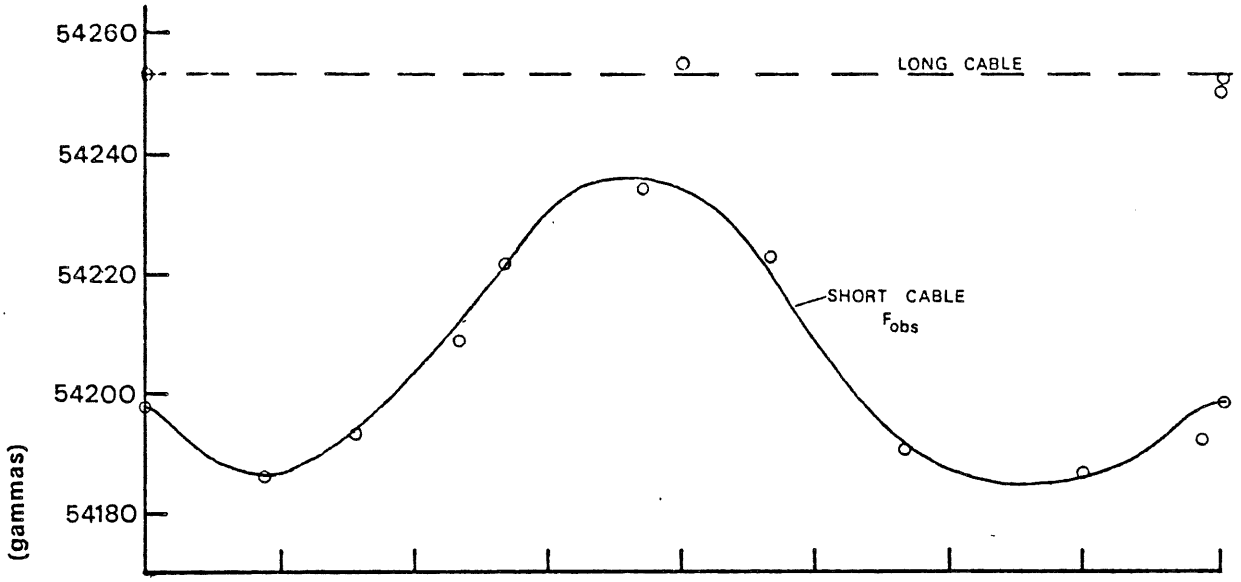

Figure II.1

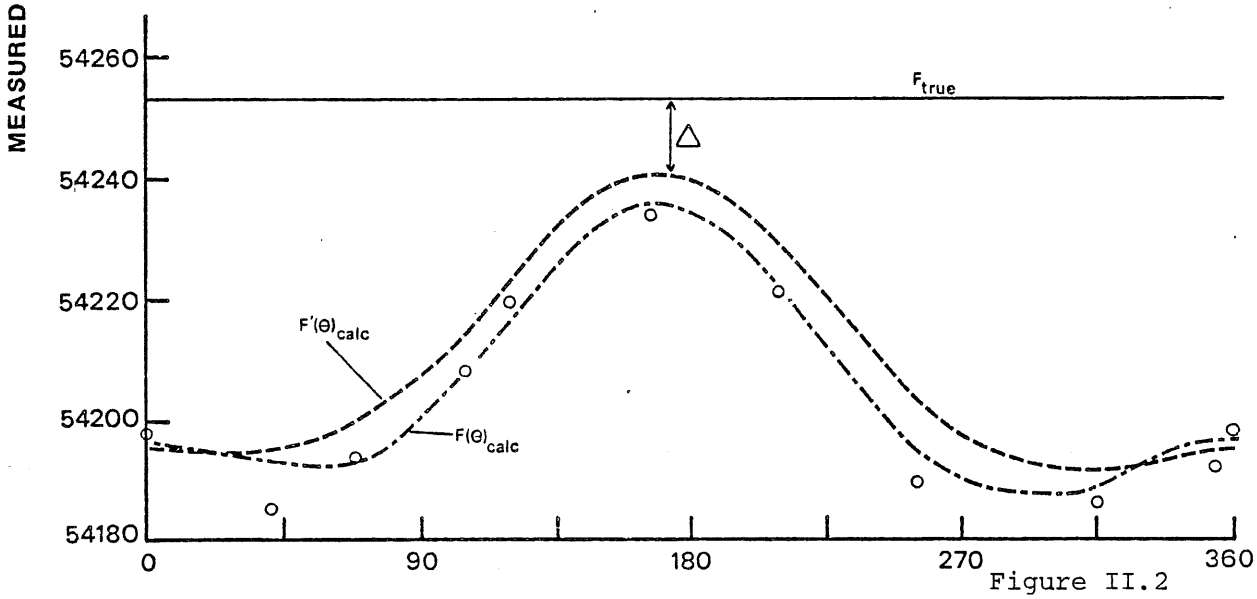

Figure II.2

Observed and calculated magnetic field variations as functions of ship's heading.

TABLE I.1

HEADING CORRECTIONS

HEADING (deg)	CORRECTION (nT)
030	58.3
060	60.2
090	53.8
120	37.8
150	21.7
180	17.7
210	29.8
240	49.7
270	64.0
300	66.1
330	60.4
360	56.5

APPENDIX II:

Petrographic and Geochemical Data: Newfoundland Seamounts

To date four of the Newfoundland Seamounts have been sampled (Table II.1). Scruncheon and Dipper Seamounts were dredged in 1974 (cruise 74-021) and Screech and Shredder Seamounts were dredged in 1975 (cruise 75-009). All in situ material, including manganese slabs and nodules and sedimentary rocks, have been catalogued; samples and complete descriptions are available from Bedford Institute of Oceanography, Dartmouth, Nova Scotia.

Thirty-eight samples (basalts and trachytes) were selected from the dredge collection for geochemical analysis. Major and trace element data are given in Table II.2, rare-earth data in Table II.3 and Figure II.1, and mineral phase chemistry in Table II.4 and Figure II.2; analytical methods and errors are given in Tables II.5 and II.6. A generalized petrographic description was given in Chapter 7; the photomicrographs in Figure II.3 illustrate the state of alteration of representative analyzed samples.

A reconaissance study of rock magnetic and magnetic mineral properties was also undertaken. The data in Table II.7 and the photomicrographs in Figure II.4 show that the seamount basalts contain highly cation-deficient titanomagnetites which display mineralogic and magnetic properties typical of advanced submarine alteration at low temperatures (probably 100°C).

TABLE II.1: DREDGE STATION DATA

II.1a DREDGE STATIONS, HU 74-021

STN. NO.	SEAMOUNT	N. LAT.	W. LONG.	RECOVERY
25	Scruncheon	43°42'	45°26'	80% granitic and gneissic erratics; 20% weathered plag. basalts and trachytes. Max. MnO_2 ca. 2 mm. Fe-Mn blocks to 20 cm; Fe rich sed.-volc. breccia.
26	Scruncheon	43°42'	45°26'	98% erratics; five small (11-15 cm) pieces basalt with MnO_2 1 mm.
30	Dipper	43°26'	45°15'	35% erratics; up to 17cm pillow fragments with MnO_2 to 4 mm; Fe-Mn blocks to 50 cm max. dimension.
31	Dipper	43°27'	45°15'	60% erratics; 2 large slabs Fe-Mn pavemt., 30 cm thick, ca. 80 cm long; ca. 50 chunks basalt (to 20 cm) with $MnO_2 \leq$ 1 mm; 2 trachytes.

II.1b DREDGE STATIONS, HU 75-009

103	Screech	44°06'	46°48'	glacial erratics (95%); MnO_2 nodules and crusts; volcanogenic sediments; cobbles of altered basalt.
104	Screech	44°07'	46°47'	glacial erratics
105	Screech	44°07'	46°47'	glacial erratics (98%); volcanogenic sediments; cobbles of altered basalts with white veins (calcite according to XRD).
106	Shredder	43°44'	43°47'	glacial erratics (95%); MnO_2 crusts and nodules
110	Shredder	43°51'	43°43'	glacial erratics (80%); MnO crusts; volcanogenic sediments; large slab 70cm x 50cm x 15cm coarse calcareous-volcanic conglomerate with graded bed imbricate bedding.

TABLE II.2 MAJOR ELEMENTS

SCRUNCHEON SEAMOUNT

	25/1	25/2	25/3	25/4	25/15	25/9	25/11	25/19	25/20	25/26	25/29	25/32	26/1
SiO_2	61.98	61.16	61.23	60.38	56.02	49.53	44.89	47.45	46.65	46.39	45.66	45.54	43.82
TiO_2	.54	.54	.55	0.54	0.49	3.11	3.27	3.82	3.28	2.68	3.31	3.35	3.48
Al_2O_3	19.28	19.28	18.46	18.32	16.14	16.55	14.69	15.45	14.79	12.36	15.50	14.57	14.26
Fe_2O	2.94	2.43	2.88	3.87	1.98	9.81	15.30	13.89	9.85	13.97	12.67	12.47	17.34
FeO	0.00	.46	0.00	0.20	0.31	0.58	0.94	.79	.21	0.00	0.98	0.84	.20
MnO	.09	.08	.14	0.12	0.08	0.29	0.09	.16	.16	0.18	0.12	0.10	.42
MgO	1.17	1.21	1.12	1.08	0.32	1.62	2.39	1.74	1.73	3.40	1.95	2.46	1.66
CaO	.93	1.06	1.01	1.10	7.83	3.84	3.86	3.10	4.95	0.69	3.65	3.17	4.50
Na_2O	6.70	6.78	6.52	6.80	6.37	3.34	2.37	2.90	2.39	1.45	2.36	1.97	2.65
K_2O	2.59	2.37	2.41	2.61	4.13	3.55	3.67	3.42	4.87	4.31	3.54	4.52	3.76
P_2O_5	.08	.08	.09	0.09	4.53	1.09	1.24	.32	2.63	0.36	0.86	1.36	1.46
CO_2	.02	.08	0.00	0.00	0.51	0.04	0.09	.12	.30	0.04	0.05	0.05	.56
H_2O^T	4.60	4.59	4.96	5.73	1.72	6.31	8.92	7.50	7.71	15.45	9.04	9.77	5.36
TOTAL	100.92	100.09	99.37	100.84	100.43	100.66	99.72	100.56	99.52	101.28	100.69	100.27	99.47

DIPPER SEAMOUNT

	30/1	30/2	30/5	30/11	31/2	31/4	31/5	31/6	31/14	31/17	31/21	31/25
SiO_2	48.60	50.10	47.78	52.21	50.39	51.11	50.34	49.55	52.26	52.49	50.84	48.33
TiO_2	2.43	3.43	2.78	3.32	2.90	1.87	2.87	2.93	2.08	3.46	2.91	1.92
Al_2O_3	17.21	18.70	16.90	19.29	19.97	18.25	18.86	20.09	20.38	19.84	19.52	19.60
Fe_2O	9.43	7.24	9.90	6.94	6.48	7.82	6.01	6.99	8.16	7.13	7.25	8.91
FeO	0.19	1.05	0.54	.69	1.08	1.11	0.99	0.69	0.00	.68	0.82	0.54
MnO	0.49	.19	0.36	.09	0.11	0.11	0.06	0.27	.24	.08	0.12	0.31
MgO	1.50	1.19	1.66	1.09	1.11	1.16	1.05	1.09	1.11	1.18	1.02	1.24
CaO	4.71	3.97	3.79	4.00	4.16	5.15	3.81	4.05	4.17	3.91	4.04	4.52
Na_2O	3.02	3.79	2.99	3.95	3.97	4.65	3.41	3.85	4.01	3.50	3.73	4.14
K_2O	3.85	3.87	3.69	3.90	3.04	2.51	3.68	3.16	3.04	3.43	3.80	1.96
P_2O_5	1.33	.96	1.08	0.00	0.59	1.44	0.76	0.67	.68	.70	0.77	0.87
CO_2	0.12	.10	0.06	.02	0.00	0.05	0.00	0.00	0.00	.07	0.00	0.00
H_2O^T	7.62	4.94	8.18	5.01	6.60	4.22	6.27	6.14	4.53	4.41	5.46	6.88
TOTAL	100.50	99.53	99.71	100.51	100.40	99.95	98.11	99.48	100.66	100.88	100.28	99.22

TABLE II.2 TRACE ELEMENTS

SCRUNCHEON AND DIPPER SEAMOUNTS

SCRUNCHEON SEAMOUNT

	25/1	25/2	25/3	25/4	25/9	25/11	25/15	25/19	25/20	25/26	25/29	25/32	26/1
Rb	20	19	20	17	36	59	45	65	80	100	40	71	48
Sr	170	209	185	201	346	306	329	309	230	46	309	288	269
Ba	1258	1178	1180	1130	370	245	1073	293	441	150	239	193	312
Ni	36	36	38	45	39	45	30	55	49	77	59	55	53
Cr	5	5	2	3	11	17	5	19	13	28	27	17	23
Zr	522	586	503	440	237	138	492	164	244	119	139	139	148
Y	39	50	nd	52	102	40	187	40	147	nd	43	64	28
Nb	119	121	122	122	59	37	119	32	nd	32	29	35	35
Cu	34	36	28	32	30	51	14	46	41	100	50	106	80
Zn	225	229	228	209	169	205	105	177	210	162	165	179	151

DIPPER SEAMOUNT

	30/1	30/2	30/5	30/11	31/2	31/4	31/5	31/6	31/14	31/17	31/21	31/25
Rb	40	50	46	40	31	19	35	26	34	47	34	23
Sr	311	330	309	364	331	463	373	365	485	387	484	578
Ba	437	410	512	369	430	445	381	328	618	370	308	474
Ni	88	55	70	35	67	32	45	76	26	58	69	55
Cr	21	29	23	30	82	14	44	46	10	38	34	9
Zr	168	230	167	212	188	328	203	202	408	240	211	386
Y	51	49	53	39	49	49	61	58	56	78	75	59
Nb	43	50	41	47	47	71	55	46	81	42	48	81
Cu	111	97	101	58	98	16	71	103	10	110	78	52
Zn	176	152	142	185	130	159	140	139	128	148	154	174

TABLE II.2 MAJOR AND TRACE ELEMENTS

	SCREECH SEAMOUNT								SHREDDER SEAMOUNT				
	103/1 core	103/1* outer	103/2 outer	103/4	103/5	105/2*	105/3	105/4	106/1	106/2*	106/3	106/4*	106/5
SiO_2	50.03	47.45	46.56	46.76	48.56	54.16	45.35	48.35	43.04	42.74	43.37	44.29	42.38
TiO_2	2.77	2.63	2.54	2.68	3.08	1.69	3.28	3.36	2.66	2.54	2.60	2.37	0.68
Al_2O_3	16.72	14.47	13.74	13.77	15.25	18.99	18.33	16.71	18.17	17.84	18.11	16.20	8.92
Fe_2O_3	9.73	13.40	12.31	12.57	9.46	6.33	11.76	10.20	13.41	13.94	13.46	12.49	7.64
FeO	0.31	0.24	0.31	0.18	0.20	0.40	0.34	0.88	0.40	0.59	0.34	2.06	5.54
MnO	0.03	0.03	0.02	0.05	0.03	0.08	0.03	0.02	0.15	0.17	0.19	0.21	0.56
MgO	1.39	1.59	1.95	1.88	1.60	0.63	1.16	1.92	2.47	2.53	2.47	3.78	5.46
CaO	1.55	1.77	1.98	1.14	1.42	1.37	1.25	0.41	1.57	2.27	1.46	4.96	12.67
Na_2O	2.51	2.15	1.73	1.75	2.29	3.08	2.07	2.36	2.32	2.17	2.18	2.53	1.51
K_2O	5.41	5.64	5.77	5.66	5.24	7.10	4.83	5.02	3.94	3.70	3.98	2.81	1.15
P_2O_5	0.63	0.62	0.49	0.56	0.62	0.61	0.80	0.10	0.47	0.46	0.64	0.46	0.49
CO_2	0.02	0.32	0.82	0.06	0.08	0.02	0.06	0.02	0.05	0.13	0.09	0.08	14.31
H_2O^T	8.82	8.16	10.66	12.84	11.99	4.90	10.24	11.06	10.03	9.29	10.55	6.79	5.31
TOTAL	99.92	98.47	98.88	99.90	99.84	99.36	99.50	100.40	98.68	98.54	99.43	99.02	101.18

* = average of 2 analyses

Rb	71	76	73	65	71	50	62	78	64	58	61	nd	31
Sr	253	188	147	168	199	626	327	163	231	201	324	nd	382
Ba	639	538	537	1154	512	697	550	553	271	249	307	nd	228
Cr	712	622	542	470	280	nd	28	47	32	nd	45	nd	95
Zr	216	191	188	191	175	322	370	382	164	162	167	nd	87
Nb	76	71	71	68	59	170	87	112	24	nd	28	nd	nd
Zn	103	121	95	104	96	129	173	51	175	172	180	nd	54

TABLE II.3: RARE EARTH ELEMENT ABUNDANCES

	La	Ce	Sm	Eu	Tb	Yb	Lu
SCRUNCHEON SEAMOUNT							
25/1a	121	--	9	3	2	3	.6
25/4	106	--	10	4	2	3	.4
25/5	113	--	11	3	2	10	2
25/9	43	--	11	4	2	4	.6
25/11	51	--	11	3	1	5	.7
25/23	76	84	16	4	2	5	1
25/26	9	11	3	1	4	1	.2
25/32	41	--	8	2	1	3	.3
DIPPER SEAMOUNT							
30/1	52	90	11	3	2	4	1
30/11	29	61	7	2	1	2	.3
31/6	28	43	8	2	1	2	.4
31/25	84	163	17	5	2	5	.9
SCREECH SEAMOUNT							
103/1	54	88	10	3	1	2	.4
103/1	44	77	8	2	1	1	.3
103/2	41	90	12	3	2	3	.3
103/4	44	90	11	3	2	2	.4
105/2	76	134	10	3	1	2	.3
105/4	15	37	3	1	< .1	1	.1
SHREDDER SEAMOUNT							
106/1	30	34	8	2	2	4	.6
106/2	25	33	8	2	2	3	.6
106/5	12	33	7	3	1	3	.4

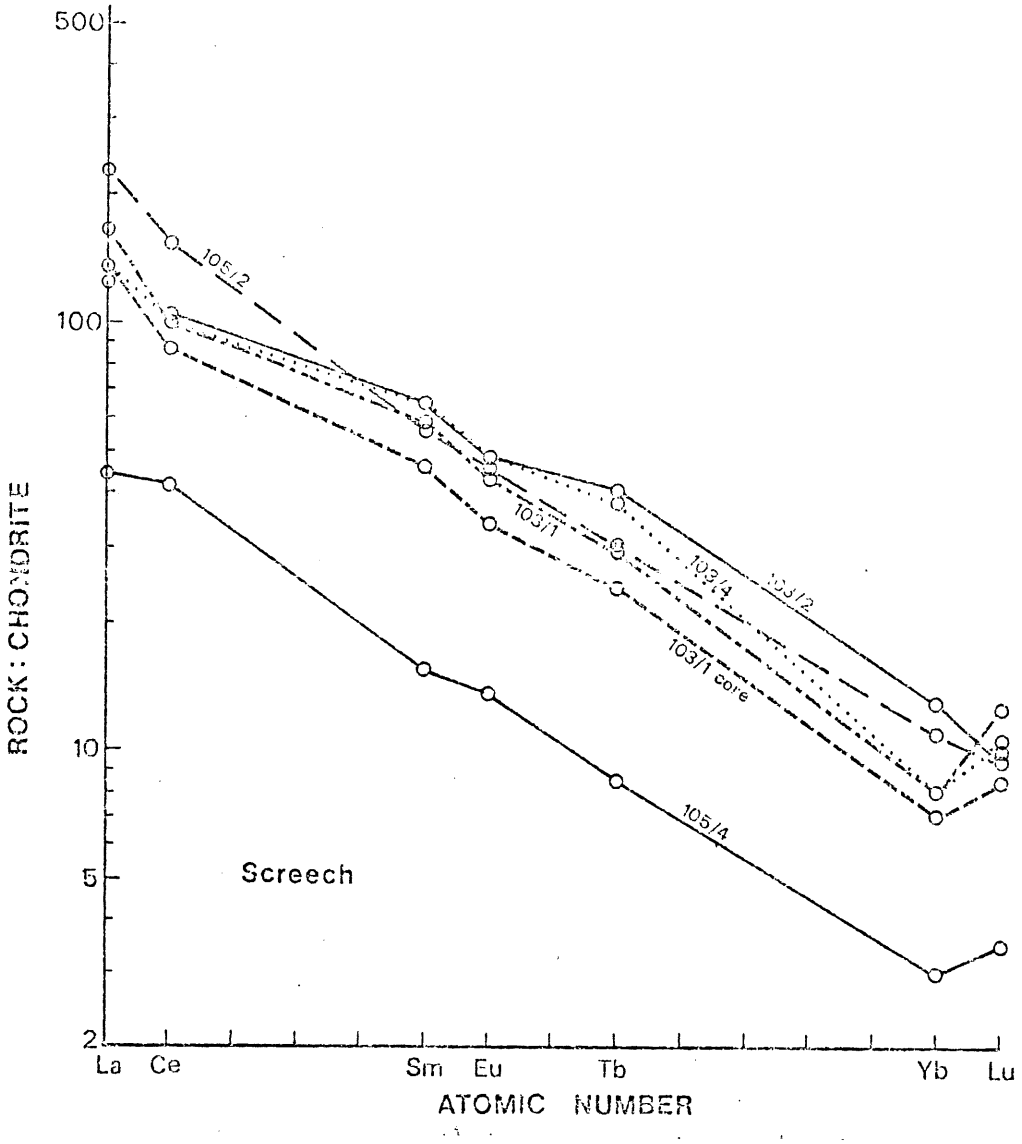

Figure II.1a
Chondrite-normalized rare-earth abundances.

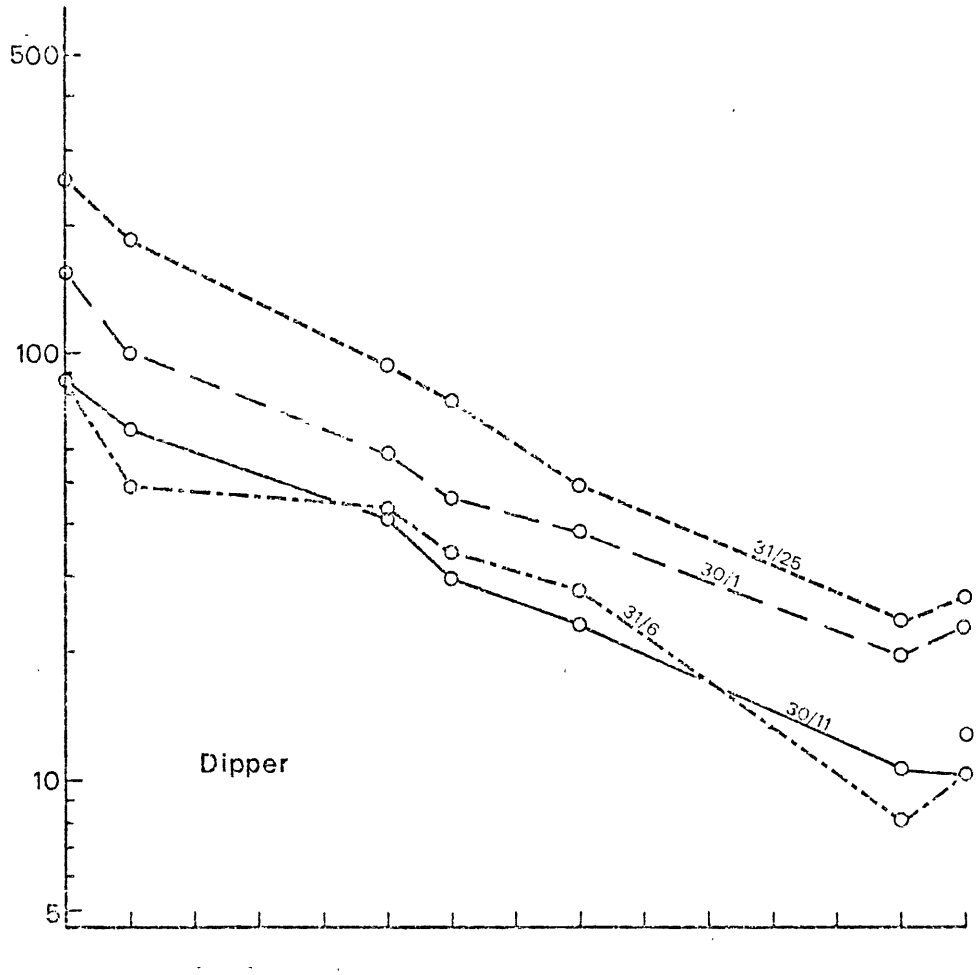

Figure II.1b

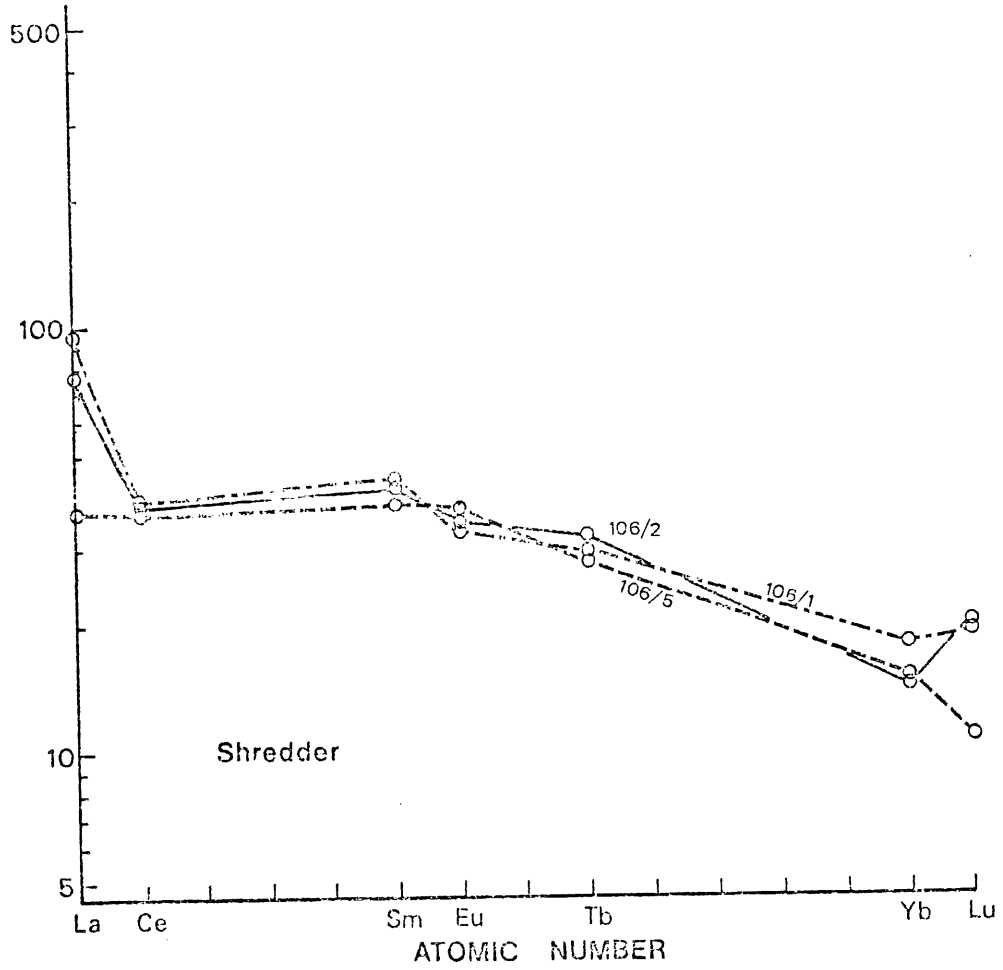
500
100
10
5
106/2
106/5
106/1
Shredder
La
Ce
Sm
Eu
Tb
Yb
Lu
ATOMIC NUMBER

Figure II.1c

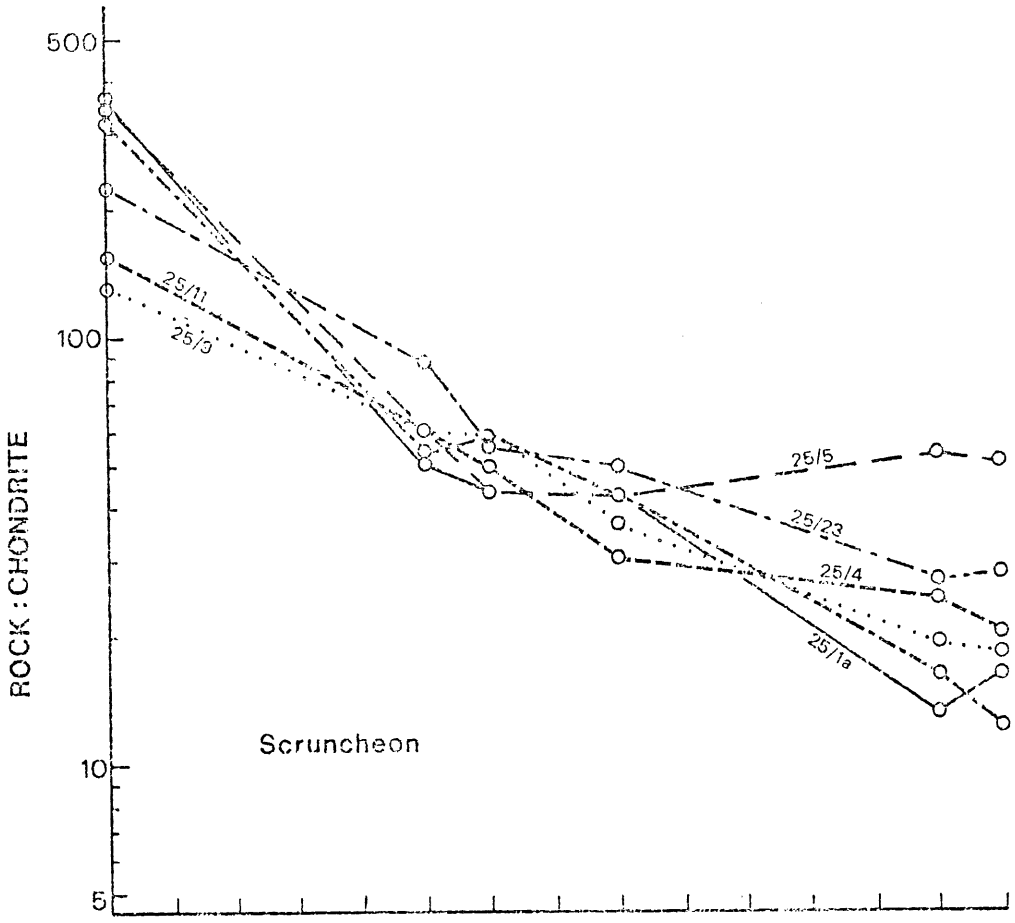
500
100
10
5
ROCK : CHONDRITE
25/11
25/3
25/5
25/23
25/4
25/1a
Scruncheon

Figure II.1d

TABLE II.4 MICROPROBE DATA

A. DIPPER SEAMOUNT PYROXENES

	31/2	31/13A	31/11A	31/13B	30/1	31/6	31/25A	31/25B
SiO_2	47.68	48.82	49.42	50.05	50.63	49.52	51.27	51.29
TiO_2	2.16	1.37	1.36	.81	1.05	1.24	1.11	1.13
Al_2O_3	5.48	6.31	5.89	5.78	3.84	6.26	2.61	2.30
Cr_2O_3	.04	.47	.31	2.04	.04	nd	.02	.04
FeO*	8.21	5.48	5.41	4.35	7.89	5.19	7.74	7.65
MnO	.20	.11	.15	.13	.22	.12	nd	nd
MgO	13.45	14.72	14.93	15.76	16.13	14.98	15.36	15.38
CaO	21.81	22.44	22.38	21.40	19.25	22.42	21.34	21.40
Na_2O	.48	.34	.34	.39	.46	.34	.42	.37
K_2O	.02	.03	.04	.03	.04	.04	.03	.04
TOTAL	99.53	100.09	100.23	100.74	99.55	100.11	99.90	99.60
WO	46.47	47.55	47.24	45.80	40.23	47.39	43.77	43.88
EN	39.87	43.39	43.84	46.93	46.90	44.05	43.83	43.87
FS	13.66	9.06	8.91	7.27	12.87	8.56	12.39	12.24

* Total Iron as FeO

TABLE II.4 (continued)

B. SHREDDER SEAMOUNT PYROXENES

	PYX 2	PYX 3	PYX 4	PYX 5	PYX 6	PYX 7
SiO_2	51.87	48.19	48.54	50.18	49.84	52.28
TiO_2	0.32	1.60	1.67	1.22	1.21	0.57
Al_2O_3	1.86	4.78	5.40	3.89	4.03	1.94
FeO*	7.05	9.52	9.89	8.81	8.75	9.25
MnO	0.00	0.00	0.00	0.00	0.00	0.00
MgO	16.61	13.84	14.02	15.01	15.00	17.07
CaO	21.34	21.27	21.06	20.93	21.64	19.60
Na_2O	0.00	0.00	0.00	0.00	0.00	0.00
K_2O	0.00	0.00	0.00	0.00	0.00	0.00
TOTAL	99.05	99.20	100.58	100.04	100.47	100.71
WO	47.72	44.35	43.62	42.99	43.98	38.76
EN	46.26	40.15	40.40	42.89	42.29	46.96
FS	11.02	15.50	15.99	14.12	13.84	14.28

* Total Iron as FeO

TABLE II.4 (continued)

C. FELDSPAR COMPOSITIONS

	SCRUNCHEON SEAMOUNT TRACHYTE 25/1				DIPPER SEAMOUNT BASALTS				
	1 RIM	1 CORE	2 GROUND-MASS	3 GROUND-MASS	31/6 A	31/6 B	31/11A A CORE	31/11A A RIM	31/11B B
SiO_2	64.48	61.21	69.53	62.70	51.38	57.44	48.79	50.31	52.53
TiO_2	.09	.12	.16	.09	.18	.19	.13	.17	.12
Al_2O_3	21.90	24.49	19.68	73.10	29.53	28.65	31.82	30.43	29.50
FeO	.31	.36	.67	.33	.72	.70	.70	.67	.44
MgO	.04	.04	.07	.04	.15	.13	.11	.13	.15
CaO	3.63	6.68	1.19	4.98	13.98	14.27	15.94	14.47	13.14
Na_2O	6.11	6.99	2.04	8.22	3.58	4.03	2.66	3.37	4.26
K_2O	.93	.50	2.67	.67	.19	.25	.13	.17	.09
TOTAL	97.52*	100.39	96.02*	100.13	99.69	99.64	100.28	97.72*	100.23
OR	7.22	2.99	39.43	3.86	1.09	1.36	.74	.97	-
AB	67.85	63.48	45.80	72.02	31.32	33.36	23.02	29.36	-
AN	22.93	33.53	19.76	24.11	67.59	65.28	76.24	69.67	-

* Sample penetrated by electron beam

Table II.4, continued

C. FELDSPAR COMPOSITIONS

	SCREECH SEAMOUNT BASALT 105/2			SHREDDER SEAMOUNT BASALT 106/4		
	1	2	3	1	2	3
SiO_2	64.08	64.90	64.33	62.59	54.78	65.79
TiO_2	0.00	0.00	0.00	0.00	0.00	0.00
Al_2O_3	18.22	17.73	18.18	20.73	27.67	19.46
FeO*	0.00	0.00	0.00	0.00	0.88	1.55
MnO	0.00	0.00	0.00	0.00	0.00	0.00
MgO	0.00	0.00	0.00	0.00	0.00	0.00
CaO	0.00	0.00	0.00	4.11	11.69	1.52
Na_2O	0.00	0.00	0.00	7.47	4.54	9.05
K_2O	17.05	16.55	0.00	1.64	0.09	1.78
TOTAL	99.35	99.18	99.41	99.93	99.65	99.15
OR	100.00	100.00	100.00	9.97	0.54	10.59
AB	0.00	0.00	0.00	69.04	41.05	81.82
AN	0.00	0.00	0.00	20.99	58.41	7.59

Table II.4, continued

D. OPAQUE MINERAL AND CLAY COMPOSITIONS

OPAQUE MINERALS
SCREECH SEAMOUNT

	1	2	3	4	5
SiO_2	0.00	0.00	0.95	0.42	0.00
TiO_2	22.43	23.57	17.72	23.40	17.55
Al_2O_3	1.59	1.73	2.57	1.96	6.04
FeO*	62.03	63.93	65.00	62.34	70.30
MnO	0.29	0.38	0.23	0.35	0.04
MgO	2.61	3.02	2.19	2.81	6.46
CaO	0.00	0.00	0.74	0.00	0.00
TOTAL	89.72	92.63	89.39	91.28	100.40

CLAYS

	SHREDDER SEAMOUNT			SCREECH SEAMOUNT		
	1	2	3	1	2	3
SiO_2	42.80	48.10	50.93	46.70	49.90	48.35
TiO_2	0.42	0.00	0.00	0.23	0.00	0.00
Al_2O_3	10.77	7.21	25.59	14.25	18.43	7.01
FeO*	28.52	27.42	7.26	20.31	10.75	28.35
MnO	0.00	0.00	0.00	0.00	0.00	0.00
MgO	3.15	2.27	1.92	1.02	2.20	2.79
CaO	0.00	0.00	0.00	0.00	0.00	0.00
Na_2O	0.00	0.00	0.00	0.00	0.00	0.00
K_2O	1.65	6.05	4.04	2.88	1.83	6.67
TOTAL	87.37	91.05	89.75	85.39	83.10	93.17

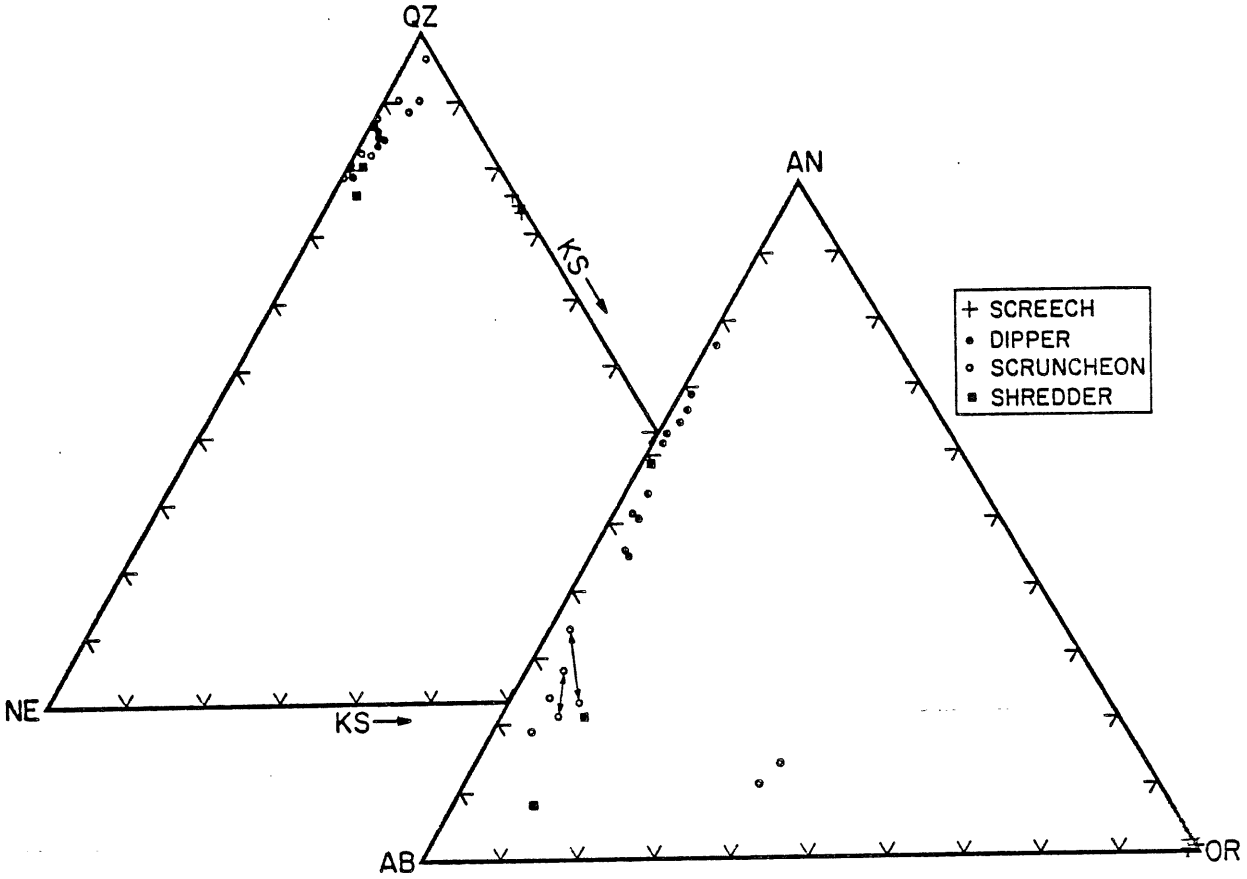

Figure II.2a: Feldspar compositions

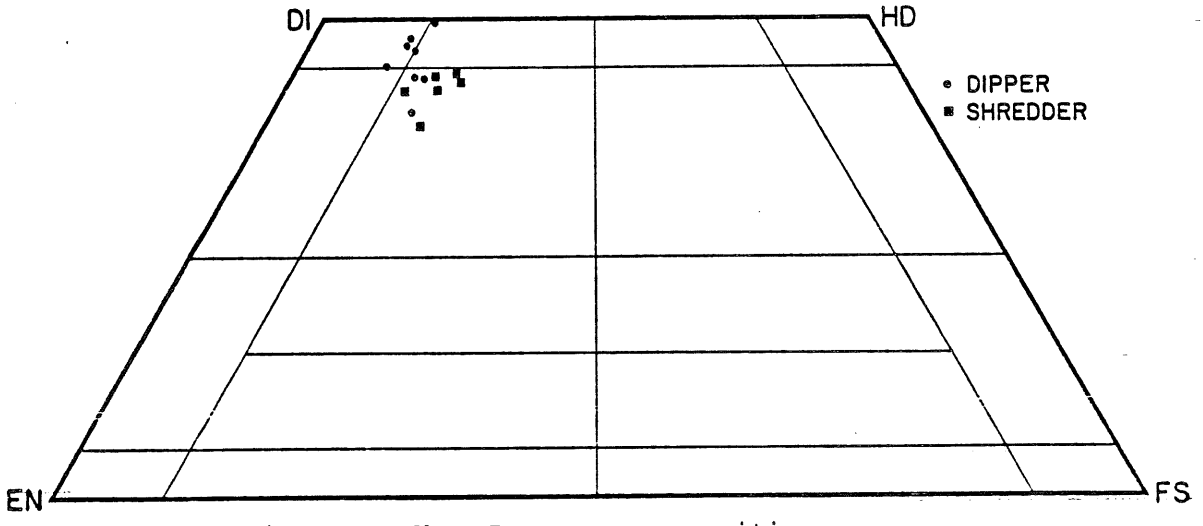

Figure II.2b: Pyroxene compositions

TABLE II.5: Analytical Methods

Element(s)	1974-1975	1975-1976
Si	INAA, Dal.	INAA, Dal.
Al, Mg, Mn, Fe, Ca, Na, K	Atomic absorption, Dal.	Atomic absorption, Dal.
Ti, P	Colorimetry, Dal.	Colorimetry, Dal; XRF, M.U.N.
CO_2	Titration, Dal.	Titration, Dal.
H_2O^T	Loss on ignition, Dal.	Loss on ignition, Dal.
Y	XRF, S.M.U.	n.d.
Rb, Sr, Zr	XRF, S.M.U. and M.U.N.	XRF, M.U.N.
Ba, Cr, Ni, Cu, Nb, Zn	XRF, M.U.N.	XRF, M.U.N.

Dal = Dalhousie University, Halifax, Nova Scotia.
S.M.U. = Saint Mary's University, Halifax, Nova Scotia.
M.U.N. = Memorial University of Newfoundland, St. John's, Nfld.

TABLE II.5 (continued)
Rare-earth element analysis

Parameter	1974-1975	1975-1976
a. Irradiation time	4 hrs	4 hrs
b. Integrated flux	6.0 MWH	6.0 MWH
c. Cooling time to:		
First counts	5 days	6 days
Second counts	12 days	17 days
Third counts	18 days	38 days
d. Detector-sample distance; counting time:		
First count	3 cm; 5,000 sec	3 cm; 1,800 sec
Second count	0 cm; 10,000 sec	0 cm; 10,000 sec
Third count	0 cm; 12,000 sec	0 cm; 10 hrs
e. Corrections applied	a. Pa (300keV) interference with Tb (299keV): Pa(300keV) = [5.8/34]x[area Pa(311keV)].	
	b. Ta (179keV) interference with Yb (177keV): 1. Use Yb (282keV) peak. 2. Calculate sum of Ta (1221keV) + Ta (1231keV): Detector 1: Ta (179)=0.5839[Ta(1221)+Ta(1231)]. Detector 2: Ta (179)=0.64[Ta(1221)+Ta(1231)].	
	c. Fe and Ce: [Fe(142keV)+Ce(145keV)]-Fe(142keV) = Ce(145keV). Fe(142keV)/fe(190keV) = 0.434.	

TABLE II.6: ANALYTICAL ERRORS

A. Major Elements: Standard rock JB-1

	Flanagan (1972)	Dal, 1974	Dal, 1976	Dal, 1976
SiO_2	52.09	52.61	nd	nd
TiO_2	1.34	1.34	1.28	1.25
Al_2O_3	14.53	14.54	14.53	14.70
Fe_2O_3	2.30*	9.14	2.22	2.34
FeO	6.06	nd	6.09	6.09
MnO	0.16	0.14	0.15	0.16
MgO	7.70	7.70	7.70	7.70
CaO	9.21	9.15	9.17	9.29
Na_2O	2.79	2.71	2.62	2.71
K_2O	1.42	1.48	1.48	1.49
P_2O_5	0.26	0.26	0.26	0.27
CO_2	0.19	0.19	0.13	nd

* Total iron as Fe_2O_3

B. Trace elements: Relative error as $2\sigma/\bar{x}$

	M.U.N.			S.M.U.	
Std.	G-2	XC-1	XC-3	BCR-1	G-2
N	10	46*	16	27	27
Zr	.04	.34	.24	.09	.25
Sr	.02	.16	.55	.04	.04
Rb	.02	.27	.14	.19	.09
Zn	.02	.30	.33	nd	nd
Cu	.22	.27	.43	nd	nd
Ba	.04	.15	.12	nd	nd
Nb	.40	.27	.32	nd	nd
Ni	.10	.50	.17	nd	nd
Cr	.29	.67	nd	nd	nd
Y	nd	nd	nd	.29	.45

* 46 separate pellets

TABLE II.6 (continued)

C. Rare-earth elements

Elements	Precision*
La, Eu, Ta	± 5%
Ce, Sm, Tb, Lu	± 10%
Yb	± 15%

* 1σ relative precision for 10,000 counts per peak; standard rock AGV-1.
Statistics from Dr. P. Jagam, Dalhousie University, Halifax, Nova Scotia; April, 1978.

TABLE II.7: PALEOMAGNETIC DATA

Sample	Oxidation $\frac{Fe\ O}{Fe\ O=FeO}$	NRM emu/cc	MDF oersteds	Curie temp. °C
25/9	1.0	.0053	150	330°; 540°
25/19	.95	--	--	485° (2nd temp)
25/29A	.95	.0027	130	412°; 418°; 220°; 398°; 543°
30/1	.97	.0092	--	358°; 543°
30/2	.87	.0085	--	380°; 543°
30/12	.90	.0093	--	425°; 550°
31/2	.90	.0058	--	335°; 540°
31/4	.96	.0048	170	420°; 520°
31/5	.91	.0107	175	347°; 526°
31/6	.93	.0110	198	361°; 550°
31/11	.98	--	--	320°; 540°
31/17	.91	.0100	--	365°; 540°

Figure II.3: Photomicrographs of selected samples, transmitted and reflected light.

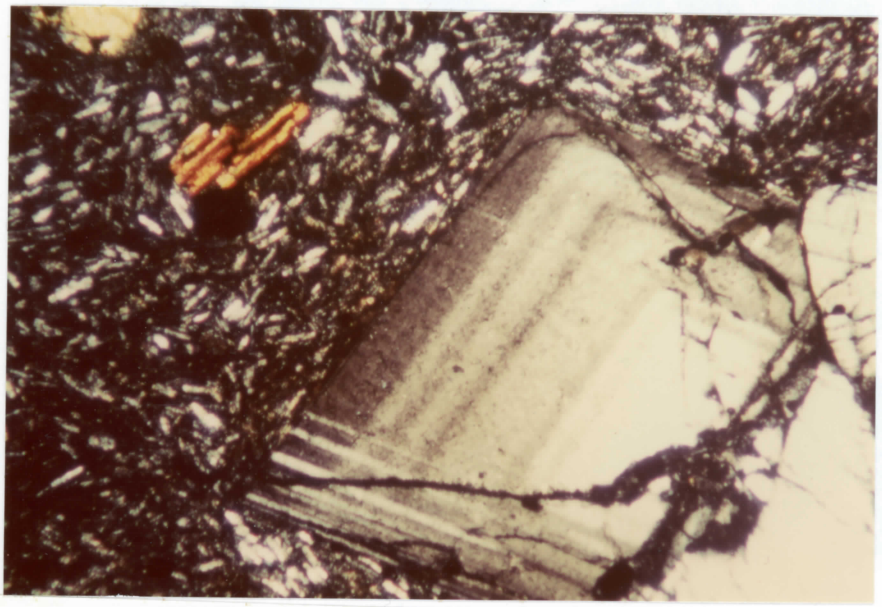

Trachyte 25/1a 31X crossed Nicols
Normally-zoned plag. (andes.-oligocl.) phenocryst in matrix of plag and K-feldspar microlites, biotite, amphibole and opaques. 25/1a is the freshest trachyte; others have varying amounts of interstitial palagonitization in the groundmass.

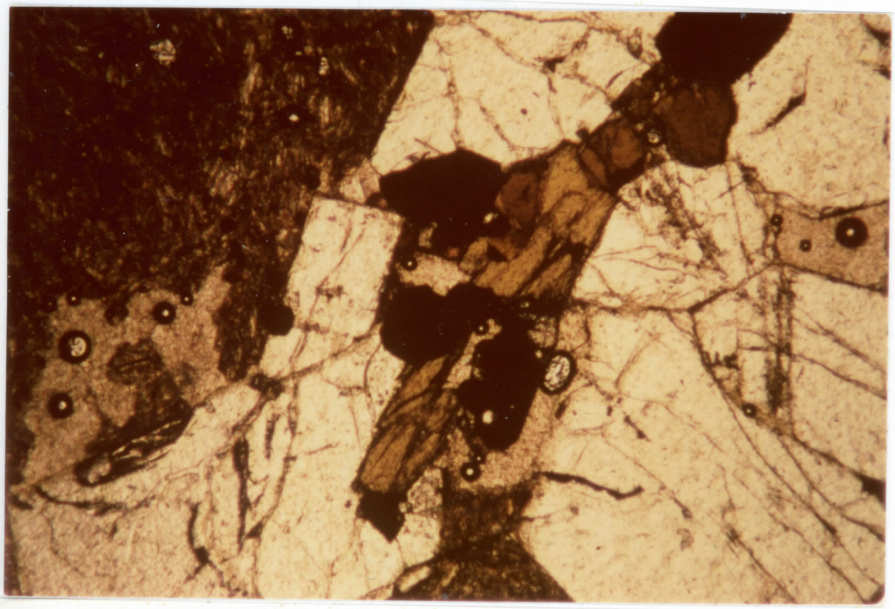

Trachyte 25/1a 31X plane-pol. light
Glomerophenocryst of plag., amphibole, biotite opaques and zircon, typical of this sample and several of the other trachytes.

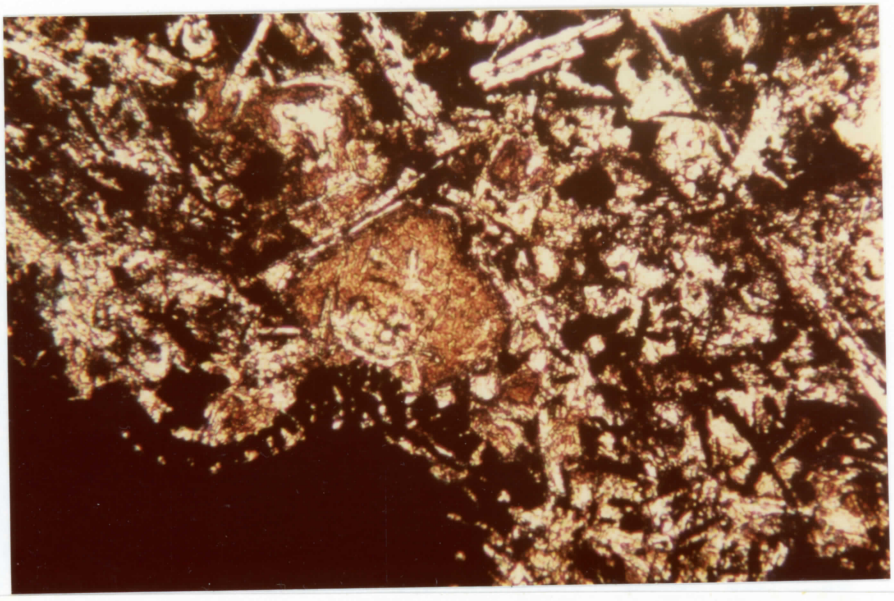

Basalt 30/5 125X plane-pol. light
Iron-titanium oxide (titanomaghemite?) phenocryst with skeletal-growth rim in typical altered matrix. Note the abundant skeletal oxides (seriate texture) in the groundmass. The bright red-orange material near the center of the photo appears to be pseudomorphous after olivine.

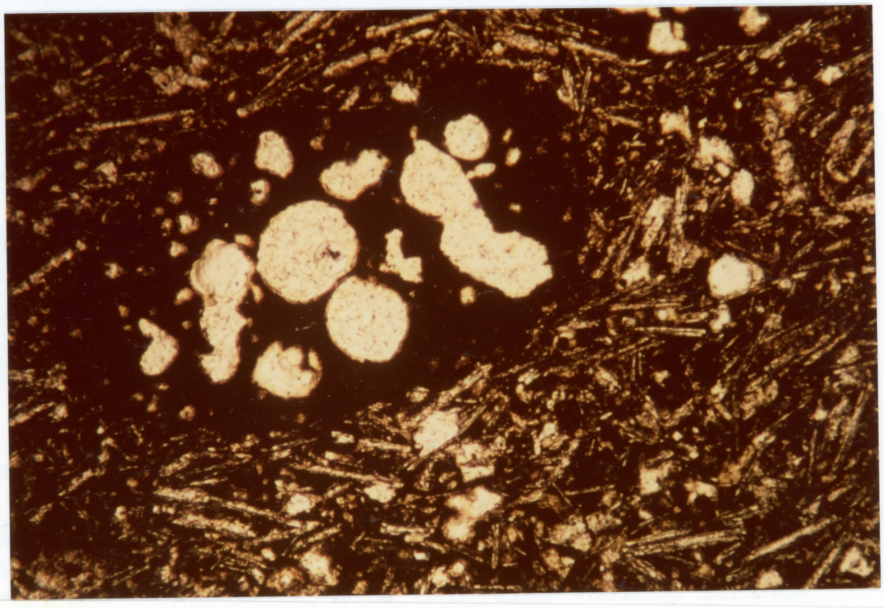

Basalt 25/9 31X plane-pol. light
Ovoid patch of iron oxide (and hydroxide?) concentration in fine-grained fluidal matrix of altered feldspar microlites, clays and opaques. The vesicles are all empty except for thin linings of orange-brown clays.

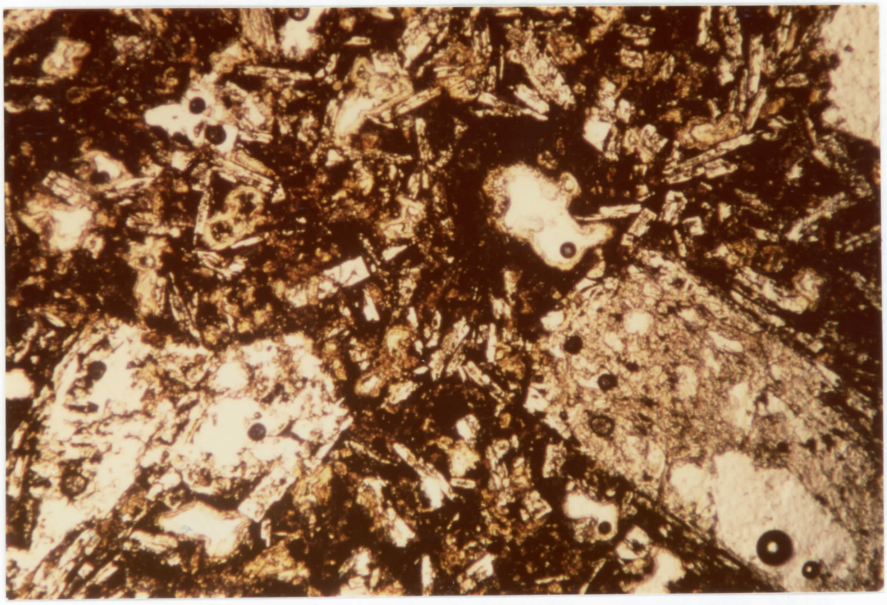

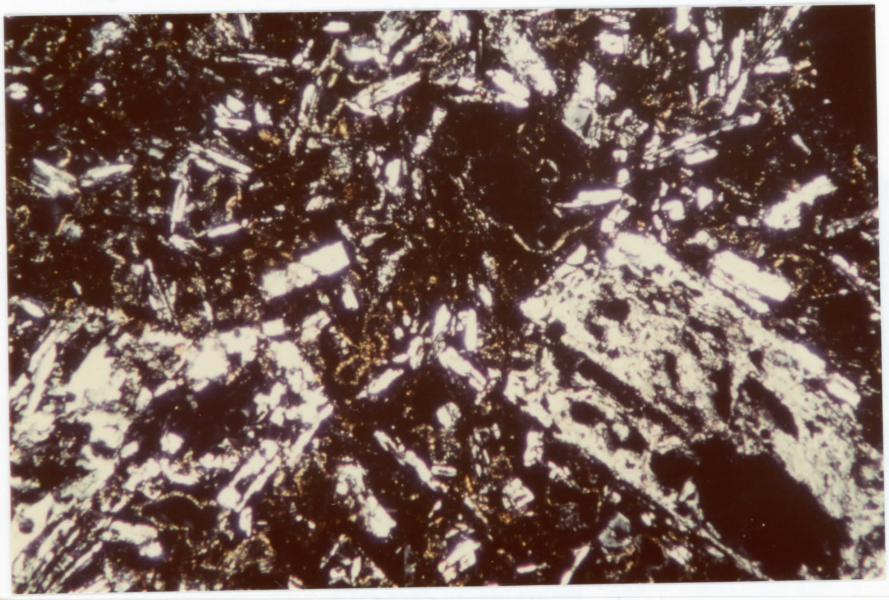

Basalt 31/6 31X plane-pol. light and crossed Nicols

Altered plagioclase phenocrysts in matrix of feldspar microlites, orange and brown clays (smectites) and seriate opaques. Note thin clay vesicle linings and opaque zone around vesicle just above and to the right of center.

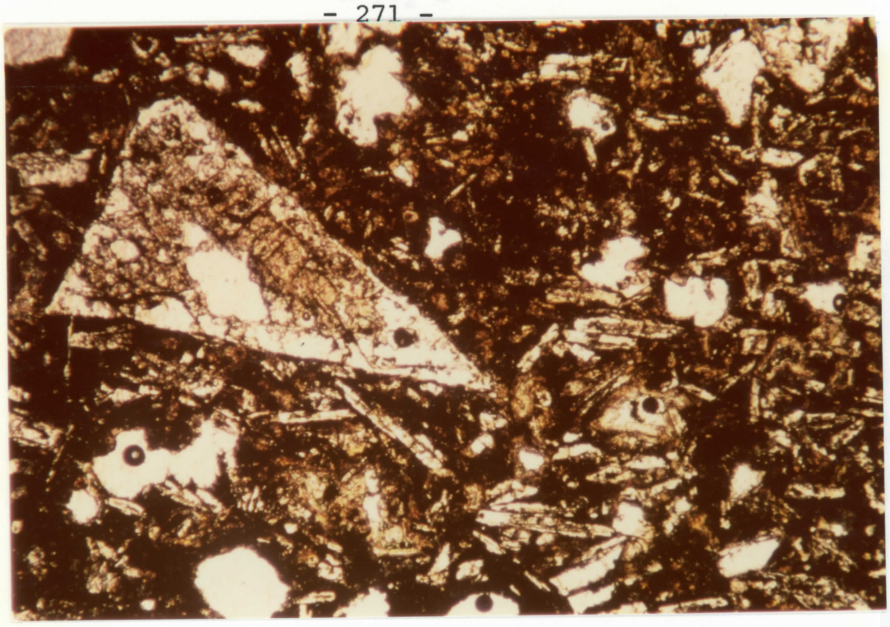

Basalt 31/5 31X plane-pol. light
Typical altered seamount basalt. Note the thin rim of still-fresh feldspar surrounding the brown-clay alteration product in the triangular phenocryst .

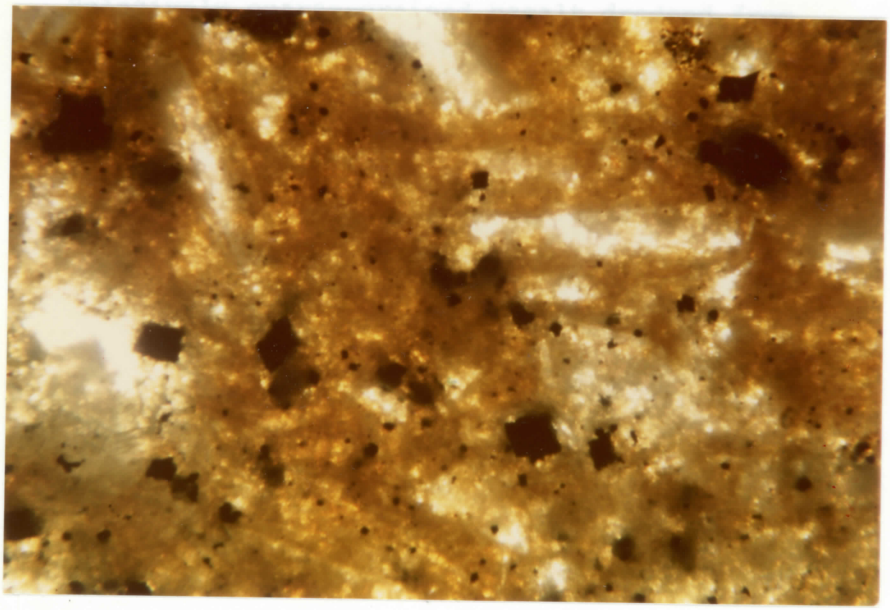

Basalt 105/2d 100X plane-pol. light
Altered glassy basalt. Outlines of several plag. laths and (possibly) altered olivines (upper left corner) are visible; abundant seriate opaques with equant habit.

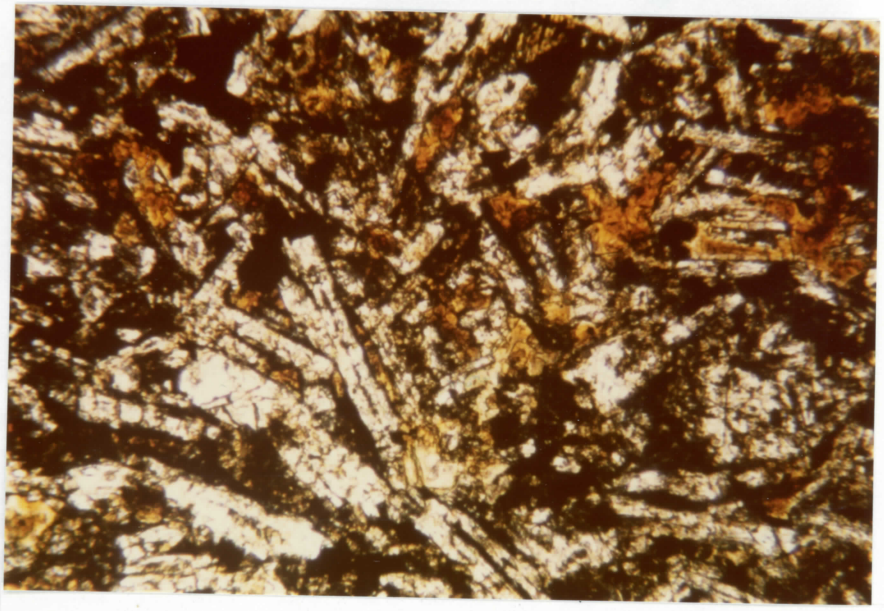

Basalt 106/1a 100X plane-pol. light
Relatively coarse-grained basalt dredged from Shredder Seamount. 106/1a contains abundant fresh phenocryst and groundmass clinopyroxenes.

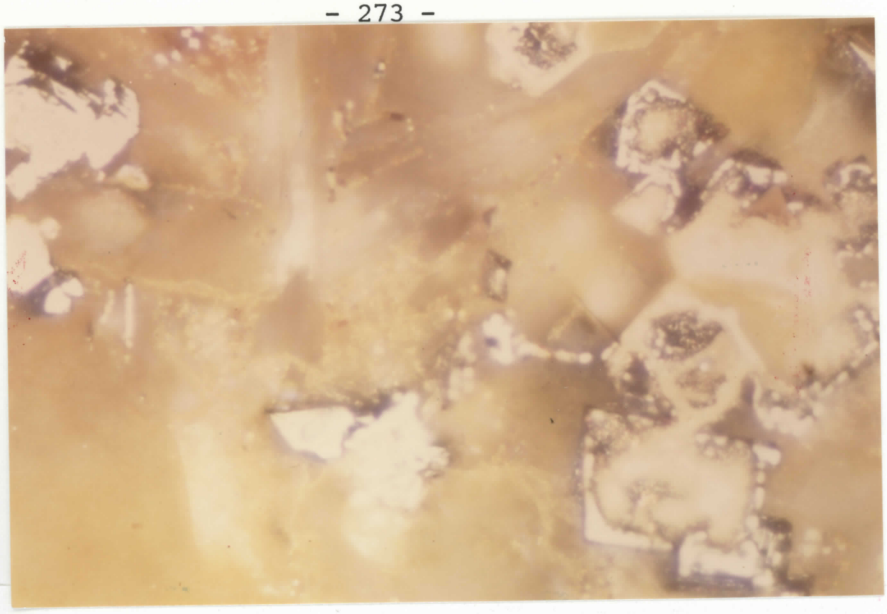

Basalt 25/10 530X; oil immers.
Highly-altered subhedral and euhedral titanomagnetites. Cores of crystals at right contain spongy-looking golden yellow material (possibly sphene?). Such highly-altered grains are not common in the sea-mount samplesbut occur in patches within 25/10.

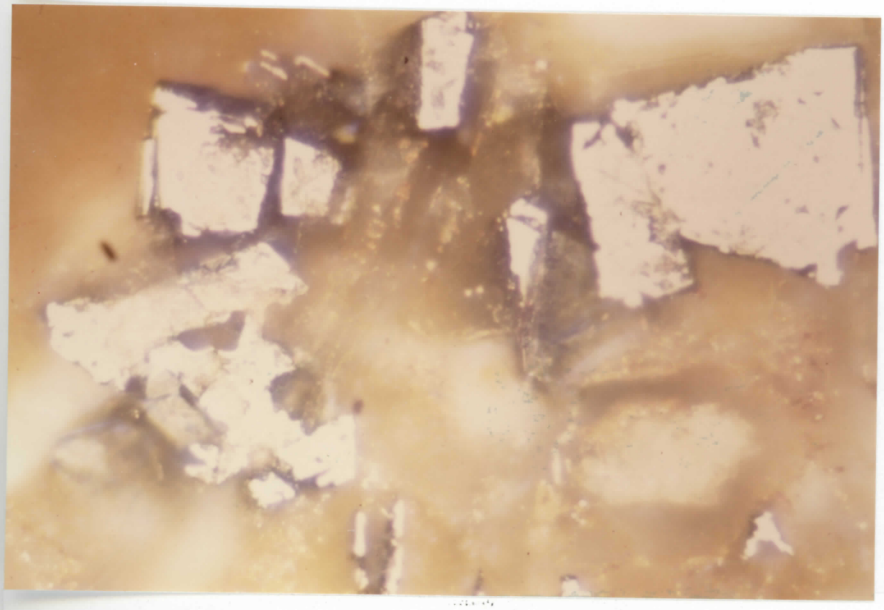

Basalt 25/10 660X; oil
Subhedral altered titanomagnetites. Cracking and granulation (in patches) are evident.

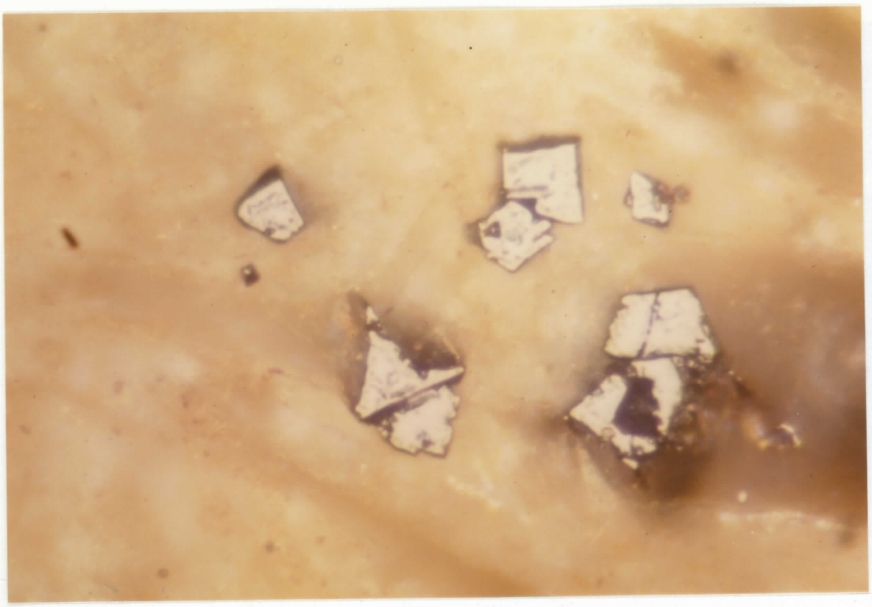

Basalt 105/1 825X; oil
Small euhedral and subhedral grains in altered glassy gasalt.

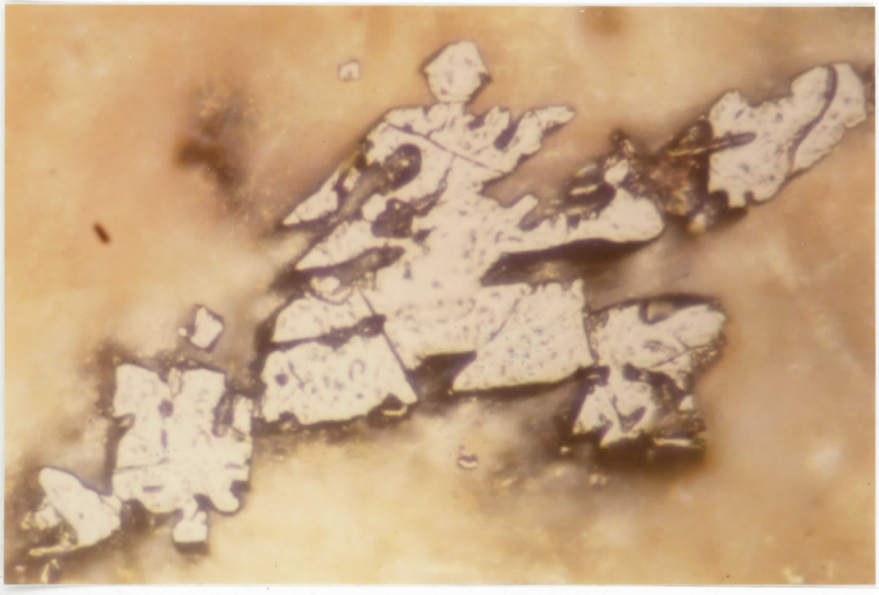

Basalt 105/1 825X; oil
Large subhedral titanomagnetite, showing cracking and pitted appearance typical of this sample.

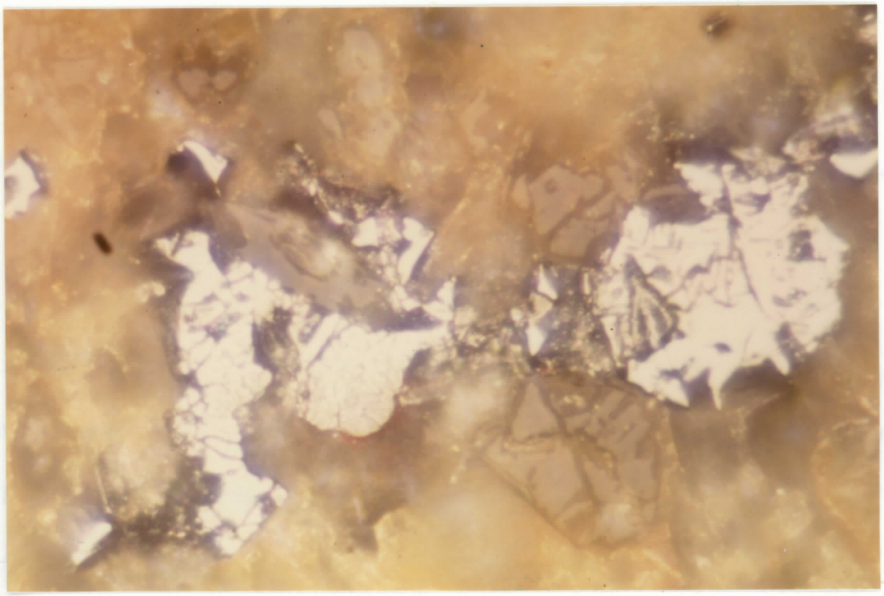

Basalt 106/4 825X; oil
Anhedral altered titanomagnetites. Note cracking of grains and the development of granulated zones (gray) along cracks in the grain at left.

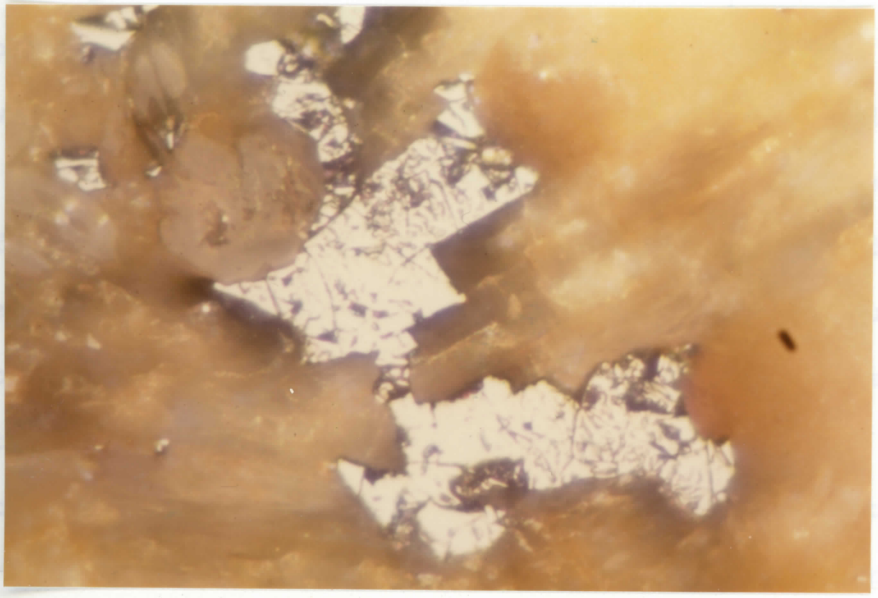

Basalt 106/4 825X; oil
Anhedral-subhedral highly-altered titanomagnetites.

APPENDIX III: EXPENDABLE SONOBUOY ANALYSIS

This appendix describes the shipboard and on-land procedures followed in analyzing wide-angle reflection and refraction data recorded at the expendable sonobuoy stations shown in Fig. III.1. This analysis is based on the principles described by LePichon et al. (1968), but rather different procedures for data recording and computation are applied. The description given here is drawn from the very detailed documentation given in M. J. Keen (1976).

Shipboard procedures

All of the expendable sonobuoys used in this study were launched from the CSS Hudson on cruises HU73-011 and HU75-009. Aquatronics 79.2 and 168 MH_Z sonobuoys are used, with a Bolt 1000 in^3 airgun with pulse-shaper as sound source. The telemetered sonobuoy signals are received with an Aquatronics receiver and recorded simultaneously on one track of a Hewlett-Packard instrumentation recorder and on a Raytheon facsimile recorder; the air-gun trigger pulse is recorded on a separate channel of the tape recorder. A second Raytheon simultaneously records the vertical-incidence record. Loran-C fixes are taken at 2-minute intervals during sonobuoy operations.

The tape-recorded sonobuoy data are subsequently played back through various filter band-widths to produce records that clearly show: water-wave (100-250 H_Z); bottom reflection (100-250 and 40-80 H_Z); sub-bottom reflections (30-60 H_Z); and refractions (7.5-15 H_Z). The

vertical-incidence data recorded during the sonobuoy operation are also filtered (30-60 H_Z) to produce a record strictly comparable to the sonobuoy record.

Analysis of records

The waterwave, bottom reflection and all possible sub-bottom reflections and refractors are identified and picked visually from the appropriate playbacks. The method used here involves tabulating, for each event, the two-way travel-time and the sweep number counted off along the horizontal axis of the records. The time (T) and sweep (SW) values are run through program BEDIT, written by M. J. Keen (see M. J. Keen, 1976) to get the waterwave distances (X) corresponding to each sweep number.

The T-X output of BEDIT then serves as input to programs TIMEX and THIN3 (Keen, 1976), which calculate interval velocities and thicknesses by the direct and ray parameter methods, respectively. Dips on reflectors are taken into account in TIMEX, but not in THIN3. Ideally, the results of both calculations are comparable (if not identical) and the results compare favorably with the vertical-incidence profile. When this is not so, there are several ways to proceed: go back to the sonobuoy records and attempt to pick reflectors again, more accurately; average the two sets of results; use the result that most closely agrees with the vertical-incidence records.

Both TIMEX and THIN3 outputs include the standard deviation and degrees of freedom of the interval solution. These values can be used

with statistical tables for Student's t-test to find the error associated with the solution at any desired confidence limit. On average, the error limits for velocity and thickness determinations proved to be ± 0.2 km/sec or less and ± 0.1 km or less, respectively, at the 95% confidence level.

Refractors are also picked visually, from the very low frequency playbacks. The two-way travel times (t_2) and sweep numbers give an apparent velocity ($V_a = \frac{1.5 \times \text{WATERWAVE TIME}}{t_2 - t_0}$). The value of the intercept time, t_0, is found by extrapolating the refractor back to the zeroth sweep.

Apparent velocity, observed intercept time and a simple layered model of the section above the refracting half-space (including the length, R, of the sonobuoy profile) are the inputs for programs FINT and FIND. Layer interfaces may have different dips at each end of the section in FIND; FINT requires a constant dip across the length of the section. Both programs give true velocity, actual intercept time and critical distances as output. Comparison of the true and observed intercept times and of the critical distances and observed vertical-incidence section constitute two good checks on the quality of the results.

APPENDIX IV

Bedford Institute Cruises to the Newfoundland Basin, 1965-1977

This appendix lists the B.I.O. cruises that have been undertaken in the Newfoundland Basin and adjacent areas between 1965 and 1977, and indicates the types of data collected on each one (Table IV.1). Figure IV.1 shows track plots for all cruises at a scale of 1:6.5 million (Mercator projection). The coastline of southeastern Newfoundland and the approximate location of the 200 m isobath are shown as solid and dashed lines, respectively.

65-006 HUDSON

1-6.5 MILLION AT 46N

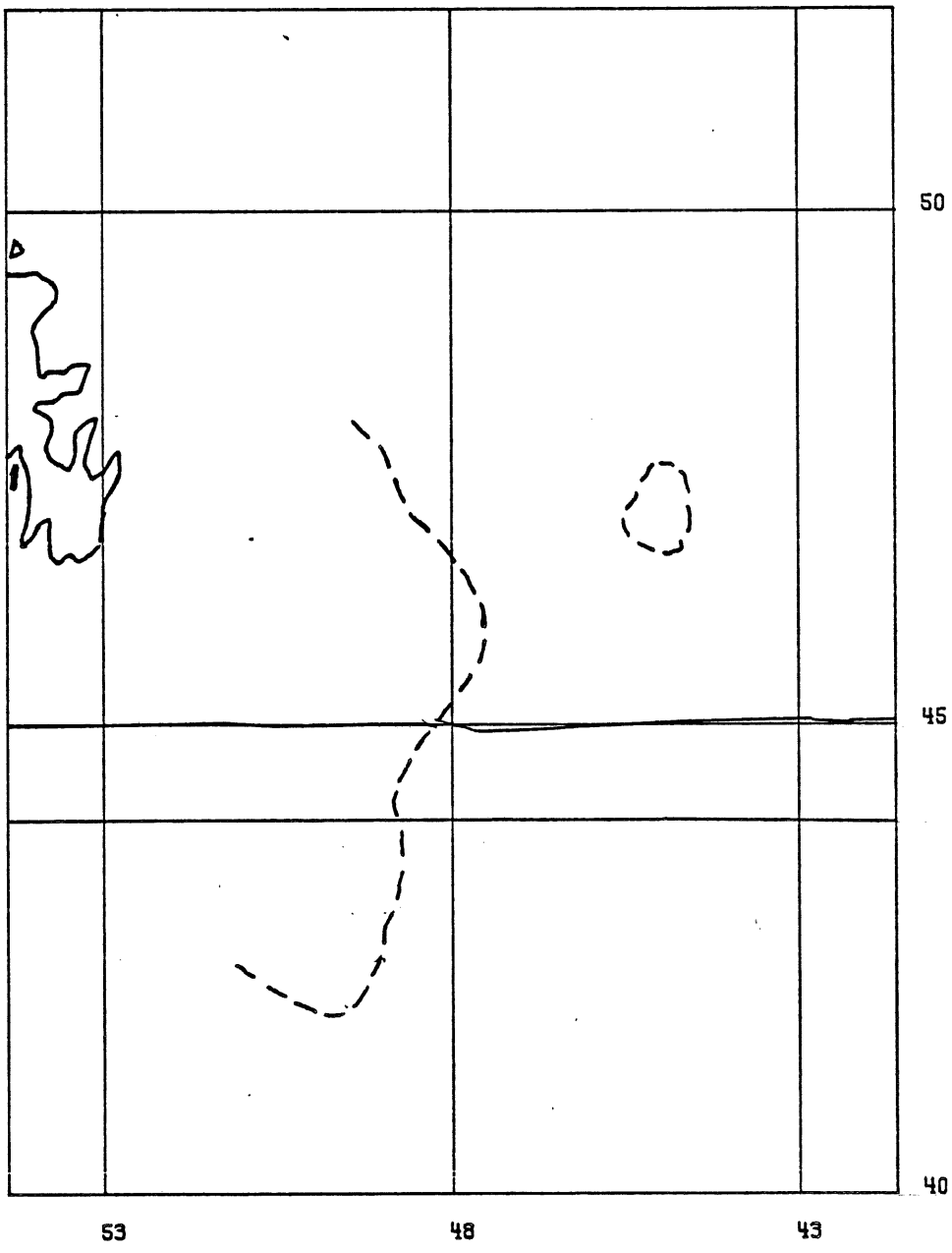

66-008 BAFFIN

1-6.5 MILLION AT 46N

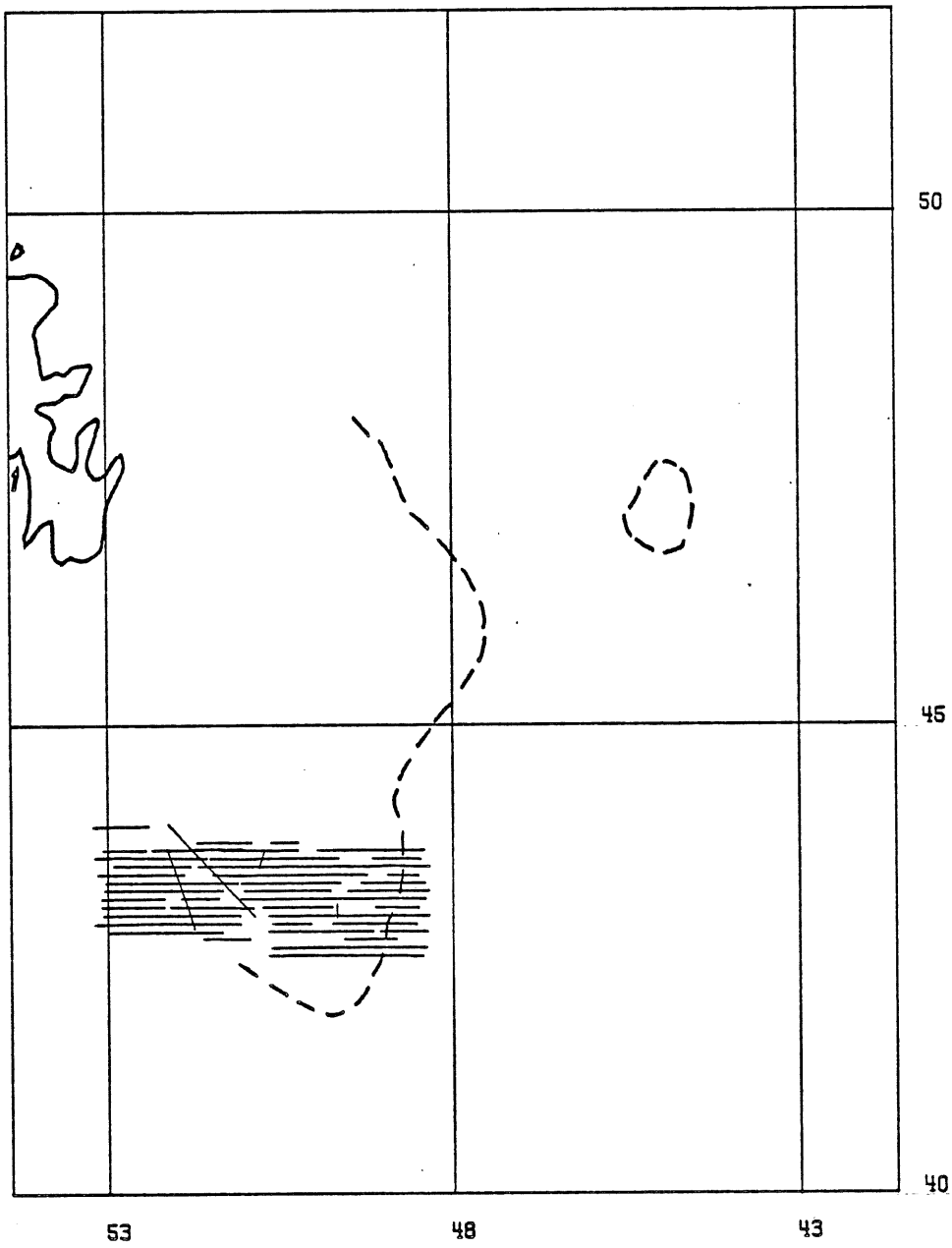

68-022 HUDSON

1-6.5 MILLION AT 46N

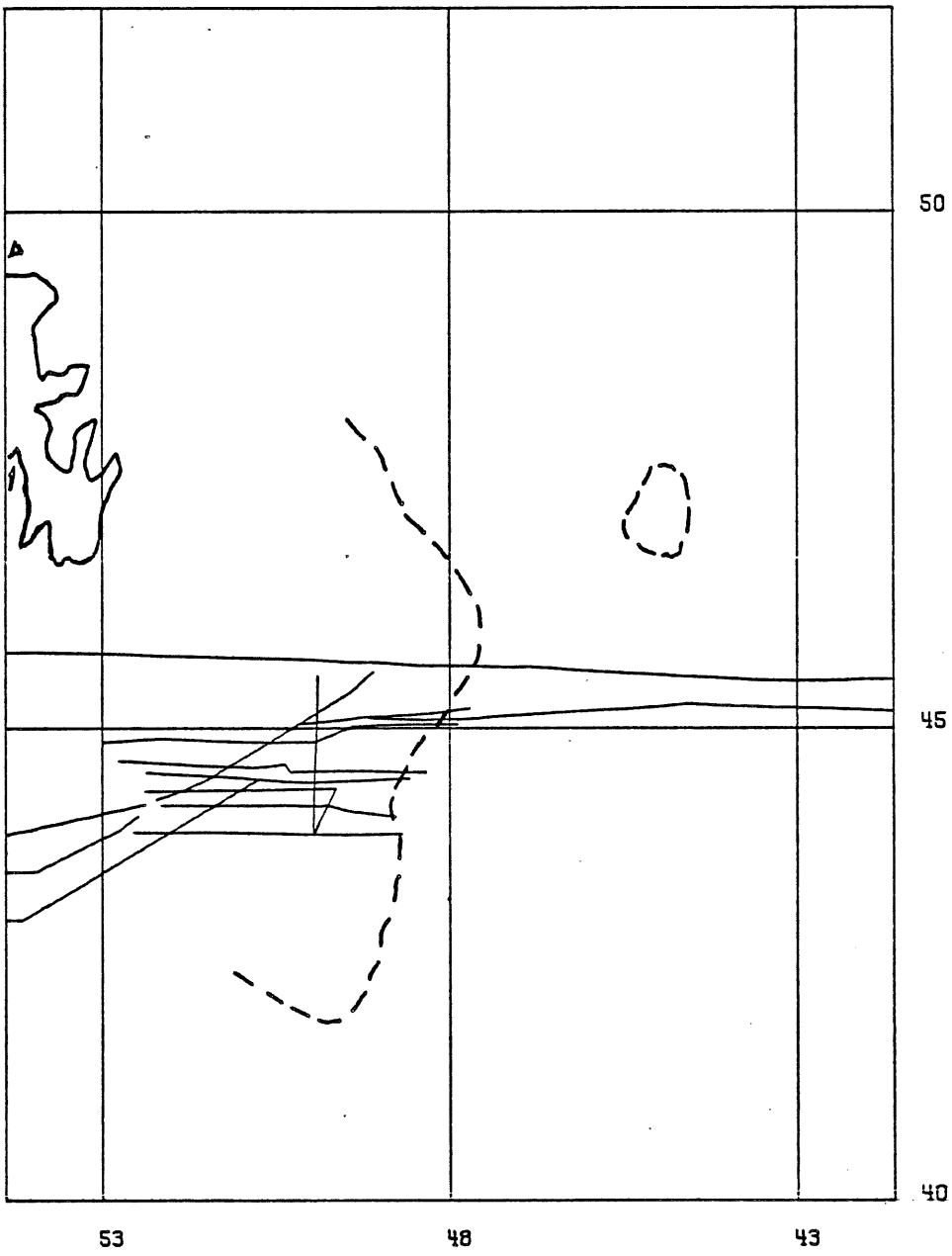

67-014 BAFFIN

1-6.5 MILLION AT 46N

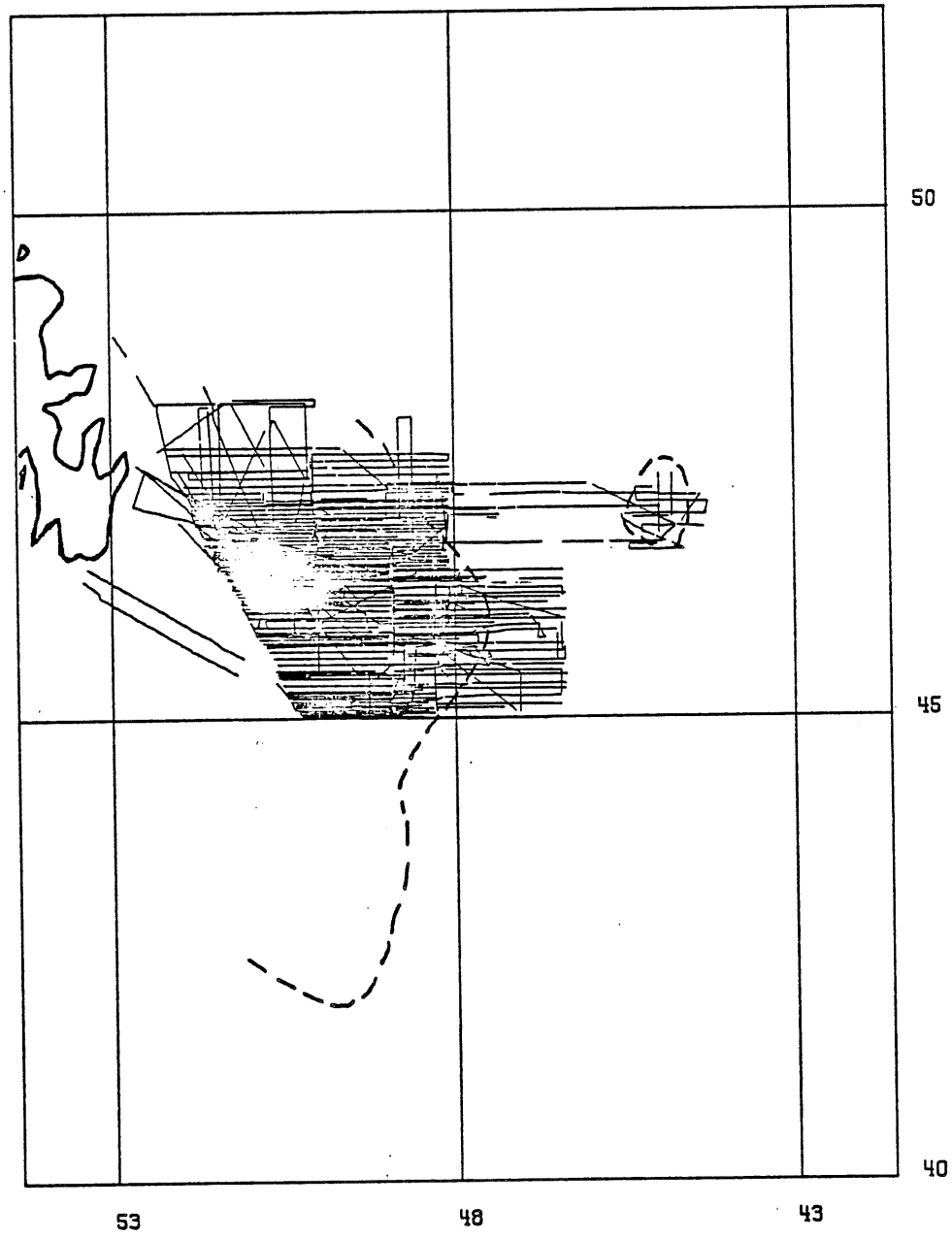

71-017 BAFFIN

1-6.5 MILLION AT 46N

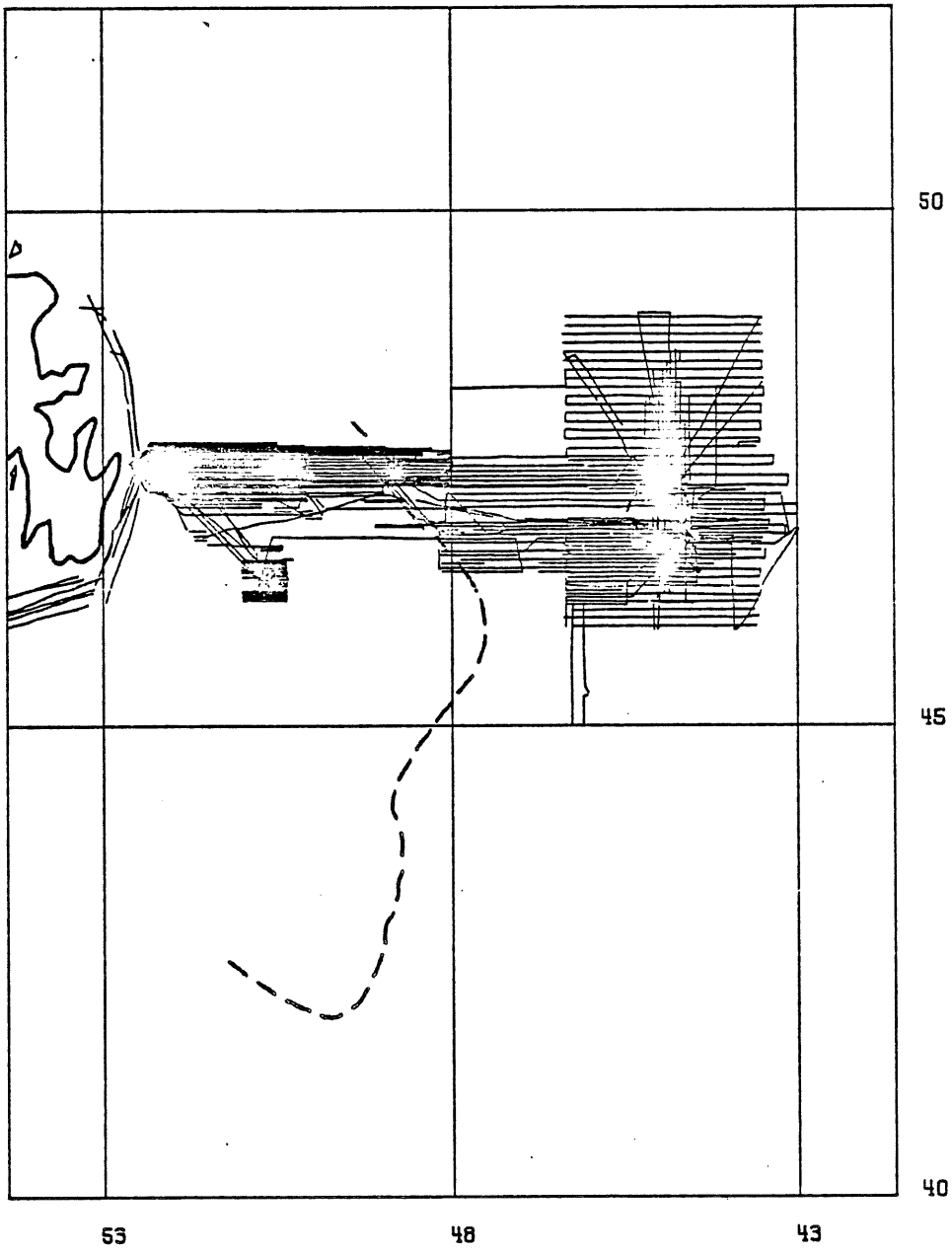

72-015 MINNA

1-6.5 MILLION AT 46N

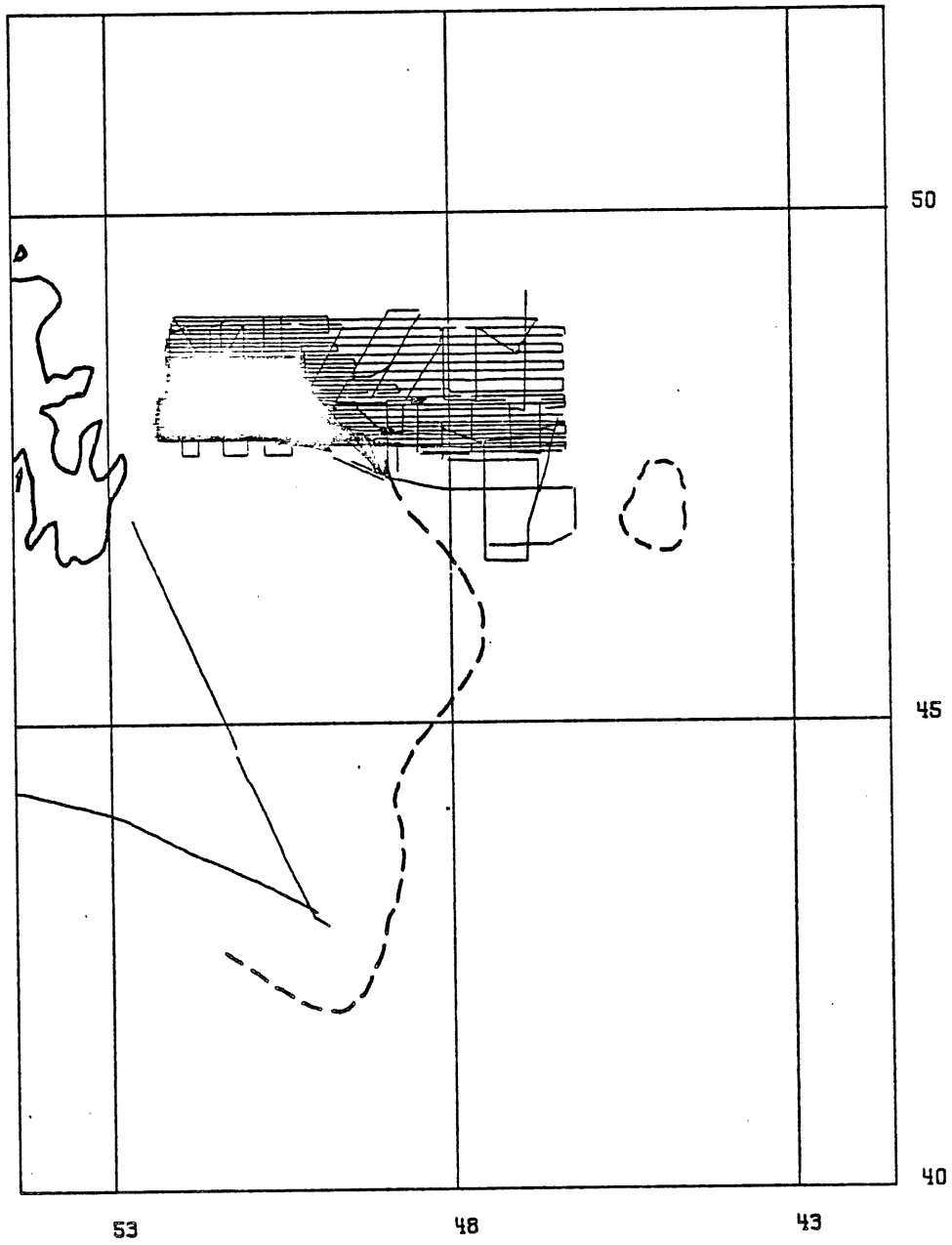

73-011 HUDSON

1-6.5 MILLION AT 46N

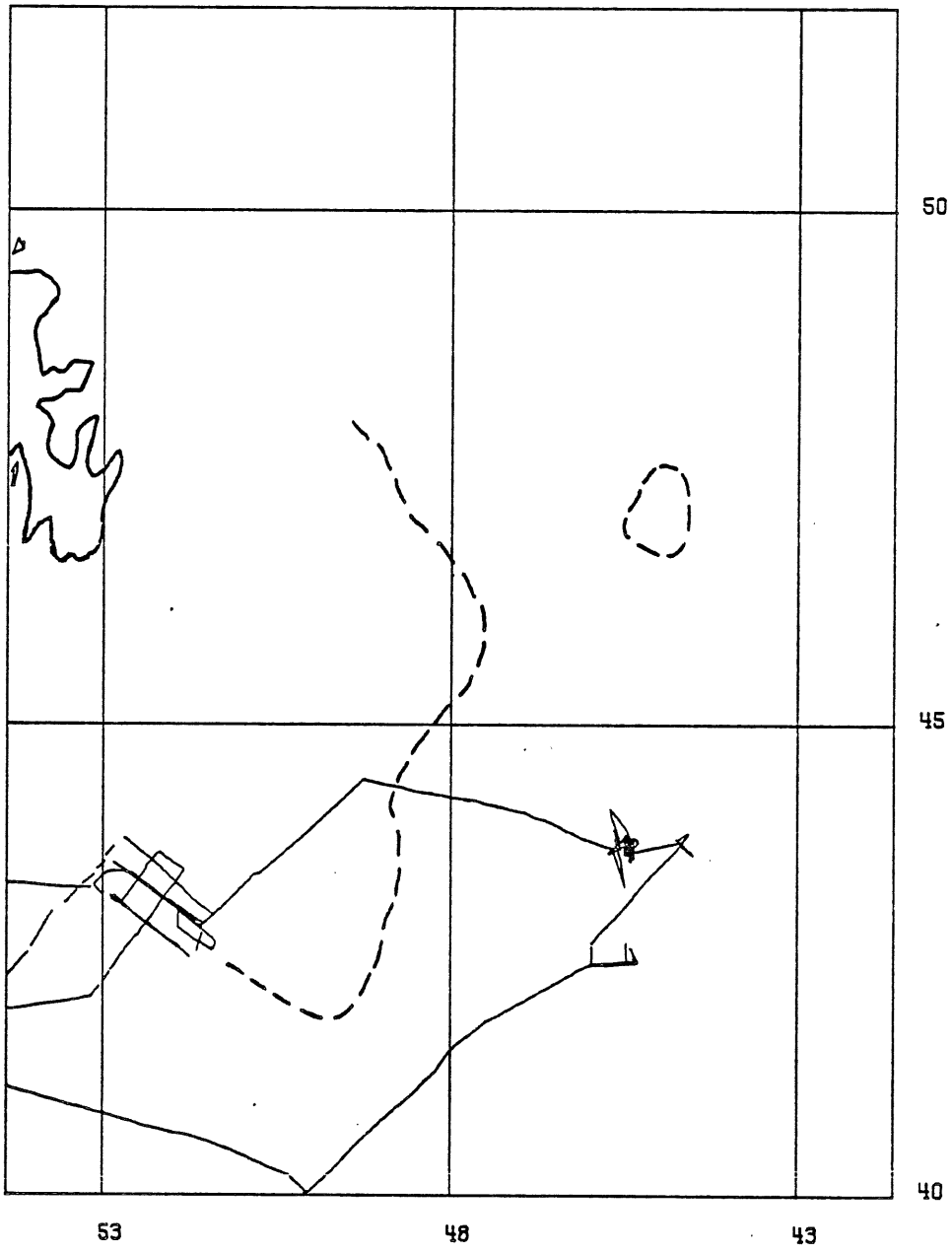

73-034 DAWSON

1-6.5 MILLION AT 46N

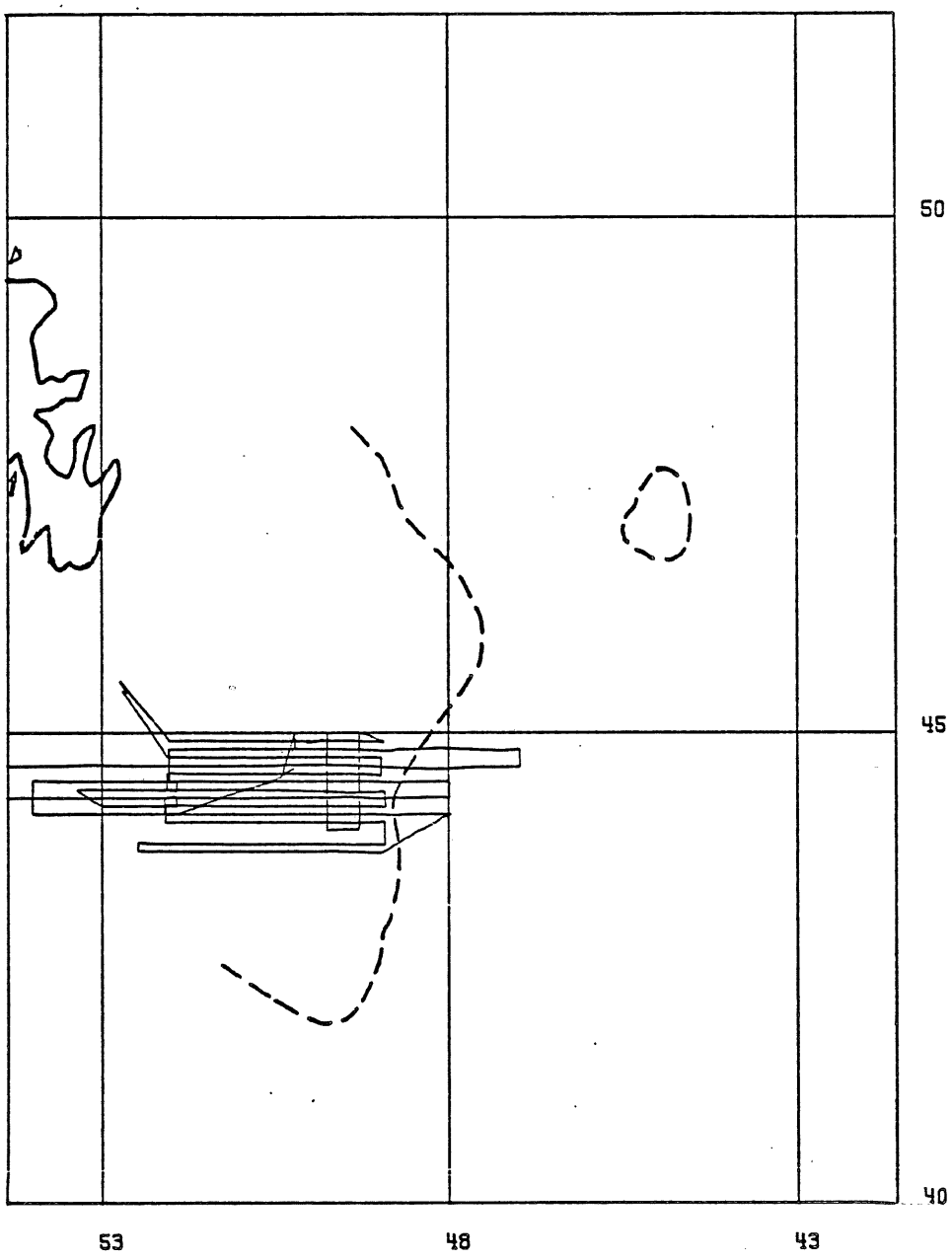

74-019 SACKVILLE

1-6.5 MILLION AT 46N

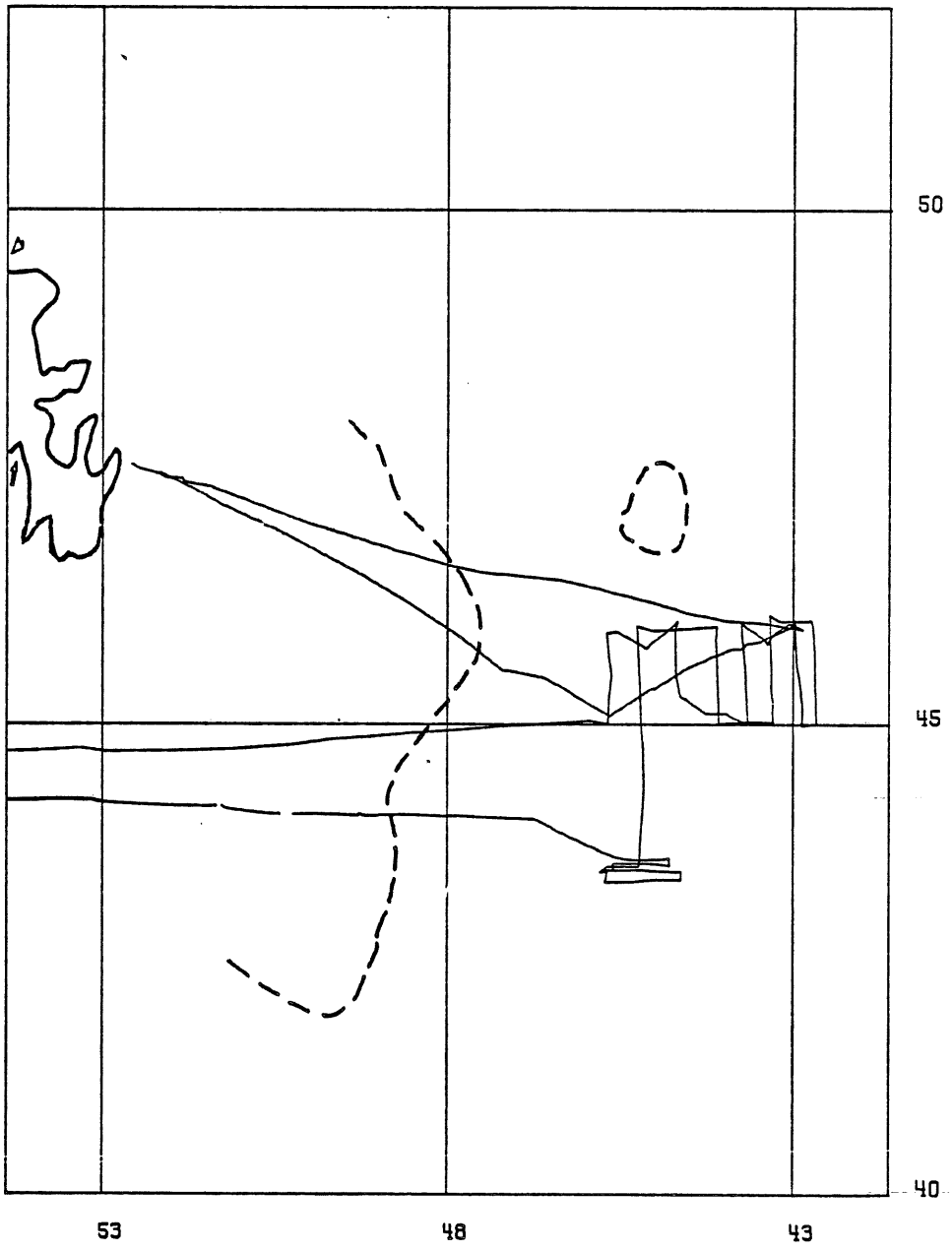

74-021 HUDSON

1-6.5 MILLION AT 46N

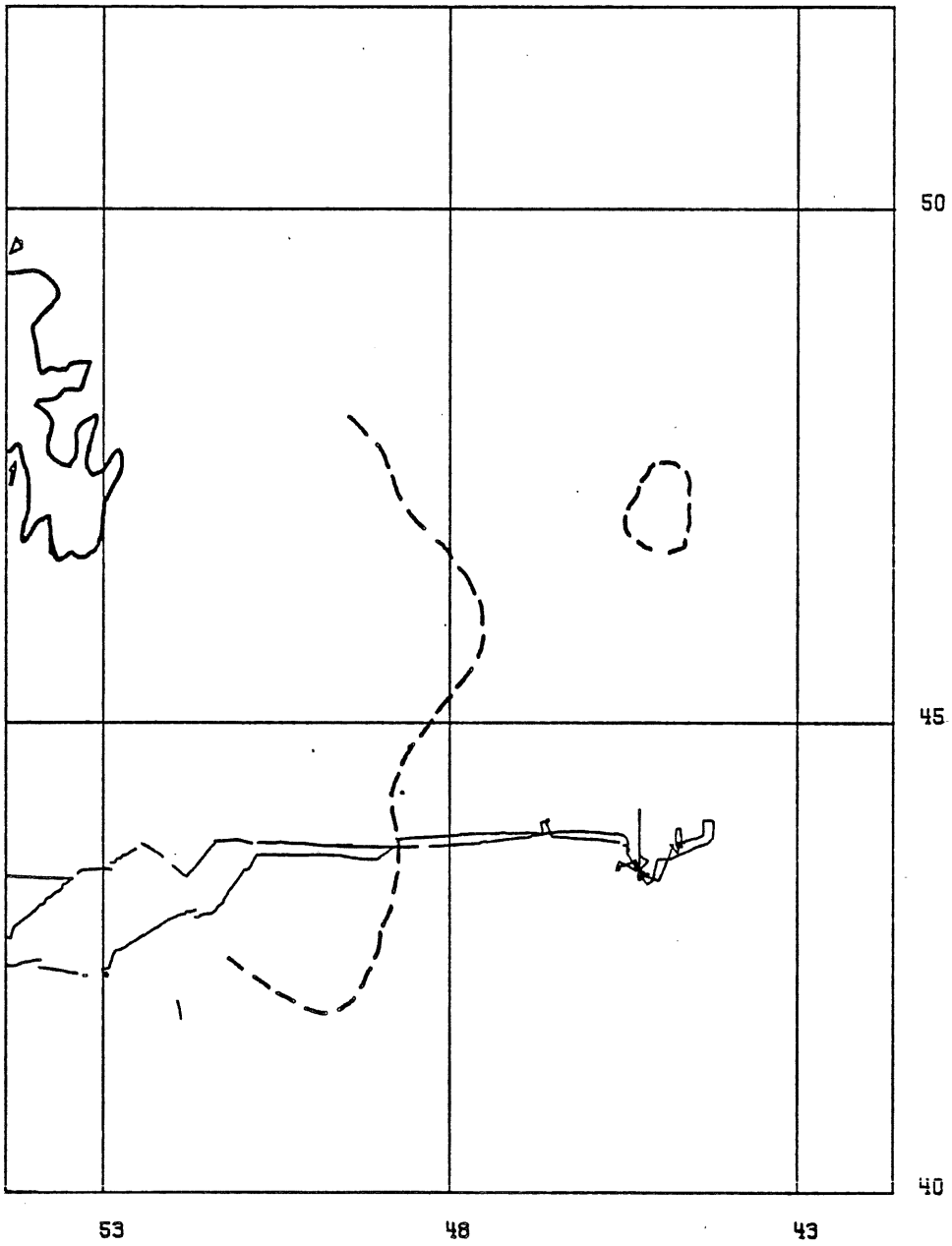

75-009 HUDSON

1-6.5 MILLION AT 46N

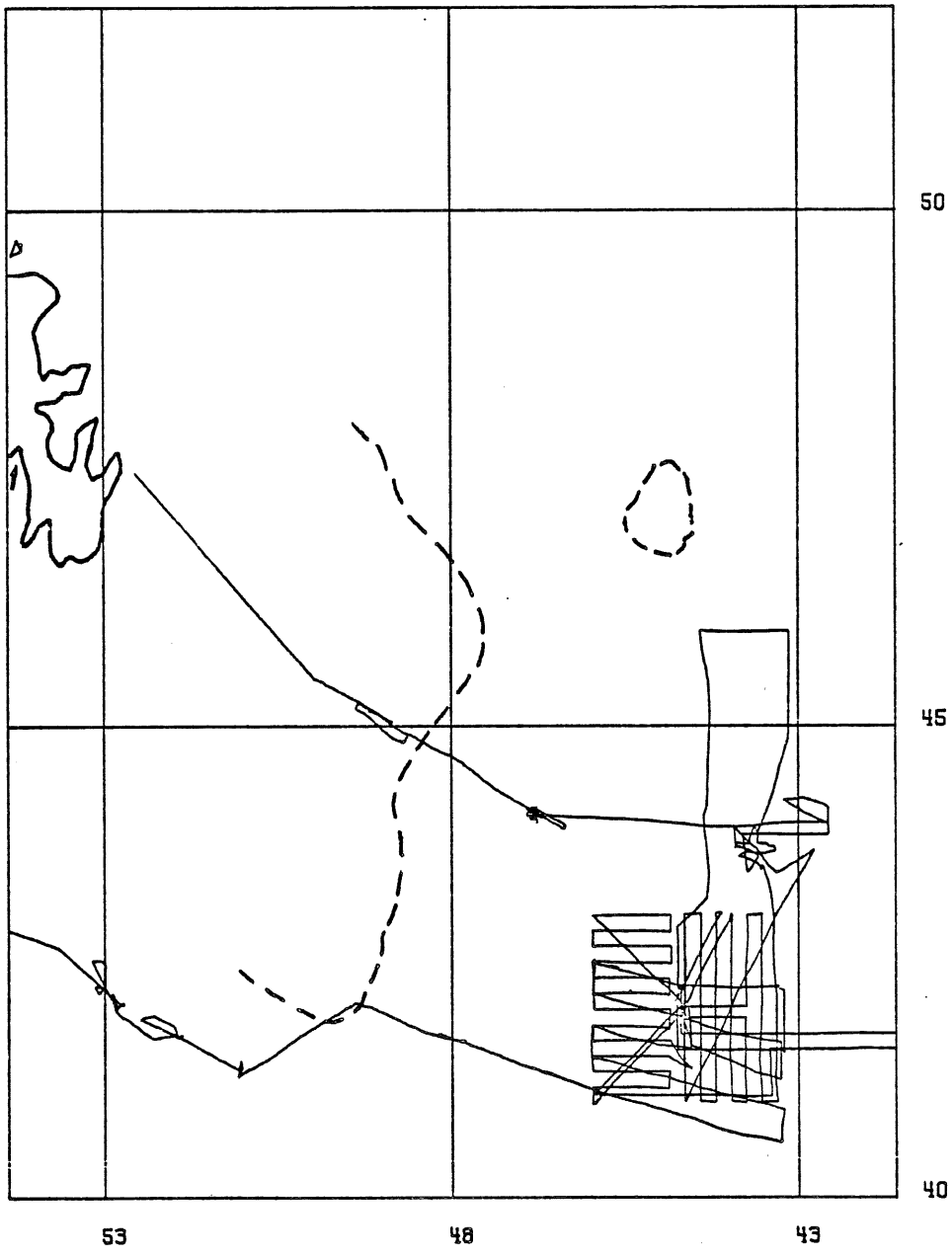

76-031 KARLSEN

1-6.5 MILLION AT 46N

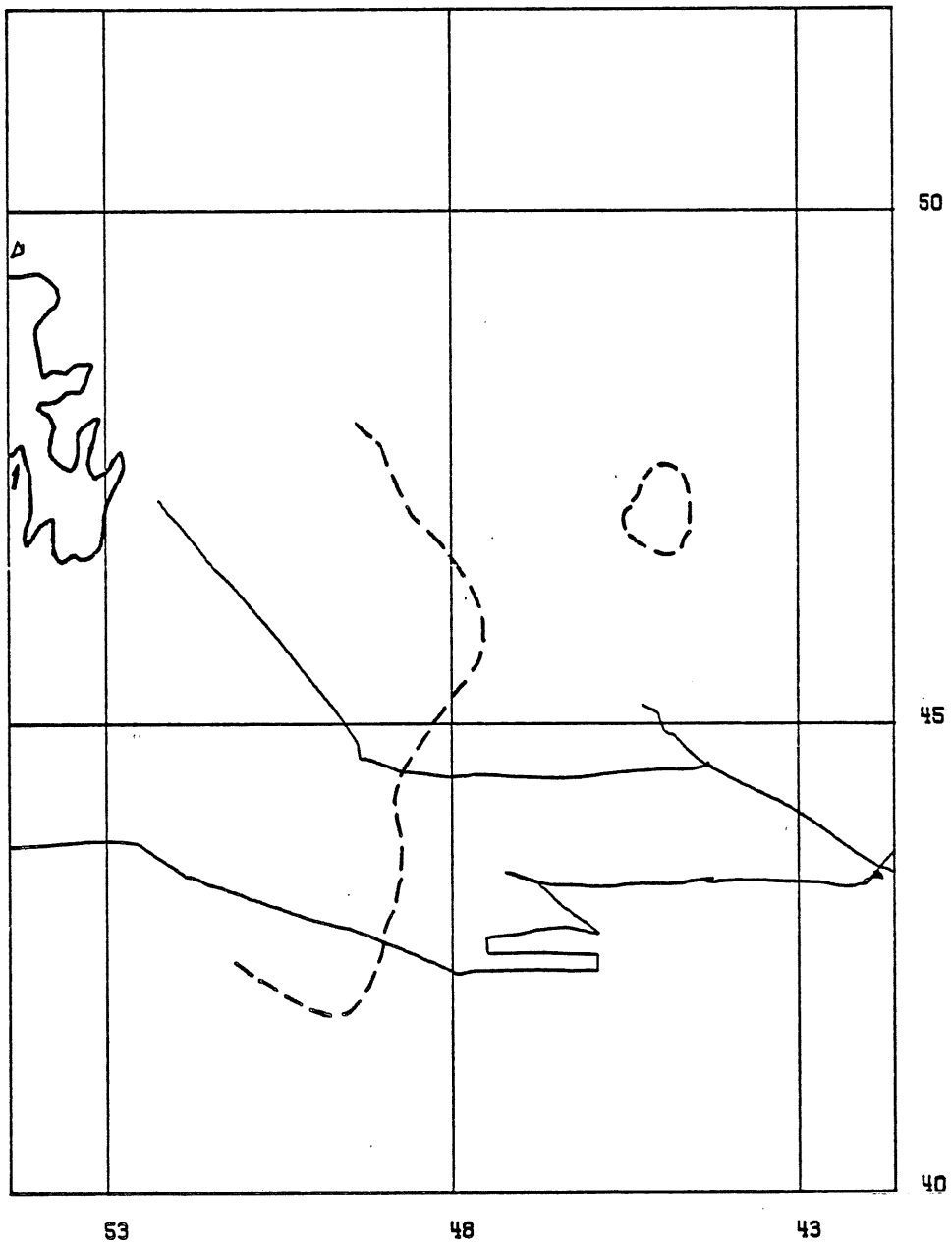

77-014 HUDSON

1-6.5 MILLION AT 46N

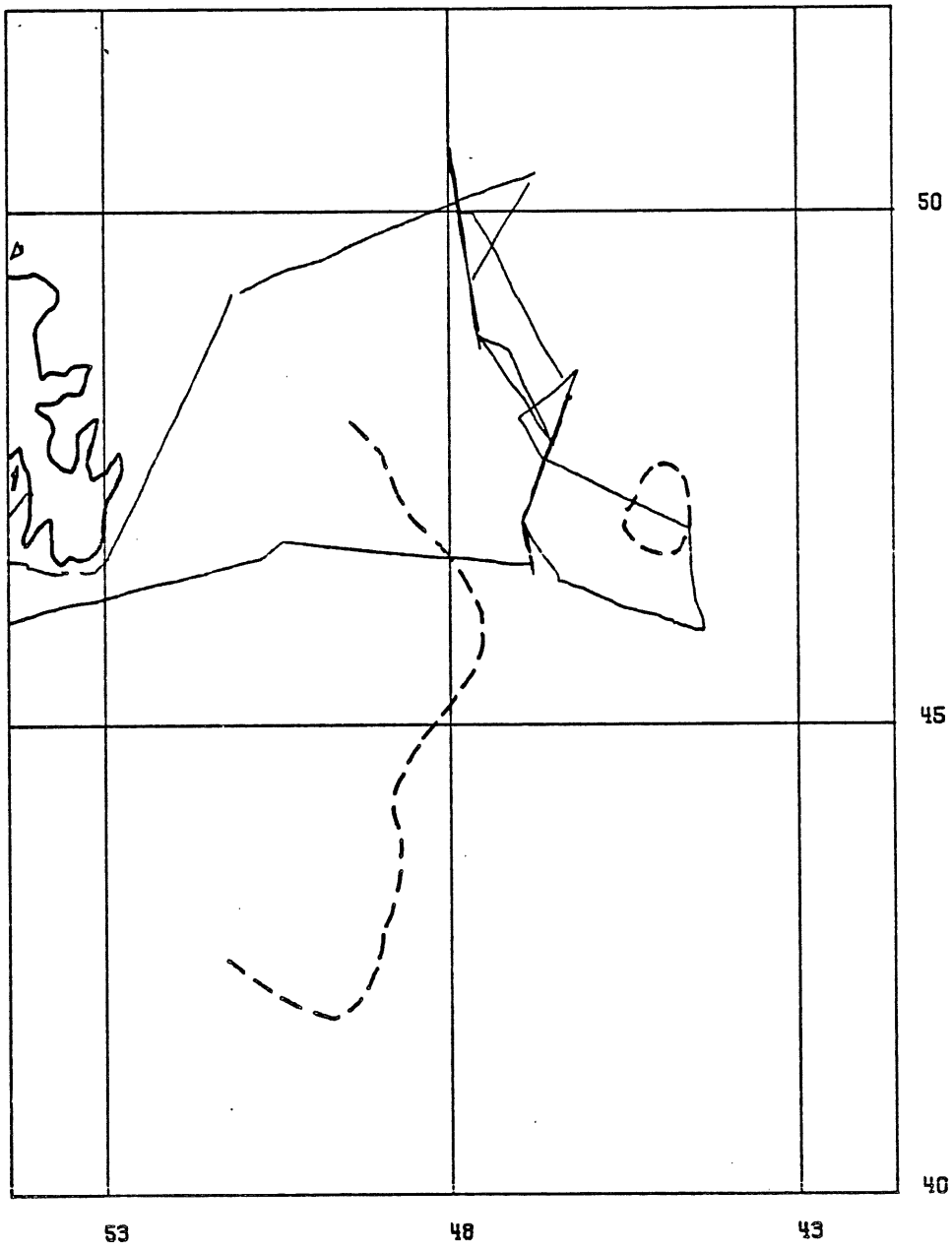

APPENDIX V

Original Seismic Reflection Records.

Hard-bound copies of this thesis will contain copies of all original B.I.O. single-channel seismic profiles in the Newfoundland Basin (see Figure 4.1a), made at 50% reduction (in pocket inside back cover). Requests for additional copies of these data should be addressed to Dr. Charlotte E. Keen, Bedford Institute of Oceanography, Dartmouth, Nova Scotia; the request should include cruise and line numbers as given in Table 4.1.